SENESCENT WHITE BLOOD CELLS IN COLORECTAL CARCINOMA PATIENTS

Miss Khin Aye Thin

เม็ดเลือดขาวชราของผู้ป่วยมะเร็งลำไส้ใหญ่

น.ส.ขิ่น อาย ธิน

Thesis Title	SENESCENT WHITE BLOOD CELLS IN COLORECTAL CARCINOMA PATIENTS
By	Miss Khin Aye Thin
Field of Study	Biomedical Sciences and Biotechnology
Thesis Advisor	Professor APIWAT MUTIRANGURA, Ph.D.
Thesis Co Advisor	Professor Steven W. Edwards
	Dr. CHAROENCHAI PUTTIPANYALEARS

Accepted by the FACULTY OF MEDICINE, Chulalongkorn University in Partial Fulfillment of the Requirement for the Doctor of Philosophy

-------------------------------------- Dean of the FACULTY OF MEDICINE
(Associate Professor CHANCHAI SITTIPUNT)

DISSERTATION COMMITTEE

-------------------------------------- Chairman
(Professor Chanitra Thuwajit (Toraksa))

-------------------------------------- Thesis Advisor
(Professor APIWAT MUTIRANGURA, Ph.D.)

-------------------------------------- Thesis Co-Advisor
(Professor Steven W. Edwards)

-------------------------------------- Thesis Co-Advisor
(Dr. CHAROENCHAI PUTTIPANYALEARS)

-------------------------------------- Examiner
(Dr. AMORNPUN SEREEMASPUN)

-------------------------------------- Examiner
(Associate Professor Nakarin Kitkumthorn)

-------------------------------------- Examiner
(Professor NATTIYA HIRANKARN)

-------------------------------------- External Examiner
(Professor Anne McArdle)

ขิ่น อาย ธิน : เม็ดเลือดขาวชราของผู้ป่วยมะเร็งลำไส้ใหญ่. (SENESCENT WHITE BLOOD CELLS IN COLORECTAL CARCINOMA PATIENTS) อ.ที่ปรึกษาหลัก : อภิวัฒน์ มุทิรางกูร, อ.ที่ปรึกษาร่วม : สตีเว็น ดับบลิว เอ็ดเวิร์ด,เจริญชัย พุฒิปัญญาเลิศ

การเกิดมะเร็งลำไส้ (CRC) และอายุที่เพิ่มมากขึ้นส่งผลต่อการเปลี่ยนแปลงของเซลล์ในระบบภูมิคุ้มกัน โดยเฉพาะเกิดการเสื่อมของระบบภูมิคุ้มกัน การศึกษานี้มีวัตถุประสงค์เพื่อตรวจสอบการแสดงออกของตัวบ่งชี้การแก่เซลล์ ($p16^{INK4A}$) ว่ามีการแสดงออกมากขึ้นหรือไม่ในเซลล์เม็ดเลือดขาวของผู้ป่วยมะเร็งลำไส้เมื่อเปรียบเทียบกับกลุ่มควบคุมที่มีสุขภาพดี วัตถุประสงค์อีกประการหนึ่งคือเพื่อศึกษาผลของอายุที่มากขึ้นและมะเร็งลำไส้ต่อการเปลี่ยนแปลงฟีโนไทป์ของทีเซลล์ เอ็นเคเซลล์ และเซลล์เม็ดเลือดขาวชนิดโมโนไซต์ โดยมีกลุ่มตัวอย่างที่ใช้ศึกษาสองกลุ่มคือกลุ่มผู้ป่วยมะเร็งลำไส้เปรียบเทียบกับกลุ่มควบคุมที่สุขภาพดีในช่วงอายุเดียวกัน และกลุ่มคนสูงอายุสุขภาพดีเปรียบเทียบกับกลุ่มควบคุมอายุน้อยสุขภาพดี โดยทำการศึกษาการแสดงออกของยีน $p16^{INK4A}$ ในเซลล์ภูมิคุ้มกันส่วนปลาย (Peripheral immune cells) ด้วยเทคนิค immunofluorescence และการจำแนกรูปแบบทางอิมมูนของเซลล์เม็ดเลือดขาว (immunophenotypes) ด้วย เทคนิค flow cytometry

การศึกษาความสัมพันธ์ระหว่างอายุและข้อมูลทางคลินิก พบว่ามีการแสดงออกของ $p16^{INK4A}$ ที่เพิ่มขึ้นในเซลล์ภูมิคุ้มกันส่วนปลาย ซึ่งเป็นการตรวจสอบที่มีความไว 78% และความจำเพาะ 71% โดยพบว่าเซลล์เม็ดเลือดขาวชนิดลิมโฟไซต์และโมโนไซต์มีระดับของยีน $p16^{INK4A}$ สัดส่วนของเซลล์โมโนไซต์เพิ่มขึ้นควบคู่ไปกับการลดลงของเซลล์ลิมโฟไซต์ ซึ่งบ่งชี้ว่ามะเร็งลำไส้และอายุที่มากขึ้นมีผลต่อการเกิด myeloid skew และยังพบอีกว่า T cells ส่วนใหญ่มีปริมาณลดลงเมื่ออายุมากขึ้น ยกเว้น helper T cells และรูปแบบย้อนกลับพบได้ในผู้ป่วย CRC เซลล์ NK พบว่ามีการขยายตัวในช่วงอายุที่มากขึ้น แต่มีแนวโน้มลดลงในผู้ป่วย CRC รูปแบบของเซลล์ monocytes มีความคล้ายคลึงกันในกลุ่มคนสูงอายุและกลุ่มผู้ป่วย CRC โดย classical monocytes ลดลงในขณะที่ intermediate monocyte และ non-classical monocyte มีจำนวนเพิ่มขึ้น ในส่วนของ T cells และเซลล์ monocytes ที่เพิ่มขึ้นส่วนใหญ่เป็นเซลล์ที่มีลักษณะเหมือนเซลล์แก่ซึ่งส่งผลต่อการกดระบบภูมิคุ้มกันในผู้ป่วย CRC ดังนั้นการแสดงออกของ $p16^{INK4A}$ และ CD^{4+} monocytes สามารถใช้เป็นตัวบ่งชี้การเกิดโรคและ/หรือตัวบ่งชี้การแก่ของเซลล์

สาขาวิชา	ชีวเวชศาสตร์และชีวเทคโนโลยี	ลายมือชื่อนิสิต ....
ปีการศึกษา	2565	ลายมือชื่อ อ.ที่ปรึกษาหลัก ....
		ลายมือชื่อ อ.ที่ปรึกษาร่วม ....
		ลายมือชื่อ อ.ที่ปรึกษาร่วม ....

6278307430 : MAJOR BIOMEDICAL SCIENCES AND BIOTECHNOLOGY
KEYWORD: colorectal cancer/ immuno-senescence/ immunophenotypes/ p16INK4A

Khin Aye Thin : SENESCENT WHITE BLOOD CELLS IN COLORECTAL CARCINOMA PATIENTS. Advisor: Prof. APIWAT MUTIRANGURA, Ph.D. Co-advisor: Prof. Steven W. Edwards,Dr. CHAROENCHAI PUTTIPANYALEARS

Colorectal cancer (CRC) and ageing can contribute to changes in immune cells including immuno-senescence. The objectives of the study were to determine if the senescence marker ($p16^{INK4A}$) was expressed more at higher levels in peripheral white blood cells in CRC compared to age-matched healthy controls. Another aim was to determine the phenotypic changes of T cells, NK cells and monocytes during ageing and CRC in case-control studies. Cases were patients with CRC and controls were matched with cases based on age. Peripheral immune cells were analysed for $p16^{INK4A}$ using immunofluorescence and immunophenotypes were determined with flow cytometry. Correlation studies with age and clinical data were performed. Increased $p16^{INK4A}$ expression in peripheral immune cells had 78% sensitivity and 71% specificity. T lymphocytes and monocytes had increased intensity of $p16^{INK4A}$. The proportion of monocytes increased alongside a reduction of lymphocytes, indicating myeloid skew in CRC and aging. Most T cells subsets decreased during ageing except helper T cells, and the reverse patterns were observed in CRC. NK cells expanded during ageing but showed a decreased trend in CRC. Immunophenotypes in monocytes were similar in ageing and CRC: classical monocytes decreased while intermediate monocytes and non-classical monocytes both increased. Most of the increased T cells and monocytes were senescent-like cells with immunosuppressive phenotypes in CRC. The potential of $p16^{INK4A}$ expression and CD4+ monocytes as disease-related and/or age-related biomarkers is discussed.

Field of Study:	Biomedical Sciences and Biotechnology	Student's Signature ....
Academic Year:	2022	Advisor's Signature ....
		Co-advisor's Signature ....
		Co-advisor's Signature ....

ACKNOWLEDGEMENTS

TABLE OF CONTENTS

Page

List of Tables

List of Figures

CHAPTER I: INTRODUCTION

1.1 Background

CRC is the third most common cancer and second highest leading cause of cancer deaths in the world (Inadomi and Jung, 2020). The incidence of the disease can vary with sex, age and geographical regions and because of lifestyle differences: incidence is higher in males than in females and higher in more-developed regions than less-developed regions (Rawla et al., 2019). It is a heterogeneous disease caused by genetic mutation and epigenetic alterations, but also affected by environmental factors such as the gut microbiome, and lifestyles such as alcohol intake, smoking, red meat consumption and increased body weight (Clinton et al., 2020). Some CRC cases are hereditary, but the majority of CRC patients are of the sporadic type with no family history of the disease (Kuipers et al., 2015).

The major risk factor for CRC is ageing with the majority of sporadic CRC patients greater than 50 years old at the time of diagnosis: 75% of rectal cancer and 80% of colon cancer patients are in their 60s and above (Kuipers et al., 2015). During ageing, there is increased genome-wide hypomethylation and accumulation of temporary DNA modifications such as epigenetic marks, DNA damage or lesions (Mutirangura, 2019). DNA damage and genome-wide hypomethylation leads to genomic instability which is a hallmark of cancer (Meirson et al., 2019; Mutirangura, 2019). In addition, inflammation may be increased during ageing, which is termed "inflamm-aging", and has tumor-promoting effects (Franceschi et al., 2000). Moreover, colonic epithelial proliferation increases in old age (Roncucci et al., 1988) which may increase susceptibility of development of CRC.

One of the hallmarks of cancer is evasion of the immune system (Meirson et al., 2019). Immuno-senescence is defined as the decline in immune function with age and an increased risk of cancers (Lian et al., 2020). One such senescence marker is p16^{INK4A} which is a cell cycle regulator and has been used as a biomarker for chronological, as well as biological, age (Liu et al., 2009; LaPak and Burd, 2014). Although there are several available blood-based biomarkers for CRC, their diagnostic and prognostic values are variable but some of them are useful for monitoring of CRC. For example, carcinoembryonic antigen (CEA) is not specific for CRC, but its level

increases with increased tumor size and decreases after resection of tumor (Hauptman and Glavač, 2017). Colonoscopy is currently the "gold standard" for the diagnosis of CRC (Kuipers et al., 2015).

Ageing and CRC can both cause changes in immunophenotypes. Different phenotypes of immune cells have specific functions in tumor immunology and these immune cell phenotypes can be categorized according to their specific cell surface markers as follows:

Table 1: Immunophenotypes of T lymphocytes, NK cells and monocytes

T lymphocytes	
Helper T cells	CD3+ CD4+ CD8-
Cytotoxic T cells	CD3+ CD4- CD8+
Double negative (DN) T cells	CD3+ CD4- CD8-
Double positive (DP) T cells	CD3+ CD4+ CD8+
Natural killer (NK) T cells	CD3+ CD56+
early-activated (EA) helper T cells	CD3+ CD4+ CD28+ CD57-
senescence-like (SL) helper T cells	CD3+ CD4+ CD28- CD57+
DN helper T cells	CD3+ CD4+ CD28- CD57-
DP helper T cells	CD3+ CD4+ CD28+ CD57+
EA cytotoxic T cells	CD3+ CD8+ CD28+ CD57-
SL cytotoxic T cells	CD3+ CD8+ CD28- CD57+
DN cytotoxic T cells	CD3+ CD8+ CD28- CD57-
DP cytotoxic T cells	CD3+ CD8+ CD28+ CD57+
CD8^{low} T cells	CD3+ CD8+
CD8^{high} T cells	CD3+ CD8++
CD4+ NK T cells	CD3+ CD56+ CD4+ CD8-
CD8+ NK T cells	CD3+ CD56+ CD4- CD8+
DN NK T cells	CD3+ CD56+ CD4- CD8-
HLA-DR-positive T cells	CD3+ HLA-DR+
HLA-DR-negative T cells	CD3+ HLA-DR-

NK cells		
	NK^{bright}	CD3- CD56++
		CD3- CD56^{bright} CD16-
		CD3- CD56^{bright} CD16+
	NK^{dim}	CD3- CD56+
		CD3- CD56^{dim} CD16-
		CD3- CD56^{dim} CD16+
	CD4+ NK	CD3- CD56+ CD4+ CD8-
	CD8+ NK	CD3- CD56+ CD4- CD8+
	DN NK	CD3- CD56+ CD4- CD8-
Monocytes		
	classical monocytes	CD14++ CD16-
	intermediate monocytes	CD14++ CD16+
	non-classical monocytes	CD14+ CD16+
	CD4+ monocytes	CD14+ CD4+
	CD56+ monocytes	CD14+ CD56+
	HLA-DR^{low} monocytes	CD14+ HLA-DR+
	HLA-DR^{high} monocytes	CD14+ HLA-DR++

1.2 Colorectal Carcinoma (CRC)

Approximately 5-10 % of all CRC cases are hereditary and the most common hereditary form is Lynch syndrome, which is associated with mutations in DNA mismatch-repair genes (Vasen et al., 2015). Another type of hereditary CRC is familial adenomatous polyposis, which has mutations in the adenomatous polyposis coli (*APC*) gene that is involved in WNT signaling (Vasen et al., 2015). The risk of CRC occurrence increases if a first degree relative has CRC and it will be increased if there is more than one CRC case in the family history. Therefore, people with family history of CRC are recommended for CRC screening every 5 years after the age of 40y (Wilkinson et al., 2019).

The majority of CRC patients have sporadic type of diseases with no family history of CRC. In many of these sporadic cases, genomic instabilities have been

reported and arise from 3 fundamental processes: chromosomal instability (CIN), microsatellite instability (MSI) and serrated neoplasia (Nguyen et al., 2019). CIN accounts for 65-70% of all sporadic CRC and is characterized by loss of chromosomal heterozygosity, that leads to activation of proto-oncogenes (eg; *KRAS*) and inactivation of tumor suppressor genes (eg; *APC*, *TP53*) by genetic and epigenetic processes (Kuipers et al., 2015). About 15% of sporadic CRC patients have MSI which has a high frequency of genomic copy number alterations and mutations in DNA mismatch repair genes (Kuipers et al., 2015). The serrated neoplasia pathway is associated with *BRAF* mutations together with MSI or *TP53* mutations (Nguyen et al., 2019). In addition, an epigenetic form of genomic instability, CpG island methylator phenotype (CIMP), can be seen together with these other processes (Kuipers et al., 2015).

The incidence of CRC is increasing especially in developing regions, which may be explained by environmental factors such as smoking, alcohol intake, increased body weight and red/processed meat consumption; these expose the colonic environment to chemical damage and chronic inflammation. Moreover, dysbiosis of the intestinal microbiome may also contribute to the development of CRC, as the healthy intestinal microbiota protects against pathogenic microorganisms and maintains physiological functions (Zhang et al., 2019; Cheng et al., 2020). Contrarily, a decreased risk of CRC is associated with healthy lifestyles, such as daily physical activities and daily intake of fiber/calcium/milk which reduce inflammation and maintain intestinal cell function. Low dose aspirin can prevent the occurrence and spread of CRC through its proapoptotic effects and control of platelet action in metastasis (Algra and Rothwell, 2012; Zhang et al., 2019).

1.2.1 Immune Response in CRC

Outer mucus layer
Inner mucus layer
Colonic epithelium
Lamina Propria
Intestinal crypt
Masularis mucosa
Lymphoid follicle
Submucosa
Blood vessel

DC
T cell
Treg
B cell
NK cell

Neutrophil
Macrophage
Eosinophil
Mast cell
Monocyte

Stem cell
Paneth cell
Goblet cell
Colonic epithelial cell
Phage
Bacteria
Mesenchymal cell
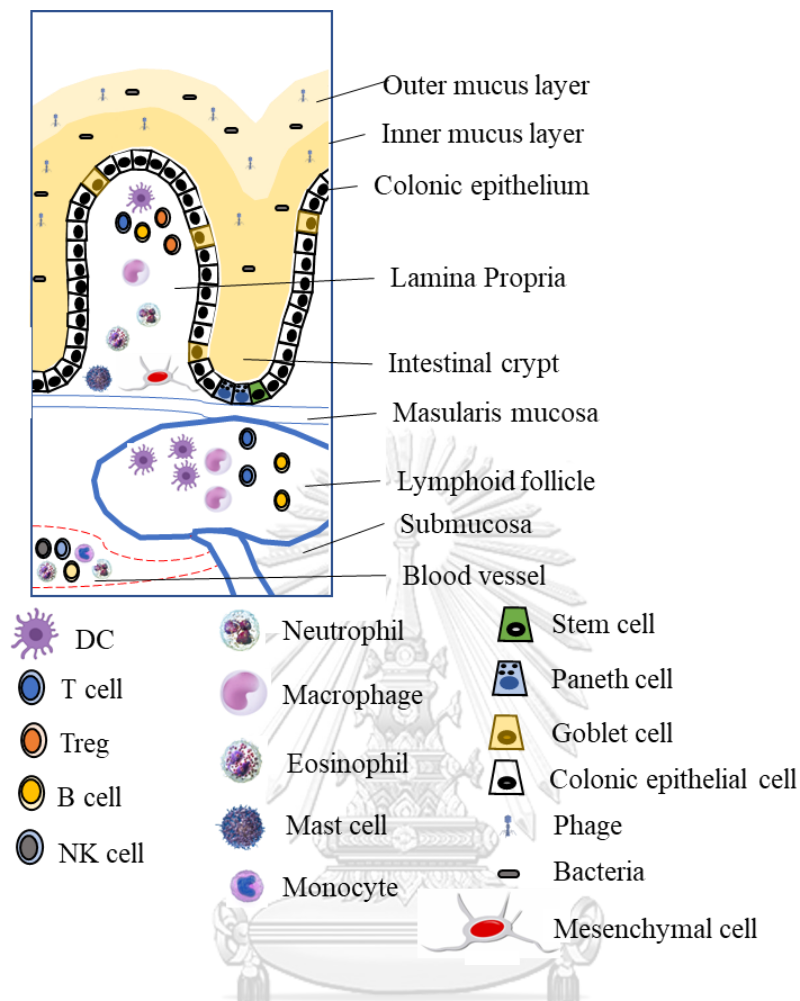
Figure 1: *Schematic representation of colonic microenvironment with predominant immune cells*
(Sipos et al., 2010; Qv et al., 2021)

The immune response is important in both the development and progression of CRC. As shown in Figure 1, the colonic environment contains different types of cells such as epithelial cells, the colonic mucosa, innate and adaptive immune cells which all contribute to maintain the normal gut physiology and the immune response of CRC. The symbiotic microbiome can maintain the gut physiology by breaking down possible toxic substances, synthesizing particular vitamins and amino acids, modulating metabolites and stimulating the immune cells (den Besten et al., 2013; Qv et al., 2021). Although the immune response may inhibit cancer growth, it can also stimulate cancer

growth and metastasis, as a consequence of tumor-associated inflammation (Grizzi et al., 2013).

Chronic inflammation of the gut mucosa is one of the causes of adenoma to carcinoma changes in CRC (Cheng et al., 2020). Healthy intestinal mucosa is maintained by the gut microbiome, which consists of 10^{13} to 10^{14} microbes, about 10 times greater than the number of human cells (Gill et al., 2006). Intestinal microbiota are important for acquiring energy, maintaining immunity and the integrity of the intestinal epithelium through the synthesis of short chain fatty acids (Natividad and Verdu, 2013). Dysbiosis of microbiota can disrupt the physiological function of the gut (Cheng et al., 2020). For example, when some microbes invade colonic epithelial cells, inflammatory cytokines such as TNF-α, IL-8 and IL-6 are released as a consequence of the immune response (Ohkusa et al., 2009). In CRC, if the intestinal microbiome has changed then it can favor disease progression; one possible mechanism is that microbial products affect the extent of immune response and inflammation (Formica et al., 2014).

The tumor microenvironment (TME) is important for immune responses. It contains mesenchymal cells, endothelial cells, infiltrating immune cells, extracellular matrix (ECM) and inflammatory mediators, and can contribute to local inflammation, systemic inflammation, and metastasis (Lin et al., 2020; Kasprzak, 2021). The TME of CRC is infiltrated by diverse immune cells: these include natural killer (NK) cells, which provide immediate responses to tumor cells; macrophages, dendritic cells (DC) and mast cells (MC), which recognize and present tumor antigens to T lymphocytes; CD8^{+} cytotoxic T cells which can have antitumor efficacy by killing tumor cells; CD4 T cells, which also enhance the antitumor immune response via secretion of regulatory cytokines; B lymphocytes, which have a role in suppression of tumor progression by producing tumor-specific antibodies in association with helper T cells (Xiong et al., 2019). However, the immune cells can be re-programmed by tumor cells to create an immunosuppressive TME which includes T regulatory cells (Treg), tumor-associated macrophages (TAM), myeloid-derived suppressor cells (MDSC), cancer-associated fibroblasts, MCs, and a group of newly identified bone marrow myeloid cells (Zhang et al., 2020b).

Moreover, the TME can support the generation of a niche which maintains the function of intestinal epithelial stem cells (IECS) (Lin et al., 2020), which are located at the crypt together with colonic epithelial cells (Figure 1). The mesenchymal cells around the niche generate Wnt protein signals to stimulate the epithelial cells to divide. Then, IESC transform into transit amplifying cells and proliferation occurs along the crypt axis. Alterations in stem cells and niche function can thus promote neoplasia (Seidelin, 2004; Ong et al., 2014).

Excessive and unresolved innate immune responses can also lead to tumorigenesis and metastasis (Formica et al., 2014). Inflammatory cells of the innate immune system are active in the epithelium as well as in the lamina propria, and MDSCs create a TME that is permissive for tumor growth (Formica et al., 2014). These MDSCs can further differentiate into TAM which can trigger metastasis by secretion of growth factors such as epidermal growth factors, TGF-β, vascular endothelial growth factor (VEGF), and several proteolytic enzymes including matrix metalloproteinases that are responsible for degradation of ECM proteins (Pancione et al., 2014). Short-lived innate immune cells such as DC and tumor-associated neutrophils (TAN) also play key roles in tumor progression: for example, TAN can synthesize TNF, hepatocyte growth factor and VEGF (Pancione et al., 2014). Inflammatory monocytes are highly infiltrative and differentiate into inflammatory macrophages that can contribute to local and systemic inflammation by producing inflammatory cytokines such as TNFα and IL-6 (Yang et al., 2014).

Crosstalk between cancer cells and their milieu can cause local as well as systemic changes. For example, in the serum of CRC patients, levels of IL-4, IL-6, IL-8, IL-10, IL-17A, IL-22, IL-23, IFNγ, TGFβ, TNF and VEGF are increased (Mager et al., 2016). These elevated levels of cytokines may be linked to immune dysfunction (Xia et al., 2016) as proinflammatory cytokines such as TNFα, IFNγ, IFNβ, IL-6 and IL-8 can induce cellular senescence. TNFα, IFNγ and IFNβ can also trigger epithelial cell senescence by producing reactive oxygen species through the ATM/p53/p21 pathway (Xia et al., 2016). They can also increase the level of p16^{INK4A} (Brenner et al., 2020; Wang et al., 2020). IL-6 and IL-8 can be released following DNA damage through the NF-kB signaling pathway (Xia et al., 2016), while IL-4 is involved in cell

cycle arrest at the G1 phase by increasing p21 protein levels (Kim et al., 2013). IL-10 and IL-22 can cause hepatic stellate cell senescence through the p53 pathway (Kong et al., 2012; Huang et al., 2020) and IL17 can generate cellular senescence in osteoarthritis (Faust et al., 2020). TGFβ is involved in cellular senescence by increasing the levels of p16^{INK4A} in bone marrow-derived MSCs (Tominaga and Suzuki, 2019). However, IL-23 can inhibit cellular senescence in castration-resistant prostate cancer cell lines (Gupta et al., 2020) and VEGF delays cellular senescence in human endothelial cells (Hasan et al., 2011). These potential roles of anti-inflammatory and pro-inflammatory cytokines in CRC and senescence are shown in **Fig 2**.
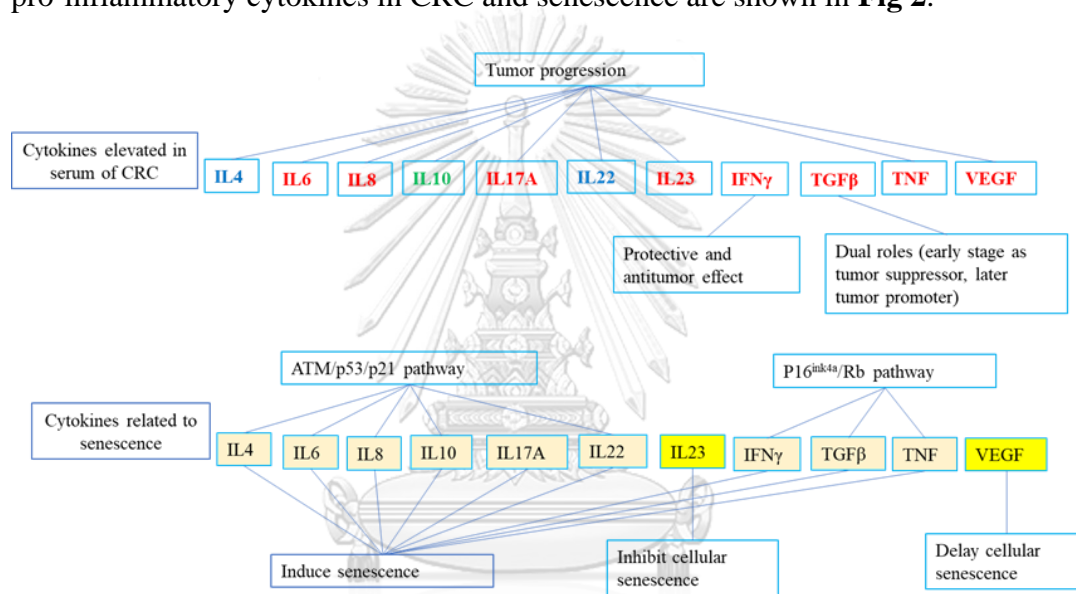
Figure 2: *Anti-inflammatory and pro-inflammatory cytokines that relate to CRC and senescence.*
Cytokines in green mostly relate to anti-inflammation, red to pro-inflammation and blue to both anti-inflammation and pro-inflammation.

There is also evidence that the colon stroma is surrounded by senescent stromal cells in advanced colon cancer (Guo et al., 2019). On the other hand, immune cell function can be altered by secretion of factors by cancer cells. For example, STAU2 expression is increased in lymphocytes after incubation with breast cancer cell lines and higher intragenic MMP9 methylation was found in WBCs after incubation with colon cancer cell lines (Boonsongserm et al., 2019; Puttipanyalears et al., 2021). This, at least *in vitro*, cancer cells can induce changes in the functions of immune cells.

Tumor development can result in changes in immune cells. For example, malignant transformation of cells and low-grade systemic inflammation can elevate cytokines in serum, including KITLG, G-CSF, GM-CSF, and M-CSF, that are involved in controlling hematopoiesis (Kiss et al., 2020). Hamm *et al* (2016) analyzed the transcriptional profiles of monocytes in CRC patients and showed that changes of monocytes occurred in early as well as disseminated stages of CRC, compared to healthy controls. After surgical removal of the tumor, previously upregulated genes of monocytes in CRC patients returned to levels comparable to those of healthy individuals (Hamm et al., 2016). Therefore, the tumor can induce systemic changes in immune cells, and after removal of the tumor, these changes in the immune cells are reprogrammed back to homeostasis.

Local immune cell infiltrates into tumors are often associated with genetic instability of CRC (MSI and CIN), but this can have a positive effect on outcomes. The interplay between antitumor immune responses and genetic instability of CRC is mediated by CD8+ T cells (Pancione et al., 2014). The degree of CD8+ T cell infiltration into tumors associates with the prognosis of CRC: a higher degree of infiltration was seen in MSI-H (microsatellite instability high) CRCs (Prall et al., 2004). MSI-H CRCs are more immunogenic than CIN CRCs and have better prognosis because they exhibit strong local immune reactions and heavy infiltration of tumor infiltrating lymphocytes, leading to better clinical outcomes (Pancione et al., 2014). CIN CRC have reduced numbers of cytotoxic T cells but increased numbers of intratumoral Treg cells, which attract immunosuppressive cells and can lead to tumor progression (Pancione et al., 2014).

1.2.2 Blood-Based Biomarkers in CRC

Biomarkers are "biological molecules found in blood, other body fluids, or tissues that are a sign of a normal or an abnormal process, or of a condition or disease", as defined by the National Cancer Institute (Henry and Hayes, 2012). The ideal biomarker should distinguish between cancers and advanced adenoma from other lesions, and be absent or at very low levels after the cancer is treated or removed (Kuipers et al., 2015). Proteins, DNA, RNA and metabolites from tissue, blood, stool

and urine have been used in CRC for screening, diagnosis and monitoring, but have varying degrees of success as effective biomarkers (Loktionov, 2020).

Protein biomarkers in blood have been used for CRC diagnosis and monitoring. For the detection of CRC in blood samples, the most promising biomarkers are CA11-19 marker protein (Sensitivity 98%, Specificity 84%), cysteine-rich 6 protein of the CCN family (Cyr 61) (Sensitivity 83%, Specificity 97%), trefoil factor 3 (TFF3) (Sensitivity 74.20%, Specificity 94.80%) and combined measurements of lectins DCSIGN and DC-SIGNR (Sensitivity 98.70%, Specificity 94.80%) (Loktionov, 2020). Carcinoembryonic antigen (CEA) and CA19-9 antigen can be used as biomarkers for prognosis, treatment response and recurrence (Hauptman and Glavač, 2017). CEA is a commonly used blood-based marker for monitoring because its levels decline after tumor resection and combined use of CEA and tissue polypeptide antigen is more sensitive for detection of CRC recurrence (Hauptman and Glavač, 2017).

Measurements of genetic markers in the blood of CRC patients are relatively unsatisfactory and inconsistent. For example, assays detecting mutations and methylation of genes such as BMP3, NDGR4, septin 9 (SEPT9), SFRP2, SPG20, TFPI2 and vimentin (VIM) have sensitivities between 50% and 92% and specificities between 80% and 100% (Loktionov, 2020). The popular marker miR-21 has generated conflicting results while the downregulated miR-139-3p has high diagnostic sensitivity (96.6%) and specificity (97.8%) (Ng et al., 2017). Generally, assays using a panel of genetic markers results in improved sensitivity and specificity. For example, assays measuring downregulated miR-144-3p, miR-425-5p and miR-1260b, miR-335 and miR-18a, and upregulated miR-19a, miR-19b, miR-15b, miR-29a can give over 90% sensitivity and specificity (Loktionov, 2020). Quantification of cfDNA can also be used for monitoring of CRC, but levels are influenced by the other conditions such as inflammatory- and autoimmune-diseases (Hauptman and Glavač, 2017).

Assays for detection of metabolites in serum have high cost and complexity issues. For example, although some studies have shown >90% sensitivity and specificity, there are several technical issues to overcome, as some metabolites are volatile metabolic compounds (VOCs), and most studies have used various types of mass spectrometry for detection of non-VOCs. Although mass spectrometry can be

considered as the technical gold standard, it has high cost, complex techniques and requires sophisticated equipment and specialized operators: hence, it is not feasible for large screening purposes in centres that do not have such facilities (Loktionov, 2020).

The immunological profile of the patient is important for outcomes in cancer, as immune cell subsets are associated with prognosis of many diseases (Nixon et al., 2019). For example, PD1 expressed on peripheral lymphocytes is associated with poor patient outcome in renal cell carcinoma (MacFarlane et al., 2014) and higher tumor burden in melanoma (Dronca et al., 2015). Immune-based markers may also be useful for monitoring the success of treatment responses. For example, peripheral immune cells have been used as a biomarker for cancer immunotherapy: patients with high expression of PD1 on CD4+ and natural NK cells in advanced stages of cancer respond better to therapy and have better outcomes (Du et al., 2018). Increased STAU2 protein expression in WBCs can be used as a novel breast cancer marker (Puttipanyalears et al., 2021).

1.3 Ageing, CRC and the immune system

Factors that alter immune cells' function
- Changes of organs
- Genomic instabilities
- Changes in immune cells
- Changes in cytokines and complement profiles
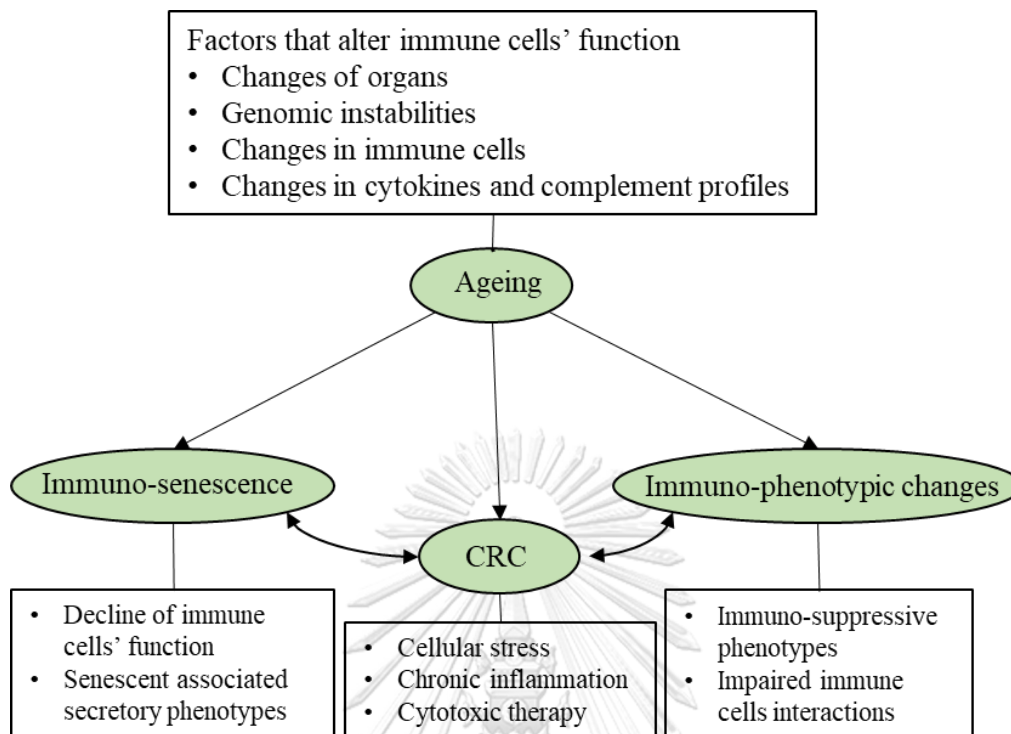
Figure 3: Possible relationships of Ageing to CRC and decline in immune function

Ageing can adversely affect the hematopoietic organs that can impair immune cell numbers and function. For example, bone marrow cellularity declines with age: hematopoietic tissue is approximately 90% at birth, 50% by the age of around 50 year and declines to around 30% at the age of 70 and above (Ricci et al., 1990). Changes can also occur in the thymus, the T cell development site, throughout life. Thymic involution starts in the early years of life as the total body mass increases and this progressively occurs up to around 45 years of age and declines for the rest of life (Mamatha et al., 2009). During ageing, disturbances in the organization of lymph nodes and nodal zones can compromise intercellular interactions (Cakala-Jakimowicz et al., 2021).

One of the hallmarks of ageing is genomic instability, which could result from mutations of the hypomethylated genome in response to accumulated DNA damage (Mutirangura, 2019). On the other hand, DNA damage can trigger innate immune responses, followed by adaptive immune responses. Consequently, unrepaired DNA

damage responses can lead to inflammation (Pilger et al., 2021) and such DNA-damage driven chronic inflammation can promote cancer development (Chatzinikolaou et al., 2014).

The numbers and functions of both adaptive and innate immune cells change in ageing. A myeloid skew (increased myeloid cells: lymphocytes ratio) can result from progenitor niche changes, which favor myeloid gene expression in progenitor cells (Sun et al., 2012). NK cell expansion especially of NK^{dim} cells could be connected to the accumulation of long-lived NK cells during ageing (Sun et al., 2011) while decreases in naïve T cell production can occur after 50 y of age, and TCR diversity (number of unique TCR sequences in a T cell population) of naïve T cells reduced 2 to 5 times in those aged 60 and above compared to young adults (Zhang et al., 2021a). Loss of B cell precursors, together with an increased number of age-associated B cells is also observed during ageing (de Mol et al., 2021). Aged monocytes are hyperactivated with higher expression of co-inhibitory molecules (Cao et al., 2022). Moreover, collaborative functions among immune cells also declines with age. For example, lower numbers of TCR on CD8+ T cells plus higher number of NK cells result in poor resistance to solid tumors (Shanker et al., 2010). In addition, decline in helper function of CD4+ T cells can contribute to defects in humoral responses of B cells (Eaton et al., 2004).

Inflamm-aging is chronic, sterile, low-grade inflammation that occurs during ageing and can result from chronic physiological stimulation of innate immune cells (Franceschi et al., 2018). Proinflammatory cytokines such as TNF, IL-1, IL-6 and IL-8 and complement C3 and C4 are often increased during unhealthy ageing (Franceschi et al., 2018; Zheng et al., 2022).

Immuno-senescence refers to a functional decline of the immune system during ageing and affects both innate and adaptive arms of the immune system. The proliferative capacity of adaptive cells and phagocytotic capacity of innate cells can decrease and these contribute to increased susceptibility to infections and occurrence of cancers. Moreover, senescence-associated secretory phenotype (SASP) is associated with inflamm-aging (Maijó et al., 2014).

CRC is a heterogeneous disease with chromosomal instabilities such as genetic mutations, epigenetic alterations and environmental factors which are all involved in pathogenesis (Holt et al., 2009). Moreover, colonic epithelial proliferation increases during ageing (Roncucci et al., 1988) and cumulative molecular and pathophysiological changes in the homeostasis of colonic epithelial cells throughout life can lead to neoplasia in the elderly (Holt et al., 2009).

1.4 Immuno-senescence

Immuno-senescence is a state of declining immune functions that can result in decreased regenerative capacity, vaccine inefficacy and increased risk of diseases. It is also an age-dependent behavior of immune functions found in older individuals and associated with detrimental clinical outcomes (Maijó et al., 2014; Stahl and Brown, 2015; Pawelec, 2018; Aiello et al., 2019). Ageing contributes to immuno-senescence and one of the contributing factors is changes in the organs of the immune system, such as thymic involution and decreased hematopoiesis, which leads to decreased numbers of naïve T cells and B cells. Another factor is the prolonged exposure and recognition of various antigens throughout lifetime, that can result in oligoclonal expansion and accumulation of memory cells (Salam et al., 2013b). Other important hallmark of immuno-senescence is inflamm-aging (Aiello et al., 2019) which is a low-grade chronic inflammation due to the accumulation of molecular damage that contributes to loss of proteostasis, genomic instability and altered cell signaling (Teissier et al., 2022). Immuno-senescence affects both innate and adaptive immunity (Maijó et al., 2014), and results in an increased risk of cancer (Pawelec, 2017).

1.4.1 T cells

During ageing, the number of naïve T cells decreases, while memory T cells increase (Abbas et al., 2022). Senescent T cells have a loss of proliferative capacity, but are highly inflammatory cells secreting cytotoxic mediators such as TNF and IL-1β (Covre et al., 2020). They have erosions in their telomeres and accumulation of DNA damage (Xu et al., 2020). Typical phenotypic changes of senescent T cells are downregulation of the co-stimulatory molecules CD27 and CD28 and decreased expression of the effector molecule perforin and granzyme B, resulting in suppressed immunity within the tumor microenvironment (Zhao et al., 2020). Other changes

include elevated expression of senescence-associated-β-galactosidase, CD57, killer cell lectin-like receptor subfamily G member 1 (KLRG-1), Tim-3, CD45RA and cell cycle regulators (p16^{INK4A}, p21, and p53) (Zhao et al., 2020). They can produce proinflammatory cytokines (IL-2, IL-6, IL-8, TNF, and IFN-γ) and the suppressive cytokines (IL-10 and TGF-β) (Zhao et al., 2020).

Senescence-Like (SL) cytotoxic T cells (CD3+ CD8+ CD28- CD57+) are considered as senescent and terminally differentiated cells as they have shortened telomeres with low telomerase activity (Vallejo, 2005). However, they can proliferate under specific stimulation of cytokines such as IL-2, IL-15 by transient up-regulation of telomerase activity. Production of the immunomodulatory cytokine IFN-γ and the pro-inflammatory cytokine TNF-α is more prominent in SL cytotoxic T cells than in Early-Activated (EA) cytotoxic T cells (CD3+ CD8+ CD28+ CD57-) (Strioga et al., 2011).

1.4.2 NK cells

Immuno-senescence of NK cells impairs their defense functions, such as induction of adaptive immune responses, elimination of senescent cells and resolution of inflammation, which can lead to cancer induction (Gounder et al., 2018b). In ageing, the number of total NK cells increases, and the majority are CD56^{dim}, but their proliferation capacity decreases. CD56^{dim} cells have decreased migration activity which is responsible for defects in the mechanisms of NK cell-mediated cytolysis (Gounder et al., 2018b).

1.4.3 B cells

Reduction in the number of B cells, as well as changes in the B cell repertoire, also occur during ageing. Naive B cells, which are important for responses to new antigen, are decreased in the elderly (Buffa et al., 2011). In contrast, late memory B cells (IgD−/CD27−, CD95^{high},CD21^{low}, high T-bet and CD11c+) are increased in number in the elderly and they can secrete proinflammatory cytokines (Frasca, 2018). They have highest levels of the SASP marker amongst memory B cells (Frasca, 2018). During physiological ageing, age-associated B cells (ABCs) accumulate in the peripheral blood and they can enhance innate immune responses with low affinity antibodies and increased inflammatory processes (Ma et al., 2019).

1.4.4 Monocytes

Immuno-senescence is also associated with inflamm-aging and macroph-aging (senescence-associated macrophages). Macrophages are crucial cells in induction and maintenance of inflamm-aging as they increase in numbers in tissue in ageing and they are responsible for senescence bystander effects, such as accumulation of senescent cells and chronic low grade inflammation (Franceschi et al., 2000; Prattichizzo et al., 2016). Circulating monocyte subsets can be classified into three types: classical, intermediate and non-classical monocytes (Ziegler-Heitbrock et al., 2010). Non-classical monocytes (CD14^{low}/ CD16+) are pro-inflammatory and associated with senescence, and these cells secrete TNF-α, IL-6, IL-8, IL-1β, CCL3, CCL4 and CCL5 (Ong et al., 2018), but have reduced phagocytic activity (Yang et al., 2014).

1.4.5 DCs

DCs are responsible for age-associated chronic inflammation, loss of immune tolerance and decline in adaptive immune responses (Agrawal et al., 2017). In ageing, secretion of anti-inflammatory and immune-regulatory cytokines decreases, but secretion of pro-inflammatory cytokines by DCs increases. The number of plasmacytoid DCs and CD141+ myeloid DCs is decreased in the circulation of the elderly (Agrawal et al., 2017).

1.4.6 Granulocytes

Neutrophils are the major population of immune cells in the circulation. They are short-lived cells (half-life 12-18 h) (Butcher et al., 2000) and in the elderly, neutrophil numbers do not decrease and their migratory responses are unaltered (MacGregor and Shalit, 1990) or slightly reduced (McLaughlin et al., 1986). However, their phagocytic activity and proliferative responses of neutrophil precursor cells decline with age (Butcher et al., 2000) and their proinflammatory activity in the circulation correlates with age. Decreased phagocytic functions of neutrophils leads to apoptosis at the site of infection which can enhance inflammation (Zhang et al., 2015). Eosinophils also have decreased effector functions in ageing, especially in degranulation (Mathur et al., 2008).

1.5 Factors affecting immuno-senescence

Immuno-senescence is multifactorial and can be affected by: unmodifiable factors like sex and genetics; modifiable factors such as lifestyles and diet patterns; and pathological factors, such as persistent stressors of immune responses and immunological- and infection-history (Aiello et al., 2019).

Particular lifestyles and diet patterns can induce immuno-senescence via inflamm-aging (Aiello et al., 2019). For example, smoking can be considered as enhancing immuno-senescence because oxidative stress associated with smoking can accelerate age-related inflammation, and serum antioxidant levels are decreased in chronic smokers (Nicita-Mauro et al., 2008). Healthy diets, such as those rich in fruits, vegetables, whole grains, legumes, and olive oil have anti-inflammatory and anti-oxidant properties (Aiello et al., 2019).

Age is an important factor for the development of immuno-senescence. In ageing, the production of immune cells declines as the immune system organs change, for example by involution of the thymus and decreased cellularity of bone marrow, as well as reduction of T cell diversity to new antigens (Weiskopf et al., 2009; Joseph et al., 2022). Moreover, elevated complement levels (e.g. C3 and C4) occur in ageing which can serve as immunomodulatory elements and represent accumulation of harmful substances in the body, which in turn relate to inflammation and metabolism (Zheng et al., 2022). Immuno-senescence is initiated earlier in men than in women, likely due to hormonal differences between males and females, as estrogen enhances immune responses, while progesterone and androgens favor immune suppressive actions (Ostan et al., 2016). Genetic and epigenetic mechanisms can also be involved in immuno-senescence and it was shown that centenarians can efficiently regulate the release of inflammatory mediators, and their genomes are epigenetically more stable (Ostan et al., 2008).

Immuno-senescence can result from various external stressors such as obesity, sleep deprivation, gut dysbiosis, stress, dysregulation of immune cells, chronic infections and accumulation of SASP cells (Xu et al., 2020). Defects in ability to cope with a variety of stressors leads to a pro-inflammatory status (Franceschi et al., 2000) and cancers can cause biological and psychological stressors in the immune system.

Oxidative stress, cellular and DNA damage, chronic inflammation and cytotoxic therapy can also lead to premature ageing of the immune system (De Padova et al., 2021).

1.6 Immunophenotypes and their roles in immune response and cancer

1.6.1 T cells

Cells of the T cell lineage are characterised by expression of the CD3 protein complex. Different types of T cells can have different CD3 membrane density (El Hentati et al., 2010; Valle et al., 2015) and CD3 expression can influence their response to activation: cells with higher CD3 expression require higher activation levels (El Hentati et al., 2010). This also correlates with anti-CD3-mediated immune re-setting levels (Valle et al., 2015).

T cell progenitors arise in the bone marrow or fetal liver, and maturation of T cells occurs in the thymus. The earliest thymic progenitors become CD4-negative and CD8-negative (DN) thymocytes through Notch signaling (Sambandam et al., 2005), and then become CD4-positive CD8-positive (DP) thymocytes through pre-TCR signaling (von Boehmer and Fehling, 1997). The T cell lineage protein CD3 complex is synthesized in the cytoplasm of prothymocytes, and in the later stage of maturation, cytoplasmic expression is lost and transmembrane CD3 is expressed (2016). DP thymocytes showing intermediate avidity to self-pMHC survive as CD4+ T or CD8+ T cells. Naïve T cells patrol in the circulation and secondary lymphoid organs and activation can occur during the immune response through TCR and co-stimulatory signals such as CD28 signaling and inducible co-stimulator (ICOS) signaling. This process can be inhibited by the signals of cytotoxic T-lymphocyte associated antigen-4 (CTLA-4) and programmed death-1. After activation, T cells proliferate and expand into effector populations. In the contraction phase of immune response, more than 90% of effector cells die and a small number of cells become memory cells (Salam et al., 2013a).

T cells are important for cell-mediated immunity. They activate phagocytes by secreting cytokines, protecting the body against pathogens and assist to eliminate tumor cells. T cells can be classified into two major types: Helper T and cytotoxic T cells (Abbas et al., 2022).

1.6.2 Helper T cells

Helper T cells are characterised by the expression of CD4, which is responsible for interacting with MHC class II molecules on the antigen presenting cells (APC) when they interact with the TCR. The expression of CD4 during TCR interactions can enhance the antigen sensitivity of T cells and reduce the number of required antigenic peptides on the APC (Glatzová and Cebecauer, 2019). Helper T cells are important for adaptive immune responses and perform their effector functions through secreted cytokines (Abbas et al., 2022). In an immune response, a naïve helper T cell is activated in the peripheral lymphoid tissue by APCs such as macrophages to become effector cells. They differentiate into different types of subclasses and activate the other immune cells, then their numbers increased by mean of positive feedback loop (Zhu, 2018). For example, the subclass Th1 cells can produce IFN-γ, IL2, TNF and lymphotoxin. They enhance the phagocytic activity of macrophages, and IgG1 and IgG3 class-switching of B cells. Th2 cells secrete IL-4, IL-5, IL-6 and IL-10. Their response is mediated by mast cells and eosinophils, and they activate IgG4 and IgE class switching of B cells. The Th17 subclass produce IL-6, IL-17, TNF and granulocyte macrophage–colony-stimulating factor. They are responsible for cell-mediated inflammation by activation of local endothelial cells and enhancing the infiltration of neutrophils (Eagar and Miller, 2023). Helper T cells can promote naïve CD8+ T cell activation by secretion of cytokines and regulating APC that presents antigen on their MHC-II molecules (Abbas et al., 2022). They can also stimulate inflammatory responses by secreting cytokines to recruit monocytes and neutrophils (Zhu, 2018). In tumor immunity, they support the anti-tumor cytotoxic T cells and can also kill the autologous cancer cells in an MHC-II dependent fashion (Oh et al., 2020).

Based on the expression of CD28 and CD57, helper T cells can be grouped into four types: early activated cells (EA) (CD28+, CD57-); senescence-like cells (SL) (CD28- CD57+); double positive cells (DP) (CD28+ CD57+); and double negative cells (DN) (CD28- CD57-). Elderly people have increased number of highly differentiated and memory cells such as CD28- T cells (Moro-García et al., 2013). CD4+ CD28- cells can also secrete INF-γ and perforin and have cytolytic function. These cells can be found in autoimmune diseases and their numbers increase after recovery from CMV

infection (van Leeuwen et al., 2004). In contrast, CD57 expression on CD4+ T cells correlates with the expression of cytoplasmic granules, granzyme B and perforin, and CD4+/CD57+ cells can be found in chronic HIV infection (Phetsouphanh et al., 2019). CD4+ T cells with cytotoxic function can expand in solid tumors such as lung cancer, colorectal cancer, hepatocellular carcinoma, breast cancer, head and neck cancer, osteosarcoma and malignant melanoma (Cenerenti et al., 2022).

1.6.3 Cytotoxic T cells

T lymphocytes expressing CD8+ have cytotoxic granules and can proliferate and differentiate into cytotoxic T cells. Naïve CD8 T cells are activated by antigen presented with MHC class I molecules on antigen presenting cells. Their cytotoxic functions are important for eradication of intracellular microorganisms and tumors. They produce interferon-γ (IFN-γ) which can activate macrophages to destroy the ingested microorganisms and also promote immune defense against many cancers (Abbas et al., 2022).

These cells can be classified into four groups according to their expression of CD28 and CD57 (EA, SL, DN, DP). DP and SL cells have the shortest telomeres therefore, they are considered they have undergone the highest number of divisions. CD8+ CD57- cells have undergone fewer cell divisions compared to CD8+ CD57+ cells and so CD57 can be used as a replicative senescence marker. CD8+ CD28- cells are absent in cord blood and neonatal blood and they expand throughout life with loss of CD28 assumed to be the consequence of chronic antigenic stimulation. Based on these facts, CD8+ CD28- CD57- cells are considered markers towards terminal differentiation, and cells gain CD57 expression later. Numbers of late differentiation SL cells increased in patients with solid tumors as well as in other diseases such as chronic viral infection and tuberculosis, or bone marrow transplantation and chronic alcoholism (Strioga et al., 2011). These cells may have an active immune response against tumors because they highly express perforin (Casado et al., 2005).

Subsets of CD8 cells have varying levels of expression of this receptor. Low CD8 expressing cytotoxic cells can be found in peripheral blood, and they have effector/cytotoxic functions. However, most show lower expression of CD28, CD62L and CD45RO, and higher expression of CD25, CD45RA, and CD95L. They may result

from immune responses because they have specific TCR variable beta regions, such as Vβ9, Vβ14 and Vβ23 expression (Trautmann et al., 2003). In contrast, CD8 expression relates to the immune response, as increased CD8 expression can be found in COVID-19 infections (Ganji et al., 2020).

1.6.4 NK T cells

A subset of immune cells in the peripheral blood show characteristics of both innate and adaptive immunity. They are termed NK T cells having both the TCR and CD56 (neural cell adhesion molecule) and they can crosstalk with innate as well as adaptive immune cells. They are potent stimulators of DC functions (Wu and Van Kaer, 2011) and their proliferative capacity decreases in ageing (Papadogianni et al., 2020). Based on the TCR rearrangement and glycolipid reactivity, there are two categories of these cells: NK T I (invariant NK T) and NK T II. Generally, NK T I has an anti-tumor role while NK T II has a pro-tumor role. NK T I has anti-tumor immunity by means of direct lysis of tumor cells as well as recruitment cytotoxic immune cells and inhibition of suppressive cells. They also promote tumor-targeted immune memory and cause downstream immune activity upon glycolipid antigen stimulation (Nelson et al., 2021). NK T II cells regulate NK T I cells in the tumor microenvironment, and their activation relates to tumor progression (Nelson et al., 2021). However, chronic stimulation of NK T cells can lead to anergy, and immune escape in cancer patients (Krijgsman et al., 2018).

Human NK T cells can express CD4 or CD8 and therefore, 3 types of cells can be classified: CD4+ NK T; CD8+ NK T; and DN NK T cells. CD4+ NK T cells are required for the generation of cytotoxic CD8+ Treg (Nakamura et al., 2003), which can suppress autoimmunity and regulate the immune response by killing activated CD4+ T cells and follicular T cells (Mishra et al., 2021). CD8+ NK T cells can regulate the immune response in an antigen-specific manner by killing the antigen-presenting DCs (Wang et al., 2015). The origin of DN NK T cells may be different from other NK T cells as they may derive from DN thymocytes due to the fact that DN thymocytes have highest expression of the NK cell lineage marker CD56 (Hu et al., 2019). They have T_H1-like functions as they can produce an effective pro-inflammatory immune cascade through their secreted cytokines (Krijgsman et al., 2018).

1.6.5 DN T cells

These cells are CD3 positive and express TCR (either TCRαβ or TCRγδ), but are negative for the co-receptors CD4 and CD8 (Wu et al., 2022). They can arise from thymic origins or extrathymic origins (Wu et al., 2022) and from their transcriptomic profiles, DN T cells can be characterized as cytotoxic, helper or innate cells (Yang et al., 2021). Those with helper functions secrete cytokines including IL-4, IL-17, IFN-γ and tumor necrosis factor-α (TNF-α) and are involved in infections and autoimmune diseases. Those with cytotoxic functions secrete IFN-γ, perforin and granzyme B to mediate the killing of tumor cells. Those with innate function recruit other immune cells by secreting cytokines such as IL-1, IL-8, IL-10, IL-17, CXCL-2, CXCL-3, TNF-α and IFN-γ (Wu et al., 2022). Their higher numbers of DN T cells in the elderly relate to increased comorbidity of diseases (Marrero et al., 2023).

1.6.6 DP T cells

DP T cells express both CD4 and CD8 receptors are a heterogenous population of cells. They are believed to originate from MHC class II restricted CD4+ T cells, as the CD8α can be re-expressed by gene regulation such as down-regulation of ThPOK, which has negative regulation on the expression of CD8 linage genes (Overgaard et al., 2015). In contrast, naïve CD8+ T cells can also express CD4 after *in vitro* activation of PBMCs and have increased antiviral effector functions (Kitchen et al., 2002). DP T cells are activated cytotoxic cells and express cytotoxicity-related, MHC class I-restricted, T cell-associated molecule (CRTAM), CD244, granzyme B, perforin, and IFN-γ (Mucida et al., 2013). They can recognize higher amounts of antigen peptide and are prone to apoptosis. Clonal expansion of DP T cells, especially CD4^{high} CD8^{low} subset, have been observed in the elderly (Ghia et al., 2007). The DP T cells have anti-tumor activities by means of expressing class I MHC and the cytokines IL-2, IL-4, IL-5, IL-13 and GM-CSF. In contrast, they favor tumor growth and metastasis by means of secretion of IL-4, IL-5, IL-13 and TNF-α (Overgaard et al., 2015).

1.6.7 HLA-DR T cells

HLA-DR is the class II MHC molecule that is involved in antigen presentation and HLA-DR positive cytotoxic T lymphocytes are activated cells (Tippalagama et al., 2021). They enhance T cell effector function by mutual antigen presentation to

bystander T cells and produce IFN-γ to induce differentiation of more protective T cells (Holling et al., 2004). HLA-DR positive cytotoxic T cells have increased IFN-γ and IL-2 levels and can result in more effective immune responses (Chen et al., 2019). HLA-DR positive helper T cells associate with effector memory cells and have increased expression of the pro-inflammatory cytokine, TNF (Tippalagama et al., 2021). In ageing, there is expansion of HLA-DR positive T cells, both CD4+ and CD8+ subsets, perhaps as a result of immune activation and these cells correlate with upregulation of CD25 and increased levels of serum IL-2 receptor and TNF-α (Rea et al., 1999). In contrast, HLA-DR positive cytotoxic T cells may have antitumor functions as they express IFN-γ, Granzyme B, Perforin, Eomes and TNF-α, which are important for CTLs cytolytic activity. Moreover, their levels inversely correlate with TGF-β, PD-L1, IL-6, IL-1β and IL-8 which are pro-tumorigenic molecules. However, HLA-DR is also expressed by Tregs and their presence in cancers positively correlates with levels of pro-tumorigenesis molecules (Saraiva et al., 2018).

1.6.8 NK cells

NK cells can be identified by their expression of CD56 and the absence of CD3. CD56 is the neural cell adhesion molecule (NCAM) which is important for calcium-dependent cell-cell interactions (Abbas et al., 2022). CD56+ NK cells are cytotoxic cells of innate immunity and can kill other cells without further differentiation: hence they are called natural killer cells. They have important roles in viral infection, graft rejection, tumor remission and surveillance of tumors (Zaidi et al., 2015; Abbas et al., 2022).

Dependent on their CD56 surface intensity, cytotoxicity, and cytokine production, NK cells can be divided into two major types: NK CD56^{bright} and NK CD56^{dim}. CD56^{bright} cells are immature and main source of cytokines. NK CD56^{dim} cells comprise about 90% of CD56+ NK cells. They are considered as mature cells and derived from NK CD56^{bright} cells because NK CD56^{bright} cells appear before NK CD56^{dim} cells after HSC transplantation; they can also be differentiated from NK CD56^{bright} cells *in vitro* in a cytokine-driven model, and have shorter telomeres than NK CD56^{bright} cells. They have more cytotoxic activity than NK CD56^{bright} cells and contain more perforin, granzymes and cytolytic granules (Poli et al., 2009; Moretta, 2010).

CD56$^+$ NK cells can be divided into subpopulations according to CD16 expression as: CD56^{bright} CD16$^-$; CD56^{bright} CD16$^+$; CD56^{dim} CD16$^-$; CD56^{dim} CD16$^+$. CD16 is important for antibody-dependent cellular cytotoxicity and the CD56^{dim} CD16$^+$ population is predominant in blood and can attack tumor cells. CD56^{bright} CD16$^-$ cells have less ability to kill the cancer cells but they can produce higher amounts of cytokines (Fu et al., 2014). Another subset of NK cells has been identified with the markers of CD56$^-$, CD3$^-$ and CD7$^-$, and they relate to immune response to viral infection (Poli et al., 2009; Müller-Durovic et al., 2019).

NK cells can express CD4 or CD8 on their plasma membrane. CD4+ NK cells are efficient cytotoxic cells, and they can migrate to the site of IL-16 production, which is a CD4-mediated chemotactic factor (Bernstein et al., 2006). CD8+ NK cells are highly functional cells with more cytotoxic activity (Abdalla, 2012), and they have increased perforin and granzyme B (Chidrawar et al., 2006).

1.6.9 Classical monocytes

These cells can be distinguished from other monocytes by their high expression of CD14 and absence of CD16. They comprise 90% to 95% of blood monocytes and can rapidly recruit to the site of infection, producing inflammatory mediators (Abbas et al., 2022).

They are robustly recruited to the tumor site in a CCL-2-dependent manner. After activation of IFN-γ or IFN-α expression, they can induce cancer cell death via cytokine-mediated apoptosis, and phagocytosis by means of TRAIL-mediated-apoptosis or secretion of pro-tumoral cytokines such as CCL-2 and IL-8. They can also kill cancer cells by antibody-dependent cellular toxicity. They cross talk with lymphocytes by paracrine signaling and antigen presentation and their recruitment to the site of tumor is inversely associated with the presence of cytotoxic CD8+ T cells in the tumor environment (Li et al., 2017). However, classical monocytes are the source of tumor-associated macrophage (TAM) and CCR-2 -recruited classical monocytes express TAM markers such as F4/80, CD11c, MHCII, and V-CAM1 after arriving the tumor site. TAM support angiogenesis, tumor growth and metastasis (Olingy et al., 2019).

1.6.10 Intermediate monocytes

Intermediate monocytes are distinct from other monocytes and express CD14 and CD16. They have the same potential for phagocytosis and ROS production as classical monocytes, but decreased ability to adhere to surfaces and have increased levels of antigen presenting molecules (Kapellos et al., 2019a). They promote inflammation and disease pathogenesis (Wong et al., 2012). TIE2-expressing monocytes (TEMs) are part of the intermediate monocytes subset and can enhance tumor growth by secretion of angiogenetic factors (Schauer et al., 2012).

1.6.11 Non classical monocytes

These cells express low levels of CD14 and are positive for CD16 expression. They are recruited into tissue after infection or injury, where they may contribute to repair mechanisms. They are "patrolling" monocytes as they survey endothelial surfaces by scavenging luminal microparticles and repairing endothelial barrier defects (Abbas et al., 2022). Because of their patrolling function and long lifespan, they are responsible for scavenging of tumor cells and debris (Olingy et al., 2019).

1.6.12 CD4+ monocytes

CD4 is a membrane bound glycoprotein (55-59 kDa) and can bind to MHC class II molecules. It can be expressed on monocytes and its possible function is differentiation of monocytes to functional macrophages due to the following facts: CD4 ligation on monocytes together with MHC-II molecules can induce the differentiated macrophage markers, such as CD163, CD209, C-type lectin and CD16; it can also increase the expression of functional molecules such as TLR8, calcium influx and phosphorylation of NF-κB. After ligation and activation, the expression of proinflammatory cytokines, leptin and IGF-1, and the chemokines CXCL1, CXCL5, CXCL6, CCL26, CCL1, CCL9, and CCL13 are increased, and expression of IL-4, IL-15, and IFN-γ is decreased (Zhen et al., 2014).

1.6.13 CD56+ monocytes

CD56 is the neural cell adhesion molecule of 175–185-kD expressed on the cell surface (Zaidi et al., 2015). CD56+ monocytes can be detected in the peripheral blood and are linked to T cell proliferation because T cell proliferation increases in *in vitro* cultures simulated with antigen and CD56+ monocytes. They release the cytokines IL-

1β and IL-6 which are required for the induction of CTL responses and alloantigen presentation of B cells (Sconocchia et al., 2005).

1.6.14 HLA-DR^{low} monocytes

HLA-DR expression on monocytes is crucial for their ability to perform antigen presentation. Therefore, its expression indicates the competency of monocytes in an immune response. However, there is low positivity of HLA-DR in peripheral monocytes subsets and levels of HLA-DR^{low} monocytes relate to disease conditions such as inflammatory bowel diseases and severe COVID-19 infection (Tillinger et al., 2013; Hammad et al., 2022). HLA-DR$^{low/neg}$ cells have low antigen presentation capacity to activate T cells. They have an immunosuppressive phenotype and negatively affect immunotherapy but are important mediators of tumor-induced immunosuppression (Mengos et al., 2019).

1.7 p16^{INK4A}

P16^{INK4A} is involved in cell cycle regulation as it is a cyclin-dependent kinase inhibitor (CKI). There are two families of CKI (Laphanuwat and Jirawatnotai, 2019), the first includes INK4 (INhibitor of cyclin-dependent Kinase 4) containing the members INK4A (p16), INK4B (p15), INK4C (p18) and INK4D (p19). These INK4 inhibitors target the major cell-cycle-related kinase CDK4 (cyclin-dependent kinase) and its subfamily member CDK6, which are activated by cyclin D during the G1 phase of the cell cycle (Malumbres, 2014). The second is the Cip/Kip (CDK interacting protein/Kinase inhibitory protein) family comprising p21^{CIP1}, p27^{KIP1} and p57^{KIP2} and they inhibit the CDK2/1, which can bind to cyclin E, cyclin A, cyclin D and cyclin B in the late G1, S, G2 and M phases (Malumbres, 2014; Laphanuwat and Jirawatnotai, 2019).

1.7.1 Properties of p16^{INK4A}

P16^{INK4A} was discovered in 1993 by searching for the binding partner for CDK4 (Serrano et al., 1993). P16^{INK4A} is encoded by *CDKN2A* (cyclin-dependent kinase 2A) located on the short arm of chromosome 9 (9p21.3) (LaPak and Burd, 2014) and the *CDKN2A* gene has 5 exons (E1β, E1α, E2, E2γ and E3) and 1 intron (In1). The p16^{INK4A}

transcript (alpha transcript) is formed by the splicing of exons E1α, E2 and E3 (**Fig 4a**). Alternative splicing of the gene results in variant transcripts such as beta (p14), p16γ and p12 (Serra and Chetty, 2018b). Several mutations of the gene are observed in different types of cancers such as head and neck squamous cell carcinomas and pancreatic carcinomas (Serrano, 1997; Serra and Chetty, 2018b). P16^{INK4A} deletion can be seen in pancreatic carcinomas (Serra and Chetty, 2018a) There are also germline mutations of p16^{INK4A} which are found in specific types of cancer such as melanoma, pancreas and liver cancers (Bisio et al., 2010).
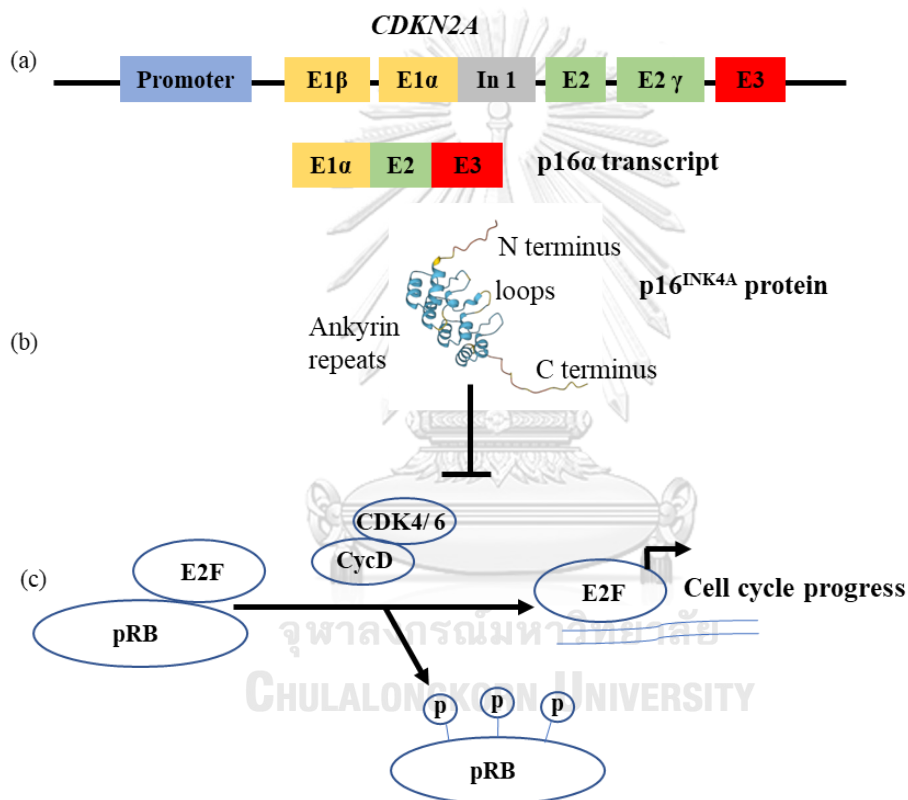
Figure 4: *p16^{INK4A} gene, protein and its canonical function*
(a) p16^{INK4A} gene, (b) p16 ^{INK4A} protein and (c) its canonical function (Jumper et al., 2021)

The p16^{INK4A} protein comprises 156 amino acids and has a molecular mass of 16 kDa, with four ankyrin repeats (Serrano et al., 1993; Li et al., 2011), which are ~30 amino acid structural motifs. Ankyrin repeats (AR) have two anti-parallel helices with a structure resembling the letter 'L' and the motifs stack together forming an extended concave surface (Russo et al., 1998) which are important for protein-protein

interactions. The second and third ankyrins of p16^{INK4A} bind to CDK4 and decrease its affinity to cyclin D (Serrano, 1997; Mosavi et al., 2004). The first and fourth ankyrins are important for binding of non-CDK proteins such as TFIIH in the inhibition of RNA polymerase II and AP-1 in prevention of cell transformation. They are also crucial for post-translational modification of the p16^{INK4A} protein, such as phosphorylation of p16^{INK4A} which has better association with CDK4; phosphorylation of p16^{INK4A} at Ser-8 can bind to IKKβ and inhibit the NFκB pathway (Li et al., 2011). In the tertiary structure of p16^{INK4A}, four ankyrin repeats are linked by three loops while the first half of the second ankyrin has only one helical turn. The linking loops are perpendicular to the helical axes (Byeon et al., 1998). P16 exhibits low stability because its tertiary structure is the molten globule which is a protein-folding intermediate **(Fig 4b)** (Boice and Fairman, 1996).

Deletion of one or more amino acid residues can disturb the tertiary structure and can affect the function of p16^{INK4A}. Single amino acid substitutions at the flexible N-terminal or C-terminal domains does not affect its structure or function (Byeon et al., 1998), but phosphorylation of Ser7, Ser8, Ser140 or Ser152 can perturb the function, structure and stability of the protein (Li et al., 2011). Although p16^{INK4A} has 4 ARs, its stability is lower, with a conformational stability of 1.94 ± 0.1 kcal mol^{-1}, lower than the common range of 5-15 kcal mol^{-1}(Li et al., 2011). The half-life of p16^{INK4A} is 3.5 h but mutant forms have shorter half-lives than the wild type in human leukemic cell lines (Gombart et al., 1997). Therefore, p16^{INK4A} is an unstable protein and this fact should be considered when conducting functional studies of protein. It is involved in the cell cycle inhibition from G1 to S phase by inhibition of cyclin D, which is responsible for phosphorylation of pRb in E2F transcription (**Fig 4c**) (Rayess et al., 2012)

1.7.2 Regulation of p16^{INK4A}

Epigenetic regulation at the INK4/ ARF locus is important for the expression of p16 (Li et al., 2011). Chromatin modifiers, either repressors or activators, can control the locus in alternate ways (D'Arcangelo et al., 2017), the most notable regulation is by the Polycomb Repressive Complexes (PRC) and ANRIL (Anti-sense non-coding RNA in the INK4/ARF Locus) (Popov and Gil, 2010). Under normal circumstances, the locus is repressed by PRC with the help of ANRIL generated from the locus (D'Arcangelo et

al., 2017). PRC2 triggers the H3K27met3 epigenetic mark which is recognized by PRC1 and repression of the gene is maintained (Rayess et al., 2012). Activation of the locus occurs rapidly when expression is activated (Popov and Gil, 2010). During activation of p16 expression, the repressive epigenetic marks are removed by decreasing the levels of enzymes that regulate methylation, while increasing the level of enzymes involved in demethylation and direct modification by phosphorylation (Popov and Gil, 2010). Epigenetic regulation of p16 is a complex process because other transcription factors, as well as histone deacetylases, can be involved in the methylation of the p16 promoter (Rayess et al., 2012). There is evidence of ROS-mediated p16 expression through epigenetic mechanisms: DNA damage/ROS production can inhibit DNMT1 causing reduced methylation of H3K9, resulting in increased expression of the p16 gene (Rayess et al., 2012).

The p16 promoter contains various regulatory elements that can control activation or repression of p16 (D'Arcangelo et al., 2017). It has binding sites for various transcription factors such as: GC boxes in the GC-rich region of the promoter for SP1 transcription factor; specific binding sites for Ets1, Ets2 and HMG box-containing protein 1 which are the downstream targets of Ras-Raf-Mek signaling; E-box elements for E-proteins; Ap1 sites for Ap1 proteins; peroxisome proliferator response element for PPARα protein; unspecified elements for chromatin remodeling complex; and INK4a transcription silence element for Myb-related protein B (Li et al., 2011).

Although p16 ^{INK4A} protein levels increase in the transition state of G0 to S phase, mRNA level showed no fluctuation during the cell cycle phases, perhaps because p16^{INK4A} RNA is relatively stable and post-translational modifications are important in the regulation of p16^{INK4A} (Hara et al., 1996). Post translational modifications of p16 are also important for its functional regulation (Li et al., 2011). Senescence cells have the novel phosphorylated form which showed higher affinity for CDK4/6 (Sandhu et al., 2000). However, phosphorylation can be regulated by cellular oxidative stress (Zhang et al., 2021c), and phosphorylation at Ser8 diminishes its CDK4-inhibitory activity (Gump et al., 2003). The cellular level of p16 also depends on its rate of degradation, which is regulated by the REGγ-20S proteasome, a ubiquitin- and ATP-

independent process (Li et al., 2011). The proteosome activator REGγ can be overexpressed in cancer cells causing the degradation of tumor suppressor proteins and enhancing tumorigenesis (Okamura et al., 2003; Ali et al., 2013). On the other hand, there is evidence of an age-associated decline of REGγ activity (Tu et al., 2022) and it could be one of the possible explanations for p16^{INK4A} increase in old age. Smoking is also reported to increase the levels of p16 via a defect in degradation (Tsygankov et al., 2009). The degradation of p16^{INK4A} can also occur in lysosomes in the case of autophagy (Coryell et al., 2020).

Changes in levels of other proteins that interact with p16 and its target CDK4 can also influence p16^{INK4A} protein levels and function (Li et al., 2011). For example, overexpression of cyclin Ds (activators of CDK4), can result in more CDK4-cyclinD complexes thereby blocking the inhibitory function of p16^{INK4A} (Li et al., 2011). Also, CKI Cip/ Kip family members can compete with p16^{INK4A} for CDK4/6 binding and can drive p16 into degradation (Li et al., 2011). There are also interactions between the regulators of NFκB signaling and the p16-Rb pathway as follow. Although p16 can bind and suppress NFκB, inhibitors of NFκB can bind CDK4 and interfere with p16 function by phosphorylation at Ser8: NFκB may also compete with CDK4 for p16 resulting in cell proliferation. This can result in both downregulation of p16 and activation of NFκB (Li et al., 2003; Ghiorzo et al., 2004; Li et al., 2011).

1.7.3 Other proteins regulating p16^{INK4A}

Other proteins from different pathways can also influence the function of p16^{INK4A}. For example, GRIM-19, a cell death regulatory protein, can promote the p16^{INK4A} function by enhancing the binding of p16 and CDK4, inhibiting the activity of cyclin D (Sun et al., 2010). In addition, the oncogene protein p34^{SEI-1} can bind to p16/ CDK4/ cyclin D complexes and antagonize the inhibitory effect of p16^{INK4A} at low levels but can inhibit the action of CDK4 at higher levels (Li et al., 2004). Gankyrin, a negative regulator of the tumor suppressor pathway, can counteract the function of p16^{INK4A} by competing for the binding site for CDK4 (Li and Tsai, 2002). The infection-related protein Tax, the transcription activator of HTLV-1, can indirectly disturb the inhibitory function of p16^{INK4A} in cell cycle, by enhancing the CDK4 activity through direct binding with CDK4 (Matsuoka and Jeang, 2011).

1.7.4 Clinical significances of p16^{INK4A}

p16^{INK4A} can have an antitumor effect and high levels of p16^{INK4A} are associated with decreased regenerative capacity, while an absence of p16^{INK4A} function by genetic mutations or epigenetic alteration predisposes to cancer. In early tumorigenesis of tumors, inactivation of p16^{INK4A} occurs and this is followed by intense activation of its promoter, as an attempt to inhibit oncogenic proliferation (LaPak and Burd, 2014). Increased expression of p16^{INK4A} can be seen in pathophysiological conditions such as tumorigenesis and senescence, as well as in other situations, e.g. response to chemotherapy (Muss et al., 2011) and smoking (Liu et al., 2009). Neoplasms can also induce p16^{INK4A} expression in cells within the tumor microenvironment (LaPak and Burd, 2014). In tissue transplantation, the p16^{INK4A} level of the donor tissue has been used to assess the biological age, to predict the potential for successful transplantation (LaPak and Burd, 2014).

p16^{INK4A} levels increase during human ageing and so can be used as an indicator of chronologic ageing (LaPak and Burd, 2014). However, its expression is more relevant for use as a biological ageing marker because its expression is associated with intrinsic cellular stressors like DNA damage and telomere erosion (LaPak and Burd, 2014). It is not only a biomarker of ageing, but also the cause of ageing for many cell types (LaPak and Burd, 2014). For example, deletion of p16^{INK4A} expressing cells in a mouse model decreases ageing phenotypes, such as delay in sarcopenia, cataracts and loss of adiposity (Baker et al., 2011). p16^{INK4A} levels significantly increase in T cell immuno-senescence of testicular cancer survivors (Bourlon et al., 2020).

1.8 Summary

CRC is one of the most common cancers worldwide and its etiology relates to ageing-related immune dysfunction. Immune responses in CRC can favor immuno-senescence and other immuno-phenotypic changes can result in defective functions of the immune system that can enhanxce tumorigenesis and metastasis of CRC. While p16^{INK4A} is a well-known ageing marker and its levels in white blood cells can increase in patients with certain cancers, it is unknown if this protein is upregulated in CRC and hence its potential as a biomarker for CRC in undefined. Several changes in immune phenotypes have been identified in CRC but again, these have not been fully defined.

Understanding these changes in immune cell phenotype in CRC is important not only to identify new biomarkers but also, in the longer term, to determine how CRC may disrupt immune function and evade immune-surveillance.

1.9 Research questions

- Can expression of the senescent marker (e.g., p16^{INK4A}) in peripheral immune cells be used as the biomarker for CRC?
- Can we detect changes in circulating immune cells that relate to either immuno-senescence or altered immunophenotypes during ageing and CRC?
- Are these changes associated with ageing or CRC, or both?

1.10 Objectives of the research

- To determine if WBCs in CRC express markers that indicate that they have a senescent phenotype.
- To identify immunophenotypic changes of T cells, NK cells and monocytes in ageing and in CRC and to distinguish immune cell subtypes that are specifically associated with CRC.
- To determine if p16^{INK4A} can be used as a biological marker for CRC.

1.11 Hypothesis

CRC patients exhibit immuno-senescence and immunophenotypic changes that result in defects in their immune function in response to CRC.

Changes of T cells, NK cells and monocytes occur in CRC as well as in ageing, but some of these changes are CRC-dependent changes.

The senescence marker p16^{INK4A} increases in peripheral immune cells in CRC and this can be used as a potential biomarker for CRC.

CHAPTER II: RESEARCH METHODOLOGY

2.1 Materials

Cell lines

- Jurkat (ATCC TIB-152; a clone of the JURKAT-FHCRC cell line)

- HeLa (American Type Culture Collection: ATCC® CCL-2™)

- HCT116 (American Type Culture Collection: ATCC® CCL-247™)

- Rat Primary Dermal Epidermal Keratinocytes (RA-6066K, Cell Biologics Inc)

Reagent for immunofluorescent staining

Antibodies:

- Mouse anti-human CD14; mouse anti-human CD3; anti-mouse Cy3; anti-rabbit FITC; rabbit anti-human $p16^{INK4A}$ (clone D3W8G); rabbit anti-human $p16^{INK4A}$ (clone D7CM1) from Cell Signaling, USA

- Mouse anti-human CD45 from Abcam, USA

Reagents:

- 4', 6-diamidino-2-phenylindole, dihydrochloride (DAPI); Bovine serum albumin from Cell Signaling, USA

- Ammonium sulphate lysis solution from Abcam, USA

- Disodium hydrogen phosphate; Paraformaldehyde; Potassium chloride; Potassium dihydrogen phosphate; Sodium chloride; Triton X-100; Tween 20 from Sigma, USA

Reagent for Flow Cytometry

Antibodies:

- DuraClone IM Phenotyping Basic tubes (CD45-KO, CD3-APC Cy7, CD4-APC, CD8-A700, CD19-texa, CD56-PE, CD14-PC7, CD16-FITC) from Beckman Coulter, USA

- Mouse anti-human CD8-PE; mouse anti-human CD28-FITC; mouse anti-human CD3-PerCP; mouse anti-human CD57-APC from BioLegend, USA

- Mouse anti-human CD4-PE; muse anti-human HLA-DR-APC from BD Biosciences, USA

- Mouse anti-human CD14-PE from R&D Systems, USA

- Rabbit anti-human Caspase 3-PE from Cell signaling, USA

- Recombinant human IgG1 p16-PE from Miltenyibiotec, USA

Reagents:

- Digitonin; disodium hydrogen phosphate; ethanol; paraformaldehyde; potassium chloride; potassium dihydrogen phosphate; propidium iodide from Sigma, USA

- DuraClone IM Phenotyping cleaning solution for flow cytometry; cytoflex sheath fluid; QC beads for Cytoflex from Beckman Coulter, USA

- BD FaCSDivaTM CS&T Research Beads from BD Bioscience, USA

- CellEvent^{TM} Senescence green flow cytometry assay kit from Thermo Fisher, USA

- Formaldehyde from Acros organics, Belgium

- Hetasep solution from Stemcell, USA

- Lymphoprep solution from Stemcell, Germany

- Trypan blue stain from Sigma, UK

- Virkon powder from Lanxess, German

- EDTA from Promega, USA

Reagents for cell culture

- Etoposide from Sigma, USA

- FBS; RPMI media from Gibco, UK

- Non-essential amino acids from Gibco, USA

RNA extraction reagents

- Chloroform; isopropanol from Sigma, USA

- DNase from ThermoFisher, USA

- RNA extraction kit from Qiagen, Germany

- Trizol from Life Technologies, USA

Reagent for cDNA synthesis

- M DTT; 5Xfirst strand buffer; dNTP; Random hexa primers; RNase OUT^{IM} Recombinant (5000 U); Superscript (10000 U) from Invitrogen, USA
- 25mM Magnesium Chloride from Bioline, USA

Reagent for RT-PCR

- p16^{INK4A} (CDKN2A) Human qPCR primer pair from Origene, USA
- QuantiNova SYBR Green PCR kit from Qiagen, Germany

2.2 Samples and ethical approval

CRC blood samples were collected from Center of Excellence for Colorectal Cancer, King Chulalongkorn Memorial Hospital, Thailand and from the colon cancer service, Aintree University Hospital, Liverpool. Control blood samples were collected from the colonoscopy unit, King Chulalongkorn Memorial Hospital, and volunteers from Aintree University Hospital and University of Liverpool.

This study was conducted under the regulations of the Institutional Review Board, Faculty of Medicine, Chulalongkorn University, COA number: 1580/2021, and the University of Liverpool, protocol number: UoL001136, REC reference: 15/NW/0477, IRAS project ID: 174008. This study was conducted in accordance with the Declaration of Helsinki. All study participants provided informed consent.

2.3 Methods

2.3.1 Buffy coat layer preparation

Whole EDTA-blood (5-10 mL) was centrifuged at 1000g for 12 min at room temperature. The buffy coat layer was collected, and the red blood cells (RBCs) were lysed with 20 volumes of RBC lysis solution. The lysis reaction was terminated by adding an equal volume of phosphate-buffered saline (PBS) and centrifuged for 5 min at 400g. Cells were washed with PBS 3 times and the white blood cells (WBCs) were counted with a counting chamber. WBCs were then fixed with 4% paraformaldehyde for 15 min (1 million cells/mL fixative) and washed 3 times with deionized water. WBCs were placed in 96-well plates (approximately 40,000 cells/well) and stored at room temperature before immuno-fluorescence staining.

2.3.2 Immunofluorescence staining of p16^{INK4A}

Sample wells containing WBCs were washed with PBS 3 times. One hundred microliter of 0.5% (v/v) Triton X-100 was added into each well and incubated for 10 min at room temperature. Wells were then washed with PBS 5 times. Then, 100μl of 5% (w/v) BSA was added into each well for 30 min. One hundred μL of 1:1000 diluted anti-p16^{INK4A} in 1% (w/v) BSA, were added into each well and incubated overnight (16 h) at 4°C. Wells were washed with 100 μL of 0.1% Tween PBS 3 times. One hundred μL of 1:1000 diluted anti-rabbit FITC secondary fluorescent antibodies in 1% (w/v) BSA, were added into each well and incubated for 2 h at room temperature in the dark. Wells were washed with PBS 3 times. One hundred μL of DAPI (final concentration of 1μg/mL) (for nuclear staining) was added into each well for 10 min and washed with PBS 3 times.

2.3.3 Double immunofluorescence staining

Sample wells containing WBCs were washed with PBS 3 times. One hundred microliter of 0.5% Triton X-100 was added into each well and incubated for 10 min at room temperature. Wells were then washed with PBS 5 times. Then, 100μl of 5% (w/v) BSA was added into each well for 30 min. One hundred μL of diluted primary antibodies (anti-p16^{INK4A} and anti-CD45) in 1% (w/v) BSA, were added into each well and incubated overnight (16 h) at 4°C. Dilutions of anti-p16^{INK4A} primary rabbit antibody and anti-CD45 primary mouse antibody were 1:1000. Anti-CD3 primary

mouse antibody and anti-CD14 primary mouse antibody were diluted 1:500. Wells were washed with 100 μL of 0.1% (v/v) Tween PBS 3 times. One hundred μL of 1:1000 diluted secondary fluorescent antibodies (anti-rabbit FITC and anti-mouse Cy3) in 1% (w/v) BSA, were added into each well and incubated for 2 h at room temperature in the dark. Wells were washed with PBS 3 times. One hundred μL of DAPI (final concentration of 1μg/mL) (for nuclear staining) was added into each well for 10 min and washed with PBS for 3 times.

2.3.4 Image analysis

Three-color images were captured as follows: blue (DAPI 358 - 461 nm); green (FITC 500 - 520 nm) and red (Cy3 560 - 570 nm) with a motorized fluorescence microscope IX83 (Olympus Co., Ltd., USA). All images were acquired using a defined experimental protocol throughout the study. Briefly, 20 fields of 20X objective (5 columns and 5 rows) were taken with the fixed exposure time for DAPI (7s), FITC (200ms) and Cy3 (300ms). The fluorescence intensity of each cell was calculated using CellSens imaging software after setting the range of intensity values (70 to 150) and perimeter values (18 to 55 nm). Mean fluorescence intensity (MFI) was then acquired from the average fluorescence intensity of cells from the whole image. In double immunofluorescence staining, the positive region was identified by using CancerScreen.exe program (Puttipanyalears et al., 2021). P16^{INK4A}-positive/CD-positive cells were identified by the signals of red and green in the same spot with the criteria of intensity value (60 to 150) and perimeter value (18-100 nm)

2.3.5 Validation of anti-p16^{INK4A} for immunofluorescent staining

Differences in p16^{INK4A} clones used to generate monoclonal antibodies, that may use different antigens, can affect target identification and the outcomes of the experiments. Therefore, p16^{INK4A} antibodies from two different sources were validated with cell lines: HeLa, HCT116 and rat epidermal keratinocytes. Antibodies to p16^{INK4A} were rabbit monoclonal antibodies. D3W8G (92803) was raised against synthetic peptide residues surrounding Ala34 of human p16^{INK4A} protein while D7CM1(80772) was produced from synthetic peptide residues surrounding Ala143 of human p16^{INK4A} protein. Hct116 cells were used as negative control for p16^{INK4A} staining. Staining

patterns of each antibody, whether cytoplasmic or nuclear patterns, were observed for each cell line.

2.3.6 Jurkat cells experiments with inhibitor

Jurkat cells were maintained at a concentration of approx. 0.5 million cells/mL and treated with or without inhibitor for the times specified in Results. The concentration of additions was etoposide at 0.5 μM (final conc) in cultures containing 0.5 million cells/mL. After incubation periods (defined in the text), the cells were washed with fresh RPMI media.

2.3.7 PBMC preparation

Ten mL of Lymphoprep solution was added into a universal tube, and layered with EDTA-anticoagulated whole blood at a ratio of 1:1. The tube was centrifuged at 1000g for 30 min without the brake applied. The layer of PBMCs was collected and washed with fresh RPMI media at 400g for 5 min. After washing, the cell pellet was suspended in 1mL RPMI media and the number of cells was counted with a cell counter. The cells were diluted with RPMI media to obtain a concentration of 0.5 million in 100 μL.

2.3.8 Storage of PBMC for RNA analysis

Ten million PBMC in RPMI media were spun down at 4°C to obtain a pellet, that was thoroughly mixed with 1mL Trizol until the cell suspension was homogenous. This was stored at -20°C until the RNA was extracted.

2.3.9 HetaSep separation

Five parts of heparinized blood were diluted with 1 part of Hetasep solution, and incubated at 37°C until the 50% of red blood cells had sedimented. The upper layer, was carefully transferred into a universal container (avoiding disturbance of the red cells), washed with fresh RPMI, and centrifuged at 400g for 5 min. The supernatant was discarded while the pellet was gently dispersed by tapping the bottom of the tube and then mixed with 1 mL RPMI media before adding 9 mL ammonium chloride solution. The suspension was incubated at room temperature for 4 min to lyse the remaining red blood cells. Then, the lysis reaction was stopped by adding equal volume of RPMI and the mixture was centrifuged at 400 g for 5 min. The supernatant was

removed and 1 mL RPMI media was added to the pellet which was then gently dispersed. The number of cells was counted with a cell counter. The cells were diluted with RPMI media to obtain a concentration of 0.5 million in 100 μL.

2.3.10 Flow cytometry surface markers staining

Compensation for the fluorophores was given for each experiment. QC assessment was checked daily with standard fluorescent beads before analysis of the samples. One hundred μL of PBMC suspension containing 0.5 million cells was washed with 1mL 0.2% (w/v) BSA in PBS. After centrifugation to pellet the cells, they were resuspended in 100 μL of 0.2% (w/v) BSA in PBS. Then, 1 μL of each fluorescently-tagged antibody was mixed and incubated for 30 min at 4°C. After incubation, the excess antibodies were washed with 1 mL of 0.5M EDTA PBS and centrifugation. The cells were suspended in 200 μL of 0.5M EDTA/PBS and analyzed on a flow cytometer (Cytoflex) using the appropriate channels with 10,000 events recorded.

2.3.11 Beta gal staining

Two hundred μL of cell suspension of PBMC was washed with 1 mL of 0.2% (w/v) BSA PBS. The cell pellet was resuspended in 100 μL of 0.2% (w/v) BSA in PBS. Then, 1 μL of each fluorescent-tagged antibody was mixed and incubated for 30 min at 4°C. After incubation, the excess antibodies were washed with 1 mL of 0.5M EDTA/PBS and centrifugation. The cell pellet was resuspended in 400 μL of 0.2% (w/v) BSA/PBS. Equal volumes of 2% (v/v) paraformaldehyde solution were added and mixed thoroughly. The mixture was incubated at room temperature for 10 min. Then, 500 μl of 0.2% (w/v) BSA/PBS was added and centrifuged at 700g for 5 min. The supernatant was discarded and 200 μL of the assay working solution (Senescence buffer + green probe 1:1000, Thermo Fisher) was added and mixed thoroughly. The tubes were incubated at 37°C for 1 hour. The negative control tubes with senescence buffer (without green probe) were also included for each sample. After incubation, 1mL of 0.2% BSA/PBS was added into each tube, mixed and the cells centrifuged at 700g for 5 min. The pellet from each tube was resuspended with 200 μL of 0.2% (w/v) BSA/PBS and analyzed on the flow cytometer using a 488-nm laser with 10,000 events recorded.

2.3.12 Flow cytometry intracellular staining

Two hundred μL of cell suspension of PBMC was washed with 1 mL of 0.2% (w/v) BSA PBS. The cell pellet was resuspended in 100 μl of 0.2% (w/v) BSA in PBS and then 1 μl of each fluorescent-tagged antibody was mixed and incubated for 30 min at 4°C. After incubation, the excess antibodies were washed with 1 mL of 0.5M EDTA PBS. The cell pellet was resuspended in 400 μL of 0.2% (w/v) BSA/PBS and then equal volumes of 2% (v/v) paraformaldehyde solution were added and mixed thoroughly. The mixture was incubated at room temperature for 10 min. Then, 500 μl of 0.2% (w/v) BSA/PBS was added and centrifuged at 700g for 5 min. The cells were resuspended in 500 μl of 0.2% (w/v) BSA/PBS and 5 μl of 0.1% (v/w) digitonin was added to permeabilize the cells. The mixture was incubated for 10 min at room temperature. After permeabilization, the cells were washed and resuspended with 0.2% (w/v) BSA/PBS in a total volume of 100 μL. The fluorescent-tagged p16 and caspase-3 antibodies were added and incubated for 30 min at 4°C. After incubation, the excess intracellular antibodies were washed out with 0.2% (v/v) Tween/PBS. The pellets from each tube were resuspended with 200 μL of 0.5 M EDTA/PBS and analyzed on the flow cytometer using the appropriate wavelengths with 10,000 events recorded.

2.3.13 DuraClone IM Phenotyping

One million cells from each sample (from section 2.3.9) were added into each of the pre-prepared antibody-coated tubes and the tubes were vortexed for 6-8 s to thoroughly mix. They were incubated at 20°C for 15 min, protected from the light. After that, they were washed with 3 mL PBS at 400g for 5 min and the cells were re-suspended gently with 500 μL of 0.1% (v/v) formaldehyde. Before analysis of the samples, eight single color tubes each containing a single antibody were mixed with cells, and analysed by flow cytometry (Fortessa) these samples were used to set the compensation parameters for each fluorophore. QC assessments using standard beads were performed before analysis of each sample. For each sample, 100,000 events were recorded and analysed with FlowJo (v 10.8.1) software.

2.3.14 RNA extraction from PBMC

The tubes of PBMC with trizol solution (from 2.3.8) were placed on ice. Two hundred μL of chloroform was added into each tube and mixed thoroughly for 15 s and

then incubated at room temperature for 2 to 3 min. They were centrifuged at 12,000 g for 15 min at 4°C. The upper phase of the mixture was removed into a 1.5mL Eppendorf and added to an equal volume of isopropanol. The tubes were placed on ice for 1 h for precipitation and then the tubes were centrifuged at 12,000g for 30 min at 4°C. The supernatant was carefully removed and the precipitate was air-dried and then resuspended in 100 μL of RNase/DNase free ddH$_2$O followed by 250 μL 100% ethanol. The mixture was transferred into RNeasy spin columns prior to RNA cleaning.

2.3.15 RNA extraction from Jurkat cells

The Jurkat cells (2 million) from the experiments were spun down at 400g for 10 min at 4°C. The RNA was extracted with RNA extraction kit (Qiagen) and the pellet was lysed with 350 μL of RLT (RNeasy lysis buffer) buffer (Qiagen) and mixed with 350 μL of 70% (v/v) ethanol. The mixture was transferred into a RNeasy spin column for RNA cleaning.

2.3.16 RNA cleaning

RNA cleaning was performed using RNA extraction kit according to the manufacturer's instructions as follows. The spin column containing the RNA mixture was centrifuged for 15 s at 8000g and the flow-through was discarded. The column was washed with 350 μL of RW1 (RNeasy wash) buffer (Qiagen) for 15 s at 8000g. Then, the DNA on the column was digested with 80 μL of DNase I working-solution (a mixture of 10μL of DNase I stock solution and 70 μL of buffer RDD (RNase-Free DNase Set) (Qiagen) for 15 min at 20-30°C. After DNA digestion, the column was washed with 350 μL of RW1 buffer (Qiagen) for 15 s at 8000g. Then, 500 μL of Buffer RPE (RNeasy propriety component) (Qiagen) was used to wash the column twice: first for 15s and second for 2 min at 8000g. The spin column was transferred into a new microfuge tube. Thirty μL of RNase-free water was added directly onto the spin column membrane and the tube was centrifuged at 8000g for 1 min to elute the RNA. The RNA content was measured with a NanoDrop spectrophotometer.

2.3.17 cDNA synthesis

cDNA synthesis used 100 ng of RNA, 1 μL of random hexa primers (mixture of single-stranded random hexanucleotides with 5'- and 3'-hydroxyl ends), 1 μL of dNTP and RNase-free water in a total volume of 18 μl in a PCR tube. A mix containing

4 µL of 5X first strand buffer, 4 µl of $MgCl_2$, 2 µL of 0.1 M DTT, 1 µL of RNaseout and 1 µL of Superscript enzyme (10,000 U) was prepared. The PCR tube was incubated at 65°C for 5 min in a thermocycler to denature RNA and after cooling to 4°C, 12 µl of the superscript-containing mix was added. The tubes were loaded into the thermocycler under the following cycling conditions: 95°C for 3 min (one cycle), 95°C for 5 s and 60°C for 10 s (40 cycles). The cDNA sample was stored at -20°C.

2.3.18 RT-PCR

For each cDNA reaction, a tube was prepared by mixing cDNA and Brilliant III Ultra-Fast QPCR Master Mix (0.5 µL of cDNA and 10 µL of master mix containing SYBR™ Green I dye, AmpliTaq Gold™ DNA Polymerase, dNTPs with dUTP and optimized buffer for each reaction). A second tube contained forward and reverse primer. For the target gene (p16^{INK4A}), 1 µL of 10 µM primer-mix was added in 9 µL of H_2O. For the house-keeping gene (cycophillin A), 0.5 µL of forward primer (10 µM (final conc 250 nM) and 0.5 µL of reverse primer (10 µM) were diluted with 9 µl of H_2O. The contents of the tubes were mixed and briefly centrifuged. Then, 10.5 µL of each sample was added into the relevant wells, plus 9.5 µl of of each primer mix was added into the relevant wells of 96-well PCR plate. For each sample, triplicate wells for both the target gene and house-keeping gene were prepared. The PCR plate was centrifuged briefly before placing on Agilent machine. The cycling protocol was performed as follow: 95°C for 3 min (one cycle), 95°C for 5 s and 60°C for 10 s (40 cycles).

Table 2: Primer sequences for PCR

Primers	Sequence
p16 forward	CTCGTGCTGATGCTACTGAGGA
p16 reverse	GGTCGGCGCAGTTGGGCTCC
Cycophillin A forward	GCTTTGGGTGCAGGAATGGT
Cycophillin A reverse	GTTGTCCACAGTCAGCAATGG

2.3.19 DNA staining for Jurkat cells

The Jurkat cells were suspended in PBS at a final concentration of 1 million cells per mL. Two hundred µL of cell suspension was mixed gently with 200 µL of 70%

(v/v) ice-cold ethanol and fixed for 1 h on ice. Then, the cells were washed with 1mL PBS at 700g for 5 min. The cells were resuspended in 50 μL of 0.1% (w/v) RNAse and incubated for 5 min at room temperature. Into the mixture, 200 μL of PI working solution (1μg of PI plus 0.01 mg RNAse/mL in PBS) was added and incubated for 30 min at room temperature. Then, the cells were transferred into wells of 96-well plates and analyzed with the flow cytometer with at least 3,000 events recorded.

2.3.20 Statistical analysis

Normal distribution values of the study groups were assessed by Shapiro-wilk test. Data are expressed as mean±SD, N (%), median value, interquartile range (IQR), 95% CI and p-value. For normally distributed data, the difference between two groups was measured with an independent t test. For skewed data, the difference between two groups was assessed by Mann-Whitney test. For the paired sample data analysis, Wilcoxon matched-pair signed rank test was used. Pearson correlation was used for the correlation of normally distributed data and Spearman correlation was used for skewed data. Receiver operating characteristic (ROC) curve was used to evaluate the sensitivity and specificity of the marker. GraphPad prism-8 (GraphPad Software Inc., USA) was used for statistical analysis and graphical illustrations.

จุฬาลงกรณ์มหาวิทยาลัย

CHULALONGKORN UNIVERSITY

CHAPTER III: UPREGULATION OF P16^{INK4A} IN PERIPHERAL WHITE BLOOD CELLS AS A NOVEL SCREENING MARKER FOR COLORECTAL CARCINOMA

3.1 Introduction

Screening methods to detect colorectal cancer (CRC) are important for early detection of this disease. CRC is related to both aging and immuno-senescence. One such senescence marker is p16^{INK4A} expression in immune cells. Expression of this protein has been used to identify immuno-senescence in other cancers (e.g. breast cancer (Sanoff et al., 2014) or testicular cancer (Bourlon et al., 2020), but it has not been investigated whether the expression of this protein is elevated in the circulating blood cells on CRC patients and hence an indicator that these cells have an immuno-senescent phenotype. If so, then these circulating immune cells will have an impaired phenotype and hence altered function in CRC. The objective of this study was to investigate the protein expression of p16^{INK4A} in peripheral white blood cells as a potential screening marker for colorectal cancer.

A case-control study was conducted in which cases were patients with colorectal cancer and controls were healthy individuals matched with cases on the basis of age and sex. Peripheral blood was collected from patients and controls and protein p16^{INK4A} expression was measured by immunofluorescence techniques. Mean fluorescence intensity of p16^{INK4A} of cases and controls were analyzed in CD45+, CD3+ or CD14+ cells and also correlated with clinical data. The p16^{INK4A} levels from cases and controls were evaluated using ROC analysis for their potential use as a screening marker in CRC patients.

Statistically-significant increased expression of p16^{INK4A} levels was found in CRC cases compared to healthy controls. p16^{INK4A} in peripheral immune cells had 78% sensitivity and 71% specificity. The percentage of p16^{INK4A}-positive cells and mean fluorescence intensity were significantly higher in CD45 positive cells, CD3 positive cells and CD14 positive cells. No significant correlation was observed between the clinical data and p16^{INK4A} levels of CRC patients. The significant increase of p16^{INK4A} expression level in peripheral immune cells represents its potential for use as a CRC screening marker.
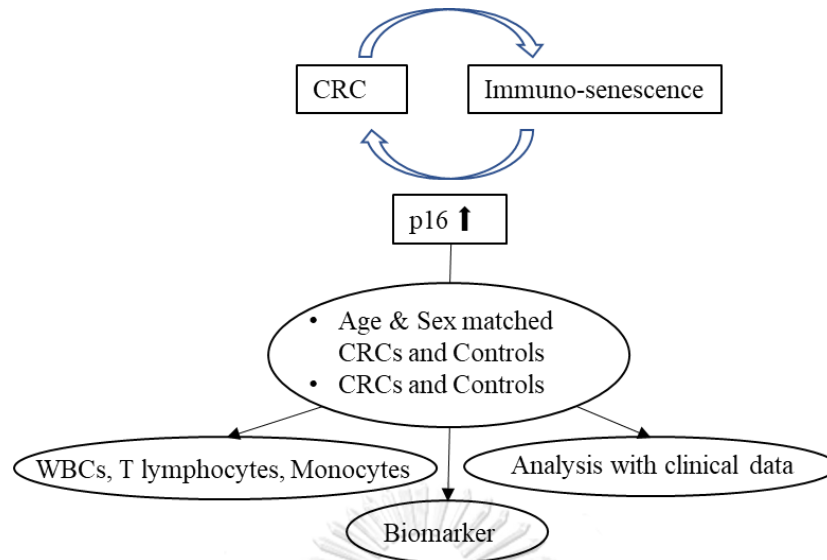
3.2 Aim

i.   To identify whether or not WBCs in CRC express a marker (p16^{INK4A}) to indicate that they have a senescent phenotype.

ii. To determine if p16^{INK4A} can be used as a biological marker for CRC.

3.3 Results

Cross-sectional case-control studies were performed at the King Chulalongkorn Memorial Hospital. All samples were collected from May 2021 to December 2021. Control samples were collected from patients without a family history of cancer, autoimmune diseases and showed negative CRC screening results from colonoscopy. This group served as normal controls for this study. Colorectal cancer staging was assessed by the American Joint Committee on Cancer TNM system by a trained pathologist. Venous whole blood (2 mL) with anticoagulant EDTA was collected from participants based on WHO guidelines and after informed consent. See Chapter 2 for Ethics approval.

3.3.1 Validation of p16 antibodies

Differences in clones that express antibodies recognizing different p16^{INK4A} epitopes can affect the outcomes of the experiments based on immuno-assays (Sawicka et al., 2013; Shain et al., 2018). The p16^{INK4A} antibodies used in this study were validated using the following cell lines: HeLa (American Type Culture Collection: ATCC$^®$ CCL-2™); HCT116 (American Type Culture Collection: ATCC$^®$ CCL-

247™); and rat epidermal keratinocytes (RA-6066K, Cell Biologics Inc). Antibodies to p16^{INK4A} (Cell Signaling) were rabbit monoclonal antibodies: D3W8G (92803) was raised against synthetic peptide residues surrounding Ala34 of human p16^{INK4A} protein, while D7CM1(80772) was raised against the synthetic peptide residues surrounding Ala143 of human p16^{INK4A} protein. D3W8G and D7CM1 antibodies showed positive staining in HeLa cells (**Fig 5a and 5b**), D7CM1 antibodies had strong cytoplasmic staining in keratinocytes (**Fig 5c**), while D3W8G antibodies showed nuclear staining in keratinocytes (**Fig 5d**). HCT116 cells were used as a negative control for p16^{INK4A} staining (**Fig 5e and 5f**) (Myöhänen et al., 1998). Cytoplasmic p16^{INK4A} could have various functions other than its canonical function of cell cycle regulation and senescence (Buj and Aird, 2019) and so D3W8G antibodies that stained nuclei were subsequently used in this study.
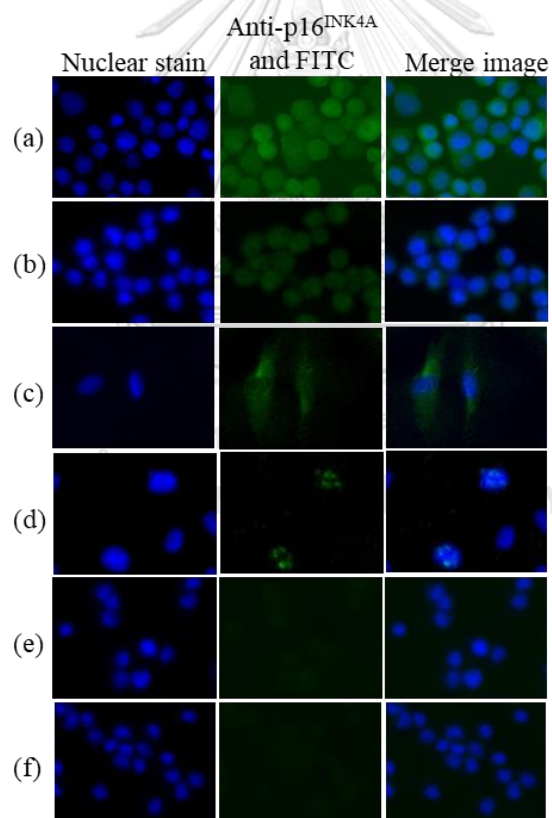
Figure 5: *Immunofluorescence staining of p16^{INK4A} antibodies in cell lines*
(a) HeLa cells with p16^{INK4A} D7CM1 antibodies showing strong cytoplasmic staining, (b) HeLa cells with p16^{INK4A} D3W8G antibodies, (c) Rat epidermal keratinocytes with p16^{INK4A} D7CM1 antibodies showing cytoplasmic staining, (d) Rat epidermal keratinocytes with p16^{INK4A} D3W8G antibodies showing nuclear staining, (e) HCT116

with p16 ^{INK4A} D7CM1 antibodies as a negative control, (f) HCT116 with p16 ^{INK4A} D3W8G antibodies as a negative control.

3.3.2 p16^{INK4A} in white blood cells of CRC patients and controls

p16^{INK4A} levels were measured in the peripheral white blood cells of CRC patients and normal controls by immunofluorescence (**Fig 6a**). Since p16^{INK4A} levels can depend on donor age, the healthy controls were age- and sex-matched to the CRC cohort. Comparison of CRC cases with healthy controls revealed a statistically-significant increase in MFI per cell between CRC patients compared to controls (**Fig 6b**) (95% CI = 2.8 to 11.9, p = 0.003).

Then, a second study was performed in which the number of samples both in CRC and control were increased (but these had a different male: female ratio because of random sampling). The total number of CRC patients was 72 with a mean age of 64.54±11.3 years, while that of healthy controls was 79 with a mean age of 63.91±8.8 years. Cases and controls demographics are shown in **Table 3**. The minimum age of the study participants was 31 years and maximum age was 89 years. The values in samples were normally distributed according to Shapiro-Wilk test. Therefore, we calculated the difference between the two groups with the independent sample t-test. Among the total number of CRC (n=72) and control (n=79), there was a statistically-significant increase MFI of p16^{INK4A} in WBC of CRC patients compared to healthy controls (**Fig 6c**) (95% CI = 4.5 to 8.3, p<0.001).
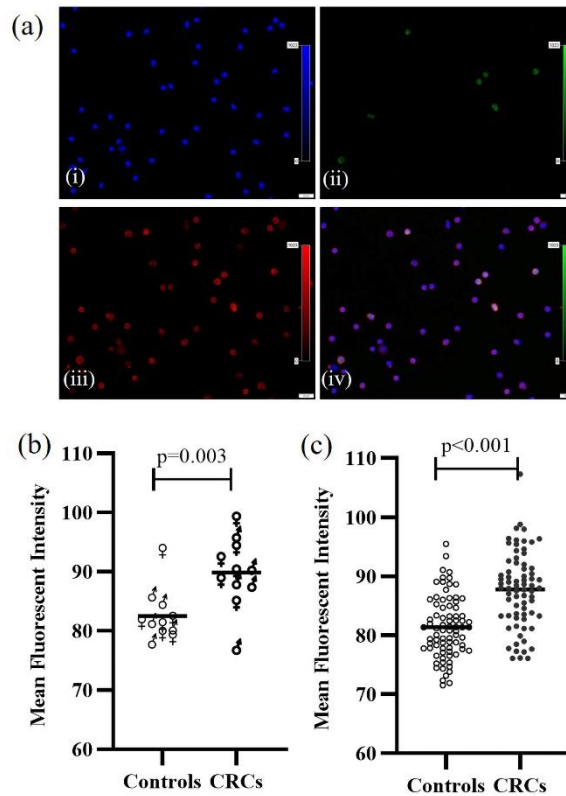
Figure 6: p16^{INK4A} immunofluorescence staining of WBCs
(a) Immunofluorescence staining of WBCs showing DAPI staining (i), p16^{INK4A} staining (ii), CD45 staining (iii) and merged image (iv). The bar marker on the images represents 20μm, (b) Scatter plot of p16^{INK4A} MFI of healthy controls and p16^{INK4A} MFI of CRC group (age and sex adjusted cohort study), (c) Scatter plot of p16^{INK4A} MFI of healthy controls and p16^{INK4A} MFI of CRC group. The bar on the scatter plot represents the mean value. a and b are data from two separate study cohorts

Table 3: *Cases and Controls demographics and clinical criteria of CRC patients for p16^{INK4A} analysis*

Parameters	N	%	Elderly population for each category (Age 65 and above) N (%)
Age (range) of Normal Controls			
<50	3	3.8	0
50-64	39	49.4	0
65 and above	37	46.8	37 (100)
Gender of Normal Controls			
Male	31	39.2	16 (51.6)
Female	48	60.8	21 (43.8)
Age (range) of CRCs			
<50	5	6.9	0
50-64	27	37.5	0
65 and above	40	55.6	40 (100)
Gender of CRCs			
Male	45	62.5	24 (53.3)
Female	27	37.5	16 (59.3)
Stages of CRCs			
I	6	8.6	3 (50.0)
II	17	24.3	13 (76.5)
III	26	37.1	12 (46.2)
IV	21	30.0	10 (47.6)
Tumor size of CRCs			
T1	4	5.7	2 (50)
T2	8	11.4	5 (62.5)
T3	42	60.0	22 (52.4)
T4	16	22.9	9 (56.3)

Lymph node involvement of CRCs			
N0	29	41.4	19 (65.5)
N1	29	41.4	15 (51.7)
N2	12	17.1	4 (33.3)
Metastasis status of CRCs			
Metastasis	21	30.0	11 (52.4)
Non metastasis	49	70.0	27 (55.1)
Tumor histological types of CRCs			
Well differentiated adenocarcinoma	14	20.0	8 (57.1)
Moderately differentiated adenocarcinoma	47	67.1	24 (51.1)
Poorly differentiated adenocarcinoma	1	1.4	1 (100)
Epithelioid cell carcinoma	1	1.4	0
Mucinous adenocarcinoma	5	7.1	4 (80)
Signet ring cell carcinoma	2	2.9	1 (50)
Left or right-side tumor of CRCs			
Left side	62	88.6	32 (51.6)
Right side	8	11.4	6 (75.0)
Tumor location of CRCs			
Cecum	2	2.9	2 (100.0)
Ascending colon	4	5.7	3 (75.0)
Hepatic flexure	1	1.4	0
Transverse colon	1	1.4	1 (100.0)
Descending colon	5	7.1	5 (100.0)
Sigmoid colon	12	17.1	7 (58.3)
Recto-sigmoid colon	2	2.9	1 (50.0)
Rectum	43	61.4	19 (44.2)

T1 = the cancer has grown through the muscularis mucosa into the submucosa, **T2** = the cancer has grown into the muscularis propria, **T3** = the cancer has grown into the outermost layers of the colon or rectum but has not gone through them, **T4** = the cancer has grown through the wall of the colon or rectum, **N0** = the cancer has not spread to nearby lymph nodes, **N1** = the cancer has spread to 1 to 3 nearby lymph nodes, **N2** = the cancer has spread to 4 to 6 nearby lymph nodes.

3.3.3 p16^{INK4A} expression in CD3+ cells, CD14+ cells and their percent positive cells

Double immunofluorescence staining was then used to investigate if lymphocytes or monocytes, or both stained positive for p16^{INK4A}. Antibodies to p16^{INK4A} and CD3 were used to detect p16^{INK4A}-positive T lymphocytes (**Fig 7a**) while for the monocyte population, antibodies against p16^{INK4A} and CD14 were used (**Fig 7b**). Mean fluorescence intensity of p16^{INK4A} in CD3+ cells and CD14+ cells were calculated in CRC patients and normal controls. A significant increase in levels of p16^{INK4A} was observed in both CD3+ cells (95% CI = 0.2 to 9.1, p = 0.04) and CD14+ cells (95% CI = 0.2 to 6.3, p = 0.04) of CRC patients compared to healthy controls (**Fig 7c**).
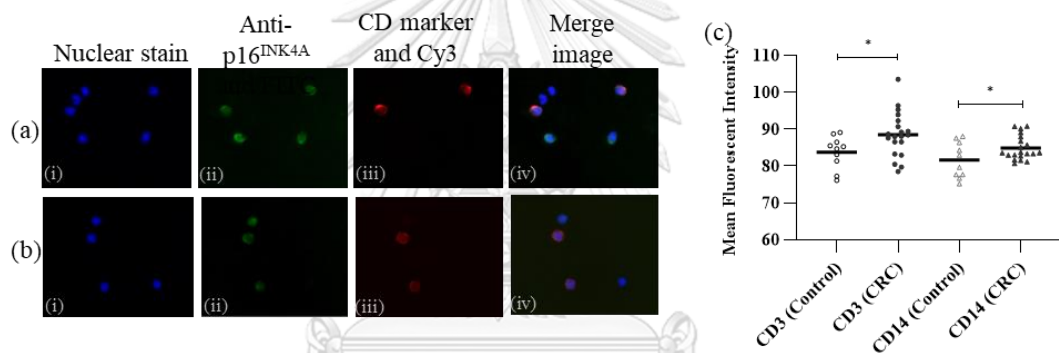
Figure 7: *p16^{INK4A} Immunofluorescence staining of T lymphocytes and monocytes*
(a) Immunofluorescence staining of CD3+ peripheral immune cells showing DAPI staining (i), p16^{INK4A} staining (ii), CD3 staining (iii) and merged image (iv),
(b) Immunofluorescence staining of CD14+ peripheral immune cells showing DAPI staining (i), p16^{INK4A} staining (ii), CD14 staining (iii) and merged image (iv),
(c) Scatter plots of p16^{INK4A} MFI of healthy controls and CRC group in CD3+ and CD14+ cells. The bar on the scatter plot represents the mean value, *=p<0.05.

The number of p16^{INK4A}-positive white blood cells also increased in CRC patients, revealing a significant difference in the CD45+ subset (95% CI = 3.2 to 24.3, p = 0.01), in the CD3+ subset (95% CI = 0.06 to 17.1, p = 0.05) and in the CD14+ subset (95% CI = 1.0 to 13.2, p = 0.02) (**Fig 8a**). When the number of p16^{INK4A} positive cells and MFI of each cell subset were combined in a graph, there was an increasing trend of higher values in p16^{INK4A} and percent positive cells in the CRC groups (**Fig 8b, 8c and 8d**).
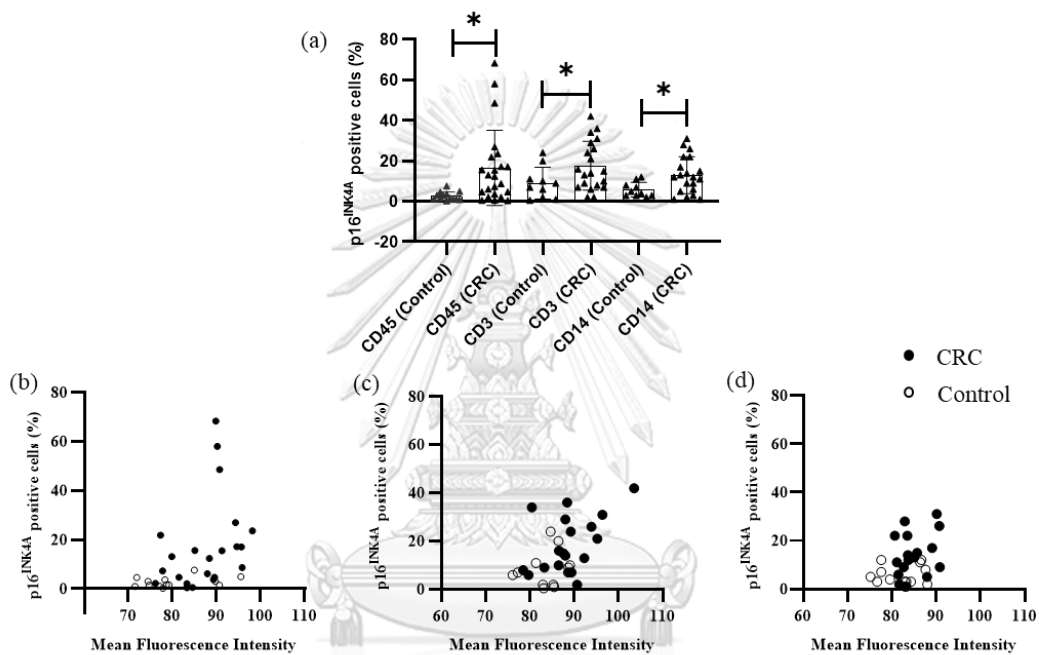
Figure 8: *p16^{INK4A} positive cells in WBCs, T lymphocytes and monocytes*
(a) Comparison of p16^{INK4A} positive cells in WBCs, CD3+ cells and CD14+ cells between CRC group and healthy control group, (b) Correlation of p16^{INK4A}-positive cells percentage and p16^{INK4A} mean fluorescent intensity of CRC patients and healthy controls in white blood cells, (c) Correlation of p16^{INK4A}-positive cells percentage and p16^{INK4A} mean fluorescent intensity of CRC patients and healthy controls in CD3+ cells, (d) Correlation of p16^{INK4A}-positive cells percentage and p16^{INK4A} mean fluorescent intensity of CRC patients and healthy controls in CD14+ cells.

3.3.4 Correlation of p16^{INK4A} mean fluorescence intensity of CRC patients with age, gender, clinical stages, tumor size, lymph node involvement, and metastasis versus non-metastasis

p16^{INK4A} protein levels in CRC samples were analyzed based on clinical parameters such as the stages of CRC, tumor size, lymph node involvement, metastasis

status, patients age and histological types of tumors (**Fig 9 a-f**). Of the 72 patients from CRC group, clinical data of 2 patients were not available, so were excluded from the analysis. CRC samples were categorized based on age as: <50-years, 50-64 years, and 65 and above years. Approximately half of the patients (55.6%) were in the population range of 65 and above. There was no significant difference in $p16^{INK4A}$ levels among the age groups (F (2, 69) = 0.4, p = 0.7). When analysed according to gender, 62.5% of patients in the study were male and showed a higher MFI of $p16^{INK4A}$, but this was not a statistically-significant difference (t=1.3, p=0.2). When the $p16^{INK4A}$ levels were observed according to the stages, size and lymph node involvement of tumors, their levels were similar, showing the statistical values of stage (F (3, 66) = 0.1, p = 0.9), tumor size (F (3, 66) = 0.3, p = 0.8) and lymph node involvement (F (3, 66) = 0.2, p = 0.8). Thirty percent of patients had metastasis, and their $p16^{INK4A}$ MFI were not statistically-different from those of non-metastasis patients (t = 0.5, p = 0.6). Clinical data of CRC patients are shown in **Table 3**.
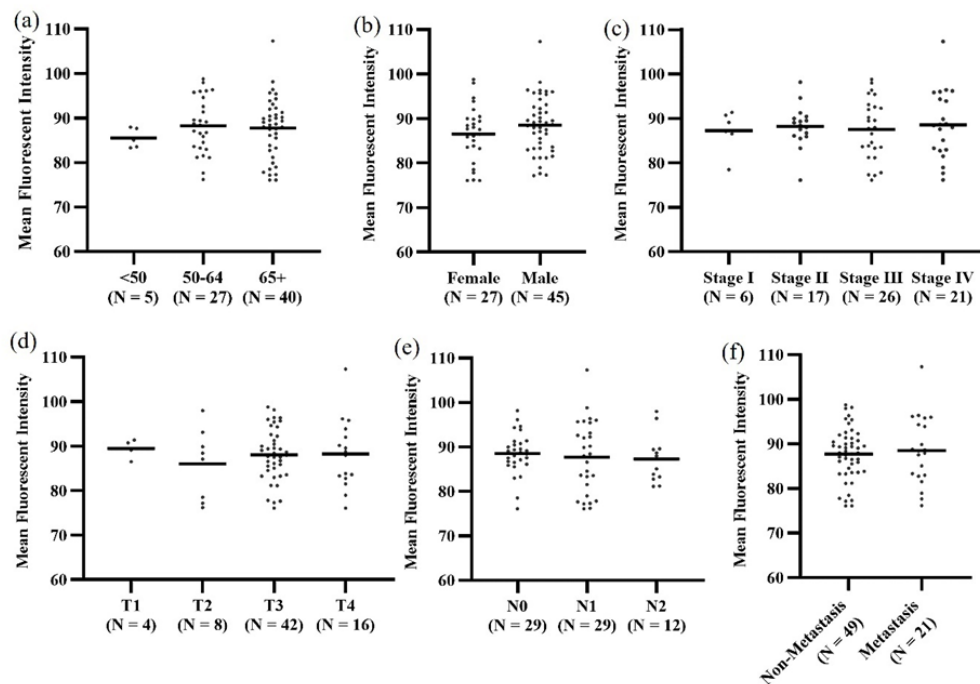
Figure 9: *Correlation of p16^{INK4A} mean fluorescence intensity of CRC patients with clinical parameters*
(a) Data from CRC patients were grouped according to age, (b) gender, (c) Clinical stages of CRC, (d) tumor sizes, (e) LN involvement and (f) metastasis or non-metastasis.

3.3.5 Evaluation of p16^{INK4A} as a marker of disease in CRC patients

These results supported the potential of p16^{INK4A} levels in peripheral immune cells to be used as a marker in CRC patients, as the p16^{INK4A} level of peripheral white blood cells increased in CRC patients compared to controls. A ROC curve was calculated using the MFI of p16^{INK4A} in CD45+ cells of patients and controls. Area under the curve was 78% (p <0.001) with the standard error value of 0.04. There was 78% sensitivity and 71% specificity with Youden index of 0.48, cut-off value of 83.26 MFI (**Fig 10**). From 2x2 table, true positive (TP) number for CRC was 56, false negative (FN) number for CRC was 16, false positive (FP) number for normal control was 23 and true negative (TN) number for normal control was 56. Therefore, sensitivity (TP/TP+FN) is 78%, specificity (TN/FP+TN) is 71%, positive predictive value (TP/TP+FP) is 71%, negative predictive value (TN/FN+TN) is 78% and accuracy (TP+TN / TP+FP+FN+TN) is 74%. The ROC curve data are available in **Appendix J**.
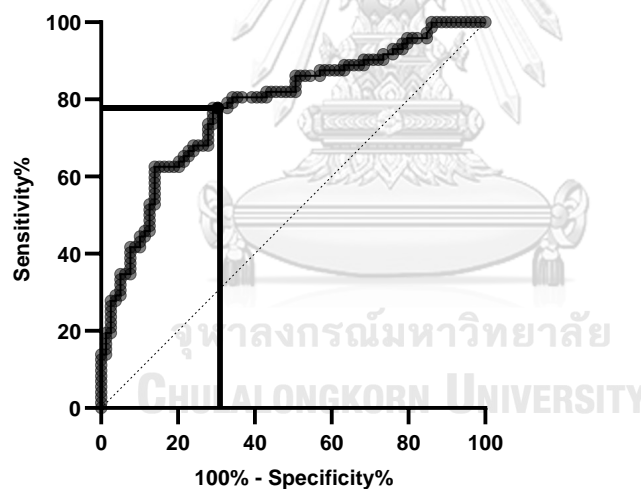
Figure 10: *ROC analysis of p16^{INK4A} in white blood cells of CRC patients and healthy controls*
The Youden index point at the vertical solid line and horizontal solid line showing 78% sensitivity and 71% specificity.

3.4 Discussion

Using an immunofluorescence technique, we measured both the intensity of staining of individual positive cells and the number of positive cells in WBC of CRC patients and healthy controls. The MFI of p16^{INK4A} in the WBC of CRC patients had a

significantly higher value than that of the healthy control group in this study. P16^{INK4A} in peripheral immune cells represents 78% sensitivity and 71% specificity for application as a potential CRC screening marker. Proteins, DNA, RNA and metabolites from tissue, blood, stool and urine have been used in CRC for screening, diagnosis and monitoring, but have varying degrees of success to be used as an effective biomarker (Loktionov, 2020). Colonoscopy has been used as the gold standard for the diagnosis of CRC (Hazewinkel and Dekker, 2011) and blood-based protein biomarkers for detection of CRC have various sensitivities and specificities, but using a protein panel rather than single proteins increases the detection rate of CRC (Loktionov, 2020).

Increased expression of p16^{INK4A} has been reported in the peripheral blood cells of testicular cancer survivors (Bourlon et al., 2020) and breast cancer survivors (Sanoff et al., 2014). The presence of p16^{INK4A} in immune cells can represent a feature of immuno-senescence (Liu et al., 2009). Immuno-senescence is initiated earlier in men than in women, likely due to hormonal differences between males and females, as estrogen enhances immune responses, while progesterone and androgens favor immune suppressive actions (Ostan et al., 2016). Therefore, age and sex-adjusted CRC patients and controls were investigated. The MFI in CRC group was significantly higher, meaning that immuno-senescence can contribute to CRC patients regardless of age and sex. Immuno-senescence can result from oxidative stress, cellular and DNA damage, chronic inflammation and cytotoxic therapy (De Padova et al., 2021). According to Giunco, *et al*, immuno-senescence in CRC patients can lead to negative consequences like disease relapse, progression and death (Giunco et al., 2019).

The CRC group showed increased p16^{INK4A} levels compared to normal controls. However, the stages of CRC were not correlated to the levels of p16^{INK4A} which is similar to the finding of Milde-Langosch, *et al* who reported p16^{INK4A} that expression was not correlated with the clinical stages of breast cancer (Milde-Langosch et al., 2001). MFI values of p16^{INK4A} were higher in some categories and found to be relatively high in the categories of late stage, male patients and old age, but there were no statistically-significant differences. The immune landscape in the elderly population and metastasis patients differ from other patients in both innate and adaptive immune system (Weng, 2006; Fulop et al., 2017; Blomberg et al., 2018). Various factors can

influence the levels of $p16^{INK4A}$ in immune cells, because $p16^{INK4A}$ has an impact on immune surveillance (Sznurkowski et al., 2017; Leon et al., 2021). Limitations of this study include the small sample size (n) of some categories and due to the nature of this cross-sectional study, and so it cannot be conclusively shown that $p16^{INK4A}$ level correlates to the prognosis of the patients.

Protein expression of $p16^{INK4A}$ was higher in T cell subsets of CRC patients and these cells are important for tumor immunity and immunotherapy (Woolaver et al., 2021). Senescent T cells relate to progression of cancers (Vicente et al., 2016) and in in CRC patients also relate to negative patient outcomes such as disease relapse, disease progression and death (Giunco et al., 2019). $p16^{INK4A}$ expression in peripheral blood T cells is associated with chronologic age, molecular age, and IL-6 production (Liu et al., 2009; Burd et al., 2020). IL-6 is important in human frailty (Soysal et al., 2016) and relates to cellular senescence (Kojima et al., 2013). $p16^{INK4A}$ protein expression increases in T cells of peripheral blood and bone marrow of acute lymphoblastic leukemia and its expression correlates to senescent features (Chebel et al., 2007).

Monocytes also expressed $p16^{INK4A}$ protein in CRC patients in this study. Monocytes are a heterogenous group of cells and a typical portion (about 85%) of monocytes are classical monocytes ($CD14^{++}$ $CD16^{-}$), the rest (5 to 10 % each) are intermediate monocytes ($CD14^{++}$ $CD16^{+}$) and non-classical monocytes ($CD14^{+}$ $CD16^{+}$) (Coillard and Segura, 2019; Kapellos et al., 2019b). Monocyte recruitment to inflammation sites and cancer tissues is an important process and it can occur within hours of onset of inflammation (Coillard and Segura, 2019). Moreover, monocytes can be transformed into monocyte-derived macrophages (Mo-mac) and monocyte-derived dendritic cells (mo-DC) (Coillard and Segura, 2019) while $p16^{INK4A}$ can stimulate the maturation of mo-DC through the MAPK pathway (Sunthamala et al., 2020). Mo-DC can be found especially in the intestines (Watchmaker et al., 2014) and $p16^{INK4A}$ is associated with macrophage polarization, as M2 macrophage showed increased level of $p16^{INK4A}$ (Hall et al., 2017).

CHAPTER IV: IMMUNOPHENOTYPIC CHANGES IN AGEING

4.1 Introduction

Different types of immune cells have distinct immune functions and can be classified based on the markers expressed on their cell surface (see Table 1). However, these sub-populations of cells are highly dynamic and can change as a result of infections or non-infectious diseases, and also during ageing. The aim of this study was to determine if these immune cell phenotypes are altered in CRC, but as CRC is a disease more commonly detected in the elderly, it was first necessary to characterize these sub-populations in a cohort of healthy individuals that cover a wide age range. Immunophenotypes of T lymphocytes, NK cells and monocytes were therefore first identified in healthy controls (HCs) and correlation studies of immunophenotypes with age were performed. The effect of ageing on immunophenotypes was examined between two groups of HCs: ≤50y group and >50y group (see later for justification). This is an investigative study in order to compare immune phenotypes of HCs and patients with CRC as a function of age (Chapter 5), and to assess whether this approach would justify a study with a larger cohort of patients with different stages of CRC.

The proportion of monocytes increased with a reduction of lymphocytes during ageing, which indicates myeloid skew (i.e., increased monocyte: lymphocyte ratio). In the >50 y group, most T cells subsets decreased in numbers, intermediate monocytes increased in most participants and CD4+ monocytes increased significantly. NK cell expansion was observed with age and CD3 intensity per cells and HLA-DR positivity increased in this group.
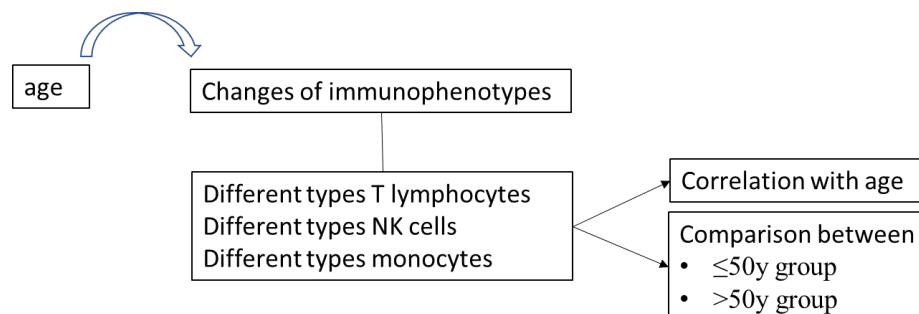
4.2 Aim

To identify immunophenotypic changes of T cells, NK cells and monocytes in ageing.

4.3 Results

Table 4: Result summary for immunophenotypic changes in ageing

+++/ ---	= significant increased or decreased (p<0.05)
++/--	= median value and interquartile values increased or decreased (>10% for value less than 50, >5% for values greater than 50)
+/ -	= median value or interquartile values increased or decreased (>10% for value less than 50, >5% for values greater than 50)
0	= no obvious change
Median	= middle value of the data set
Q1	= 25th percentile of the data set
Q3	= 75th percentile of the data set
Values in table	= percent positive cells

	≤50y (n= 11)			>50y (n = 13)			
	Median	Q1	Q3	Median	Q1	Q3	Difference (compared to ≤50y)
T lymphocytes (% of all lymphocytes)	73.05	70.93	78.1	67.75	62.6	74.75	- - -
% of T lymphocytes							
Helper T cells	40.2	34.4	57	61.8	40.8	70.2	+ +
Cytotoxic T cells	39.2	36.2	44	30.1	25.75	44.6	-
DN T cells	6.365	3.835	7.998	3.49	2.02	5.025	- - -
DP T cells	0.72	0.545	0.935	0.39	0.273	0.9	-
NK T cells	4.64	3.88	17.45	2.98	1.315	5.608	- -
% of Helper T cells							
EA helper T cells	89.3	86.8	95.4	93.6	87.7	95.55	0
SL helper T cells	5.18	1.28	7.46	0.25	0.108	1.52	- - -
DN helper T cells	1.05	0.35	1.35	0.63	0.092	1.67	-
DP helper T cells	4.54	2.21	5.54	6.04	3.23	8.615	+ +

% of cytotoxic T cells							
EA cytotoxic T cells	44.4	24.3	64.1	41.5	21.15	69.1	0
SL cytotoxic T cells	41.2	18.6	56.8	35.7	11.15	62.55	-
DN cytotoxic T cells	8.82	6.84	13.6	6.31	4.265	16.3	-
DP cytotoxic T cells	2.56	2.16	6.74	8.18	4.36	9.875	+ +
% of CD8 T cells							
CD8^{low} T cells	6.425	4.63	13.88	6.515	2.933	9.848	-
CD8^{high} T cells	93.6	86.13	95.4	93.45	90.15	97.1	0
% of NK T cells							
CD4+ NK T cells	4.32	2.85	14.25	1.855	0.893	4.383	- -
CD8+ NK T cells	73.4	59.7	81.1	62.7	55.05	79.45	-
DN NK T cells	19.5	9.755	31.5	26.25	8.758	40.88	+
% of T lymphocytes							
HLA-DR-positive T cells	13.2	6.72	22.5	16.7	11.6	26.95	+ +
HLA-DR-negative T cells	86.8	77.5	93.3	83.2	73.05	88.4	-
NK cells (% of all lymphocytes)	12.5	8.535	16.35	15.3	10.9	19.1	+ +
% of NK cells							
NK^{bright}	6.08	4.475	9.24	5.9	2.33	10.02	0
NK^{dim}	93.91	90.81	95.52	94.12	89.99	97.71	0
% of NK cells							
NK^{bright} CD16+	3.45	2.08	4.525	1.92	0.66	4.69	-
NK^{bright} CD16-	3.26	2.29	5.03	3.98	0.89	7.86	0
NK^{dim} CD16+	89.5	75.9	91.95	88.9	81.2	94.3	+
NK^{dim} CD16-	3.8	1.845	10.72	3.72	2.24	8.79	0
% of NK cells							
CD4+ NK	0.15	0.049	0.325	0.18	0.067	0.313	+

CD8+ NK	33.7	26.15	39.65	34.3	28	40.4	0
DN NK	66.1	60.3	73.6	65.3	59.3	71.9	0
Monocytes (% of PBMC)	16.2	10.3	20.3	22.9	17.55	27.55	+++
% of Monocytes							
classical monocytes	90.85	87.18	94.4	82.55	68.93	89.75	- - -
intermediate monocytes	4.47	1.838	7.008	9.26	3.398	20.95	++
non-classical monocytes	4.555	2.63	6.555	5.53	2.383	7.933	+
% of Monocytes							
CD4+ monocytes	1.7	0.715	3.773	7.41	1.973	10.3	+++
CD56+ monocytes	4.18	3.128	6.965	2.835	1.43	6.215	- -
% of Monocytes							
HLA-DR^{low} monocytes	12.2	5.46	15.4	6.82	5.65	20.05	-
HLA-DR^{high} monocytes	87.1	83.3	93.8	92.2	78.5	93.9	+

Healthy volunteers from University of Liverpool were recruited from May 2022 to November 2022. Whole blood from healthy controls (no known or disclosed illness) without a family history of colorectal cancer were collected. Ten ml whole blood with EDTA anticoagulant was collected to perform immuno-phenotyping of lymphocytes and monocytes. Healthy controls were mean age of 51.3±19 y, minimum 23 y, maximum 89 y and male: female of 12:12.

After the age of 40 y, the cellularity of bone marrow gradually declines (Mamatha et al., 2009). Moreover, the perivascular space of the thymus increases in ageing and these changes are completed by the age of 40-50 y (Weiskopf et al., 2009). Reduction of T cell diversity occurs after 50 y of age (Joseph et al., 2022). Therefore, immuno-phenotypic changes of ageing were studied in two groups of HCs: ≤50y (mean age ± SD is 30.6 ± 9.1, M:F is 5:6) and >50y (mean age ±SD is 64.5±10.8, M:F is 6:7).

4.3.1 Immuno-phenotyping of lymphocytes and monocytes and their correlation with donor age

T lymphocytes were classified with surface markers CD45, CD3, CD4, CD8, CD56, CD28 and CD57 into the following phenotypes (**Fig 11a**):

- helper T cells (CD3+ CD4+ CD8-)
- cytotoxic T cells (CD3+ CD4- CD8+)
- DN T cells (CD3+ CD4- CD8-)
- DP T cells (CD3+ CD4+ CD8+)
- NK T cells (CD3+ CD56+)

Helper T cells were sub-divided into 4 types (**Fig 11b**):

- early-activated (EA) helper T cells (CD3+ CD4+ CD28+ CD57-)
- senescence-like (SL) helper T cells (CD3+ CD4+ CD28- CD57+)
- double-negative (DN) helper T cells (CD3+ CD4+ CD28- CD57-)
- double-positive (DP) helper T cells (CD3+ CD4+ CD28+ CD57+)

Cytotoxic T cells were sub-divided into 4 types (**Fig 11c**):

- EA cytotoxic T cells (CD3+ CD8+ CD28+ CD57-)
- SL cytotoxic T cells (CD3+ CD8+ CD28- CD57+)
- DN cytotoxic T cells (CD3+ CD8+ CD28- CD57-)
- DP cytotoxic T cells (CD3+ CD8+ CD28+ CD57+)

Based on CD8 expression intensity, cytotoxic T cells were categorized into 2 types (**Fig 11a**):

- $CD8^{low}$ T cells (CD3+ CD8+/-)
- $CD8^{high}$ T cells (CD3+ CD8++)

NK T cells were sub-divided into 3 types (**Fig 11a**):

- CD4+ NK T cells (CD3+ CD56+ CD4+ CD8-)
- CD8+ NK T cells (CD3+ CD56+ CD4- CD8+)
- DN NK T cells (CD3+ CD56+ CD4- CD8-)

CD3+ staining together with HLA-DR staining identified T cells into two categories as (**Fig 11d**):

- HLA-DR-positive T cells
- HLA-DR-negative T cells

NK cells were selected from the lymphocyte region after gating out T cells (with CD3), B cells (with CD19), other cells (with CD14), and selecting cells positive for CD56. Based on CD56 expression intensity, NK cells were categorized as:

- NK^{bright} (CD56++)
- NK^{dim} (CD56+) (**Fig 12a**)

The CD56+ NK cells were then grouped into 4 types with CD16 (**Fig 12a**):

- $CD56^{bright}$ CD16-
- $CD56^{bright}$ CD16+
- $CD56^{dim}$ CD16-
- $CD56^{dim}$ CD16+

CD56+ NK cells were further sub-grouped into 3 types based on CD4 and CD8 positivity (**Fig 12a**):

- CD4 NK (CD56+ CD4+ CD8-)
- CD8 NK (CD56+ CD4- CD8+)
- DN NK (CD56+ CD4- CD8-)

Monocytes were gated with CD45, CD14, CD16, CD4 and CD56 into 5 categories (**Fig 12b**):

- classical monocytes (CD14++ CD16-)
- intermediate monocytes (CD14++ CD16+)
- non-classical monocytes (CD14+ CD16+)
- CD4+ monocytes (CD14+ CD4+)
- CD56+ monocytes (CD14+ CD56+)

CD14 antibody together with HLA-DR antibody, identified monocytes in two categories as (**Fig 12c**):

- HLA-DR^{low} monocytes
- HLA-DR^{high} monocytes

The percentage positive cells of each of these immuno-phenotypes were correlated with the age of the participants. In this study group, there were significant decreases in classical monocytes, total T cells, HLA-DR negative T cells and DN T cells, and significant expansion of NK cells, HLA-DR positive T cells, helper T cells, DP helper T cells, monocytes and intermediate monocytes in the >50 y group. Positive and negative correlations of IPs to age are shown in **Table 5**.
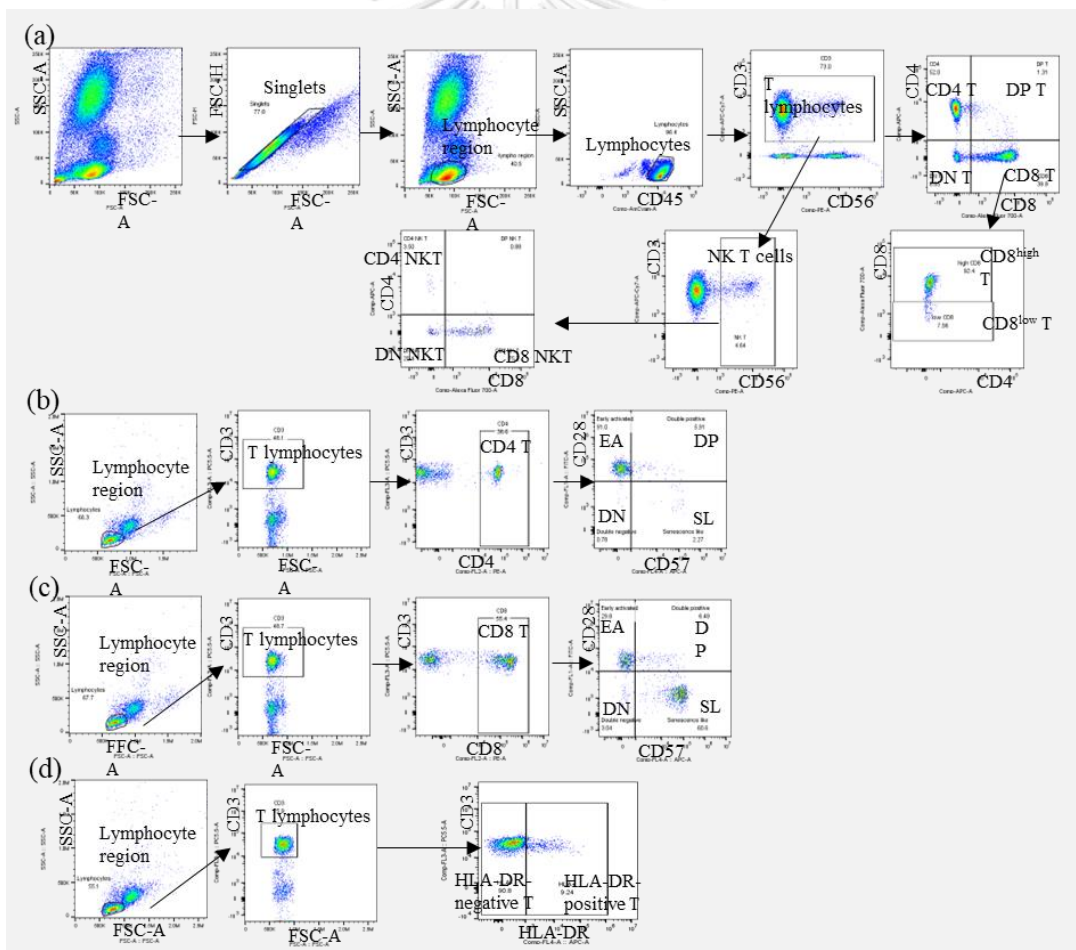
Figure 11: *Gating strategies of T lymphocytes*
(a) Gating for lymphocytes with Duraclone basic immuno-phenotyping kit, (b) Gating for different types of helper T cells, (c) Gating for different types of cytotoxic T cells, (d) Gating for HLA-DR-positive and HLA-DR-negative T cells
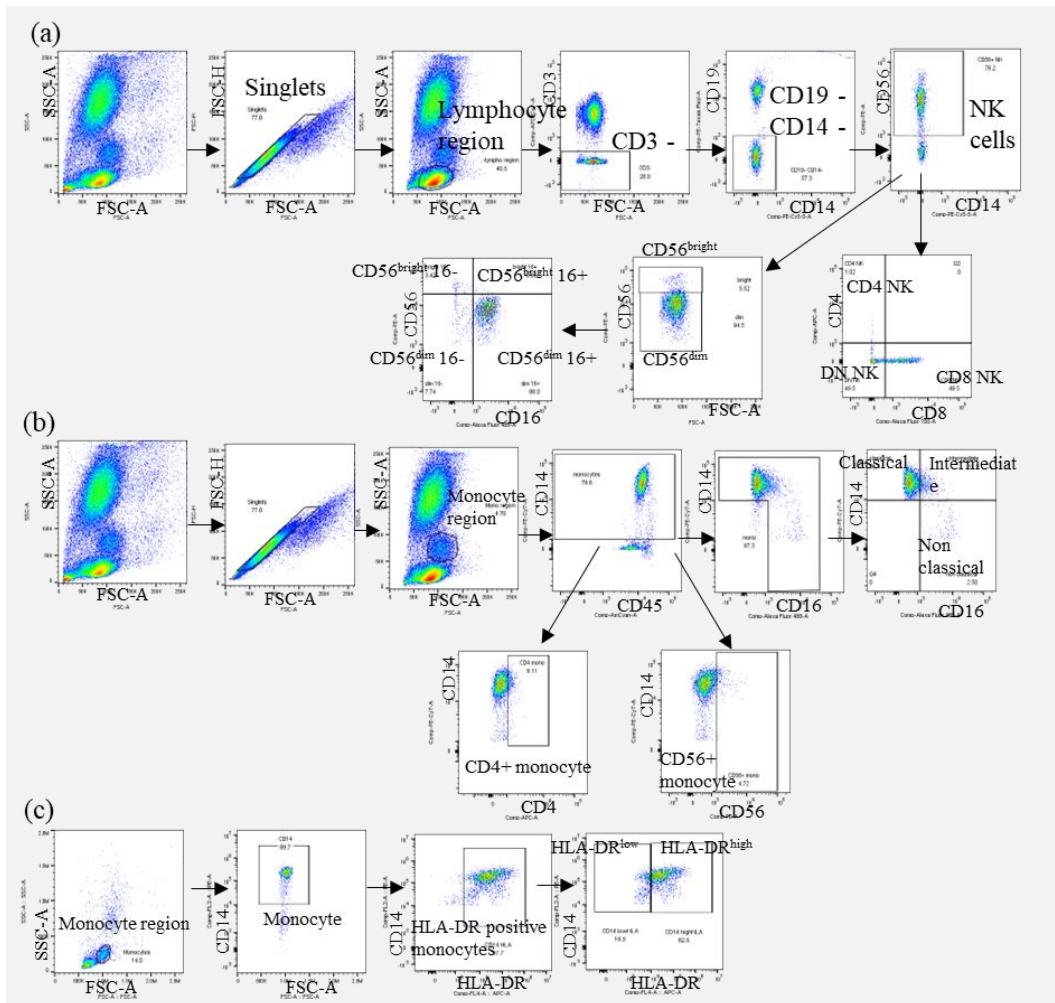
Figure 12: *Gating strategies of NK cells and monocytes*
(a) Gating for different types of NK cells, (b) Gating for different types of monocytes, (c) Gating for HLA-DR positive monocytes into HLA-DR^{low} and HLA-DR^{high} populations.

Table 5: *Correlation of immuno-phenotypes and age*

Negatively correlated IPs (decreasing with age)	r value	p	Positively correlated Ips (increasing with age)	r value	p
Classical monocytes	**-0.6**	**0.002**	NK	**0.5**	**0.03**
DN T	**-0.6**	**0.01**	HLA-DR-positive T	**0.5**	**0.02**
T lymphocytes	**-0.5**	**0.02**	Monocytes	**0.5**	**0.02**
HLA-DR-negative T	**-0.5**	**0.02**	Helper T	**0.4**	**0.04**
SL helper T	-0.4	0.1	Intermediate monocytes	**0.4**	**0.048**
NK T	-0.4	0.1	DP helper T	**0.4**	**0.049**
Cytotoxic T	-0.3	0.2	CD4+ mono	0.4	0.1
B lymphocyte	-0.3	0.2	DP cytotoxic T	0.4	0.1
CD8^{low}T	-0.3	0.2	CD8^{high}T	0.3	0.2
EA cytotoxic T	-0.3	0.2	Non classical monocytes	0.3	0.2
			HLA-DR^{high} monocytes	0.3	0.2

4.3.2 Changes in lymphocytes and monocytes

The number of T cells was significantly decreased, and the number of monocytes significantly increased in the >50y group. The interquartile range (IQR) of B lymphocytes decreased, and IQR of NK cells also increased in this population (**Fig 13a**). While the ratio of T lymphocytes to B lymphocytes was fairly consistent in the ≤50 y group (**Fig 13b**), there was a much broader ratio in the >50 y group showing greater variation and heterogeneity. The median value of the ratio of NK cells to T lymphocytes increased while that of lymphocytes: monocytes (L:M) decreased in the >50 y group (**Fig 13c, 13d**).

The intensities of expression of specific CD markers for immune cells were also analyzed. CD3 intensity on T lymphocytes was significantly increased in the >50 y group (**Fig 13e**). The intensity (MFI) of CD19 staining on B lymphocytes was also increased in the older age group **(Fig. 13f)**, as was intensity of staining of CD14 on monocytes **(Fig.13h)**, but these differences did not reach statistical significance.
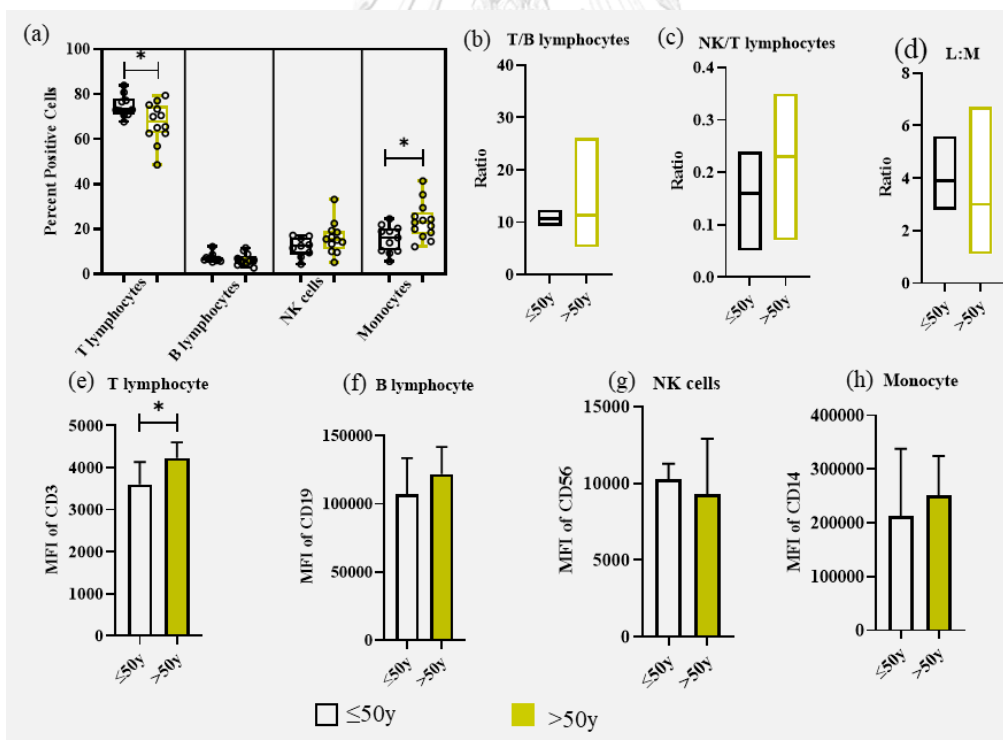
Figure 13: *Comparison of T lymphocytes, B lymphocytes, NK cells and monocytes between ≤50y and above-50y groups*
(a) percent positive cells, box represents IQR, line in box represents median, whiskers represent minimum and maximum, (b) ratio of T lymphocytes to B lymphocytes, (c) ratio of NK cells to T lymphocytes, (d) lymphocytes to monocytes ratio, bars represent range

*of ratio, lines in bars represent median, (e) CD3 intensity on T lymphocytes, (f) CD19 intensity on B lymphocytes, (g) CD56 intensity on NK cells, (h) CD14 intensity on monocytes. Bars represent median, whiskers represent 95% CI, * is p<0.05.*

4.3.3 Immunophenotypic changes of T cells

Overall, there were larger variations (larger IQR and/or longer whiskers) in the >50y group than the ≤50y group: helper T lymphocytes showed increased IQR, and the data set was left (negative)-skewed (higher values). Cytotoxic T, NK T, and DP T lymphocytes showed decreased IQR, but these differences did not reach statistical significance. However, a significant decrease in DN T cells was observed (**Fig 14a**).

Levels of CD3 expression in the different types of T cells were then compared in these two cohorts. The median values of CD3 intensities increased in all types of lymphocytes in the >50y age group, except for DP T cells, and the increased expression in helper T cells was statistically-significant (**Fig 14b**).
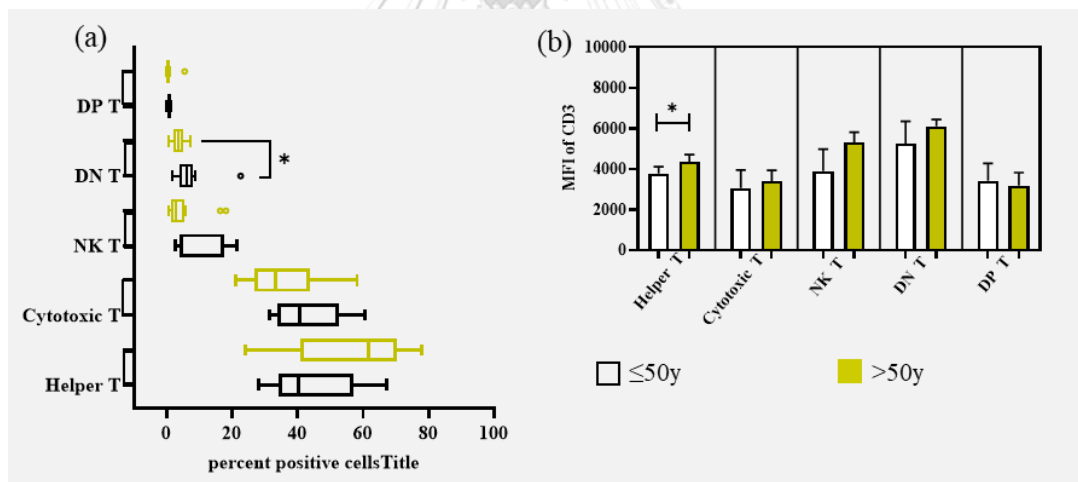
Figure 14: *Comparison of different types of T cells between the ≤50y group and the >50y group*
*(a) percent positive cells, Tukey graph: boxes represent 25% to 75% of samples, lines in boxes represent median, whiskers represent 1.5 times the IQR, dot represents outlier, * is p<0.05, (b) Intensity of CD3 staining in different types of T cells: bars represent median, whiskers represent 95% CI, * is p<0.05.*

For the different types of helper (CD4) T cells in the >50y group, the early-activated (EA) T cells were left (negative)-skewed (higher values), and senescent-like (SL) cells were significantly decreased. There were lower numbers of double negative (DN) cells (right-skewed) and double positive (DP) cells had an increased IQR (**Fig 15a**).

In the >50y group, CD3 intensity on helper T cells increased especially in EA cells and DP cells (**Fig 15b**). CD4 expression of cells tended to increase but a significant increase was observed in EA cells (**Fig 15c**).
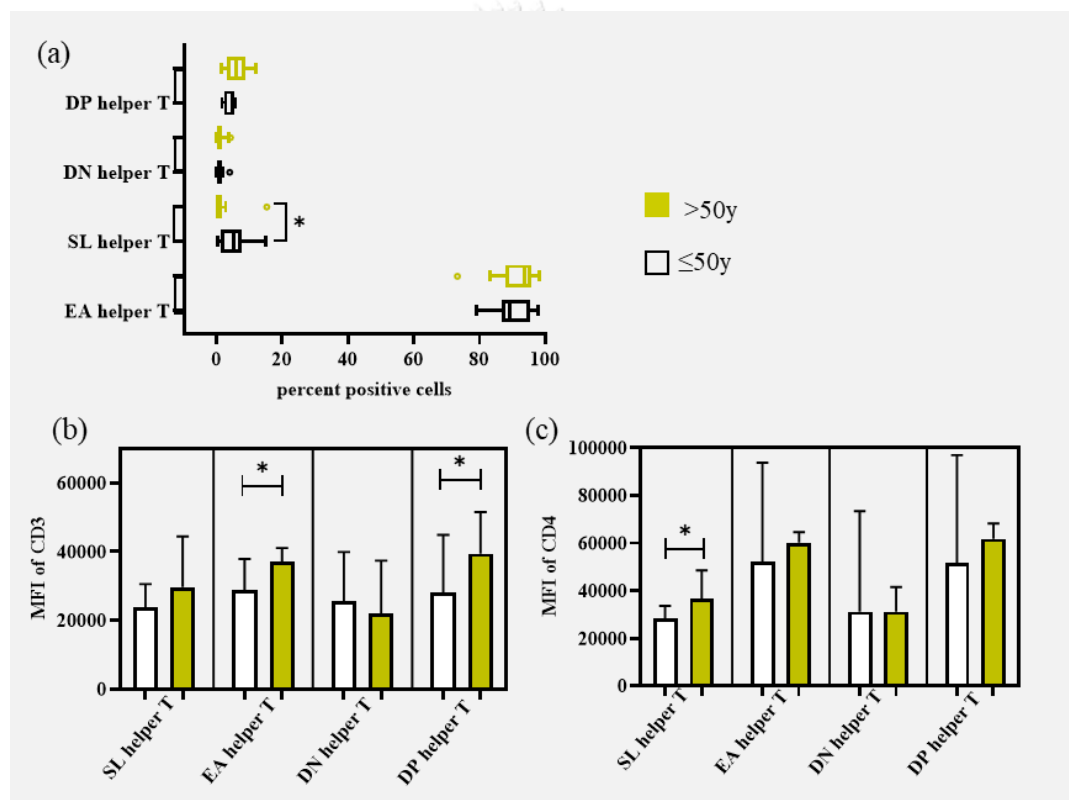
Figure 15: *Comparison of different types of helper T cells between ≤50y group and >50y group*
(a) percent positive cells, Tukey graph: boxes represent 25% to 75% of samples, lines in boxes represents median, whiskers represent 1.5 times the IQR, dot represents outlier, * is p<0.05, (b) Intensity of CD3 in different types of helper T cells, (c) Intensity of CD4 in different types of helper T cells. Bars represent median, whiskers represent 95% CI, * is p<0.05.

Cytotoxic T (CD8) cells in the >50y group had a larger IQR in EA cells, SL cells and DN cells while DP cytotoxic T cells of >50y had an increased IQR and were left-skewed (higher values) (**Fig 16a**). Cytotoxic T cells also showed increased CD3 expression; significant increases were observed in EA, DN and DP cells in the >50y group (**Fig 16b**), but no significant changes in CD8 expression were observed (**Fig 16c**).
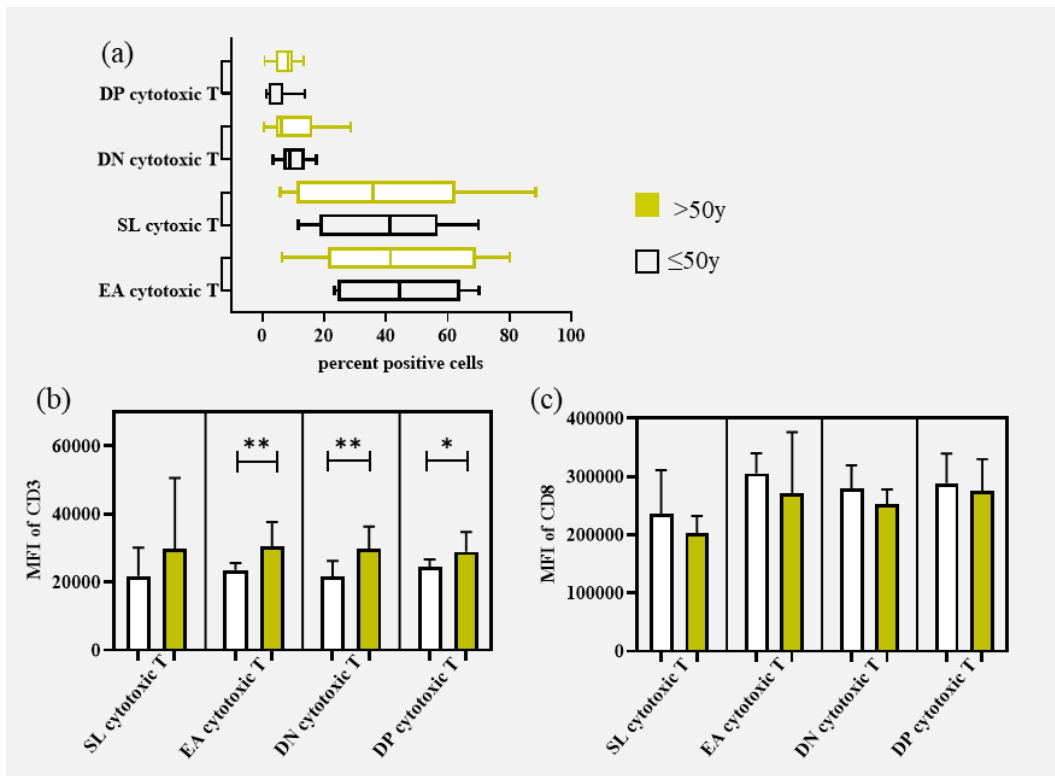
Figure 16: *Comparison of different types of cytotoxic T cells between ≤50y group and >50y group*
(a) percent positive cells, Tukey graph: boxes represent 25% to 75% of samples, lines in boxes represents median, whiskers represent 1.5 times of IQR, dot represents outlier, (b) Intensity of CD3 in different types of cytotoxic T cells, (c) Intensity of CD4 in different types of cytotoxic T cells. Bars represent median, whiskers represent 95% CI, * is p<0.05, ** is p<0.01.

SL helper T cells significantly increased (**Fig 15a**), and SL cytotoxic T cells tended to increase in the <50y group (**Fig 16a**). Other senescence markers were also examined in T lymphocytes, but no significant differences in beta-galactosidase and p16^{INK4A} expression were observed between the two groups (**Fig 17a, 17b**).
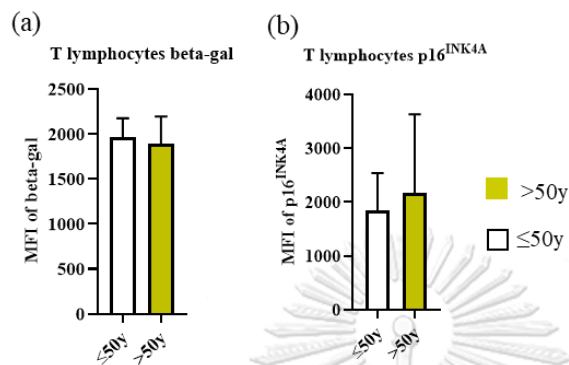
Figure 17: *Comparison of beta-gal and p16^{INK4A} expression in T lymphocytes between ≤50y group and >50y group*
(a) Beta-gal intensity, (b) p16^{INK4A} intensity. Bars represent median, whiskers represent 95% CI.

In NK T cells of the >50y group, CD4+ NK T had decreaed IQR but contained some outliers. CD8+ NK T data was right (positive)-skewed (lower values) with a larger IQR. DN NK T showed a larger IQR with the median value increased (**Fig 18a**).

CD3 intensity of DN NK T significantly increased in the >50y group (**Fig 18b**).
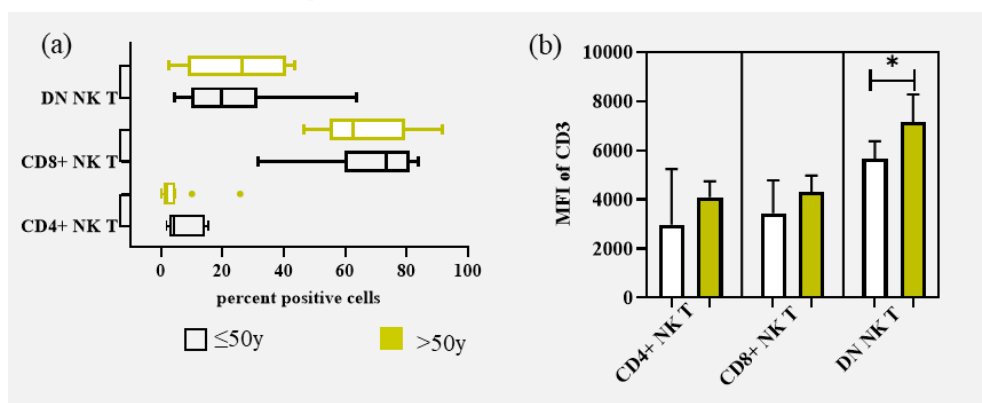
Figure 18: *Comparison of different types of NK T cells between ≤50y group and >50y group*
(a) percent positive cells, Tukey graph: boxes represent 25% to 75% of samples, lines in boxes represents median, whiskers represent 1.5 times of IQR, dot represents outlier,

* is p<0.05, (b) Intensity of CD3 in different types of NK T cells. Bars represent median, whiskers represent 95% CI, * is p<0.05.

CD8^{low} T cells of the >50y group showed decreased IQR while CD8^{high} T cells showed increased IQR (**Fig 19a**). No significant differences in CD3 and CD8 intensities were observed (**Fig 19b, 19c**).
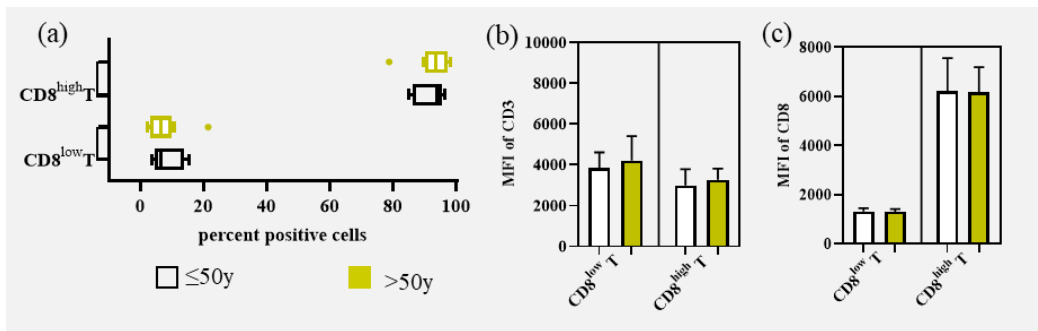
Figure 19: *Comparison of different types of CD8^{low} T and CD8^{high} T cells between ≤50y group and >50y group*
(a) percent positive cells, Tukey graph: boxes represent 25% to 75% of samples, lines in boxes represents median, whiskers represent 1.5 times of IQR, dot represents outlier, (b) Intensity of CD3 in CD8^{low} T cells and CD8^{high} T cells, (c) Intensity of CD8 in CD8^{low} T cells and CD8^{high} T cells. Bars represent median, whiskers represent 95% CI.

The IQR of HLA-DR-positive T cells was increased in >50y group (**Fig 20a**), while CD3 intensities of both groups were similar (**Fig 20b**). HLA-DR positivity significantly increased in lymphocytes of the older group (**Fig 20c**).
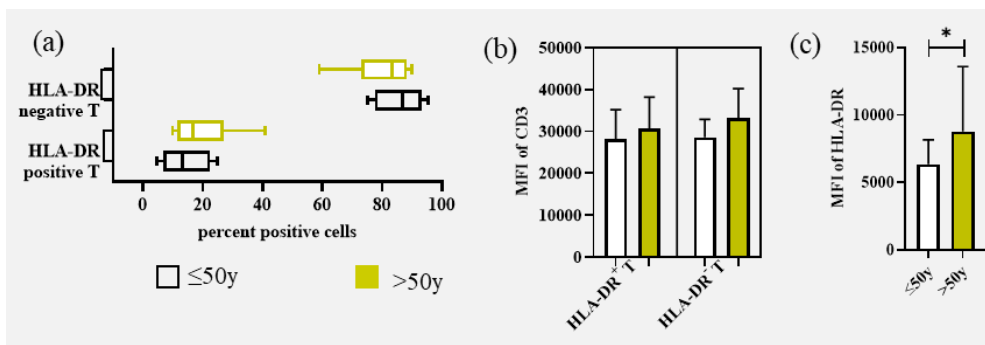
Figure 20: *Comparison of different types of HLA-DR$^+$ T and HLA-DR$^-$ T cells between ≤50y group and >50y group*
 (a) percent positive cells, Tukey graph: boxes represent 25% to 75% of samples, lines in boxes represents median, whiskers represent 1.5 times of IQR, dot represents outlier,

*(b) Intensity of CD3 in HLA-DR⁺ T and HLA-DR⁻ T cells, (c) Intensity of HLA-DR in HLA-DR⁺ T cells. Bars represent median, whiskers represent 95% CI, * is p<0.05.*

4.3.4 Immunophenotypic changes of NK cells

NK^{bright} and NK^{dim} of the >50y group had larger IQR, and NK^{bright} CD16- cells showed similar median values but with larger IQR. NK^{bright} CD16+ data were right-skewed (lower values) while NK^{dim} CD16- had similar median values. NK^{dim} CD16+ had increased IQR (**Fig 21a**). CD4 and CD8 expression in NK cells was similar in both groups (**Fig 21b**). CD56 intensities were also similar in both groups (**Fig 21c, 21d**).
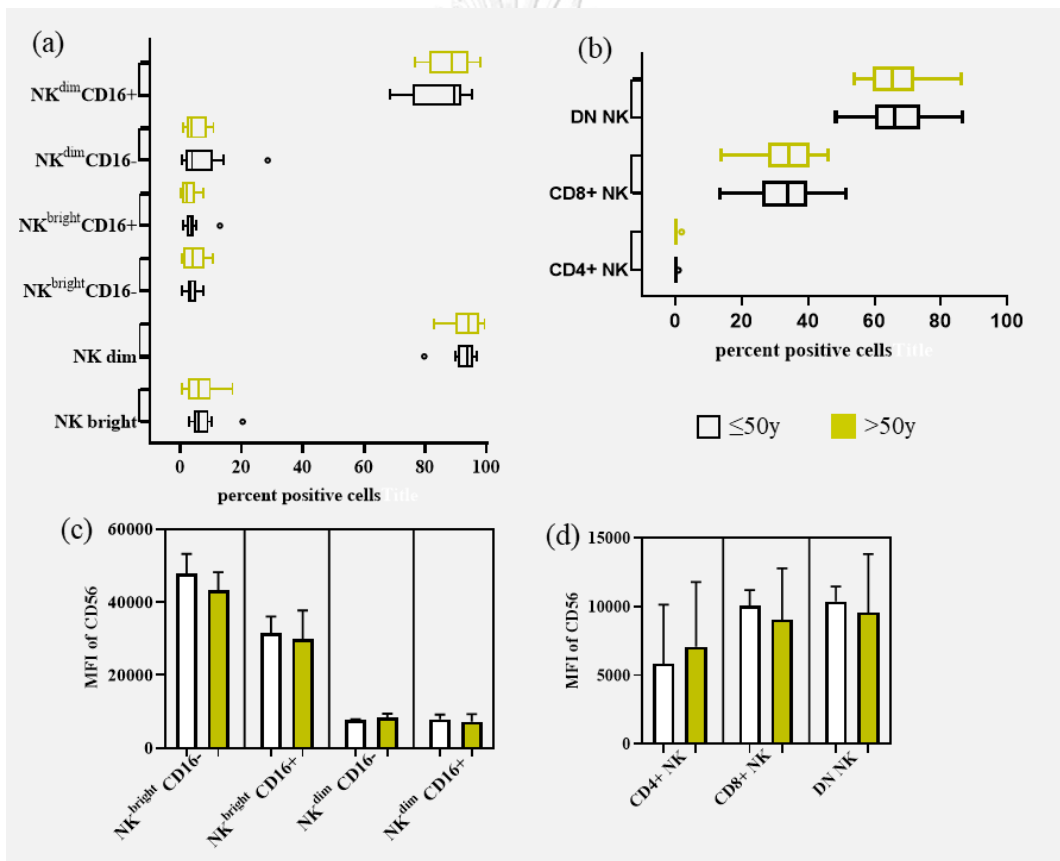
Figure 21: *Comparison among different types of NK cells between ≤50y group and >50y group*
(a) percent positive cells of NK^{bright}, NK^{dim}, NK^{bright} CD16-, NK^{bright} CD16+, NK^{dim} CD16-, NK^{dim} CD16+ cells, (b) percent positive cells of CD4+ NK, CD8+ NK and DN NK cells, Tukey graph: boxes represent 25% to 75% of samples, lines in boxes represents median, whiskers represent 3/2 of IQR, dots represent outliers, (c) Intensity of CD56 in NK^{bright} CD16-, NK^{bright} CD16+, NK^{dim} CD16-, NK^{dim} CD16+ cells, (d) Intensity of CD56 in CD4+ NK, CD8+ NK and DN NK cells. Bars represent median, whiskers represent 95% CI.

4.3.5 Immunophenotypic changes of monocytes

In monocytes of the >50y group, the number of classical monocytes significantly decreased and had a larger IQR while the intermediate monocytes population had higher median and IQR. Non-classical monocytes had a larger IQR (**Fig 22a**). The median of CD4 intensities increased and median of CD56 intensities decreased in all three monocytes of the older group (**Fig 22c, 22d**). CD4+ monocytes count significantly increased in the >50y group and CD56+ monocytes had decreased interquartile values. HLA-DR^{low} monocytes showed right-skewed data (lower values) and HLA-DR^{high} monocytes had left-skewed data (**Fig 22b**). The median value of HLA-DR positivity increased in the older group (**Fig 22e**).
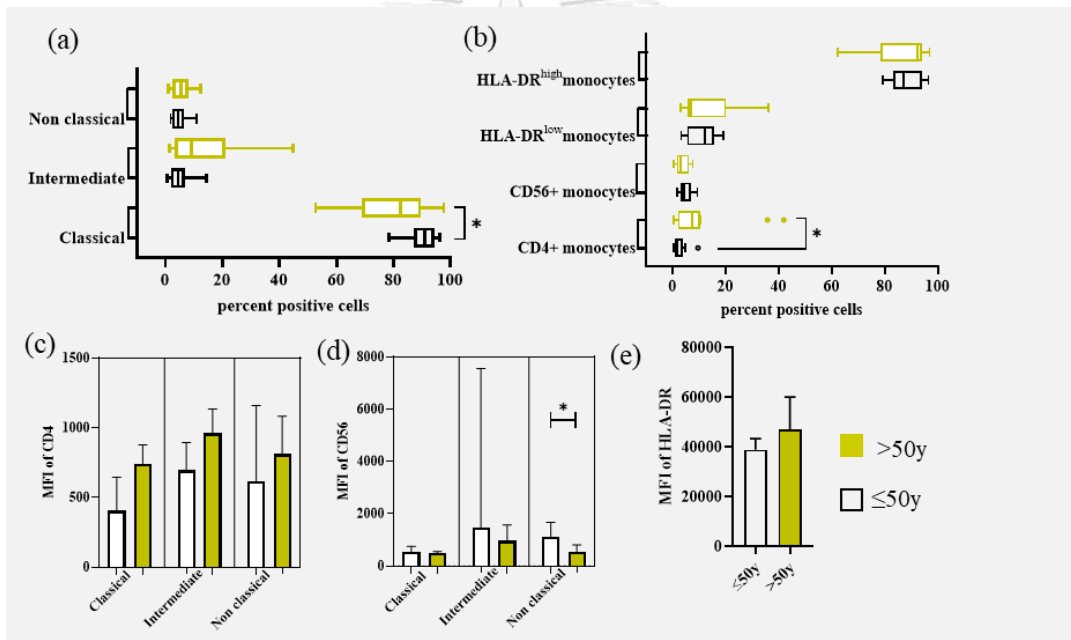
Figure 22: *Comparison of different types of monocytes between >50y group and ≤50y group*
(a) percent positive cells of classical, intermediate and non-classical monocytes,
(b) CD4+ monocytes, CD56+ monocytes, HLA-DR^{low} monocytes and HLA-DR^{high} monocytes, Tukey graph: boxes represent 25% to 75% of samples, lines in boxes represents median, whiskers represent 1.5 times of IQR, dots represent outliers,
(c) Intensity of CD4 among classical, intermediate and non-classical monocytes,
(d) Intensity of CD56 among classical, intermediate and non-classical monocytes,
(e) Intensity of HLA-DR. Bars represent median, whiskers represent 95% CI.

4.4 Discussion

Results presented in this Chapter confirm that immune cells undergo changes in their properties during ageing, and these have been determined by immuno-phenotyping. While it was not the primary aim of this thesis to undertake a detailed investigation of immune cell changes during ageing, because the incidence of CRC is higher in elderly populations (Kuipers et al., 2015), it was necessary to distinguish changes in immune cells that were either a function of ageing, associated with the disease, or a combination of both. Detailed investigations of the immune properties of CRC blood cells are described in the next Chapter, but here the same assays and measurements have been made in a broad age group of individuals who declared no current or previous cancers or inflammatory diseases, and hence for this study are classed as healthy controls.

Here, we show: CD4+ monocytes increased in ageing; most T cells subsets decreased; DN T cells decreased in >50 y group; HLA-DR positivity increased with age; NK cells were increased with age; there was a myeloid skew in ageing (significant decrease in T cells and a significant increase in monocytes so that the L:M ratio tended to decrease); and classical monocytes decreased.

In this study, significant decreases of T cells and increase of monocytes were observed during >50y. In the >50y group, the interquartile values of B cells decreased, and NK cells increased, meaning that most participants had decreased numbers of B cells and increased numbers of NK cells in ageing. However, the decreased number of T cells, B cells and increased number of NK cells, monocytes were disproportionate, as the ratios of T/B, NK/T and L:M ratio showed a wider range in >50y group. Therefore, hematopoiesis capacity in ageing is changing but, in some people, these changes are imbalanced and there is heterogeneity in the age at which these changes develop.

Different types of T cells during ageing

Different types of T cells (helper T, cytotoxic T, NK T, DN T and DP T) were examined in the study and types of T cells tended to decrease in the >50y group, except helper T cells. A significant decrease was found in DN T cells and most of the participants of the >50y group showed increased numbers of helper T cells and

decreased numbers of cytotoxic T cells. These results are similar to the findings of other studies (Li et al., 2019; Zheng et al., 2020), which showed that the T cell reservoir decreased with age (except for the CD4 subset), and the main decrease was found in the CD8 compartment (Li et al., 2019). In our study, the other phenotypes of T cells (NK T, DN T and DP T) were also studied, and these phenotypes also showed a decreased trend. To our knowledge, this has not been reported before. Increased numbers of helper T cells in the >50 y group can be explained by the following possible mechanism: there is evidence of increased numbers of CD4 Treg cells in ageing (Lages et al., 2008) and these CD4+ Tregs secrete various cytokines, such as IL-4, IL-10 and TGFβ, and inhibit the functions of other T cells (Lefebvre and Haynes, 2012). IL-4 and IL-10 favor the occurrence of Th2 phenotypes (Silva-Filho et al., 2014; Coomes et al., 2017) which are increased in normal ageing (Mansfield et al., 2012). TGFβ can impede T cells activation and inhibit the differentiation of T cells (Oh and Li, 2013). Moreover, immune organs' changes and reduction of T cell diversity in ageing may contribute to the decreased numbers of most T cells subsets in the elderly. However, there could be thymus-independent homeostatic mechanism in the total CD4 T cell pool, which can increase memory CD4 T cells with lymphopenia-induced proliferation in peripheral blood (Surh and Sprent, 2008; Unsinger et al., 2009).

T cells with functional markers

For cytotoxic T cells, there was a trend for decreased EA, SL, DN cells, and a larger IQR in each population categorized by CD28 and CD57 was observed (Fig 16a) indicating more variability in the compartment of cytotoxic T cells in >50y group. This is likely because of variations in the onset of immune changes during ageing, as a consequence of lifestyle and genetic make up. Age-associated epigenomic alterations are more prominent in CD8+ T cells than in CD4+ T cells (Hu et al., 2020) and these alterations increase chromatin accessibility to enable the cells to become terminally differentiated effector cells during ageing (Zhang et al., 2021a). However, epigenetic control of immune cells during ageing via alterations in DNA methylation, which can lead to dysfunctional changes that can compromise in immunocompetence (Jasiulionis, 2018).

When helper T cells were examined for the expression of functional markers (CD28, CD57), the SL helper T cells significantly increased in ≤50y group. (Fig 15a). Loss of CD28 expression can be seen during antigenic stimulation of T cells, while appearance of CD57 expression relates to the increased number of cell divisions. SL cells (CD28- CD57+) are terminally differentiated effector cells. Their increased number relates to pathologic conditions such as infections and autoimmune diseases (Broadley et al., 2017), and unhealthy lifestyles such as alcohol consumption and smoking (Arosa et al., 2000; Hodge et al., 2011). SL cells can result in immunocompetency as they are susceptible to apoptosis which can enable naïve T cell expansion (Strioga et al., 2011). We also showed that SL T cells are susceptible to apoptosis (**Appendix H**). Under stress conditions, the SL population of CD4+ T cells increased, together with increased expression of senescence markers (p16^{INK4A} and beta-gal): subsequent expression of activated caspase-3 in SL cells was also observed. Therefore, the increased SL T cells in ≤50y group could relate to immunocompetent immune responses to undefined underlying conditions.

The other senescent markers, p16^{INK4A} and beta-gal, were also analyzed in T cells and compared between the two age-groups of participants, however, no significant differences were observed between the two age-groups. It would be interesting, in future, to look for changes in these senescent markers in different subsets of T cells. This particular group of young healthy individuals with increased SL cells may have an undefined condition that induced these changes, but these changes did not result in increased expression of the senescent markers, beta-gal and p16INK4A. Therefore, SL helper T cells could relate more to a disease condition rather than to the age of the individuals and is not associated with the development of senescence (e.g. p16^{INK4A} and beta-gal expression) normally associated with ageing. This study has therefore identified a disconnect between appearance of SL cells and lack of correlation with expression of the other senescence markers, p16^{INK4A} and beta-gal. To our knowledge, this phenomenon has not been reported previously.

Therefore, SL T cells could be perceived as senescent-like cells. They have senescent features such as shortened telomere and senescent-associated secretions (González-Osuna et al., 2022), at the same time, they can perform effector functions

(Phetsouphanh et al., 2019). They could contribute to naïve cells expansion through the process of apoptosis (Strioga et al., 2011). However, prolonged apoptosis can impair the body's defense mechanism by means of immunosuppression (Zhang and Zheng, 2005; Hu et al., 2022). Based on these facts, it can be concluded that short-term presence of SL helper T cells could be beneficial. And these could be the reason why SL helper T cells increased in ≤50y group of the study.

CD3 expressions during ageing

CD3 plays a key role in TCR function and the TCR/CD3 complex is responsible for antigen recognition, T cell activation and subsequent triggering of the immune response (Boćko and Frydecka, 2003). T cells have heterogenous expression of CD3 while CD4+ T cells express higher levels of CD3 than CD8+ T cells (Valle et al., 2015). A study of DN thymocytes (earliest thymic progenitors) of mice showed that CD3 expression on DN thymocytes increases with age (Aw et al., 2009). In our study, CD3 expression was high-low, in the order of: DN T; NK T; CD4+ T; CD8low T; CD8+ T; DP T and CD8high T cells (**Appendix A**). There was a significant increased CD3 expression on T cells in the >50y group, especially in EA T cells (both helper and cytotoxic), DP helper T cells, DN cytotoxic T cells, DP cytotoxic T cells and DN NK T cells.

CD3 intensity of expression is related to T cell activation; higher CD3 expression requires higher activation levels (El Hentati et al., 2010). During ageing, the T cell receptor repertoire is more restricted and T cell activation is decreased (Salam et al., 2013a). Based on these facts, our finding of increased CD3 intensity suggests that higher activation levels are required, and inadequate level of stimulus levels could result in weak activation of T cells and hence immuno-compromisation during ageing. To our knowledge, this has not been reported previously.

We also examined the properties of SL cells (**Appendix B**). CD3 expression on SL helper T cells was lower than the other helper T cells. In the ≤50 y cohort of this study, there were significant increased levels of CD4+ SL cells. Therefore, interpretation of the CD3 intensities on helper T cells may be affected by the increased numbers of CD4+ SL cells. Analysis of more samples or the use of functional assays

such as activation assays, should be performed to determine the biological significance of the higher intensity of CD3 expression in ageing.

NK T cells

CD4+ NK T cells and CD8+ NK T cells play roles in regulation of the immune response, because CD4+ NK T cells relate to the generation of CD8+ Treg, while CD8+ NK T cells play a role in controlling antigen-bearing DC (Nakamura et al., 2003; Mishra et al., 2021). Immunosuppressive phenotypes were prevalent in unhealthy ageing (Salminen et al., 2020). In this study, in the >50 y group, most of participants had decreased immunoregulatory cells (CD4+ NK T and CD8+ NK T cells) and increased DN NK T cells. This may imply healthy ageing in the study group of >50y. However, the increased trend of DN NK T cells had increased intensity of CD3 expression (**Fig 18a, 18b**) indicating they could have different properties and functions.

HLA-DR positive T cells

The presence of HLA-DR positive T cells indicates activated T cells and arises from an effective immune response of the effector memory cells (Chen et al., 2019; Tippalagama et al., 2021). In this study, HLA-DR positive T cells positively correlated with age and the intensity of HLA-DR on T cells significantly increased in >50y group (**Fig 20c**). These data indicate ageing T cells had encountered more antigen than younger individuals. This interpretation is supported by observing the properties of HLA-DR positive T cells: these cells had a negative correlation with EA cells and a positive correlation with SL cytotoxic T cells (**Appendix C**) and their size and granularity were higher than those of HLA-DR negative T cells (**Appendix D**), implying they could be the late differentiated cells and have more cargo than the HLA-DR negative T cells.

NK cells

The number of NK cells increases in old age because of long-lived NK cells, and most of these cells were CD56^{dim} (Gounder et al., 2018b). In a study performed with different age groups of adults and elderly, NK^{bright} cells decreased in older people significantly (Chidrawar et al., 2006).

In this study, NK cells expanded in old age significantly. Most participants of the >50y group showed increased numbers of NK cells compared to the ≤50y group. However, some participants of the older group showed the expansion of NK[bright]. When this expansion of NK[bright] was measured together with CD16 expression, the expansion was in the NK[bright] CD16- subset. Some participants of the older group had increased numbers of NK[dim] CD16+ cells (Fig 21a).

NK^{bright} cells decreased and NK^{dim} cells increased in some participants of the older group, as found in the other studies (Chidrawar et al., 2006; Gounder et al., 2018a), but there were also increased NK^{bright} cells in some participants. The study during this thesis period was done during the COVID-19 pandemic, and the NK subsets can fluctuate during COVID-19 infection as well as during the recovery period (Varchetta et al., 2021): some NK cells may represent exhausted and depleted cells, but this may be accompanied by expansion of more mature perforin- and granzyme B-containing CD56^{bright} NK cells (Deng et al., 2022). Although total NK cells increased in ageing, subtypes of NK cells showed similar values. In retrospect, it would have been more informative to examine changes of NK cells in ageing with more participants of different age groups. However, this study was time- and volunteer-limited. In addition, clinical background information such as infection history at the time of sampling should be considered for more detailed investigation of NK cells subsets. In future studies, the cellular contents of NK cells or functional differences should be examined to assess the functional changes of NK cells.

Monocytes

In >50 y group, the total monocyte counts increased (Fig 13a) and there was a significant decrease of classical monocytes (Fig 22a). There was a trend of increases of intermediate and non-classical monocytes (Fig 22a), which can be comparable to a study of monocytes that included phenotypic and functional analysis in different age groups, where a higher percentage of intermediate and non-classical monocytes was found in the blood of elderly (Cao et al., 2022). These authors also found that monocytes of elderly people seem to be active but have decreased functional capacity: monocytes of the elderly exhibit increased expression of immune activation markers HLA-DR, adhesion molecules of CD11b and CD62L (Cao et al., 2022). CCR2 expression on

classical monocytes, which is important for migration was increased in the elderly (Cao et al., 2022). The expression of molecules involved in functional processes, such as CD200R, TIGIT, BTLA and TIM-3, was decreased. In intermediate monocytes, CX3CR1 expression, which is important for migration and control of inflammatory responses, also decreased, but the TNF-α producing capacity of intermediate monocytes increased, indicating an increase in inflammation (Cao et al., 2022).

In this study, other subtypes of monocytes in the >50 y group were also observed and the percentage of CD4+ monocytes also significantly increased (Fig 22b). This could be an indicator of monocytes' function, as CD4 expression on monocytes can relate to differentiation of monocytes towards macrophages (Zhen et al., 2014). In addition, CD56+ monocytes tended to decrease in the >50 y group (Fig 22b) which could relate to the function of monocytes, as CD56 expression relates to the activation of T cells (Sconocchia et al., 2005). Moreover, the majority of >50 y group had increased intensity of CD4, decreased intensity of CD56 and increased intensity of HLA-DR on their monocytes (Fig 22c, 22d, 22e). Therefore, they could have altered function because of their abnormal properties. Interestingly, intermediate monocytes expressed higher levels of CD4 and CD56 compared to classical monocytes and non-classical monocytes (**Appendix F**). Therefore, intermediate monocytes could have an important role in the pathogenesis of diseases in the elderly, such as interaction with T cells and their impaired properties can contribute to ineffective immune responses. The patrolling (non-classical) monocytes also showed significant decreased intensity of CD56, which could affect their interaction with T cells, and may impair their scavenger function.

HLA-DR^{low} monocytes relate to immunosuppression (Mengos et al., 2019). In this study, most participants of the >50 y group had lower numbers of HLA-DR^{low} monocytes, while some showed extremely high values. Further studies will be required to exclude the effects of other diseases because HLA-DR^{low} monocytes can be generated due to conditions, such as acute and chronic liver inflammation, pancreatitis, severe burns and immediately after surgical procedures (Mengos et al., 2019).

Conclusion

Immunophenotypic changes were observed in ageing. Decreased numbers of T lymphocytes in ageing related to reduction of different T subsets except helper T cells. To our knowledge, the following have not been reported previously:

- The number of HLA-DR positive T cells as well as staining intensity increased with age;

- CD3 staining intensity increased especially in EA T cells (both helper and cytotoxic), DP helper T, DP cytotoxic T, DN cytotoxic T cells and DN NK T cells;

- Expansion of NK cells correlated with age, but no prominent changes were observed in the NK subsets;

- Increased number of monocytes in ageing related to a decrease in classical monocytes and an increase in intermediate monocytes and non-classical monocytes;

- CD4+ monocytes significantly increased in ageing, but CD56+ monocytes tended to decrease.

CHAPTER V: IMMUNO-PHENOTYPIC CHANGES IN CRC

5.1 Introduction

Immune cells are dynamic populations of cells (Roy and Bagchi, 2020) and changes in their function and activity can be affected by: (a) unmodifiable factors such as age, gender; (b) modifiable factors such as stress, exercise and diet and (c) pathological factors such as inflammation and diseases (Hanahan and Weinberg, 2011; Klein, 2012; Maijó et al., 2014; Giunco et al., 2019; Hiam-Galvez et al., 2021). Ageing is also an important factor in inducing genomic instability in immune cells and susceptibility to diseases (Mutirangura, 2019). Colorectal cancer can result in chronic stresses to the immune system and can also contribute to changes in the functions of immune cells (Formica et al., 2014).

In this Chapter, the basic immunophenotypes of T lymphocytes, NK cells and monocytes were measured and compared in age-matched healthy controls (HCs, described in detail in Chapter 4) and CRC patients. In most patients with CRC, the numbers of NK cells decreased, helper T cells decreased, while cytotoxic T cells and NK T cells increased: intermediate monocytes with higher CD4 intensity were significantly increased, to our knowledge, a new observation. Most of the increased T cells and monocytes were senescent-like cells and with immunosuppressive phenotypes. Based on these preliminary observations, CD4+ monocytes at a level of 11.6% can be used as diagnostic marker for CRC with a 60% sensitivity and 88% specificity.
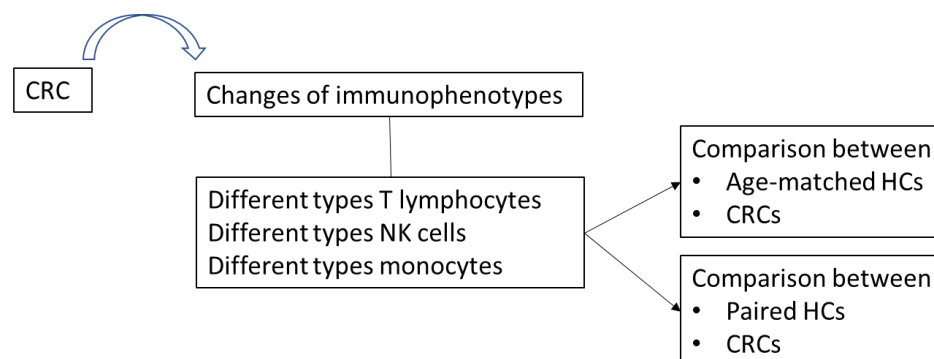
5.2 Aim

To identify immunophenotypic changes of subsets of T cells, NK cells and monocytes in CRC that may indicate altered functions as a result of cancer and may be useful as diagnostic markers of disease. It was also an aim to characterize changes in these phenotypes that were a function of disease (CRC) and not a consequence of ageing.

5.3 Results

Table 6: *Result summary for immunophenotypic changes in CRC*

+++/ ---	= significant increased or decreased (p<0.05)
++/--	= median value and interquartile values increased or decreased
	(>10% for value less than 50, >5% for values greater than 50)
+/ -	= median value or interquartile values increased or decreased
	(>10% for value less than 50, >5% for values greater than 50)
0	= no obvious change
Median	= middle value of the data set
Q1	= 25th percentile of the data set
Q3	= 75th percentile of the data set
Values in table	= percent positive cells

	age-matched HC n =17			CRC n=42			
	Median	Q1	Q3	Median	Q1	Q3	Difference (compared to age-matched HC)
T lymphocytes (% of all lymphocytes)	70.6	63.23	73.33	71.55	65.2	77.63	+
% of T lymphocytes							
Helper T cells	61.5	40.3	68.1	52.3	40.9	64.45	-
Cytotoxic T cells	36.2	27.1	45.6	41.95	29.88	55.05	++
DN T cells	3.725	2.02	5.713	2.46	1.303	4.465	- -
DP T cells	0.555	0.35	0.955	0.955	0.423	2.59	++

NK T cells	3.39	2.05	5.88	6.265	1.88	11.93	+
% of Helper T cells							
EA helper T cells	91.1	87.9	94.9	90.5	83.65	94.65	0
SL helper T cells	0.56	0.13	3.995	2.22	0.185	6.855	++
DN helper T cells	0.77	0.125	1.67	1.11	0.35	2.48	++
DP helper T cells	5.33	3.23	7.995	4.27	3.055	7.52	-
% of cytotoxic T cells							
EA cytotoxic T cells	44.4	23.8	66.05	39.3	19.65	55.55	- -
SL cytotoxic T cells	34.4	11.5	58.95	44.7	24.15	62.3	++
DN cytotoxic T cells	8.58	5.495	16.3	8.32	4.4	14.1	-
DP cytotoxic T cells	8.18	4.36	11.4	5.69	2.85	9.795	- -
% of cytotoxic T cells							
CD8^{low} T cells	6.515	3.59	10.43	6.65	3.865	11.03	0
CD8^{high} T cells	93.45	89.58	96.43	93.35	88.98	96.1	0
% of NK T cells							
CD4+ NK T cells	2.1	1.08	4.58	5.83	2.605	11.1	++
CD8+ NK T cells	69	55.2	80.9	75.95	53.98	83.58	+
DN NK T cells	20.4	8.11	35.1	10.04	4.043	25.85	- -
% of T lymphocytes							
HLA-DR-positive T cells	19.2	12.6	25.9	18.4	14.35	27.85	0
HLA-DR-negative T cells	80.7	74.1	87.4	79.8	71.8	85.55	0
NK cells (% of all lymphocytes)	15.1	11.6	18.6	13.5	9.388	18.1	- -
% of NK cells							
NK^{bright}	5.99	3.763	9.173	6.86	4.25	10.23	+
NK^{dim}	94.02	90.85	96.2	93.12	89.77	95.76	0

% of NK cells							
NK^{bright} CD16+	2.04	0.735	4.135	2.82	1.738	5.2	+ +
NK^{bright} CD16-	3.435	1.333	6.375	3.3	1.485	5.75	0
NK^{dim} CD16+	89.45	80.8	92.88	87.3	83.3	92.05	0
NK^{dim} CD16-	3.76	2.058	9.293	4.99	2.105	6.36	0
% of NK cells							
CD4+ NK	0.21	0.073	0.345	0.265	0.12	0.525	+
CD8+ NK	31.2	25.65	37.03	32.75	22.9	42.3	0
DN NK	68.7	61.63	74.28	66.65	57.6	73.73	-
Monocytes (% of PBMC)	20	13.35	24.95	22.1	13.45	27.1	+
% of Monocytes							
classical monocytes	86.05	76.88	89.88	81.05	70.9	86.18	-
intermediate monocytes	7.78	4.35	18.28	12.15	8.118	19.03	+
non-classical monocytes	5.14	2.383	7.23	4.995	3.085	9.335	+
% of Monocytes							
CD4+ monocytes	6.45	1.973	9.873	15.2	8.255	33.73	+++
CD56+ monocytes	3.265	2.375	6.215	4.61	2.353	7.23	+
% of Monocytes							
HLA-DR^{low} monocytes	6.73	5.435	13.2	16.5	5.065	21.8	+ +
HLA-DR^{high} monocytes	92.3	85.85	93.95	82.5	76.35	94.4	- -

Whole blood samples of CRC patients from the surgical units, Aintree University Hospital were collected from May 2022 to November 2022 from patients diagnosed with CRC and about to undergo surgery. White blood cells from 10 ml EDTA-anticoagulated blood were analyzed for immunophenotyping. The immuno-phenotypic changes were compared between age-matched HCs and CRCs. The age-matched HCs were selected from HCs of chapter 4 with the age range of 38 y to 89 y, mean ± SD of 59.0 ± 14.1 y and the ratio of male: female was 8:9. CRCs had a mean ±

SD of 67.1± 13.6 y with minimum 34 y, maximum 87 y and the male: female ratio was 26:16.

5.3.1 Changes in lymphocytes and monocytes

In CRCs, the IQR of T lymphocytes increased (but did not reach statistical significance), while that of B lymphocytes significantly decreased (p=0.04), compared to age matched HCs. The IQR of NK cells decreased, while in CRC monocytes showed a similar data distribution, but the median value was higher than in HC's (**Fig 23a**).

The median value of T/B lymphocytes was similar to HCs, but the range was wider (**Fig 23b**). Median values of NK/T and lymphocyte: monocytes (L:M) decreased and had a wider IQR (**Fig 23c**, **23d**). The CD3 intensity of T lymphocytes and CD19 intensity of B lymphocytes decreased in CRCs but this did not reach statistical significance (**Fig 23e, 23f**). CD56 intensity of NK cells and CD14 intensity of monocytes were similar in both groups (**Fig 23g, 23h**).
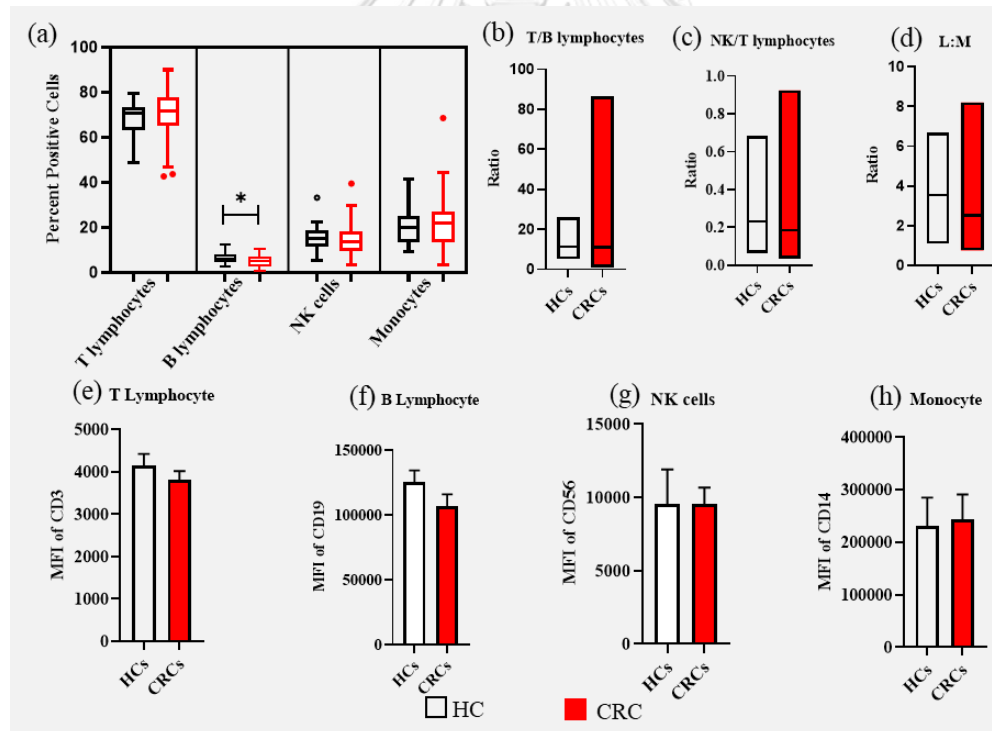
Figure 23: *Comparison of T lymphocytes, B lymphocytes, NK cells and monocytes between age-matched HCs and CRCs*
*(a) Shows percent positive cells, box represents IQR, line in box represents median, whiskers represent minimum and maximum, * is p<0.05. (b) Shows ratio of T lymphocytes to B lymphocytes; (c) ratio of NK cells to T lymphocytes; (d) lymphocytes to monocytes ratio. Bars represent range of ratios, lines in bars represent median, ** is p<0.01. (e) Shows CD3 intensity of T lymphocytes, (f) CD19 intensity of B*

lymphocytes, (g) CD56 intensity of NK cells, (h) CD14 intensity of monocytes. Bars represent median, whiskers represent 95% CI.

5.3.2 Immunophenotypic changes of T cells in CRCs

In CRCs, helper T cell counts decreased in most participants (median value decreased), while cytotoxic T cells tended to increase (median value and IQR increased). The number of NK T cells increased in most participants of CRCs while DN T cells decreased in CRCs but some extremely higher values were observed. Similar median values in DP T cells were observed in CRCs compared to HC and again some higher values were observed (**Fig 24a**).

CD3 intensities of different types of T cells tended to decrease but these were not significantly different in CRC and HC (**Fig 24b**).
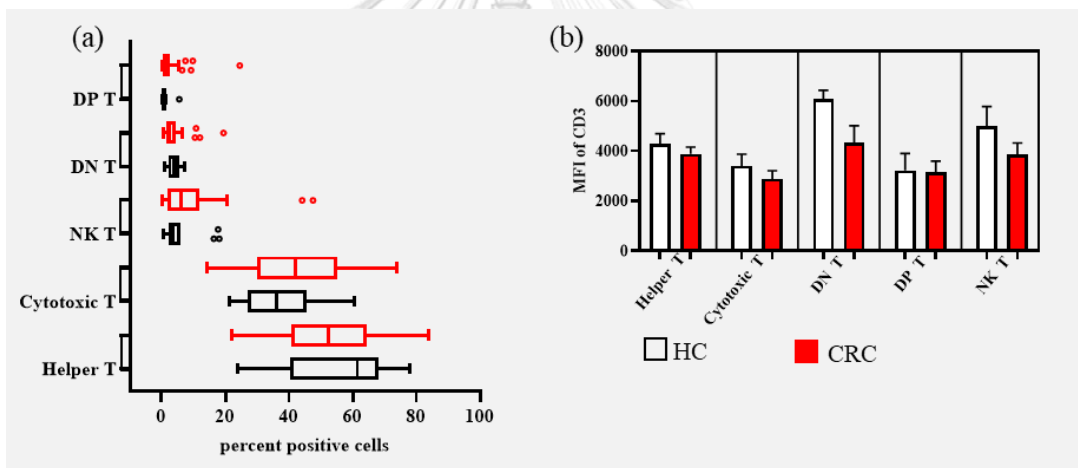
***Figure 24:** Comparison of different types of T cells between age-matched HCs and CRCs.*
***(a)** Shows percent positive cells, Tukey graph: boxes represent 25% to 75% of values of samples, lines in boxes represent median, whiskers represent 1.5 times of IQR, dot represents outliers. **(b)** Intensity of CD3 in different types of T cells, bars represent median, whiskers represent 95% CI.*

For the different types of helper T cells, CRCs samples contained more outliers. In EA cells of CRCs, most values were similar to HCs, but some individuals had lower values. SL cells tended to increase in CRCs: median value and IQR were increased. IQR of DN cells increased in CRCs while DP cells had lower median values in CRCs compared to HCs (**Fig 25a**).

The intensity of CD3 expression significantly decreased in EA cells and DP cells in CRC (**Fig 25b**), but no difference was observed in CD4 intensities between the two groups (**Fig 25c**).
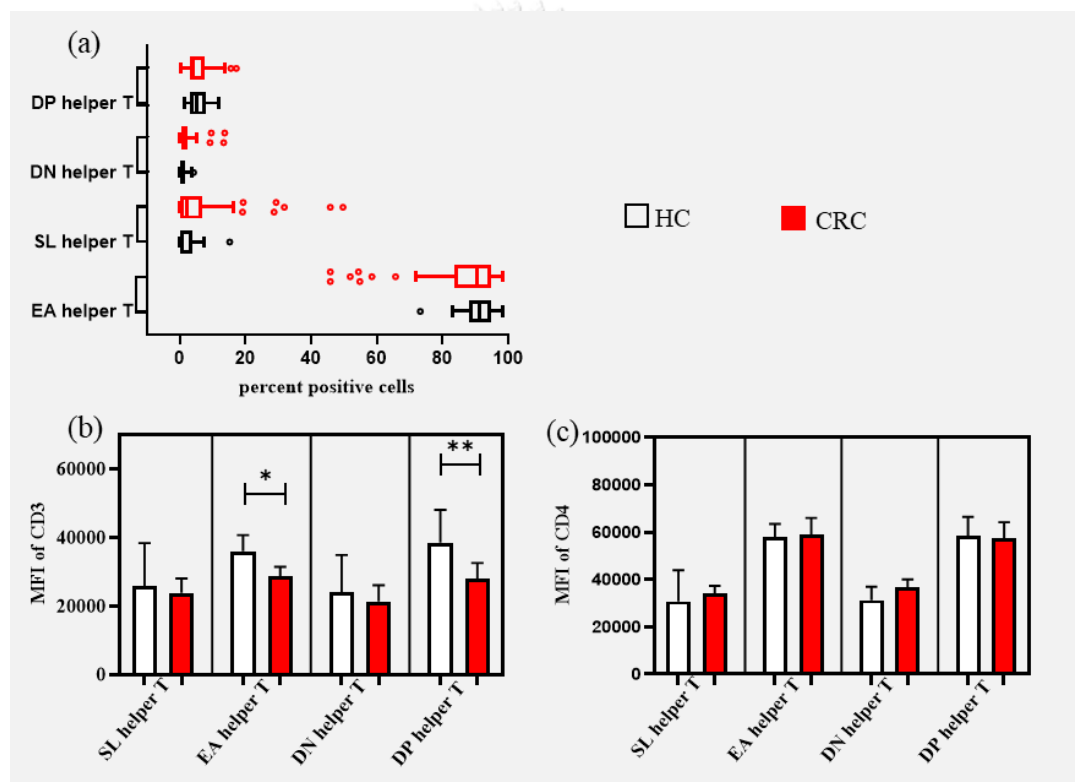
Figure 25: *Comparison of different types of helper T cells between age-matched HCs and CRCs*
(a) Shows percent positive cells, Tukey graph: boxes represent 25% to 75% of samples, lines in boxes represent median, whiskers represent 1.5 times of IQR, dot represents outlier. (b) Intensity of CD3 in different types of helper T cells. (c) Intensity of CD4 in different types of helper T cells, bars represent median, whiskers represent 95% CI, * is p<0.05.

For different types of cytotoxic T cells, the IQR and median values for SL cells increased in CRCs. The IQR of EA cells and DP cells decreased in CRCs, while DN cells showed similar values to HCs (**Fig 26a**). The intensities of CD3 expression decreased significantly in EA, DN and DP cells in CRC. CD8 intensities were similar in both CRC and HC groups (**Fig 26b, 26c**).
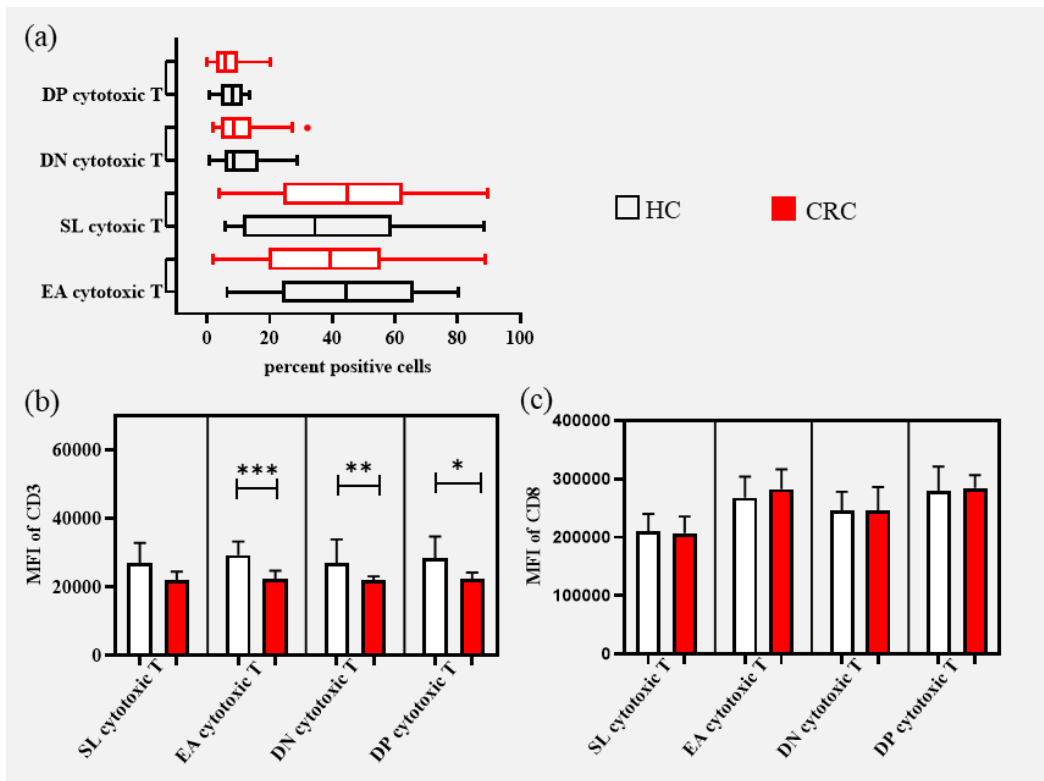
Figure 26: *Comparison of different types of cytotoxic T cells between age-matched HCs and CRCs*
(a) *Shows percent positive cells, Tukey graph: boxes represent 25% to 75% of samples; lines in boxes represents median; whiskers represent 1.5 times of IQR; dot represents outlier; * is p<0.05, ** is p<0.01, *** is p<0.001.* ***(b)*** *Intensity of CD3 in different types of cytotoxic T cells, **(c)** Intensity of CD8 in different types of cytotoxic T cells, bars represent median, whiskers represent 95% CI, * is p<0.05.*

Most of the CRC patients showed increased numbers of NK T cells (**Fig 24a**). When they were analyzed for expression of CD4 and CD8 markers, CD4+ NK T cells and CD8+ NK T cells tended to increase (median value and IQR increase) while DN NK T cells tended to decrease (median value and IQR decrease) (**Fig 27a**). The median values for the intensities of CD3 expression decreased in CRCs (**Fig 27b**).
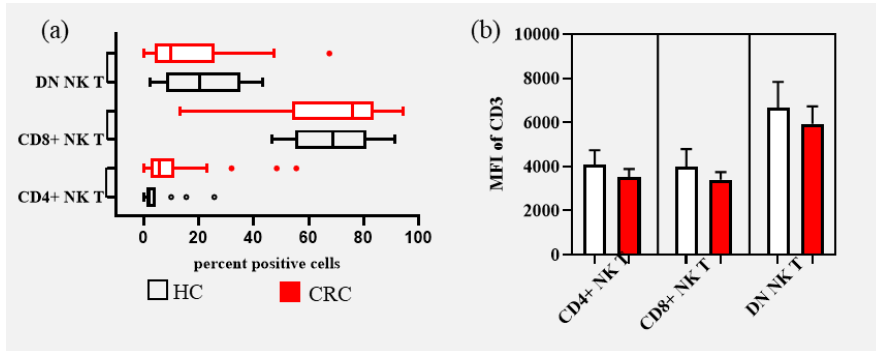
Figure 27: *Comparison of different types of NK T cells between age-matched HCs and CRCs*
(a) Shows percent positive cells, Tukey graph: boxes represent 25% to 75% of samples, lines in boxes represent median, whiskers represent 1.5 times of IQR, dot represents outlier. (b) Intensity of CD3 in different types of NK T cells, bars represent median, whiskers represent 95% CI.

CD8^{low} and CD8^{high} T cells of CRCs showed similar patterns of expression to HCs, but more outliers were observed in CRCs (**Fig 28a**). CD3 intensities tended to decrease in CRCs (**Fig 28b**), but there were no significant differences in intensity of CD8 staining (**Fig 28c**).
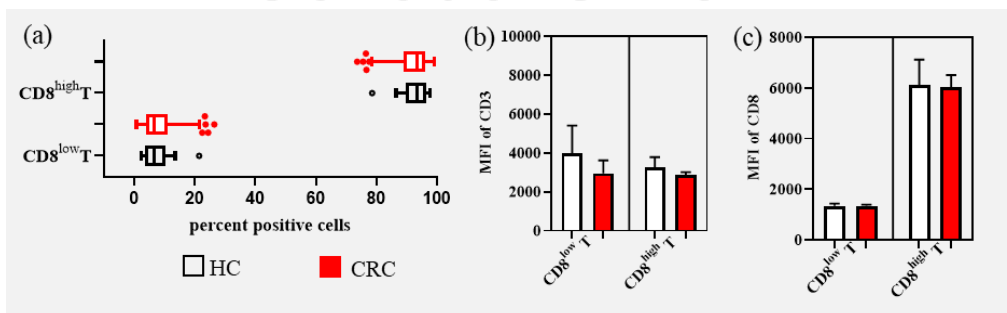
Figure 28: *Comparison of different types of CD8^{low} T and CD8^{high} T cells between age-matched HCs and CRCs*
(a) shows percent positive cells, Tukey graph: boxes represent 25% to 75% of samples; lines in boxes represents median; whiskers represent 1.5 times of IQR; dot represents outlier. (b) Intensity of CD3 in CD8^{low} T cells and CD8^{high} T cells. (c) Intensity of CD8

in CD8^{low} T cells and CD8^{high} T cells: bars represent median, whiskers represent 95% CI.

HLA-DR positivity was similar in both groups, in terms of both counts and intensity, but some outliers in CRCs were observed (**Fig 29a, 29c**). HLA-DR positive cells of CRCs showed lower intensity of CD3 than in HCs' (p= 0.01) (**Fig 29b**).
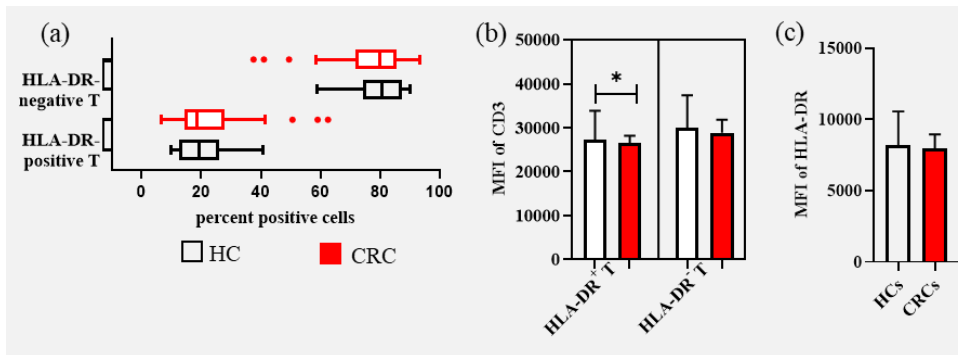
Figure 29: *Comparison of different types of HLA-DR^+ T and HLA-DR T cells between age-matched HCs and CRCs*
(a) Shows percent positive cells, Tukey graph: boxes represent 25% to 75% of samples; lines in boxes represent median; whiskers represent 1.5 times of IQR; dot represents outlier. (b) Intensity of CD3 in HLA-DR^+ T and HLA-DR^- T cells. (c) Intensity of HLA-DR in HLA-DR^+ T cells: bars represent median, whiskers represent 95% CI.

5.3.3 Immunophenotypic changes of NK cells in CRCs

The data distributions of NK^{bright} and NK^{dim} were similar in both groups, except that NK^{bright} CD16+ showed increased IQR in CRC (**Fig 30a**). In terms of CD4 and CD8 positivity in NK cells, the two groups had similar median values, but more variations were seen in CRCs (more outliers and longer whiskers) (**Fig 30b**). CD56 intensities were similar in both groups (**Fig 30c, 30d**).
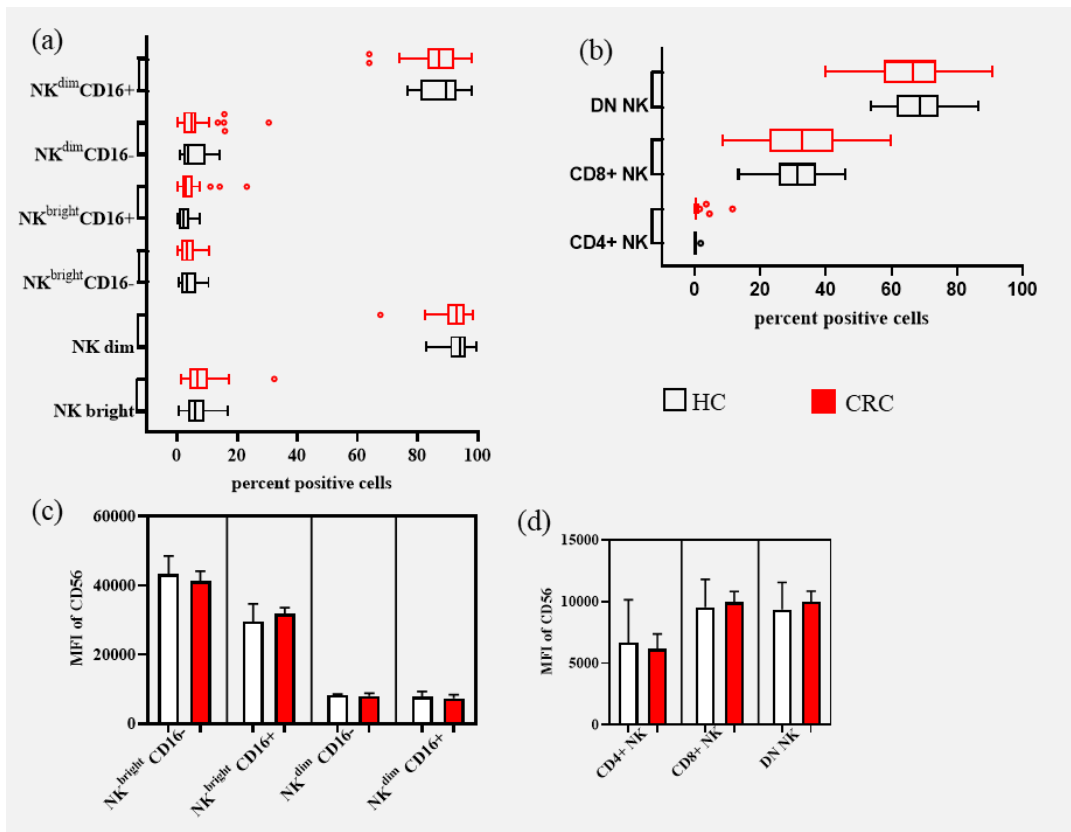
Figure 30: *Comparison among different types of NK cells between age-matched HCs and CRCs*
(a) Shows percent positive cells of NK^{bright}, NK^{dim}, NK^{bright} CD16-, NK^{bright} CD16+, NK^{dim} CD16-, NK^{dim} CD16+ cells. (b) Shows percent positive cells of CD4+ NK, CD8+ NK and DN NK cells, Tukey graph: boxes represent 25% to 75% of samples; lines in boxes represents median; whiskers represent 1.5 times of IQR; dots represent outliers. (c) Intensity of CD56 in NK^{bright} CD16, NK^{bright} CD16+, NK^{dim} CD16-, NK^{dim} CD16+ cells. (d) Intensity of CD56 in CD4+ NK, CD8+ NK and DN NK cells; bars represent median, whiskers represent 95% CI.

5.3.4 Immunophenotypic changes of monocytes in CRCs

In CRCs, numbers of classical monocytes (CD14++ CD16-) tended to decrease (decreased median value and IQR) while intermediate monocytes (CD14++ CD16+) and non-classical monocytes (CD14+ CD16+) tended to increase (increased median values and IQR) (**Fig 31a**).

CD4+ monocytes in CRCs significantly increased in CRCs (p=0.002), while CD56+ monocytes tended to increase in CRC and some higher outliers were observed. HLA-DR^{low} positive cells showed left-skewed (most participants had higher values) data in CRC while right-skewed (most participants had lower values) data in HCs. The reversed data pattern was observed in HLA-DR^{high} positive cells (**Fig 31b**).

When CD4 and CD56 positivity were compared among the 3 different types of monocytes, the median of CD4 intensities increased in all monocytes and a statistically-significant increase was observed in intermediate monocytes (**Fig 31c**). CD56 intensities of monocytes showed similar data patterns in both groups (**Fig 31d**). The median value of HLA-DR intensity increased in CRC (**Fig 31e**).

CD4+ monocytes were significantly increased in CRCs and because of this, data were further analysed by ROC analysis to determine if these numbers may have potential as a biomarker. The area under the curve was 76% (p=0.002) and the standard error was 0.07. There was 60% sensitivity and 88% specificity with a likelihood ratio of 4.8, cut-off value of 11.6% (**Fig 31f**). The ROC curve data can be seen in **Appendix K**.
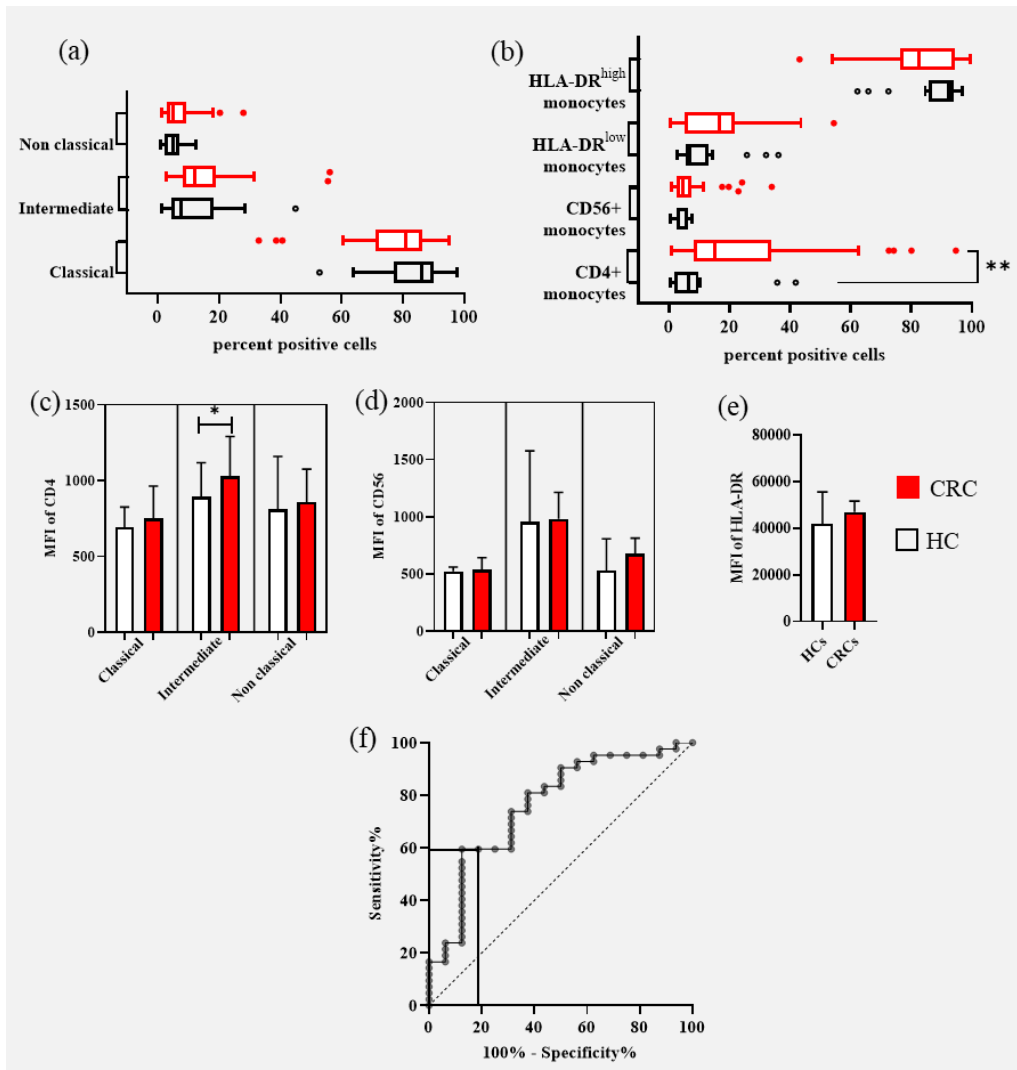
Figure 31: *Comparison of different types of monocytes between age-matched HCs and CRCs*

(a) Shows percent positive cells of classical, intermediate and non-classical monocytes, while *(b)* shows CD4+ monocytes, CD56+ monocytes, HLA-DR^low monocytes and HLA-DR^high monocytes, Tukey graph: boxes represent 25% to 75% of samples; lines in boxes represents median; whiskers represent 1.5 times of IQR; dots represent outliers. *(c)* Intensity of CD4 expression by classical, intermediate and non-classical monocytes, *(d)* intensity of CD56 expression by classical, intermediate and non-classical monocytes, *(e)* intensity of HLA-DR expression: bars represent median, whiskers represent 95% CI. *(f)* ROC analysis of CD4+ monocytes between age-matched HCs and CRCs, the cut-off value of 11.6% at the vertical solid line and horizontal solid line showing 60% sensitivity and 88% specificity.

5.3.5 Outliers of the datasets

There were outliers in the datasets, especially in CRC group, indicating greater heterogeneity as a result of the disease or treatment or both. Data were therefore analyzed again after removing the outliers.

Most phenotypes were not affected by the outliers except for DN T, CD4+ NKT and HLA-DR^{low} monocytes. In DN T, when 4 outliers from HCs were removed, then a significant decrease was observed in the CRC population (**Fig 32a**). Similarly, CD4+ NK T cells were significantly increased in CRC after removing 3 outliers from HCs and 5 outliers from CRC (**Fig 32f**). When five outliers from HLA-DR^{low} monocytes of HCs were removed then there was a significant increase in the CRC group (**Fig 32j**).
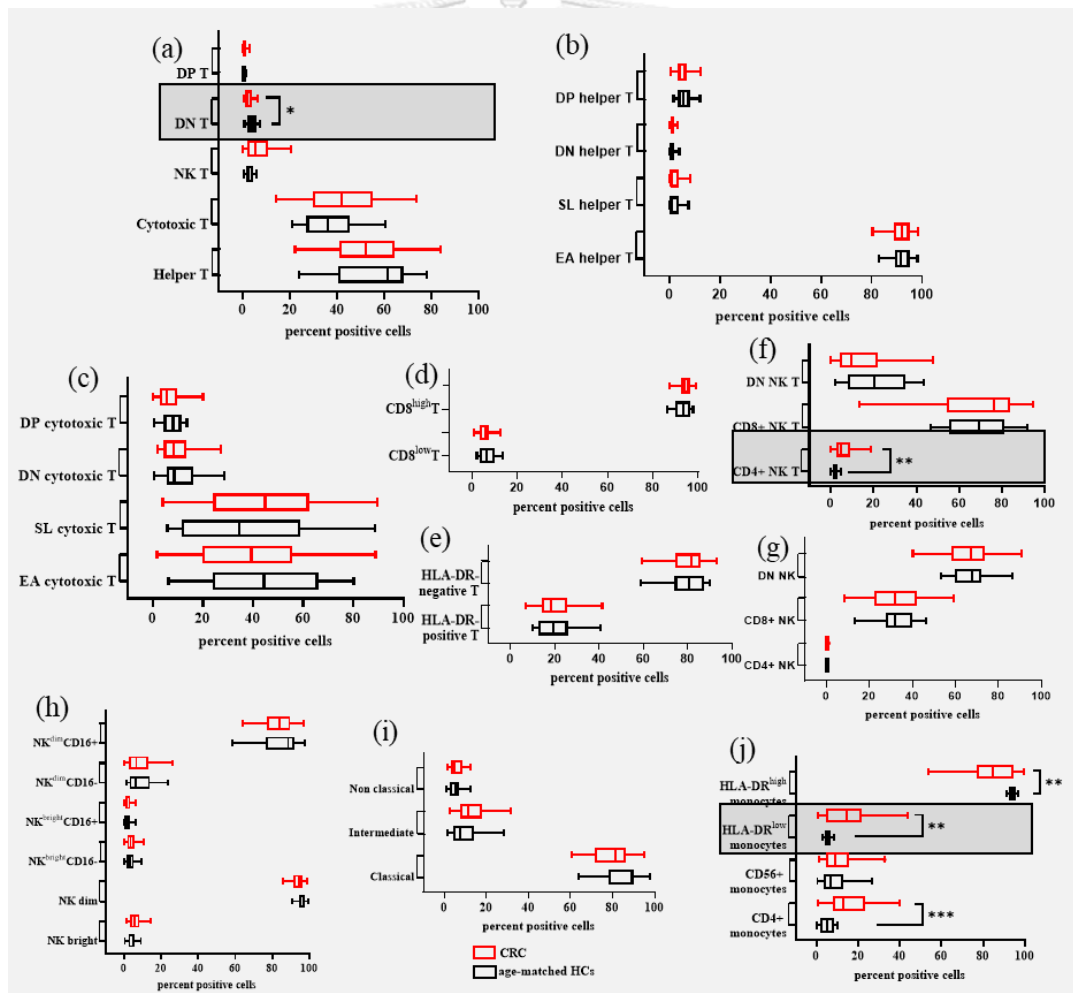
Figure 32: *Comparison of percent positive cells in different immuno-phenotypes of age-matched HCs and CRC with the outliers removed*

*(a) Shows helper T, cytotoxic T, NK T, DN T and DP T lymphocytes, (b) different types of helper T lymphocytes, (c) different types of cytotoxic T lymphocytes, (d) CD8^{low} T and CD8^{high} T lymphocytes, (e) HLA-DR-negative T and HLA-DR-positive T lymphocytes, (f) CD4+ NK T, CD8+ NK T and DN NK T lymphocytes, (g) CD4+ NK, CD8+ NK and DN NK cells, (h) NK^{bright}, NK^{dim}, NK^{bright} CD16-, NK^{bright} CD16+, NK^{dim} CD16-, NK^{dim} CD16+, (i) classical monocyte, intermediate monocyte and non-classical monocyte, (j) CD4+ monocyte, CD56+ monocyte, HLA-DR^{low} monocyte and HLA-DR^{high} monocyte, Tukey graph: box represents 25% to 75% of samples, line in box represents median, whiskers represent 3/2 of IQR, dot represents outlier, * = p<0.05, ** = p<0.01, *** = p<0.001.*

5.3.6 CD4+ monocytes in aged-and sex-matched paired samples

As changes of CD4+ monocytes were affected by age: increased in ageing (Chapter 4), pair data analysis for CD4+ monocytes was also performed. Paired samples were selected from similar age and same sex, e.g., 59y female HC and 59y female CRC. There were 15 pairs of participants of which the M: F was 7:8. CD4+monocytes showed significant differences between HCs and CRCs (p=0.003) in pair t-test (**Fig 33**).
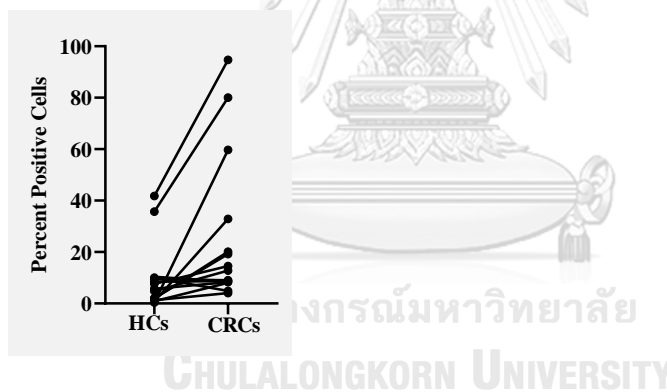
***Figure 33:** Comparison of CD4+ monocytes in paired samples of HC and CRC*

5.4 Discussion

One of the hallmarks of cancer is evasion of immune system. Immune cells are a heterogenous and dynamic population of cells and are involved in the surveillance of tumor cells, immune responses to cancers, eradication of cancers and progression of cancer. Their functional changes can be caused by various stressors and cancer is a long-term stressor to the immune system (Zhang et al., 2020a). Immune cell changes can reflect the response of the body against the cancer and therefore these changes may have potential to be used as biomarkers for cancers.

Phenotypic changes of lymphocytes and monocytes

A number of changes in immune cells have been reported in cancer, for example, cancer patients have clonotypic expansion of T cells which relates to clinical outcomes (Wu et al., 2020). Cancer-related treatments can also affect the immune cells. For example, chemotherapy can affect B cells more than T cells and NK cells, by decreasing the number of B cells, including naïve cells memory cells and class-switched B cells (Waidhauser et al., 2020).

In this study, most patients with CRCs had increased T cells and monocytes, and decreased NK cells (Fig 23a). B lymphocytes were significantly decreased, and most patients had similar T/B ratios compared to HCs. However, some patients had either very low or very high T/B ratios. Decreased NK cells with increased T cells in CRCs generate lower NK/T, which is the reverse of the trend of this ratio observed in normal ageing (NK cells increase and T cells decrease in normal aging makes higher NK/ T ratio) (chapter 4).

There are collaborative interactions of immune cells during the immune response, and coordination between T cells and B cells is important for successful T cell-dependent antibody responses (Petersone et al., 2018). In addition, communications between NK cells and T cells are important for the initial regulation of T cells (Schuster et al., 2016). Patients with extreme values of ratios and reversed ratios could have imbalances in these coordinated cooperation responses of immune cells.

Most CRC patients had lower L:M ratio, although both T lymphocytes and monocytes tended to increase in CRCs. The lower L:M ratio can be interpreted as increased levels of monocytes which were much higher than the increased level of T lymphocytes observed. Therefore, a possible myeloid skew can be observed in CRCs patients.

CD3 intensity of expression by T cells and CD19 expression intensity of B cells were lower in most participants with CRC. NK cell CD56 expression and monocyte CD14 expression were similar in both CRCs and HCs (Fig 23). However, CD3 intensity significantly decreased in EA helper T and DP helper T (Fig 25b); in EA cytotoxic T, DN cytotoxic T and DP cytotoxic T (Fig 26b); and in HLA-DR positive T (Fig 29b). There is evidence of CD3ζ chain impairment or loss in T cells can in patients with malignancy (Ishigami et al., 2004). However, there are some contradictory data: for example, no CD3ζ chain impairments were observed in another study between cancer and normal controls (Deakin et al., 1999). In contrast, CD3 expression levels were directly proportionate to the levels of T cell activation: higher CD3 level require higher activation capacity (El Hentati et al., 2010) and the TCR activation level can determine the fate of T cells: successful strong TCR activation can lead to Th1 differentiation and weak activation can lead to Th2 differentiation (van Panhuys, 2016). Therefore, studies of CD3 function and expression on T cells in malignancy are worthy of further study.

T lymphocytes

Most patients with CRC had lower numbers of helper T cells but higher numbers of cytotoxic T cells (Fig 24a). Loss of helper T cells can occur during malignancy as well as during chemotherapy (Madu et al., 2013). There is a "help program" of helper T cells for cytotoxic T cells in that helper T cells help cytotoxic T cells to mediate their effector functions through CD27 co-stimulation. Without helper T cells, cytotoxic T cells can become exhausted by the upregulation of PD-1 and co-inhibitory receptors (Ahrends et al., 2017). Therefore, loss of helper T cells can affect the cytotoxic T cells and "helpless" cytotoxic T cells can have impaired anti-tumor activity. On the other hand, the CD4+ T/ CD8+ T ratio has been used as the prognostic biomarker; a lower ratio indicates tumor progression (Liu et al., 2021). There was also evidence of exhaustion of immune cells, not only in T lymphocytes subsets but also in B

lymphocytes and NK cells of CRC patients, expressing the immune exhaustion genes such as PD-L1, LAG3 and T-bet (Sorrentino et al., 2021).

NK T cells numbers also increased in most patients with CRC (Fig 24a). NK T cells can cross talk with both innate and adaptive immune cells, but exist in different subsets which can have either pro-tumor or anti-tumor properties (Wu and Van Kaer, 2011; Nelson et al., 2021).

Most patients with CRCs had lower levels of DN T cells, but some had extreme higher values (Fig 24a). DN T cells have immunoregulatory roles, e.g. to prevent graft-versus-host-disease (Wu et al., 2022). They also have cytotoxic, helper or innate functions (Yang et al., 2021). There are two theories for the origin of DN T cells. The first is that DN T cells derive from a thymic origin. DN thymocytes with higher activity of TCR remain in this DN stage and mast cells can force them to leave the thymus. Alternatively, a second theory is DN T cells transform from TCRαβ+ CD8 T cells. This theory implies that DN T cells and CD8+ T cells have similar a TCR repertoire, and that apoptotic cell debris can induce loss of CD8 and generate the DN T cells; CD8 T cells can then differentiate into DN T cells (Wu et al., 2022). In our study, the evidence supports the alternative theory, as the number of DN T cells significantly decreased in ageing (Table 6) and there is a positive correlation with CD8+ T cells and strong positive correlation with CD8^{low} T cells (**Appendix E**).

Most patients with CRC had similar levels of DP T cells as in HCs, but some expressed higher levels (Fig 24a). However, while their numbers are very low in the blood, they can have distinct complex functions as they are positive for both CD4 and CD8 receptors. They have been shown to have anti-tumor as well as pro-tumor activities in tumor immunity (Overgaard et al., 2015).

T cells with functional markers

In this study, most patients with CRC had increased SL T cells and decreased EA cells in both compartments of helper and cytotoxic cells (Fig 25a, 26a). Helper SL cells have contrasting roles in tumor immunology. They have the features of senescence such as shortened telomeres and SASP secretion (González-Osuna et al., 2022). Because of this senescent phenotype, their helper functions decrease (Moro-García et

al., 2013). but they may have anti-tumor activity. They gain some distinct features, such as increased expression of cytoplasmic granules containing perforin and granzyme B (Phetsouphanh et al., 2019). In contrast, there is a distinct phenotype called CD4+ cytotoxic T cells. They highly express IL-7 receptors, NKG2D, granzyme B and perforin and can eradicate tumor cells in an MHC class II-dependent manner (Quezada et al., 2010). Interestingly, they can be enriched in the blood of the elderly and their NKG2D expression relates to immuno-senescence (Alonso-Arias et al., 2011). There is also evidence of increased cytotoxic CD4+ T cells in colorectal cancers (Zhang et al., 2018) and these cells can also be found in other diseases, such as viral infections and autoimmune diseases (van Leeuwen et al., 2004; Phetsouphanh et al., 2019). In contrast, cancer treatment can induce the senescent T cells and chemo/radio therapy-induced senescent T cells have been reported in colorectal carcinoma (Bruni et al., 2019). Moreover, immunosenescent characteristics such as decreased naïve cells with increased central memory CD8+ T cells and terminally differentiated effector memory T lymphocytes (CD45RA+ CCR7− CD28− CD27−) were observed in CRC patients with advanced-stages (Zhang et al., 2022).

The level of beta gal and p16^{INK4A} were also measured in these populations of HCs and CRC. The level of beta-gal of T lymphocytes significantly increased and was mostly higher in monocytes of CRC patients (**Appendix Ic**) whereas levels of p16^{INK4A} in T lymphocytes and monocytes were similar in both groups (**Appendix Id**). When p16^{INK4A} levels in different T cells were observed, increased levels were observed in EA T cells and DN T cells in most CRC patients and significant increased levels were measured in DP T cells (**Appendix If**). Moreover, the mRNA level of p16^{INK4A} from PBMCs of CRC patients significantly increased (**Appendix Ie**). These data indicate that there was stress-induced senescence in CRC T cells and monocytes.

In this study, helper DN (CD28- CD57-) cells increased in the majority of CRC patients, but no difference was observed in levels of cytotoxic DN cells. Most patients had lower numbers of DP in both helper and cytotoxic T cells (Fig 25, 26). Loss of CD28 and gain of CD57 are the features of SL cells. DN cells are considered as on a pathway to late differentiated CD57+ cells (Strioga et al., 2011). The evidence in this thesis supports this hypothesis as we measured p16^{INK4A} in EA, SL, DN and DP T cell

populations, and SL cells and DN cells had higher levels of p16^{INK4A} than EA and DP cells (**Appendix G**).

NK T cells

The majority of CRCs had increased numbers of total NK T cells, particularly in the subsets of CD4+ NK T and CD8+ NK T cells (Fig 27). DN NK T cells were lower in most CRCs and the expression of co-receptors on NK T cells relates to immunosuppression. CD4+ NK T cells are involved in CD8+ Treg generation and CD8+ NK T cells are involved in the immune response by controlling antigen-bearing DCs (Nakamura et al., 2003; Wang et al., 2015). On the other hand, DN NK T cells have Th1-like function, and they can kill tumor cells. Therefore, the increased number of NK T cells in CRCs indicates a phenotype of immunosuppression rather than anti-tumor activity.

HLA-DR positive T cells

HLA-DR positive T cells can favor anti-tumor responses as they produce INF-γ, Granzyme B, Perforin and TNF-α. Their levels negatively correlate with the expression of pro-tumorigenesis molecules such as TGF-b, PD-L1, IL-6, IL-1b and IL-8 (Saraiva et al., 2018). These cells can expand in viral infections, but no functional differences were observed in HIV-1 infection (Imamichi et al., 2012). In this study, both the proportions and positivity of HLA-DR positive cells were similar in CRCs and HCs, although a few patients showed very high values of HLA-DR positive cells (Fig 29a, 29c). CD3 intensity of HLA-DR positive T cells decreased in the CRC group (Fig 29b) indicating there could be qualitative differences in HLA-DR positive T cells in CRC.

NK cells

NK cells count decreased in the majority of CRC patients (Fig 23a). NK cells are cytotoxic cells of innate immunity and are important not only for the killing of tumor cells but also for tumor remission (Abbas et al., 2022). Tang and associates showed that the increased numbers of NK cells relate to higher survival rates in colorectal cancer (Tang et al., 2020).

When NK cells were categorised into different subsets based on their intensity of CD56 and CD16 expression, similar cell counts were observed between HCs and CRCs (Fig 30a). NK cells were also sub-divided into groups of CD4+ or CD8+ cells. CD4+ NK cells in the blood were present at low percentages in both HCs and CRCs, while CD8+ NK cells showed great variation in CRC: some patients had very low numbers, while some had much higher numbers compared to HCs (Fig 30b). The presence of CD8 on NK cells relates to an enhancement of their cytotoxic activity (Addison et al., 2005).

In this study, the total NK cells count decreased in CRC, but phenotypic subsets were similar to HCs. NK cells subsets can have dynamic fluctuations due to infections and inflammatory conditions (Gyurova et al., 2019) and therefore, longitudinal studies and functional analysis of NK cells will be required to study these NK cells changes in CRCs.

Monocytes

Most patients with CRC had lower numbers of classical monocytes and higher numbers of intermediate monocytes, with some having increased numbers of non-classical monocytes (Fig 31a). This result was similar to that of Schauer et al (2012) who showed that intermediate monocytes were increased in CRCs patients, especially in localized tumor cases. They predicted that the intermediate monocytes could be used as diagnostic markers, with 69% sensitivity and 81% specificity in CRC (Schauer et al., 2012).

HLA-DR positivity changed in CRC with the majority of CRC patients showing increased numbers HLA-DR^{low} monocytes, and decreased numbers of HLA-DR^{high} monocytes (Fig 31b). HLA-DR expression is important for antigen presentation by monocytes and so impaired expression of HLA-DR indicates a defect in this function of monocytes. In contrast, HLA-DR^{low} positivity represents immunosuppression (Mengos et al., 2019).

CD56+ monocytes increased in most CRC patients and CD4+ monocytes increased significantly (Fig 31b). CD56 expression relates to T cell proliferation (Sconocchia et al., 2005), while CD4 expression relates to differentiation of monocytes

(Zhen et al., 2014). Therefore, monocytes of CRC could be functionally active in the immune response.

When CD4 intensity and CD56 intensity were examined among the 3 types of monocytes, all types of monocytes increased in CD4 expression intensity, which was significant in intermediate monocytes (Fig 31c). The intensity of CD56 expression did not show significant differences, although the CD56+ monocytes count increased in the majority of CRC patients (Fig 31d). Intermediate monocytes had the highest intensity of expression of CD56 which could suggest that the functions of intermediate monocytes are different in CRC.

CD4+ monocytes were significantly increased in CRC (unpaired samples and paired samples) as well as in ageing (Chapter 4) indicating they relate to both age and CRC. When they were evaluated as a potential diagnostic marker in CRC, it showed a 60% sensitivity and 88% specificity with the cut-off value of 11.5% of CD4+ monocytes (Fig 31f).

Outliers in samples

In this study, there were a number of immune cell subsets that showed outliers in values (high or low) especially in the CRC group and these outliers were more prevalent in the immune subsets with skewed data (Fig 32). When outliers were removed, the qualitative observations and data interpretation were not significantly changed, but the p value decreased in some immune subsets. The outliers in CRC groups can imply there could be extreme immune response in some CRC cases.

Conclusion

The majority of CRC patients showed changes in T cell compartments: decreased helper T cells with increased SL helper T cells; increased cytotoxic T cells with increased SL cytotoxic T cells, in line with previous observations. However, these differences did not reach statistical significance in this study. We also show increased NK T cells with increases in immunosuppressive populations (CD4+ and CD8+ NK T cells) which has not been reported previously. However, these changes were also not statistically significant and so further studies, with a larger cohort of CRC patients would be needed to confirm this potentially important finding.

We show here that NK cells decreased in most CRC, while increases in monocytes in CRC patients related to increased intermediate monocytes and non-classical monocytes were observed. Previous work has confirmed the increase in intermediary monocytes in CRC and has suggested that this may be used as a biomarker for CRC (Schauer et al., 2012). Immunosuppressive HLA-DR^{low} monocytes increased in the majority of CRC patients, while CD4+ monocytes significantly increased in CRC patients. Of these novel observations, only the changes in CD4+ monocytes were statistically significant, and again suggesting that further studies with a larger patient cohort are required. ROC analysis indicates that this may have potential as a biomarker (Fig 31f), but its specificity (88%) and sensitivity (60%) are rather low. A similar analysis with a larger cohort with increased numbers of CRC patients at different disease stages may be warranted.

CHAPTER VI: IMMUNOPHENOTYPIC CHANGES IN CRC WITH CLINICAL DATA

6.1 Introduction

Chapter 5 described the immune-phenotypic changes in circulating immune cells of CRC patients and compared these to those age-matched controls. These analyses looked at the CRC cohort as a whole, only considering their age when the blood sample was obtained. However, it is possible that clinical parameters such as tumor size, lymph node involvement, metastasis status and side of tumors impacted on the immunophenotypes of these patients. Therefore, data were re-analysed according to these different clinical parameters.

Most T cells' subsets except helper T cells increased in all stages of CRC. Different cytotoxic T cells increased, especially in the early stages. Decreasing helper T cells and increasing cytotoxic T cells were more prominent in late stages. Different types of monocytes except classical monocytes increased in early stages, some of them decreased in late stages. However, these differences did not reach statistical significance due to the low numbers of patients with different diseases of the disease.

However, a number of features were statistically significant, even with this relatively small sample size: numbers of NK cells relate to tumor sizes and CD14 staining intensity on monocytes increased in metastasis. Furthermore, DP T cells increased in stage II and stage III, DP cytotoxic cells correlate with tumour site and lymph node involvement, HLA-DR^{low} monocytes increased in S-II, and SL cytotoxic T cells and HLA-DR positive T cells increased in right-sided tumours.

6.2 Aim

To determine immuno-phenotypic properties with patients' clinical data.

6.3 Results

The changes were assessed with grading as follow:

+++/ ---	= significant increased or decreased (p<0.05)
++/--	= median value and interquartile values increased or decreased
	(>10% for value less than 50, >5% for values greater than 50)
+/ -	= median value or interquartile values increased or decreased
	(>10% for value less than 50, >5% for values greater than 50)
0	= no obvious change
Median	= middle value of the data set
Q1	= 25th percentile of the data set
Q3	= 75th percentile of the data set
Values in table	= percent positive cells

Colorectal cancer staging was assessed by the American Joint Committee on Cancer TNM system by a pathologist. Tumor size can be defined as;

- T1 = the cancer has grown through the muscularis mucosa into the submucosa,
- T2 = the cancer has grown into the muscularis propria,
- T3 = the cancer has grown into the outermost layers of the colon or rectum but has not gone through them,
- T4 = the cancer has grown through the wall of the colon or rectum

Lymph node involvement can be defined as;

- N0 = the cancer has not spread to nearby lymph nodes,
- N1 = the cancer has spread to 1 to 3 nearby lymph nodes,
- N2 = the cancer has spread to 4 to 6 nearby lymph nodes.

6.3.1 Patients' demographic data

Patients' clinical data with mean age and male:female ratio is shown in **Table 7**. Sixty five percent of patients were above 65 years old. The number of males patients

was higher than females. However, females were more prevalence in younger population and right-sided tumor cases.

Table 7: *CRC Patients' demographic data for immunophenotypic study*

Parameters	N	%	Mean age ± SD (y)	M: F
Age (range)				
<50	6	12	40.8 ± 6.0	1: 5
50-64	11	23	59.64 ± 4.5	8: 3
65 and above	32	65	74.1 ± 6.9	20: 12
Gender				29: 20
Male	29	59	68.8 ± 9.6	
Female	20	41	63.9 ± 16.7	
Stages				
S-I	11	22	66.6 ± 12.5	6: 5
S-II	7	14	73.1 ± 8.2	5: 2
S-III	15	31	68.4 ± 13	8: 7
S-IV	16	33	62.6 ± 14.6	10: 6
Tumor size				
T1	1	2	38	0: 1
T2	16	34	65.4 ± 10.5	10: 6
T3	18	38	67.1 ± 13.5	9: 9
T4	12	26	71.6 ± 8.2	9: 3
Lymph node involvement				
N0	22	48	66.6 ± 12.5	13: 9
N1	15	33	68.5 ± 8.7	8: 7
N2	9	20	64 ± 15.6	6: 3
Metastasis status				
Metastasis	16	33	62.6 ± 14.6	10: 6
Non metastasis	33	67	68.8 ± 11.9	19: 14
Left- or right-sided tumor				
Left side	27	56	62.2 ± 13.6	18: 9
Right side	21	41	72.3 ± 10.2	10: 11

6.3.2 Analysis of clinical data with CRC stages

Immunophenotypic changes were first compared with stage of disease (SI-IV) Significant increases were detected in cytotoxic T cells of S-IV, DP T cells of S-II and S-III, and HLA-DR^{low} monocytes of S-II. Most increased or decreased trends were noticed starting from S II (**Table 8**). Some immunophenotypes increased throughout the stages (increased trend such as NK^{dim} CD16- and intermediate monocytes), while some decreased throughout the stages (decreased trend such as helper T cells and classical monocytes).

Table 8: *Immunophenotypic changes among stages of CRCs*

	Stages	Median	Q1	Q3	Difference (compared to S-I)	
B lymphocytes	S-I	6.79	3.49	7.81		
(% of all lymphocytes)	S-II	3.69	2.2	6.74	**- -**	
	S-III	6.41	3.79	7.3	**0**	
	S-IV	3.42	2.393	6.713	**- -**	
T lymphocytes	S-I	71.6	65.85	75.15		
(% of all lymphocytes)	S-II	70.5	58.4	79.78	**0**	
	S-III	71.9	66.5	77.5	**0**	
	S-IV	69.1	63.6	81.7	**0**	
Helper T cells	S-I	64.9	49.9	71.4		
(% of T lymphocytes)	S-II	46.5	45.7	56.5	**-**	
	S-III	52	38.1	62	**- -**	
	S-IV	45.35	39.15	59.48	**- -**	
Cytotoxic T cells	S-I	35.2	18.2	38.9		
(% of T lymphocytes)	S-II	54	23.4	56.5	+ +	
	S-III	42	25.6	52.9	+ +	
	S-IV	44.05	31.85	53.68	+ + +	p = 0.04
DN T cells	S-I	1.64	0.93	5.503		
(% of T lymphocytes)	S-II	1.605	0.9225	6.53	**0**	
	S-III	2.96	1.54	4.26	+	
	S-IV	3.79	1.95	5.08	+	
DP T cells	S-I	0.355	0.2225	0.9		

(% of T lymphocytes)	S-II	2.245	1.203	5.058	+ + +	p = 0.01
	S-III	1.37	0.77	2.94	+ + +	p = 0.02
	S-IV	0.82	0.49	5.5	+ +	
NK T cells	S-I	3.255	0.61	8.245		
(% of T lymphocytes)	S-II	8.45	2.373	17.53	+ +	
	S-III	7.07	2.55	13.4	+ +	
	S-IV	4.69	1.76	11.8	+ +	
EA helper T cells	S-I	91.6	89.4	95.5		
(% of Helper T cells)	S-II	86.1	65.7	92	**0**	
	S-III	85.8	80.3	92.5	**0**	
	S-IV	92.75	88.55	95.4	**0**	
SL helper T cells	S-I	0.34	0.097	6		
(% of Helper T cells)	S-II	8.19	0.19	19.1	+ +	
	S-III	3.56	0.4	6.96	+ +	
	S-IV	0.71	0.1925	2.955	+	
DN helper T cells	S-I	1.07	0.19	2.41		
(% of Helper T cells)	S-II	2.14	1.41	5.26	+ +	
	S-III	1.11	0.24	2.59	**0**	
	S-IV	0.665	0.4325	1.533	-	
DP helper T cells	S-I	3.97	2.48	5.91		
(% of Helper T cells)	S-II	3.56	2.9	8.88	**0**	
	S-III	6.63	3.75	10.1	+ +	
	S-IV	4.095	3.25	6.263	**0**	
EA cytotoxic T cells	S-I	49.9	21.2	62.3		
(% of Cytotoxic T cells)	S-II	31	19.2	44.5	-	
	S-III	25.5	15.6	42.8	- -	
	S-IV	47.95	20.13	60.85	**0**	
SL cytotoxic T cells	S-I	37.1	23.6	58.8		
(% of Cytotoxic T cells)	S-II	48.2	31.8	58	+	
	S-III	48.2	40.4	70.5	+ +	
	S-IV	33.45	19.08	62.35	**0**	
DN cytotoxic T cells	S-I	10.5	4.99	15.1		
(% of Cytotoxic T cells)	S-II	11	2.49	27.3	**0**	
	S-III	8.2	3.97	14.5	-	

	S-IV	7.415	4.048	12.48	- -
DP cytotoxic T cells	S-I	5.82	4.89	7.42	
(% of Cytotoxic T cells)	S-II	4.84	0.54	6.61	- -
	S-III	6.29	2.9	12.1	**0**
	S-IV	6.205	2.688	11.73	**0**
CD8^{low} T cells	S-I	6.635	3.923	13.93	
(% of Cytotoxic T cells)	S-II	4.085	1.773	12.83	-
	S-III	6.16	3.46	10.9	-
	S-IV	7.56	5.53	12.6	+
CD8^{high} T cells	S-I	93.35	86.08	96.1	
(% of Cytotoxic T cells)	S-II	95.95	87.15	98.2	**0**
	S-III	93.8	89.1	96.5	**0**
	S-IV	92.4	87.4	94.5	**0**
CD4+ NK T cells	S-I	8.08	2.38	11.75	
(% of NK T cells)	S-II	8.37	4.453	25.25	+
	S-III	5.95	3.58	14.5	**0**
	S-IV	2.86	1.19	6.65	- -
CD8+ NK T cells	S-I	74.45	49.6	82.85	
(% of NK T cells)	S-II	69.15	48.7	80.9	**0**
	S-III	74.4	65.5	83.3	**0**
	S-IV	80.6	43.5	86.8	**0**
DN NK T cells	S-I	12.04	5.655	36.78	
(% of NK T cells)	S-II	2.95	0.98	26.55	- -
	S-III	7.28	4.63	25.5	- -
	S-IV	13.7	5	18.8	**0**
HLA-DR-positive T cells	S-I	15.2	10.4	24.3	
(% of T lymphocytes)	S-II	16.5	14.2	41.4	+
	S-III	22.7	20.1	32.6	+ +
	S-IV	17.75	14.33	30.55	+ +
HLA-DR-negative T cells	S-I	84.7	75.7	89.6	
(% of T lymphocytes)	S-II	83.5	58.5	85.8	**0**
	S-III	75.6	67.4	79.5	- -
	S-IV	82.25	69.43	85.63	**0**
NK cells	S-I	14.45	10.05	18.1	

(% of all lymphocytes)	S-II	13.7	9.975	21.7	**0**
	S-III	13.3	9.84	17.1	**0**
	S-IV	9.47	7.34	18.4	**-**
NK^{bright}	S-I	5.337	3.585	8.788	
(% of NK cells)	S-II	5.805	3.965	9.38	**0**
	S-III	9.57	6.62	11.18	+ +
	S-IV	5.74	4.19	10.19	+
NK^{bright} CD16+	S-I	2.695	1.633	4.548	
(% of NK cells)	S-II	2.31	1.543	4.533	**0**
	S-III	4.52	1.32	6.99	+
	S-IV	3.14	1.77	4.39	+
NK^{bright} CD16-	S-I	1.54	0.825	5.765	
(% of NK cells)	S-II	3.285	2.228	4.723	+
	S-III	5.17	2.89	7.7	+ +
	S-IV	2.43	1.49	5.26	+
NK^{dim}	S-I	94.66	91.2	96.43	
(% of NK cells)	S-II	94.21	90.64	96.05	**0**
	S-III	90.4	88.79	93.34	**0**
	S-IV	94.3	89.79	95.76	**0**
NK^{dim} CD16+	S-I	92.6	87.05	94.95	
(% of NK cells)	S-II	88.9	83.43	92.03	**0**
	S-III	83.9	77.6	89.8	**0**
	S-IV	84.8	83.4	91.5	**0**
NK^{dim} CD16-	S-I	1.96	0.78	5.71	
(% of NK cells)	S-II	4.735	2.608	8.043	+ +
	S-III	5	3.58	8.74	+ +
	S-IV	4.99	2.25	10.4	+ +
CD4+ NK	S-I	0.12	0.0835	0.485	
(% of NK cells)	S-II	0.4	0.26	0.61	+ +
	S-III	0.24	0.102	0.43	+
	S-IV	0.31	0.15	1.525	+ +
CD8+ NK	S-I	28.7	15.28	41.4	
(% of NK cells)	S-II	41.15	28.53	51.63	+ +
	S-III	31.7	20.3	43.2	+

	S-IV	37.3	27.7	40.3	+	
DN NK	S-I	70.95	58.28	82.13		
(% of NK cells)	S-II	58.45	47.85	71.15	**- -**	
	S-III	66.8	56.7	79.7	**0**	
	S-IV	62.7	59.2	70.8	**-**	
Monocytes	S-I	20.9	16.8	23.4		
(% of PBMC)	S-II	23.5	11.3	30.8	+	
	S-III	24.8	13.2	33.6	+	
	S-IV	18.55	12	26.3	**0**	
classical monocytes	S-I	84.5	74.43	86.95		
(% of Monocytes)	S-II	81.65	65.15	87.8	**0**	
	S-III	77.4	69.5	86.1	**-**	
	S-IV	73.6	65.3	92.8	**-**	
intermediate monocytes	S-I	10.58	5.708	14.63		
(% of Monocytes)	S-II	13.15	7.895	24.98	+ +	
	S-III	12.4	9.28	23.5	+ +	
	S-IV	13.8	4.29	30.5	+ +	
non-classical monocytes	S-I	5.065	2.578	8.865		
(% of Monocytes)	S-II	5.89	2.863	9.883	+ +	
	S-III	5.5	3.98	10.2	+	
	S-IV	4.33	2.5	8.87	**-**	
CD4+ monocytes	S-I	11.14	8.638	29.23		
(% of Monocytes)	S-II	21.8	7.463	31.25	+	
	S-III	14.5	7.25	38.2	+	
	S-IV	18.7	9.07	74.2	+	
CD56+ monocytes	S-I	8.81	4.488	11.78		
(% of Monocytes)	S-II	19.55	5.665	27.88	+ +	
	S-III	9.81	7.88	16.5	+ +	
	S-IV	5.15	3.49	22.3	**-**	
HLA-DR^{low} monocytes	S-I	10.6	5.91	21.8		
(% of Monocytes)	S-II	26	16.5	43.5	+ + +	$p = 0.03$
	S-III	12.2	3.41	21.6	+	
	S-IV	11.6	3.74	20.2	**0**	
HLA-DR^{high} monocytes	S-I	88.4	76.7	93.6		

(% of Monocytes)	S-II	73.6	54.4	82.5	**- - -**	p = 0.03
	S-III	87.2	77	96.1	**0**	
	S-IV	87.2	78.48	96.03	**0**	
MFI of CD3	S-I	3881	3497	4015		
(T lymphocytes)	S-II	3879	3211	4816	**0**	
	S-III	3232	3051	3814	**-**	
	S-IV	4146	3203	4562	**0**	
MFI of CD14	S-I	20998	15579	27458		
(Monocytes)	S-II	22323	16267	29500	**0**	
	S-III	18454	12353	24530	**- -**	
	S-IV	25887	19592	29059	**+**	
MFI of CD56	S-I	9099	8282	10661		
(NK cells)	S-II	8736	8237	10749	**0**	
	S-III	11068	8234	11914	**+**	
	S-IV	9241	7978	10738	**0**	
MFI of CD19	S-I	110827	87591	124184		
(B lymphocytes)	S-II	128670	94532	134047	**+**	
	S-III	109162	92930	127525	**0**	
	S-IV	99683	93248	124485	**-**	

6.3.3 Analysis of clinical data with tumor sizes

In this study, there was only one patient with T1. Therefore, immunophenotypic changes were compared with T2 of CRCs. Most T cells subsets had increased in numbers when tumor size became larger. NK^{bright} cells significantly increased in T3 and T4 (**Table 9**). Tumor size had significant positive correlation with DP cytotoxic T cells, NK^{bright} cells and NK^{dim} CD16- cells. It had a significant negative correlation with NK^{dim} cells and NK^{dim} CD16+ cells (**Fig 34**).

Table 9: Immunophenotypic changes with tumor sizes

	Tumor size	Median	Q1	Q3	Difference (compared to T2)
B lymphocytes	T2	4.49	2.438	7.358	
(% of all lymphocytes)	T3	4.62	3.07	7.733	**0**

	T4	5.73	2.838	7.078	+	
T lymphocytes	T2	71.6	66.38	73.9		
(% of all lymphocytes)	T3	73	64.6	78.7	**0**	
	T4	69.8	63.28	74.85	**0**	
Helper T cells	T2	58.55	36.05	65.9		
(% of T lymphocytes)	T3	46.1	38.13	58.05	**-**	
	T4	55.5	47.73	72.3	**0**	
Cytotoxic T cells	T2	36.15	20.53	43.13		
(% of T lymphocytes)	T3	45.05	23.6	60.05	+ +	
	T4	41.6	26.75	51.1	+ +	
DN T cells	T2	1.715	1.03	4.093		
(% of T lymphocytes)	T3	2.24	1.31	4.26	+	
	T4	2.64	1.903	5.215	+ +	
DP T cells	T2	0.635	0.34	1.185		
(% of T lymphocytes)	T3	1.69	0.6	4.43	+ + +	$p = 0.03$
	T4	1.21	0.395	1.938	+ +	
NK T cells	T2	3.255	0.61	7.495		
(% of T lymphocytes)	T3	7.07	2.89	17.4	+ +	
	T4	5.775	2.175	11.6	+ +	
EA helper T cells	T2	91.25	86.1	95.3		
(% of Helper T cells)	T3	89.2	79.58	93.25	**0**	
	T4	91.25	81.68	93.88	**0**	
SL helper T cells	T2	1.21	0.1053	6.083		
(% of Helper T cells)	T3	3.06	0.2425	9.163	+ +	
	T4	2.37	0.4675	7.883	+ +	
DN helper T cells	T2	0.88	0.2025	1.713		
(% of Helper T cells)	T3	1.26	0.163	4.418	+	
	T4	1.515	0.6375	1.738	+	
DP helper T cells	T2	4.67	3.123	6.753		
(% of Helper T cells)	T3	4.07	3.375	10.3	**0**	
	T4	4.865	3.738	6.645	**0**	
EA cytotoxic T cells	T2	42.95	18.95	61.38		
(% of Cytotoxic T cells)	T3	35.95	19.88	57.1	**-**	
	T4	28.4	19.45	48.65	**-**	

SL cytotoxic T cells	T2	41.75	19.18	66.98		
(% of Cytotoxic T cells)	T3	44.05	23.93	60.23	**0**	
	T4	46.55	33.43	62.35	+	
DN cytotoxic T cells	T2	8.755	4.638	14.98		
(% of Cytotoxic T cells)	T3	9.795	3.97	13.9	**0**	
	T4	7.28	4.605	12.2	**-**	
DP cytotoxic T cells	T2	5.605	2.548	7.29		
(% of Cytotoxic T cells)	T3	5.9	2.645	10.8	**0**	
	T4	9.37	4.99	15.68	+ + +	p = 0.04
CD8^{low} T cells	T2	6.635	3.863	8.448		
(% of Cytotoxic T cells)	T3	4.04	2.24	6.86	**- -**	
	T4	8.265	6.37	17.55	+ +	
CD8^{high} T cells	T2	93.35	91.58	96.1		
(% of Cytotoxic T cells)	T3	96	93.1	97.8	**0**	
	T4	91.7	82.45	93.65	**0**	
CD4+ NK T cells	T2	5.475	2.903	10.3		
(% of NK T cells)	T3	5.71	1.66	12.6	**0**	
	T4	5.985	2.273	19.1	**0**	
CD8+ NK T cells	T2	79.15	64	86		
(% of NK T cells)	T3	78.6	65.5	83.4	**0**	
	T4	64.95	41.08	84.68	**-**	
DN NK T cells	T2	9.085	6.14	28.35		
(% of NK T cells)	T3	7.15	1.81	17.4	**- -**	
	T4	13.85	3.945	31.33	+	
HLA-DR-positive T cells	T2	17.2	10.75	25.28		
(% of T lymphocytes)	T3	23.5	14.28	39.73	+ +	
	T4	19.3	15.38	22.48	+	
HLA-DR-negative T cells	T2	82.8	74.73	89.25		
(% of T lymphocytes)	T3	76.5	60.28	85.73	**0**	
	T4	79.05	75.28	84.63	**0**	
NK cells	T2	14.55	11.28	17.35		
(% of all lymphocytes)	T3	9.95	5.57	14.3	**- -**	
	T4	15.25	10.24	20.23	**0**	
NK^{bright}	T2	4.305	2.58	8.688		

(% of NK cells)	T3	6.62	5.21	10.59	+ + +	p = 0.04
	T4	9.01	6.928	10.35	+ + +	p = 0.03
NK^{bright} CD16+	T2	2.37	0.85	3.375		
(% of NK cells)	T3	2.78	1.64	5.86	+ +	
	T4	3.765	2.45	6.338	+ + +	p = 0.04
NK^{bright} CD16-	T2	1.625	0.825	5.825		
(% of NK cells)	T3	4.07	3.19	5.36	+	
	T4	3.985	1.77	7.843	+ +	
NK^{dim}	T2	95.71	91.29	97.43		
(% of NK cells)	T3	93.34	89.45	94.82	0	
	T4	91	89.67	93.06	0	
NK^{dim} CD16+	T2	92.6	85.1	95.05		
(% of NK cells)	T3	85.5	83.5	89.8	-	
	T4	80.4	76.3	90.2	- -	
NK^{dim} CD16-	T2	4.7	0.915	5.71		
(% of NK cells)	T3	5.26	3.73	6.32	+ +	
	T4	7.145	3.258	15.63	+ + +	p = 0.049
CD4+ NK	T2	0.12	0.0835	0.405		
(% of NK cells)	T3	0.485	0.18	0.67	+ +	
	T4	0.24	0.111	0.5125	+ +	
CD8+ NK	T2	32	25.45	41.4		
(% of NK cells)	T3	33.3	20.3	40.3	0	
	T4	35.9	23.8	48.7	+	
DN NK	T2	67.9	58.28	74.1		
(% of NK cells)	T3	66.5	59.2	79.7	0	
	T4	62.8	51.08	70.65	-	
Monocytes	T2	20.8	14.33	23.55		
(% of PBMC)	T3	24.2	13.23	31.65	+	
	T4	21.35	12.83	31.78	0	
classical monocytes	T2	84.75	74.35	88		
(% of Monocytes)	T3	75.9	60.5	86.1	-	
	T4	80.85	72.7	83.63	0	
intermediate monocytes	T2	11.15	6.263	15.15		
(% of Monocytes)	T3	14.4	8.53	30.5	+ +	

	T4	13.1	10.83	18.15	+ +	
non-classical monocytes	T2	4.655	2.458	7.773		
(% of Monocytes)	T3	5.25	3.28	9.41	+ +	
	T4	4.76	3.25	8.085	**0**	
CD4+ monocytes	T2	14.1	8.638	23.73		
(% of Monocytes)	T3	10.82	5.35	43.58	**-**	
	T4	29.6	9.07	52.5	+	
CD56+ monocytes	T2	8.81	4.533	11.78		
(% of Monocytes)	T3	10.4	5.15	26.3	+ +	
	T4	8.78	4.685	20.53	**0**	
HLA-DR^{low} monocytes	T2	18.9	6.633	25.53		
(% of Monocytes)	T3	14.35	5.338	22.7	**- -**	
	T4	18.2	4.148	21.48	**-**	
HLA-DR^{high} monocytes	T2	80.1	73.05	92.9		
(% of Monocytes)	T3	84.85	76.15	93.85	**0**	
	T4	80.7	76.53	95.58	**0**	
MFI of CD3	T2	3983	3690	4232		
(T lymphocytes)	T3	3243	3113	4648	**-**	
	T4	3460	3014	4131	**-**	
MFI of CD14	T2	24102	17786	28684		
(Monocytes)	T3	20018	12468	26144	**-**	
	T4	18432	16814	22899	**-**	
MFI of CD56	T2	8458	7368	9948		
(NK cells)	T3	9241	8199	11419	+	
	T4	10720	8876	11420	+ + +	p = 0.02
MFI of CD19	T2	111398	92400	135991		
(B lymphocytes)	T3	103627	92863	128458	**0**	
	T4	103678	93551	124630	**0**	
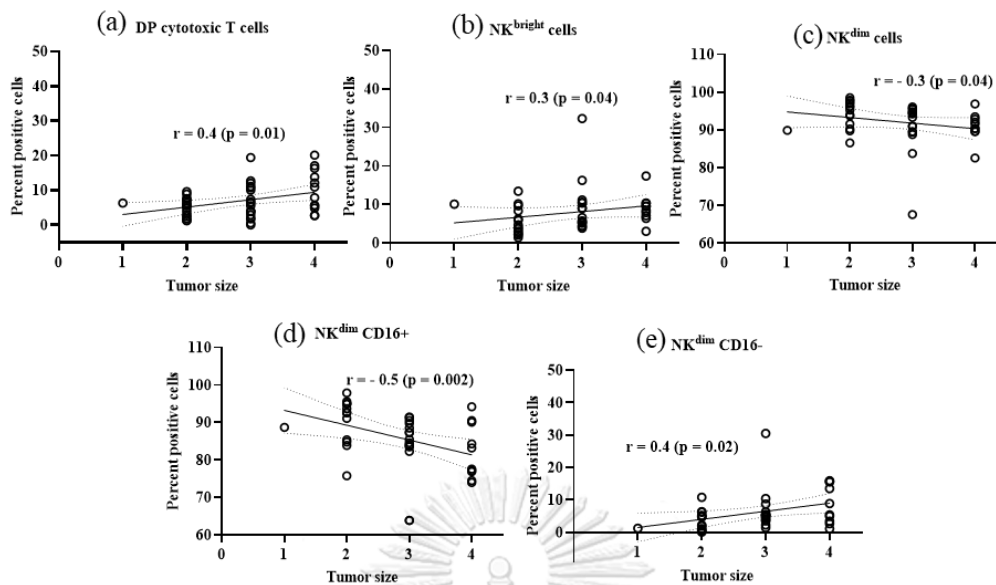
Figure 34: *Significant correlation of immunophenotypes and tumor size of CRC*
(a) DP cytotoxic T cells, (b) NK^{bright} cells, (c) NK^{dim} cells, (d) NK^{dim} CD16+ cells, (e) NK^{dim} CD16- cells, line in graph represents best fit line with 95% CI.

6.3.4 Analysis of clinical data with LN involvement

No obvious changes were observed in T cells compartment. The DN T cells and DP T cells tended to increase. NK^{bright} increased in most lymph-node-involved CRC: NK^{bright} CD16+ increased in N1, and NK^{bright} CD16- increased in N2. No obvious changes in 3 major types of monocytes, however, CD56+ monocytes and HLA-DR^{low} monocytes tended to decrease in N1 CRC (**Table 10**). DP (CD28+ CD57+) cytotoxic T cells significantly increased in N2 CRC (**Table 10**), and positively correlate with lymph nodes involvement (**Fig 35**).

Table 10: *Immunophenotypic changes in lymph nodes involvement*

	Lymph Node Involve-ment	Median	Q1	Q3	Difference (compared to N0)
B lymphocytes	N0	4.475	2.733	7.585	
(% of all lymphocytes)	N1	5.07	2.83	7.57	+
	N2	5.05	3.77	6.415	+
T lymphocytes	N0	71.6	65.55	76.15	
(% of all lymphocytes)	N1	70.7	60.88	80.4	**0**

	N2	71.9	65.45	75.65	**0**
Helper T cells	N0	51.3	40.58	65.5	
(% of T lymphocytes)	N1	52.3	42.9	57.7	**0**
	N2	59.1	37.4	67.2	+
Cytotoxic T cells	N0	38.25	23.23	54.45	
(% of T lymphocytes)	N1	41.1	30.2	45.7	**0**
	N2	41.9	24.6	57.8	**0**
DN T cells	N0	1.715	1.01	4.055	
(% of T lymphocytes)	N1	4.225	2.063	5.488	+ +
	N2	2.59	1.34	3.37	+
DP T cells	N0	0.845	0.34	1.648	
(% of T lymphocytes)	N1	0.865	0.485	2.165	+
	N2	1.44	0.585	2.73	+ +
NK T cells	N0	4.6	1.898	10.25	
(% of T lymphocytes)	N1	9.165	1.848	13.48	+
	N2	4.02	1.9	15.7	**0**
EA helper T cells	N0	90	83.15	95.43	
(% of Helper T cells)	N1	92	83.9	94.6	**0**
	N2	91.3	82.05	93.75	**0**
SL helper T cells	N0	2.515	0.16	7.845	
(% of Helper T cells)	N1	3.1	0.17	6.11	**0**
	N2	0.49	0.22	5.035	-
DN helper T cells	N0	1.435	0.1665	2.64	
(% of Helper T cells)	N1	1.11	0.44	2.59	**0**
	N2	0.43	0.2	2.14	-
DP helper T cells	N0	4.085	2.915	6.895	
(% of Helper T cells)	N1	4.27	3.62	6.63	**0**
	N2	8.19	3.55	11.65	+ +
EA cytotoxic T cells	N0	42.7	20.7	55.85	
(% of Cytotoxic T cells)	N1	23.7	15.6	53.5	-
	N2	42.8	27.1	62	+
SL cytotoxic T cells	N0	40.8	26.93	58.2	
(% of Cytotoxic T cells)	N1	56.7	24.4	70.5	+
	N2	40.4	16.9	48.15	-

DN cytotoxic T cells	N0	9.905	4.873	14.73		
(% of Cytotoxic T cells)	N1	9.59	5.58	14.5	**0**	
	N2	6.88	3.32	12.6	**- -**	
DP cytotoxic T cells	N0	5.68	3.34	7.03		
(% of Cytotoxic T cells)	N1	3.93	2.65	10	**-**	
	N2	11.1	5.655	16.7	+ + +	p = 0.01
CD8^{low} T cells	N0	5.915	3.573	8.635		
(% of Cytotoxic T cells)	N1	7.025	4.613	13.7	+ +	
	N2	6.16	2.995	13.65	**0**	
CD8^{high} T cells	N0	94.1	91.35	96.4		
(% of Cytotoxic T cells)	N1	92.95	86.3	95.4	**0**	
	N2	93.8	86.35	97	**0**	
CD4+ NK T cells	N0	6.365	2.523	10.5		
(% of NK T cells)	N1	4.995	2.598	11.02	**-**	
	N2	3.65	1.53	15.6	**-**	
CD8+ NK T cells	N0	78.3	55.83	86.5		
(% of NK T cells)	N1	73.1	55.7	85.53	**-**	
	N2	79.2	67.9	83.35	**0**	
DN NK T cells	N0	9.085	3.27	26		
(% of NK T cells)	N1	19.6	6.613	29.85	+ +	
	N2	7.17	4.07	15.7	**-**	
HLA-DR-positive T cells	N0	16.8	13.6	27.18		
(% of T lymphocytes)	N1	21.7	14.4	32.6	+	
	N2	21.8	14.55	25.65	+	
HLA-DR-negative T cells	N0	83.2	72.83	86.4		
(% of T lymphocytes)	N1	77.4	67.4	85.4	**-**	
	N2	78.1	74.05	85.45	**-**	
NK cells	N0	14.25	10.58	18.1		
(% of all lymphocytes)	N1	13.5	5.133	19.75	**0**	
	N2	10.6	8.645	20.35	**-**	
NK^{bright}	N0	5.772	3.993	9.535		
(% of NK cells)	N1	9.315	6.593	10.74	+ +	
	N2	6.62	4.56	13.89	+ +	
NK^{bright} CD16+	N0	2.695	1.698	4.205		

(% of NK cells)	N1	5.325	2.515	6.473	+ + +	p = 0.03
	N2	2.45	1.31	4.84	**0**	
NK^{bright} CD16-	N0	3.285	1.218	5.638		
(% of NK cells)	N1	3.325	1.995	5.665	**0**	
	N2	4.68	2.705	8.7	+ +	
NK^{dim}	N0	94.2	90.47	96.02		
(% of NK cells)	N1	90.69	89.29	93.4	**0**	
	N2	93.34	86.1	95.47	**0**	
NK^{dim} CD16+	N0	88.7	84.8	93.7		
(% of NK cells)	N1	84.15	82.98	91.03	**-**	
	N2	83.9	75.45	90.65	**-**	
NK^{dim} CD16-	N0	5	1.96	6.32		
(% of NK cells)	N1	4.995	2.058	6.313	**0**	
	N2	5	4.185	11.95	+	
CD4+ NK	N0	0.28	0.12	0.54		
(% of NK cells)	N1	0.16	0.075	0.695	**-**	
	N2	0.28	0.18	0.52	**0**	
CD8+ NK	N0	32.05	20.8	41.8		
(% of NK cells)	N1	32.4	18.55	40	**0**	
	N2	33.9	24	41.75	**0**	
DN NK	N0	67.8	58.03	78.03		
(% of NK cells)	N1	65.1	59.83	80.78	**0**	
	N2	65.8	57.95	76	**0**	
Monocytes	N0	21.1	15.98	26.25		
(% of PBMC)	N1	24	11.3	33.3	+	
	N2	24.2	13.3	25.25	+	
classical monocytes	N0	81.85	72.45	85.48		
(% of Monocytes)	N1	77.35	70.03	87.23	**0**	
	N2	81.2	55.05	88.65	**0**	
intermediate monocytes	N0	12.45	7.568	16.98		
(% of Monocytes)	N1	10.85	7.793	17.88	**0**	
	N2	12.4	7.48	27.6	**0**	
non-classical monocytes	N0	5.065	2.935	9.2		
(% of Monocytes)	N1	5.635	3.085	10.73	+	

	N2	4.79	3.13	6.005	**0**
CD4+ monocytes	N0	14.35	8.433	29.13	
(% of Monocytes)	N1	11.39	8.435	57.5	**0**
	N2	20.15	6.92	36.88	**+**
CD56+ monocytes	N0	9.865	5.17	20.03	
(% of Monocytes)	N1	8.355	4.418	10.01	**- -**
	N2	10.4	4.46	22.3	**0**
HLA-DR^{low} monocytes	N0	18.9	8.928	26.7	
(% of Monocytes)	N1	10.5	3.41	21.6	**- -**
	N2	18	5.335	20.65	**-**
HLA-DR^{high} monocytes	N0	80.1	71.8	90.43	
(% of Monocytes)	N1	88.7	77	96.3	**+ +**
	N2	81.2	77.85	94.3	**0**
MFI of CD3	N0	3950	3387	4135	
(T lymphocytes)	N1	3199	2904	4528	**-**
	N2	3381	3182	3980	**-**
MFI of CD14	N0	22513	16079	28905	
(Monocytes)	N1	20018	12353	25887	**- -**
	N2	18565	16764	25573	**-**
MFI of CD56	N0	9039	8249	10526	
(NK cells)	N1	10820	9085	11638	**+ +**
	N2	8652	7143	12349	**0**
MFI of CD19	N0	111803	92960	129672	
(B lymphocytes)	N1	111815	96808	134292	**0**
	N2	96438	92331	107883	**-**

DP cytotoxic T cells

r = 0.4 (p = 0.005)
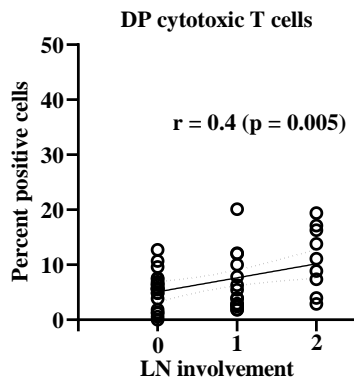
Figure 35: *Significant correlation of DP cytotoxic T cells and LN involvement of CRC line in graph represents best fit line with 95% CI.*

6.3.5 Analysis of clinical data with metastasis status

Most cells subsets showed decreased trend in metastasis compared to non-metastasis, however, CD14 staining intensity increased in metastatic cases (**Table 11**).

Table 11: *Immunophenotypic changes in metastatic status*

	Meta-static status	Median	Q1	Q3	Difference (compared to NM)
B lymphocytes	NM	6.41	3.59	7.405	
(% of all lymphocytes)	M	3.42	2.393	6.713	-
T lymphocytes	NM	71.9	66	76.9	
(% of all lymphocytes)	M	69.1	63.6	81.7	**0**
Helper T cells	NM	52.7	42.95	65.7	
(% of T lymphocytes)	M	45.35	39.15	59.48	-
Cytotoxic T cells	NM	38.9	23.5	53.15	
(% of T lymphocytes)	M	44.05	31.85	53.68	+
DN T cells	NM	2.11	1.1	4.26	
(% of T lymphocytes)	M	3.79	1.95	5.08	+ +
DP T cells	NM	0.99	0.34	2.52	
(% of T lymphocytes)	M	0.82	0.49	5.5	**0**
NK T cells	NM	6.56	2.26	12.3	
(% of T lymphocytes)	M	4.69	1.76	11.8	-
EA helper T cells	NM	89.7	81.2	93.75	

(% of Helper T cells)	M	92.75	88.55	95.4	**0**
SL helper T cells	NM	3.56	0.185	7.96	
(% of Helper T cells)	M	0.71	0.1925	2.955	**-**
DN helper T cells	NM	1.46	0.27	2.645	
(% of Helper T cells)	M	0.665	0.4325	1.533	**-**
DP helper T cells	NM	5.14	2.945	8.115	
(% of Helper T cells)	M	4.095	3.25	6.263	**-**
EA cytotoxic T cells	NM	28.7	18.7	51.45	
(% of Cytotoxic T cells)	M	47.95	20.13	60.85	**+ +**
SL cytotoxic T cells	NM	48.1	29.45	64.25	
(% of Cytotoxic T cells)	M	33.45	19.08	62.35	**-**
DN cytotoxic T cells	NM	9.31	4.755	14.8	
(% of Cytotoxic T cells)	M	7.415	4.048	12.48	**- -**
DP cytotoxic T cells	NM	5.69	3.37	9.225	
(% of Cytotoxic T cells)	M	6.205	2.688	11.73	**0**
CD8^{low} T cells	NM	6.3	3.57	10.9	
(% of Cytotoxic T cells)	M	7.56	5.53	12.6	**+ +**
CD8^{high} T cells	NM	93.7	89.1	96.4	
(% of Cytotoxic T cells)	M	92.4	87.4	94.5	**0**
CD4+ NK T cells	NM	6.78	3.21	14.5	
(% of NK T cells)	M	2.86	1.19	6.65	**- -**
CD8+ NK T cells	NM	74.4	56.8	81.4	
(% of NK T cells)	M	80.6	43.5	86.8	**0**
DN NK T cells	NM	7.63	3.51	26.9	
(% of NK T cells)	M	13.7	5	18.8	**+**
HLA-DR-positive T cells	NM	20.1	14.55	27.85	
(% of T lymphocytes)	M	17.75	14.33	30.55	**-**
HLA-DR-negative T cells	NM	79.5	71.8	85.45	
(% of T lymphocytes)	M	82.25	69.43	85.63	**0**
NK cells	NM	13.7	9.95	17.2	
(% of all lymphocytes)	M	9.47	7.34	18.4	**-**
NK^{bright}	NM	7.89	4.27	10.39	
(% of NK cells)	M	5.74	4.19	10.19	**-**
NK^{bright} CD16+	NM	2.77	1.64	5.65	

(% of NK cells)	M	3.14	1.77	4.39	**0**
NK^bright CD16-	NM	4.07	1.3	5.87	
(% of NK cells)	M	2.43	1.49	5.26	**-**
NK^dim	NM	92.1	89.6	95.76	
(% of NK cells)	M	94.3	89.79	95.76	**0**
NK^dim CD16+	NM	87.35	82.98	92.6	
(% of NK cells)	M	84.8	83.4	91.5	**0**
NK^dim CD16-	NM	4.995	1.84	6.265	
(% of NK cells)	M	4.99	2.25	10.4	**+**
CD4+ NK	NM	0.26	0.09975	0.4875	
(% of NK cells)	M	0.31	0.15	1.525	**+ +**
CD8+ NK	NM	31.7	19.9	43.2	
(% of NK cells)	M	37.3	27.7	40.3	**+**
DN NK	NM	67.4	56.7	80	
(% of NK cells)	M	62.7	59.2	70.8	**-**
Monocytes	NM	23.4	15.1	29.4	
(% of PBMC)	M	18.55	12	26.3	**- -**
classical monocytes	NM	81.1	71.5	85.8	
(% of Monocytes)	M	73.6	65.3	92.8	**-**
intermediate monocytes	NM	11.9	8.53	17.7	
(% of Monocytes)	M	13.8	4.29	30.5	**+**
non-classical monocytes	NM	5.15	3.28	9.41	
(% of Monocytes)	M	4.33	2.5	8.87	**-**
CD4+ monocytes	NM	14.5	8.03	29.6	
(% of Monocytes)	M	18.7	9.07	74.2	**+ +**
CD56+ monocytes	NM	9.81	6.04	16.5	
(% of Monocytes)	M	5.15	3.49	22.3	**-**
HLA-DR^low monocytes	NM	18	5.76	22.35	
(% of Monocytes)	M	11.6	3.74	20.2	**-**
HLA-DR^high monocytes	NM	81.2	75.95	93.5	
(% of Monocytes)	M	87.2	78.48	96.03	**0**
MFI of CD3	NM	3622	3172	4015	
(T lymphocytes)	M	4146	3203	4562	**+**
MFI of CD14	NM	19483	15783	25002	

(Monocytes)	M	25887	19592	29059	+ + +	p = 0.04
MFI of CD56	NM	9846	8249	11419		
(NK cells)	M	9241	7978	10738	**0**	
MFI of CD19	NM	110827	93068	130674		
(B lymphocytes)	M	99683	93248	124485	**-**	

6.3.6 Analysis of clinical data with left- or right- sided tumor

Most immunophenotypes between left- and right- sided tumor were similar. But SL T cells and HLA-DR positive T cells significantly increased; intermediate monocytes, non-classical monocytes and CD4+ monocytes tended to decrease in right-sided tumor (**Table 12**).

Table 12: Immunophenotypic changes between Left- and Right-sided tumor

	left-sided or right-sided tumor	Median	Q1	Q3	Difference (compared to left-sided tumor)
B lymphocytes	L	4.97	3.69	7.7	
(% of all lymphocytes)	R	5.07	2.495	7.005	**0**
T lymphocytes	L	71.55	64.15	77.35	
(% of all lymphocytes)	R	70.5	65.55	81.25	**0**
Helper T cells	L	54.7	39	64.4	
(% of T lymphocytes)	R	52.3	43.25	68.15	**0**
Cytotoxic T cells	L	40.3	23.6	47.4	
(% of T lymphocytes)	R	42.9	24.6	55.25	**0**
DN T cells	L	3.785	1.333	5.335	
(% of T lymphocytes)	R	2.11	1.425	3.51	**-**
DP T cells	L	0.895	0.3775	2.313	
(% of T lymphocytes)	R	1.05	0.405	3.525	**+**
NK T cells	L	5.625	1.703	12.18	
(% of T lymphocytes)	R	5.97	2.01	14.4	**+**
EA helper T cells	L	92	89.4	95.5	

(% of Helper T cells)	R	86.1	76.15	93.2	**-**	
SL helper T cells	L	0.4	0.16	3.11		
(% of Helper T cells)	R	4.51	0.565	12.3	+ + +	p = 0.02
DN helper T cells	L	0.91	0.19	1.74		
(% of Helper T cells)	R	1.48	0.64	3.675	+ +	
DP helper T cells	L	4.15	2.94	7.83		
(% of Helper T cells)	R	5.13	3.34	6.72	+	
EA cytotoxic T cells	L	44.5	24.1	58.6		
(% of Cytotoxic T cells)	R	25.6	18.7	51.1	**- -**	
SL cytotoxic T cells	L	35.8	18.7	58.3		
(% of Cytotoxic T cells)	R	48.8	36.4	67.85	+ +	
DN cytotoxic T cells	L	10.5	3.97	14.6		
(% of Cytotoxic T cells)	R	7.94	4.755	13.55	**-**	
DP cytotoxic T cells	L	5.82	2.9	8.86		
(% of Cytotoxic T cells)	R	5.69	2.665	10.45	**0**	
CD8^{low} T cells	L	6.88	3.675	12.18		
(% of Cytotoxic T cells)	R	6.3	3.75	9.64	**0**	
CD8^{high} T cells	L	93.1	87.83	96.3		
(% of Cytotoxic T cells)	R	93.7	90.35	96.25	**0**	
CD4+ NK T cells	L	3.895	2.313	14.03		
(% of NK T cells)	R	6.65	3.095	10.03	+	
CD8+ NK T cells	L	73.3	53.5	82.63		
(% of NK T cells)	R	78.5	49	85.25	**0**	
DN NK T cells	L	13.45	6.678	29.05		
(% of NK T cells)	R	7.28	3.18	15.25	**- -**	
HLA-DR-positive T cells	L	17.1	14.2	24.4		
(% of T lymphocytes)	R	22.6	15.95	36	+ + +	p = 0.04
HLA-DR-negative T cells	L	82.9	75.6	85.8		
(% of T lymphocytes)	R	77.3	64	83.45	**-**	
NK cells	L	13.9	9.553	17.85		
(% of all lymphocytes)	R	11.6	8.985	17.65	**-**	
NK^{bright}	L	7.255	4.103	10.3		
(% of NK cells)	R	6.41	4.23	10.05	**0**	
NK^{bright} CD16+	L	2.775	1.433	5.038		

(% of NK cells)	R	3.04	1.755	5.985	+
NK^{bright} CD16-	L	3.69	1.865	5.488	
(% of NK cells)	R	3.19	1.105	6.365	**-**
NK^{dim}	L	92.72	89.72	95.91	
(% of NK cells)	R	93.54	89.95	95.76	**0**
NK^{dim} CD16+	L	85.45	83.43	91.4	
(% of NK cells)	R	90.3	79.18	94.08	**0**
NK^{dim} CD16-	L	5	1.685	6.295	
(% of NK cells)	R	3.895	2.033	6.163	**0**
CD4+ NK	L	0.25	0.14	0.56	
(% of NK cells)	R	0.24	0.08625	0.4875	**-**
CD8+ NK	L	31.6	21.7	40.15	
(% of NK cells)	R	33.3	22.3	44.45	**0**
DN NK	L	67.6	59.43	76.58	
(% of NK cells)	R	65.8	55.3	75.35	**0**
Monocytes	L	22.2	16.8	27	
(% of PBMC)	R	21.3	11.4	29.4	**0**
classical monocytes	L	76.65	67.88	86.08	
(% of Monocytes)	R	84.1	73.45	87.9	+
intermediate monocytes	L	12.35	8.718	22.78	
(% of Monocytes)	R	12.4	6.23	15.4	**-**
non-classical monocytes	L	5.375	3.373	9.385	
(% of Monocytes)	R	4.4	2.275	8.85	**-**
CD4+ monocytes	L	17.3	8.763	39.63	
(% of Monocytes)	R	12.8	7.635	25.4	**- -**
CD56+ monocytes	L	8.95	4.76	14.03	
(% of Monocytes)	R	9.81	5.31	19.4	+
HLA-DR^{low} monocytes	L	18	5.91	22.9	
(% of Monocytes)	R	10.5	3.725	21.15	**-**
HLA-DR^{high} monocytes	L	81.2	75.9	93.3	
(% of Monocytes)	R	88.7	77.4	95.9	+
MFI of CD3	L	3858	3171	4527	
(T lymphocytes)	R	3791	3186	4133	**0**
MFI of CD14	L	19538	13937	28486	

(Monocytes)	R	20846	17916	25209	**0**
MFI of CD56	L	8869	7864	11249	
(NK cells)	R	10620	8689	11282	+
MFI of CD19	L	102558	93205	118536	
(B lymphocytes)	R	111969	92724	138937	**0**

6.4 Discussion

Helper T cell and cytotoxic T cells

In most participants of >50 y healthy controls, helper T cells increased, and cytotoxic T cells decreased (Chapter 4). The reverse pattern (helper T cells decreased, and cytotoxic T cells increased) was seen in CRC (Chapter 5). Decreased helper T cells and increased cytotoxic T cells were observed throughout the stages of CRC (Table 8). Cytotoxic T cells increased in larger tumors in most cases (Table 9).

Cytotoxic T cells are powerful effectors cells in tumor immunology (Raskov et al., 2021). Their functions can be enhanced by the helper T cells, and they become exhausted without the helper T cells (Ahrends et al., 2017). There is also evidence of heterogenous cytotoxic T cells exhaustion in solid cancers (Dolina et al., 2021). Based on these facts and the results, there may be exhausted cytotoxic T cells in CRC starting from early states.

NK cells in tumor size

When tumor size increased, NK^{bright} increased and NK^{dim} decreased especially in NK^{dim} CD16+ cells (Fig 34). NK^{bright} number significantly increased in T3 and T4 than T2 tumors (Table 9). These cells are considered immature cells with increased production of cytokines such as IFN-γ, TNF-α, GM-CSF, IL10 and IL13 and have less cytotoxic activity than NK^{dim} cells (Poli et al., 2009). Their numbers increased in larger tumors and this implies that the immune response was enhanced by interacting with other immune cells. However, the major population, NK^{dim} CD16+ decreased which may indicate decrease ability to target tumor cells, as NK^{dim} CD16+ are important for cytotoxicity of NK cells (Poli et al., 2009). Therefore, immunophenotypic changes of NK cells in CRC could lead to inefficient tumor cells clearance in CRC.

DP cytotoxic cells

Another immunophenotype that correlated with tumor size was DP (CD28+ CD57+) cytotoxic T cells (Fig 34). DP cytotoxic T cells also correlate with LN involvement (Fig 35). They have undergone cell divisions and possess the same telomere length as SL cytotoxic T cells (Strioga et al., 2011). They are a mixed population of cells and contain effector memory cells, terminally differentiated effector memory T cells, central memory cells and naïve cells. Their cytokine production is similar to SL cytotoxic T cells but have higher levels of IL-10 (Pangrazzi et al., 2020). IL-10 has a role in immune regulation as anti-inflammatory cytokines and can be involved in SASP (Huang et al., 2020).

In this study, there is a trend that these cells increase in ageing (Chapter 4) and decrease in CRC (Chapter 5). They tended to decrease in S-II (Table 8), but significantly increased in T4 tumor size compared to T2 (Table 9) and N2 lymph node involvement (Table 10) disease. Their presence in CRC could be an indicator of tumor progression relating to both tumor size and LN involvement.

SL helper T cells

SL helper T cells can be late-stage effector cells (Moro-García et al., 2013) and can perform cytolytic functions in immune response (van Leeuwen et al., 2004; Phetsouphanh et al., 2019). In this study, SL helper T cells significantly increased in younger individuals (Chapter 4) and tended to increase in CRC (Chapter 5). They showed increased trend in early stages (highest level in S-II) and enlarged tumor size, indicating they are immunocompetent cells perhaps responding to the disease conditions.

However, they also have the role in tumor immune invasion through SASP and immunosuppressive functions (Zhang et al., 2021b). Their presence can indicate poor prognosis in cancers, which can be partially explained by the fact of tumor-induced apoptosis, and they can trigger the apoptosis of activated T cells (Zhang et al., 2021b). Failure of clearance of apoptotic cells can lead to tumor progression through the process of inflammation (Shin et al., 2019). SL helper T cells themselves are also prone to

apoptosis (Appendix H). Moreover, they significantly increased in right-sided tumors (poor prognosis) compared to left-sided tumors (Table 12).

Therefore, they could be immunocompetent cells, but their existence could result in poor outcome partly due to the process of apoptotic cells clearance.

Immunophenotypic changes in S-II CRC

Immunophenotypic changes started in S-II. There were basically four patterns:

(1) Immunophenotypes increased in S-II and increased in later stages such as cytotoxic T, HLA-DR positive T, NK^{bright} CD16-, NK^{dim} CD16-, CD4+ NK, intermediate monocytes and CD4+ monocytes. Most of them increased in larger tumor size as well. But there were no obvious changes with lymph node involvement.

(2) Immunophenotypes decreased in S-II and decreased in later stages, such as B lymphocyte, helper T cells and classical monocytes.

(3) Immunophenotypes increased in S-II and decreased in later stages, such as DP T, NK T, SL helper T, DN helper T, SL cytotoxic T, CD4+ NK T, CD8+ NK, non-classical monocytes, CD56+ monocytes and HLA-DR^{low} monocytes.

(4) The immunophenotypes that decreased in S-II and increased in later stages were EA cytotoxic T, DP cytotoxic T, DN NK T and DN NK.

There were no obvious changes in most immune cells between non-metastasis (S-I, S-II and S-III) and metastasis patients in this study. Moreover, these data indicate that immunophenotypes were different in each stage, possibly indicating altered functions in different stages of CRC.

Immunophenotypes in right-sided tumor

Right-sided (proximal) CRC have different biologic characteristics from left-sided (distal) CRC, such as different histological types, different genetic mutation and different epigenetic landscape (Lee et al., 2017). They have inferior clinical outcomes such as lower prognosis and decreased response to therapy (Moretto et al., 2016). Their incidence is associated with old age and 1.5 times increased risk in the female population (Reif de Paula et al., 2021).

In this study, right-sided cases were higher mean age (72.3±10.2 y) than left-sided cases (62.2±13.6 y), and male to female ratio is 10:11 (Table 7). The prominent immune landscape in right-sided CRC were increases of SL T cells (significant in SL helper T cells), significant increase of HLA-DR positive T cells, decrease trend of CD4+ monocytes, with increased trend of CD56+ monocytes. Increased levels of SL T cells could be one of the factors of poor prognosis in right-sided CRC.

Overview of T cells

T subsets except helper T cells decreased in majority of >50 y group (Chapter 4). The reversed patterns (decreased helper T, increased cytotoxic T, increased DP T and increased NK T) were observed in CRC (Chapter 5).

Further analysis of CRC patients showed a decrease in helper T cells and increase in cytotoxic T cells throughout all stages of the disease. T cells (DP T, NK T, cytotoxic T, SL helper T and DP helper T) which can perform cytotoxic activity, increased in all stages. These data indicated immunophenotypic changes in CRC can occur in all stages, even in the early stage. The schematic diagram of T cells subsets can be seen in **Fig 36**.
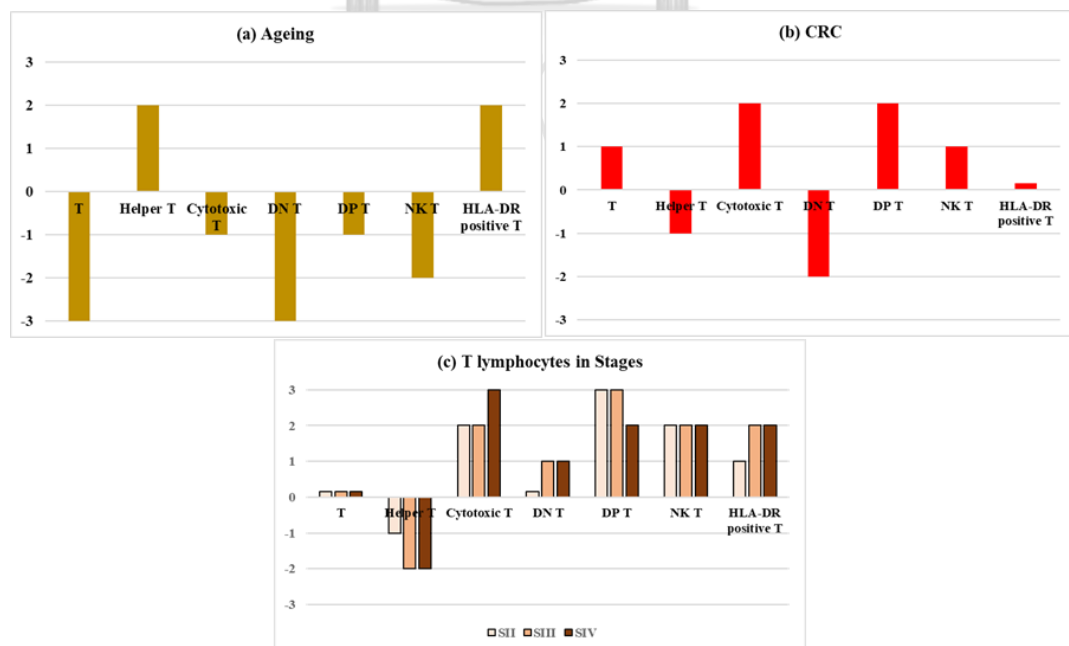

Figure 36: *Schematic diagram of T cells subsets*

(a) in ageing, *(b)* in CRC, *(c)* among stages of CRC, 1 and 2 represent increased levels, 3 represents significantly increased (p< 0.05), -1 and -2 represent decreased levels, -3 represents significantly decreased.

In S-II, the numbers of decreased helper T cells were lower when compared to other stages. There was an increased number of SL cells of the helper T cells. DP T cells, which are activated cytotoxic cells (Mucida et al., 2013), increased. The increased level of NK T cells included increased levels of CD4+ NK T cells, which have immunosuppressive properties such as generating cytotoxic Treg and killing activated helper T (Nakamura et al., 2003; Mishra et al., 2021). This could indicate that active immune cells as well as suppressive immune cells can be seen in S-II of CRC.

In S-III, the number of helper T decreased compared to S-II. Increased cytotoxic T cells included increased SL cells indicating changes in the CD8 compartment. DN T cells, which could have helper function as well cytotoxic function (Yang et al., 2021), tended to increase while DP T cells (activated cytotoxic cells) increased. NK T cells were at the same levels as S-II. HLA-DR positive T cells (activated T cells) were higher than in S-II, implying more antigens had been encountered. Therefore, changes in cytotoxic T cells were more prominent and immunoregulation had potentially changed in S-III.

The prominent features in S-IV were significant increase in cytotoxic T cells with a relative decrease of SL cells. The other cytotoxic cells (DP T and NK T) were slightly decreased compared to S-II and S-III. In the NK T cells population, DN NK T, which could have a pro-inflammatory immune response (Krijgsman et al., 2018), become prominent in most patients compared to those with non-metastasis (Table 11). DN T cells tended to increase in metastasis cases compared to non-metastasis (Table 11) while HLA-DR positive T cells (activated T cells) were higher than S-II. Taken together, these data imply that the cytotoxic functions of adaptive immune cells decreased, and pro-inflammatory responses increased in S-IV.

Overview of NK cells

The number of NK cells increased in ageing (Chapter 4), but no obvious changes were observed in CRC compared to age-matched HCs (Chapter 5). In this analysis, NK cells correlated with tumor sizes: NK^{bright} increased and NK^{dim} decreased in enlarged tumors (Fig 34). The schematic diagram of NK cells subsets can be seen in **Fig 37**.

Figure 37: *Schematic diagram of NK cells*
(a) in ageing, (b) in CRC, (c) among stages of CRC, 1 and 2 represent increased levels, 3 represents significantly increased (p< 0.05), -1 and -2 represent decreased levels, -3 represents significantly decreased.

CD4 positivity in NK cells can indicate efficient cytotoxic activity because of increased migration to the target (Bernstein et al., 2006). CD8 positivity in NK cells relates to increased cytotoxic activity (Abdalla, 2012). CD4+ NK cell numbers increased in all stages compared to S-I (Table 8) and increased in metastasis compared to non-metastasis (Table 11). CD8+ NK cells tended to increase in all stages but were relatively higher in S-II. Therefore, NK cells migration and cytotoxicity are likely to be increased in CRC.

Overview of monocytes

In the >50 y group, the total monocyte counts increased, with significant decrease in classical monocytes, and increased trend of intermediate monocytes and non-classical monocytes. CD4+ monocytes significantly increased (Chapter 4). A similar pattern was observed in CRC (Chapter 5). A schematic diagram of different types of monocytes at different stages of CRC is shown in **Fig 38**.
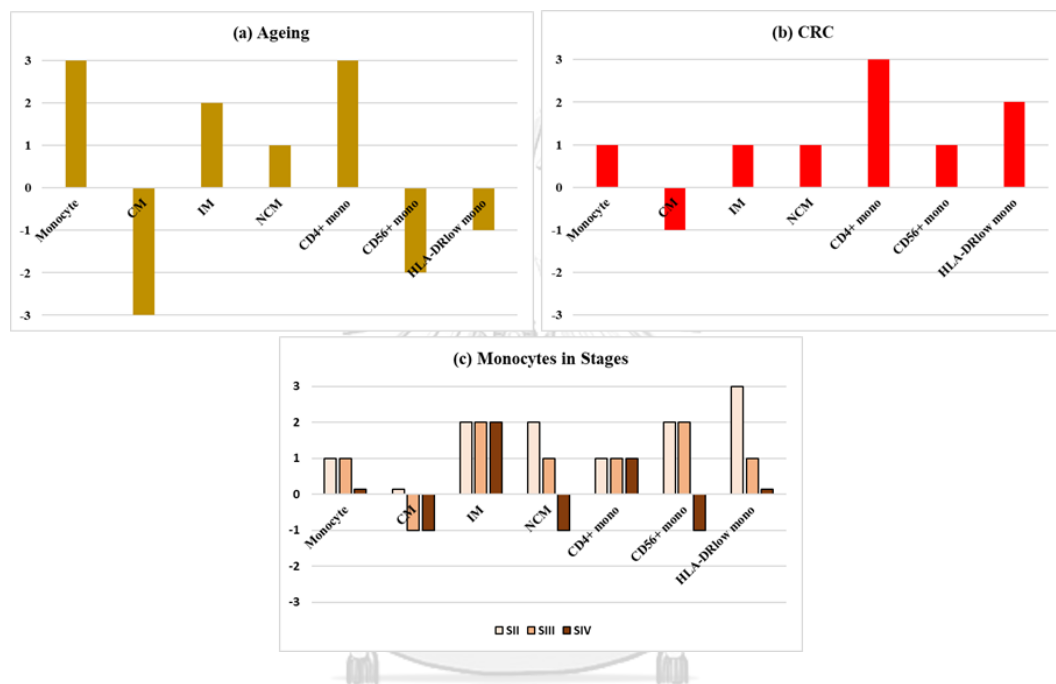
Figure 38: *Schematic diagram of different types of monocytes*
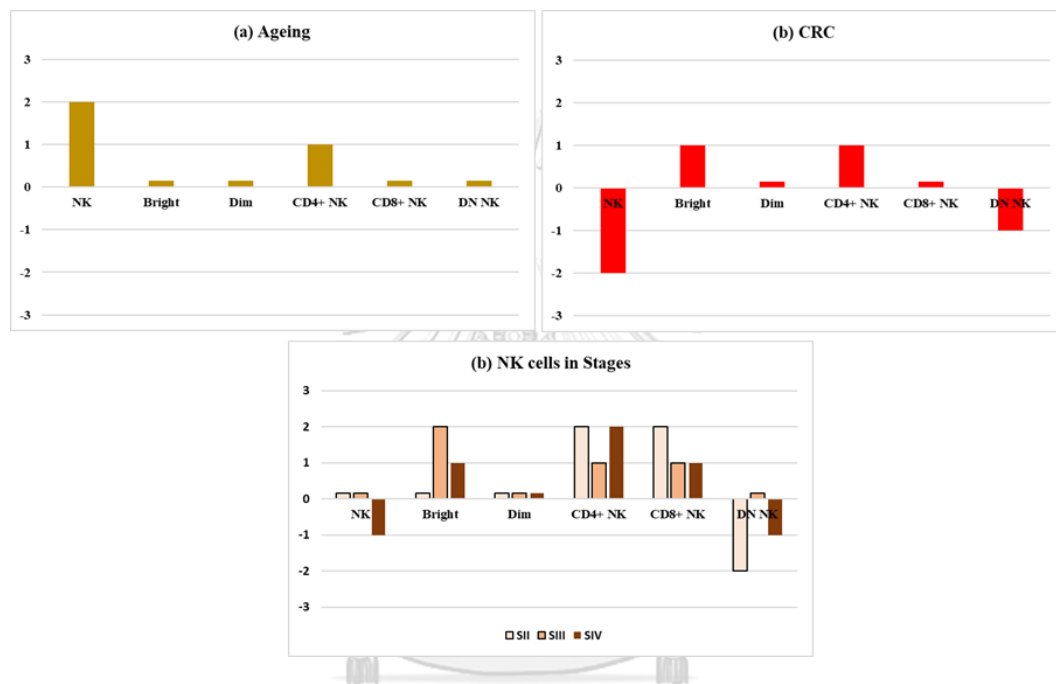*(a) in ageing, (b) in CRC, (c) among stages of CRC, 1 and 2 represent increased levels, 3 represents significantly (p<0.05) increased, -1 and -2 represent decreased levels, -3 represents significantly decreased, CM: classical monocyte, IM: intermediate monocyte, NCM: non-classical monocytes.*

Most CRC patients had increased intermediate monocytes throughout all stages, but non-classical monocytes showed an increase in S-II and a decrease in late stages. The effector function of immune cells as well as their ability to phagocytose and clear debris should be in balance for a successful immune response. Defects in clearance functions can lead to tumor progression especially through the inflammation process (Shin et al., 2019). As non-classical monocytes have the role in patrolling and scavenging debris, their decreased levels could relate to impaired clearance of debris in response to the tumor.

CD4+ monocytes and CD56+ monocytes showed similar patterns (increased trends) in S-II and S-III. However, CD56+ monocytes showed a decreased trend in S-IV. Therefore, the functional properties of monocytes could be decreased in CRC, as CD56 on monocytes is responsible for T cell activation (Sconocchia et al., 2005). Moreover, the immunosuppressive phenotypes HLA-DR^{low} monocytes significantly increased in S-II and decreased in later stages. Therefore, the functional properties of monocytes were changing throughout the stages.

CD14 staining intensity in metastasis significantly increased (Table 11) and this is the coreceptor for immune recognition function of monocytes (Zanoni and Granucci, 2013). CD14-dependent activation can regulate metabolic processes and can cause the accumulation of lipids in the body (Zanoni and Granucci, 2013). In renal cell carcinoma, increased intensity of CD14 on infiltrating immune cells related to poor prognosis (Yap et al., 2023). Their increased expression in metastasis CRC could also be an indicator for patients' outcome.

Conclusion

In spite of the relatively low numbers of patients with different CRC pathologies and features, significant changes were observed in the following cell types:

- numbers of NK cells relate to tumor sizes
- CD14 staining intensity on monocytes increased in metastasis
- DP T cells increased in S-II and S-III
- DP cytotoxic cells correlate with tumour size and lymph node involvement
- HLA-DR^{low} monocytes increased in S-II
- SL helper T cells and HLA-DR positive T cells increased in right-sided tumours.

Further studies with larger numbers of patients with different disease properties are required to determine if any of these properties of circulating immune cells can be used as biomarkers.

CHAPTER VII: GENERAL DISCUSSION, KEY CONCLUSIONS, AND FUTURE PERSPECTIVES

7.1 Summary of approaches

Both the ageing process and development of diseases such as CRC, can result in changes to the immune system that are characterised by immuno-senescence and other phenotypic changes in immune cells. CRC can also induce stresses on the immune system, such as oxidative stress, induction of inflammation or generation of other factors that can influence immune function. In addition, cytotoxic therapy can induce changes in immune cell function during cancer therapy. All of these factors must be considered when determining immune cell properties in diseases such as CRC.

In this study, we aimed to determine if the properties of circulating immune cells could act as potential as biomarkers in CRCs. However, because the prevalence of CRC increases with age, it was important to distinguish whether any changes in immune cell function were a feature of ageing or CRC, or a combination of both. The established senescent marker p16^{INK4A} (Rayess et al., 2012) was first evaluated as a potential biomarker in peripheral immune cells of CRC patients using immunofluorescent techniques. The advantage of this technique is that it is readily available in most laboratory settings as it does not have sophisticated equipment. In addition, this technique was used on WBCs, previously stored at room temperature in 96 well plates for subsequent analysis. However, great care must be taken when quantifying fluorescence images obtained by this technique, and especially quantitative determination of images taken on different days. Standardisation of fluorescence values between samples was achieved by internal controls for every batch of samples. This technique showed 78% sensitivity and 71% specificity for the diagnosis of CRC.

Lymphocytes as well as monocytes have important functions in tumorigenesis and there are many different subgroups of these cells that have different functions that can be determined by their cell surface properties. The immunophenotypes of lymphocytes and monocytes were therefore studied using flow cytometry and comparing aged-matched HCs and CRC cohorts. Based on literature reports (George and Ritter, 1996; Mamatha et al., 2009; Cakala-Jakimowicz et al., 2021) these cohorts

were subdivided into ≤50y and >50y and the surface properties compared between HC and CRCs. A graphical abstract of thesis was summarized in **Fig 39**.
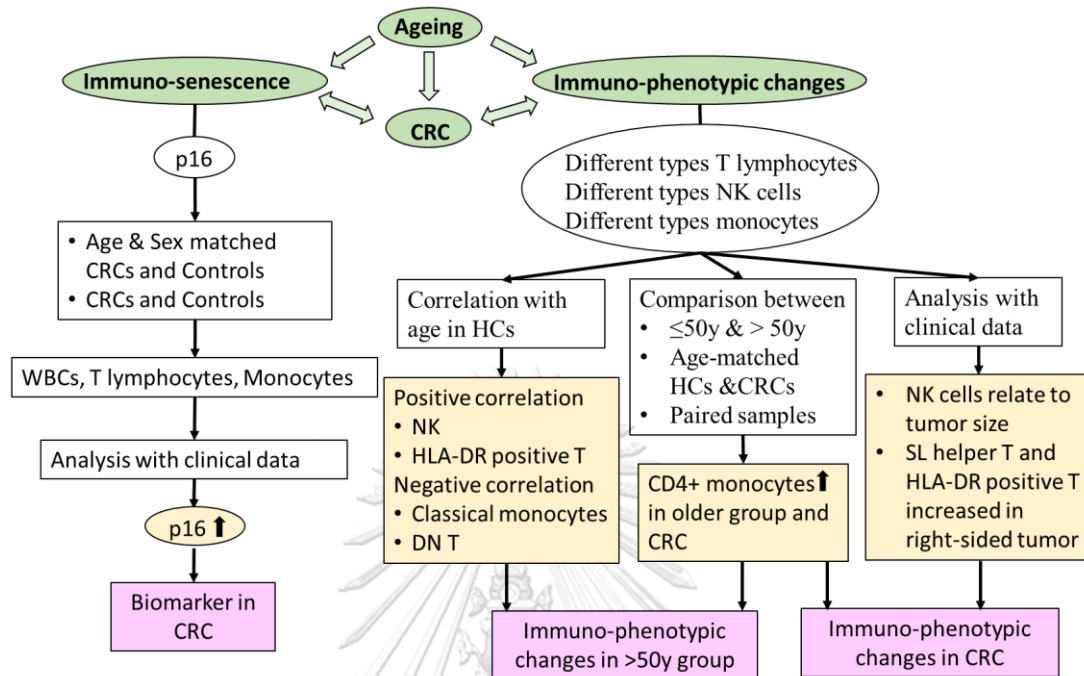
Figure 39: *Graphical abstract of thesis; green boxes represent rational, yellow boxes represent main findings and pink boxes represent the clinical applications.*

7.2 Key conclusions

Overall findings were summarized in **Fig 40**. New findings were shown in **Fig 41**.

In CRC group:

- $p16^{INK4A}$ increased in peripheral white blood cells, in both T lymphocytes and monocytes.
- Increased $p16^{INK4A}$ in peripheral immune cells had 78% sensitivity and 71% specificity which can possibly be used as a diagnosis tool for colorectal cancer.
- There was a possible myeloid skew present in most participants (i.e., increased monocytes/lymphocytes).
- The level of decreased helper T and increased cytotoxic T were more prominent in late stages.
- Significant changes were observed for:

- o decreased B lymphocyte numbers.
- o CD3 staining intensity decreased in EA T cells (both helper and cytotoxic), DP helper T cells, DN cytotoxic T cells and DP cytotoxic T cells and HLA-DR positive T cells.
- o increased CD4 positivity in intermediate monocytes.
- o increased CD4+ monocytes:

  CD4+ monocytes can be used as a diagnostic marker for CRC at the cut off value of 11.5% with 60% sensitivity and 88% specificity.

- o DP cytotoxic T cells correlate with tumor size and lymph nodes involvement.
- o DP T cells increased in S-II and S-III.
- o NK^{bright} cells positively correlate with tumor size.
- o NK^{dim} cells negatively correlate with tumor size.
- o CD14 staining intensity increased in metastasis.
- o SL helper T cells and HLA-DR positive T increased in right-sided tumor.

- • There was a trend for:
  - o increased numbers of T lymphocytes.
  - o decreased helper T cells.
  - o increased cytotoxic T cells.
  - o increased NK T cells, especially immunosuppressive phenotypes of CD4+ NK T cells and CD8+ NK T cells.
  - o decreased DN T cells in early stage and increased in metastasis.
  - o Increased DP T cells.
  - o increased SL T cells (both helper and cytotoxic) in early stages.
  - o decreased CD3 staining intensity in T lymphocytes.
  - o decreased NK cells.
  - o increased CD4+ NK cells and CD8+ NK cells from S-II onwards.
  - o increased monocytes: intermediate monocytes and non-classical monocytes were increased while classical monocytes decreased. Intermediate

monocytes increased in all stages, but non-classical monocytes increased in early stages then decreased in late stages.

- o increased HLA-DR^{low} monocytes and CD56+ monocytes increased in early stages and decreased in late stages.

In >50y age group:

- There was a possible myeloid skew present in most participants (i.e., increased monocytes/lymphocytes).
- Significant changes were observed for:
  - o decreased T lymphocytes.
  - o decreased DN T cells.
  - o increased in CD3 staining intensity in T lymphocytes, especially in helper T cells, EA cytotoxic T cells, DN cytotoxic T cells, DP cytotoxic T cells and DN NK T cells.
  - o increased in HLA-DR staining intensity.
  - o increased monocytes.
  - o decreased classical monocytes.
  - o increased CD4+ monocytes.
- There was a trend for:
  - o increased NK cells.
  - o decreased B lymphocytes.
  - o increased helper T cells with decreased cytotoxic T, NK T, DN T and DP T cells.
  - o decreased SL T cells, but beta-gal and p16^{INK4A} of T lymphocytes did not show significant decreased.
  - o decreased NK T cells with decreased CD4+ and CD8+ NK T cells.
  - o increased HLA-DR positive T lymphocytes
  - o increased intermediate monocytes and non-classical monocytes.
  - o decreased CD56+ monocytes.
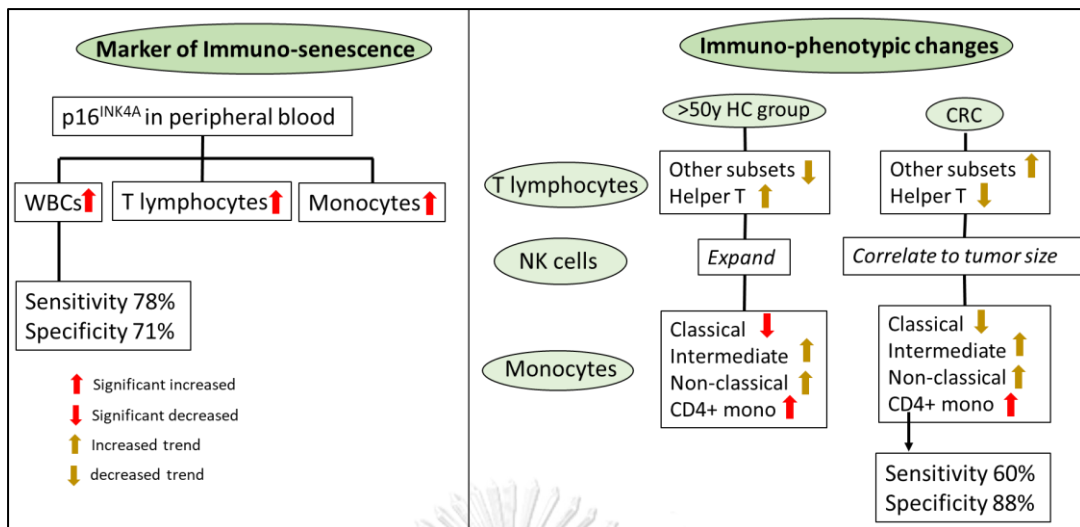
Figure 40: *Schematic diagram of overall findings*
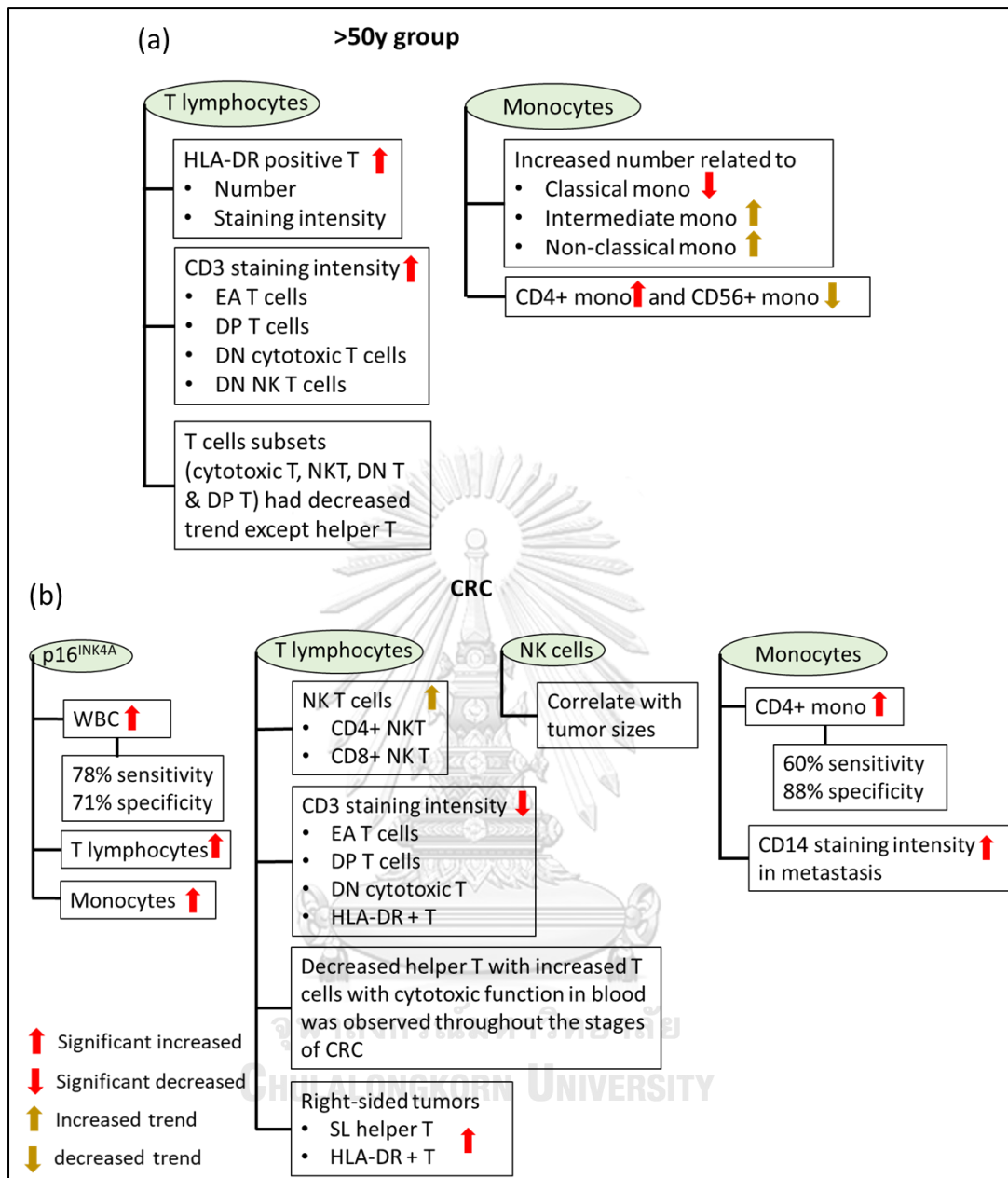
Figure 41: *Schematic diagram of new findings*
(a) in >50y group, (b) in CRC group.

7.3 Limitations of the study

The study period was during the COVID-19 pandemic and so it is possible that the immuno-senescence and phenotypic changes of some participants may be influenced by post-COVID consequences. Differences in lifestyles and infection history of participants, which may impact on immune cells, were not recorded in the datasets. Because of the time limitation of the study, the number of samples collected

as HCs was 24 and CRCs was 42 for immunophenotyping and so while trends were observed, many differences did not reach statistical significance because of this relatively small sample size.

7.4 Future perspectives

The expression of p16^{INK4A} significantly increased in peripheral immune cells of CRC patients. The canonical function of p16^{INK4A} is in the nucleus and it is involved in cell cycle regulation. However, p16^{INK4A} may also be expressed in the cytoplasm where it may have different functions to that in cell cycle regulation as it has been shown to interact with other proteins such as β-catenin, laminin-5 and $α_vβ_3$ integrin (Romagosa et al., 2011). Therefore, future experiments should characterise the function of p16^{INK4A} in immune cells.

CD3 is an important receptor in TCR signaling and in this study, CD3 staining intensity of lymphocytes was significantly decreased in SL cells of HCs, significantly increases in >50y and showed a decreased trend in CRC. Therefore, the functional consequences of these changes associated with altered CD3 in cancers and ageing should be investigated. SL T cells can relate to other diseases and conditions such as viral infections, chronic infections, alcoholism, smoking and acute physical exercises (Strioga et al., 2011; Phetsouphanh et al., 2019). In this study, these were increased in the ≤50y group and the CRC group. For all of these changes, it would be important to perform longitudinal studies to determine if these changes are associated with different disease outcomes. Other potentially compounding variables, drug treatments should also be recorded to see if these correlate with any of the observed changes in immune function. This would require a significantly increased sample size.

NK cells significantly increased in most people in the >50y cohort and most participants of CRC had lower number of NK cells. NK^{bright} cells increased and NK^{dim} cells decreased in enlarged tumors. However, there were similar patterns of NK^{bright} and NK^{dim} in HCs and CRCs. Therefore, longitudinal studies and functional analysis of NK cells will be required to determine the significance of these NK cells changes in CRCs and ageing.

A possible myeloid skew (increased myeloid: lymphocyte ratio) was observed in the >50y cohort people and most patients with CRC. CD4 positivity of monocytes significantly increased in the >50y group and CRC, especially in intermediate monocytes. Therefore, the role of monocytes in tumor immunology and ageing should be investigated in more detail.

In summary, this research has highlighted both age-dependent and CRC-dependent changes in immune cell phenotypes. However, the functional consequences of these changes need to be fully investigated and increased cohort sizes will be needed to see if any of the changes that showed increased or decreased trends are statistically-significant. A larger study would also be important to correlate these changes with disease outcomes or drug therapy, while longitudinal studies would be required to determine if these changes are stable or fluctuate during disease progress/remission.
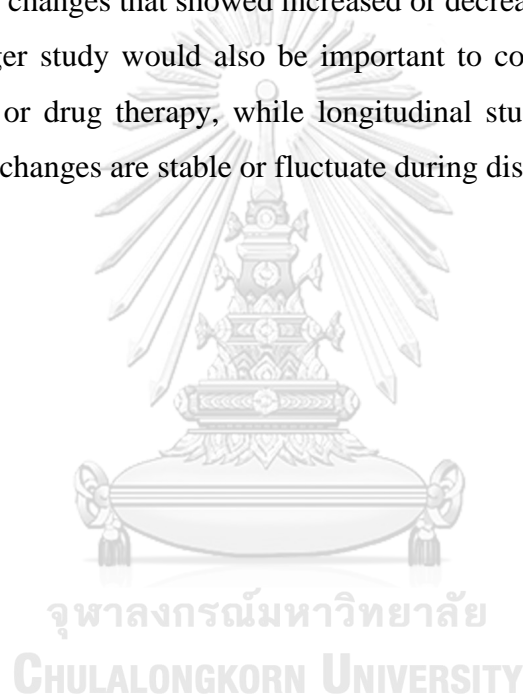
CHAPTER VIII: APPENDIX

Appendix A: CD3 expression of different types of T cells

   The CD-markers on cells have distinct functions. CD3 involve in the signaling of T cells (Ryan, 2010). Intensity of CD3 on lymphocytes relate to activation level: higher CD3 expression can reach higher activation level (El Hentati et al., 2010).

   The intensities of CD3 for different types of T cells from the samples prepared in the same conditions were investigated and compared. The DN T cells showed the highest intensity of CD3, while CD8^{high} T cells showed lowest intensity (**Fig 42**).
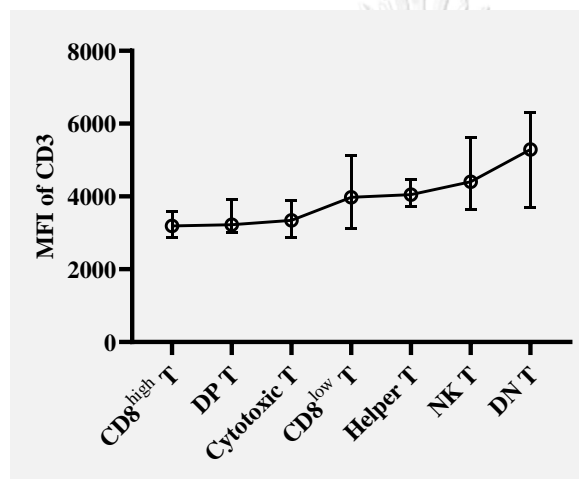

Figure 42: *Different types of T cells showing the order of CD3 increasing intensity. Bars represent IQR, circles represent median.*

Appendix B: Properties of senescent T cells

CD4 and CD8 are important for T cells signaling and activation: CD4 has a role in communication with antigen presenting cells and CD8 plays as a co-receptor (Mørch et al., 2020). The expressions of CD3, CD4 and CD8 together with cells size and cellular content were examined in T cells populations with CD28 and CD57.

In helper T cells, generally, SL cells had decreased expression of CD3 and CD4, and increased in size and cellular content. In detail, CD3 expression decreased in SL cells and DN cells compared to EA cells and DP cells (**Fig 43a**); CD4 expression showed the similar pattern (**Fig 43b**); EA cells were the smallest among the four types (**Fig 43c**); the cellular contents of EA cells were also the lowest one among these cells (**Fig 43d**).

The CD3 expression of different cytotoxic T cells were similar (**Fig 43e**). EA cells had the highest intensity of CD8 (**Fig 43f**). SL cells and DP cells are bigger (**Fig 43g**), as well as had more cellular contents than EA cells and DN cells (**Fig 43h**).
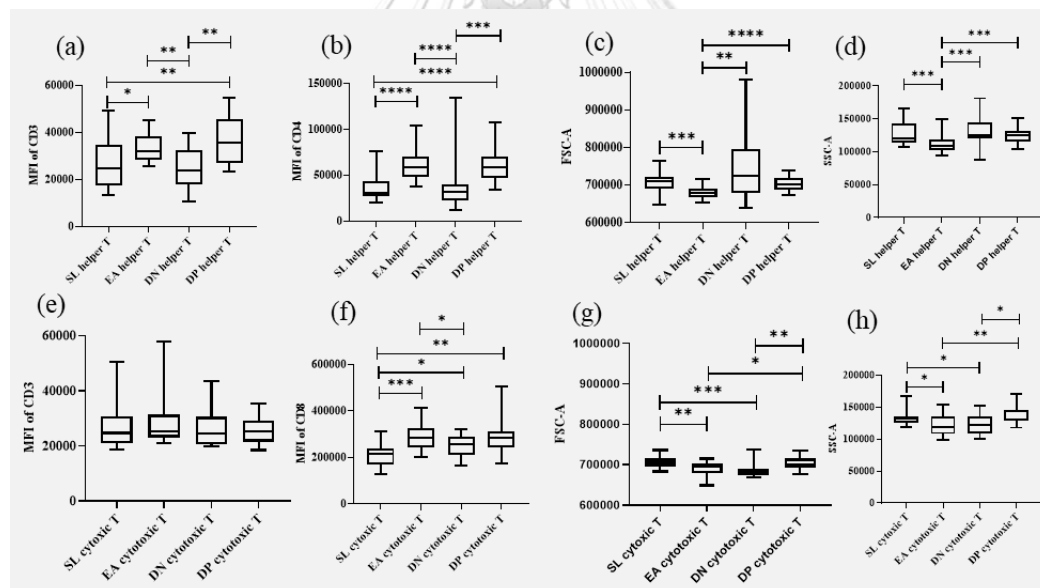
Figure 43: *Comparison of CDs expression, cell size and cellular contents of helper T cells and cytotoxic T cells.*
*(a) CD3 intensity in different types of helper T cells, (b) CD4 intensity in different types of helper T cells, (c) size of different types helper T cells, (d) cellular content of different types of helper T cells, (e) CD3 intensity in different types of cytotoxic T cells, (f) CD4 intensity in different types of cytotoxic T cells, (g) size of different types cytotoxic T cells, (h) granularity of different types of cytotoxic T cells, boxes represent IQR, bars in boxes represent median, whisker represent minimum and maximum value, * = p<0.05, ** = p<0.01, *** = p<0.001, **** = p<0.0001.*

Appendix C: Correlation of HLA-DR-positive T cells with other immunophenotypes

According to the data, HLA-DR-positive T cells were expanded at the old age of the study groups. Therefore, their correlation to other immune cells, especially with senescent cells, is worth examining. They showed moderate uphill correlations with SL cytotoxic cells, DN helper T cells and DP helper T cells. And moderate downhill correlations with EA T cells (both helper and cytotoxic), DN T cells, classical monocytes and HLA-DR^{low} monocytes were noted (**Fig 44**).
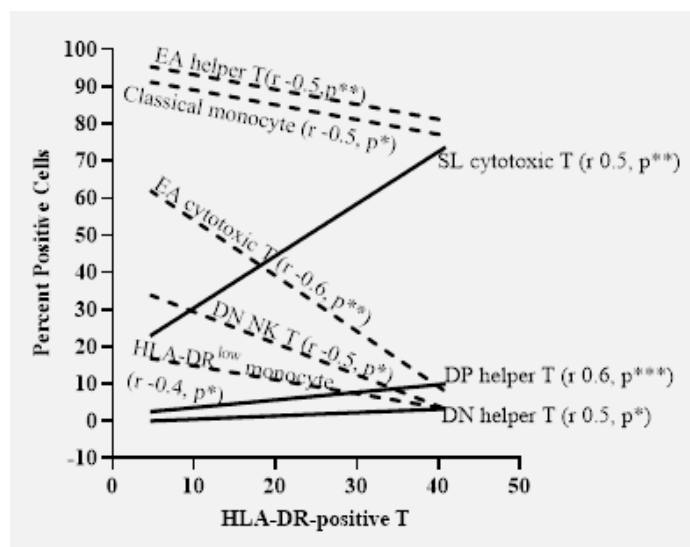
Figure 44: *Correlation of HLA-DR-positive T cells with other immuno-phenotypes.*
* = p<0.05, ** = p<0.01, *** = p<0.001.

Appendix D: Properties of HLA-DR positive T cells

   The expression of HLA-DR on T cells relates to effector T cells and CD3 is important for T cells function (El Hentati et al., 2010; Tippalagama et al., 2021). The intensity of CD3, size and granularity were investigated between HLA-DR-positive T cells and HLA-DR-negative T cells. The result revealed HLA-DR-positive T cells showed slightly decreased intensity of CD3 (**Fig 45a**), increased size (**Fig 45b**) and more complexity (**Fig 45c**).
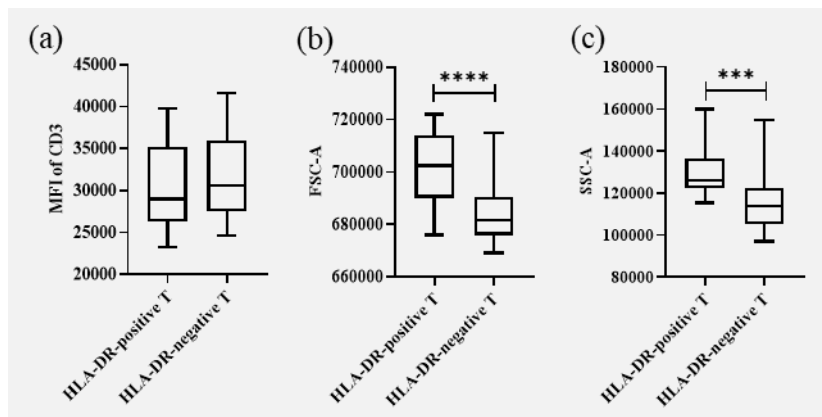
Figure 45: *Comparison of the intensity of CD3 in HLA-DR-positive T cells and HLA-DR-negative T cells.*
(a) CD3 intensity, (b) size of cell, (c) Granularity of cell, Tukey graph: boxes represent IQR, bars in boxes represent median, whisker represent minimum and maximum value, *** = p<0.001, **** = p<0.0001.

Appendix E: Correlation of DN T cells with other immuno-phenotypes

According to the data, DN T cells decrease in old age. Their correlation with other immunophenotypes were observed. There were moderate positive correlations with cytotoxic T and NK T cells, and strong positive correlation with $CD8^{low}$ T and DN NK T. Strong negative correlation with helper T cells and $CD8^{high}$ T cells were observed (**Fig 46**).
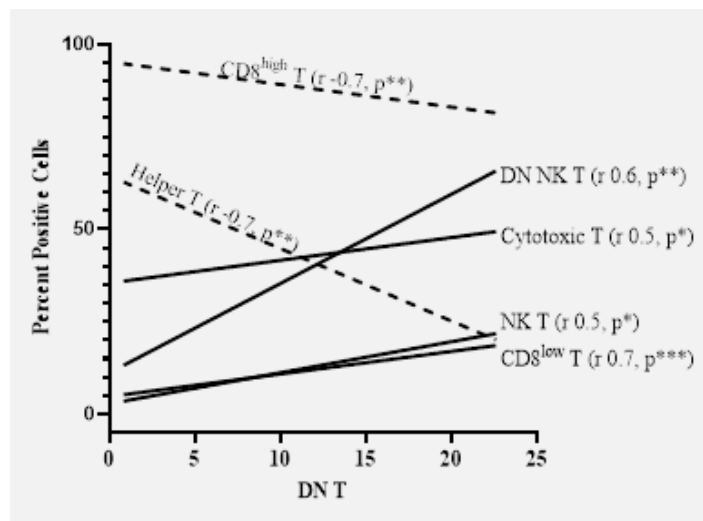
Figure 46: *Correlation of DN T cells with other immuno-phenotypes.*
* = p<0.05, ** = p<0.01, *** = p<0.001.

Appendix F: Positivity of CD56 and CD4 in monocytes

CD56 on monocytes relate to the proliferation of T cells (Sconocchia et al., 2005). CD4 on monocytes is important for macrophage differentiation (Zhen et al., 2014). Therefore, expression of these markers on monocytes are important for monocytes' function. Their intensities on classical monocyte, intermediate monocyte and non-classical monocyte were observed. Among these three monocytes, CD4 expression was high in intermediate monocytes and non-classical monocytes (**Fig 47a**). CD56 expression was high in intermediate monocyte (**Fig 47b**).
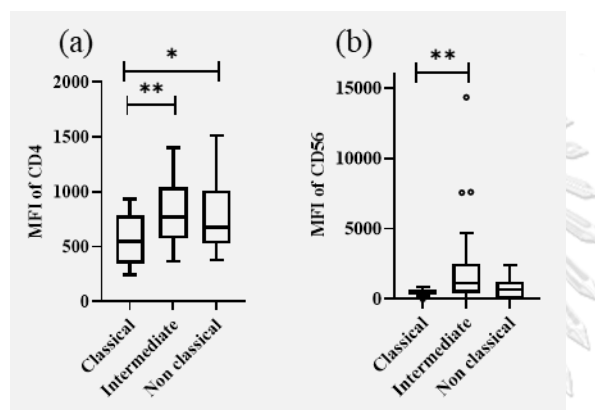
Figure 47: CD4 and CD56 expressions on classical monocytes, intermediate monocytes and non-classical monocytes.
(a) MFI of CD4 on HCs' monocytes, *(b)* MFI of CD56 on HCs' monocytes, Tukey graph: box represents 25% to 75% of samples, line in box represents median, whiskers represent 3/2 of IQR, dot represents outlier, * is p<0.05, ** is p<0.01.

Appendix G: p16^{INK4A} expression with CD28 and CD57 markers in PBMCs
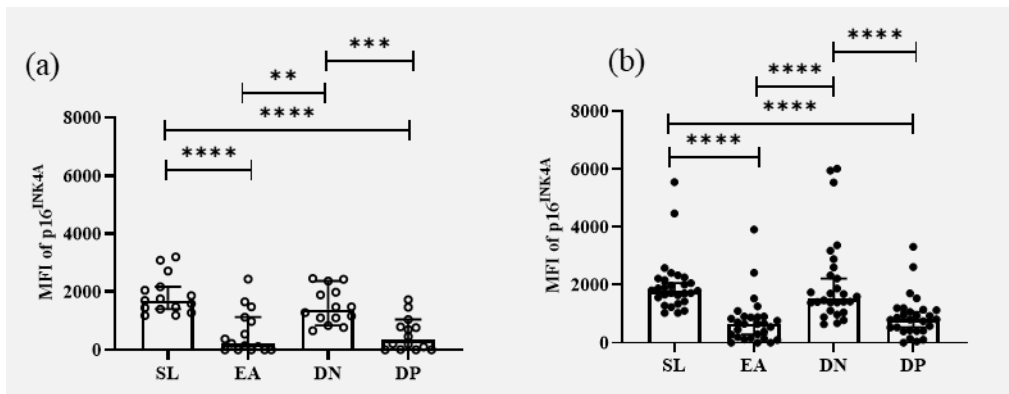
Figure 48: *p16^{INK4A} with CD28 and CD57 expressions in PBMCs of HCs and CRCs.* ***(a)*** *comparison of p16^{INK4A} expression in SL, EA, DN and DP T lymphocytes of HCs,* ***(b)*** *comparison of p16^{INK4A} expression in SL, EA, DN and DP T lymphocytes of CRCs, boxes represent 25% to 75% of samples, lines in box represent median, whiskers represent 3/2 of IQR, dots represent outlier, * is p<0.05, ** is p<0.01, *** is p<0.001, **** is p<0.0001.*

Appendix H: Senescent markers expression in Jurkat cells

Jurkat cells were treated with low dose of Etoposide upto 48 h. Shift-to-left population (low FSC and high SSC) population was prominent at 24 h (**Fig 49a**). Shift-to-left population had a higher number of SL cells and DN cells (**Fig 49b**). The levels of p16^{INK4A} increased after 5 h treatment and similar levels were observed at 24 h and 48 h (**Fig 49c**). The levels of beta-gal increased after 5 h of treatment and became higher at 48 h (**Fig 49d**). The mRNA level of p16^{INK4A} was also higher at 5 h treatment (**Fig 49e**). G2 cells were accumulated at 24 h and 48 h of treatment (**Fig 49f**). Caspase-3 activity was studied in EA, SL, DN and DP cells. Caspase-3 intensity increased in SL cells of 24 h and 48 h treatment (**Fig 49g**).
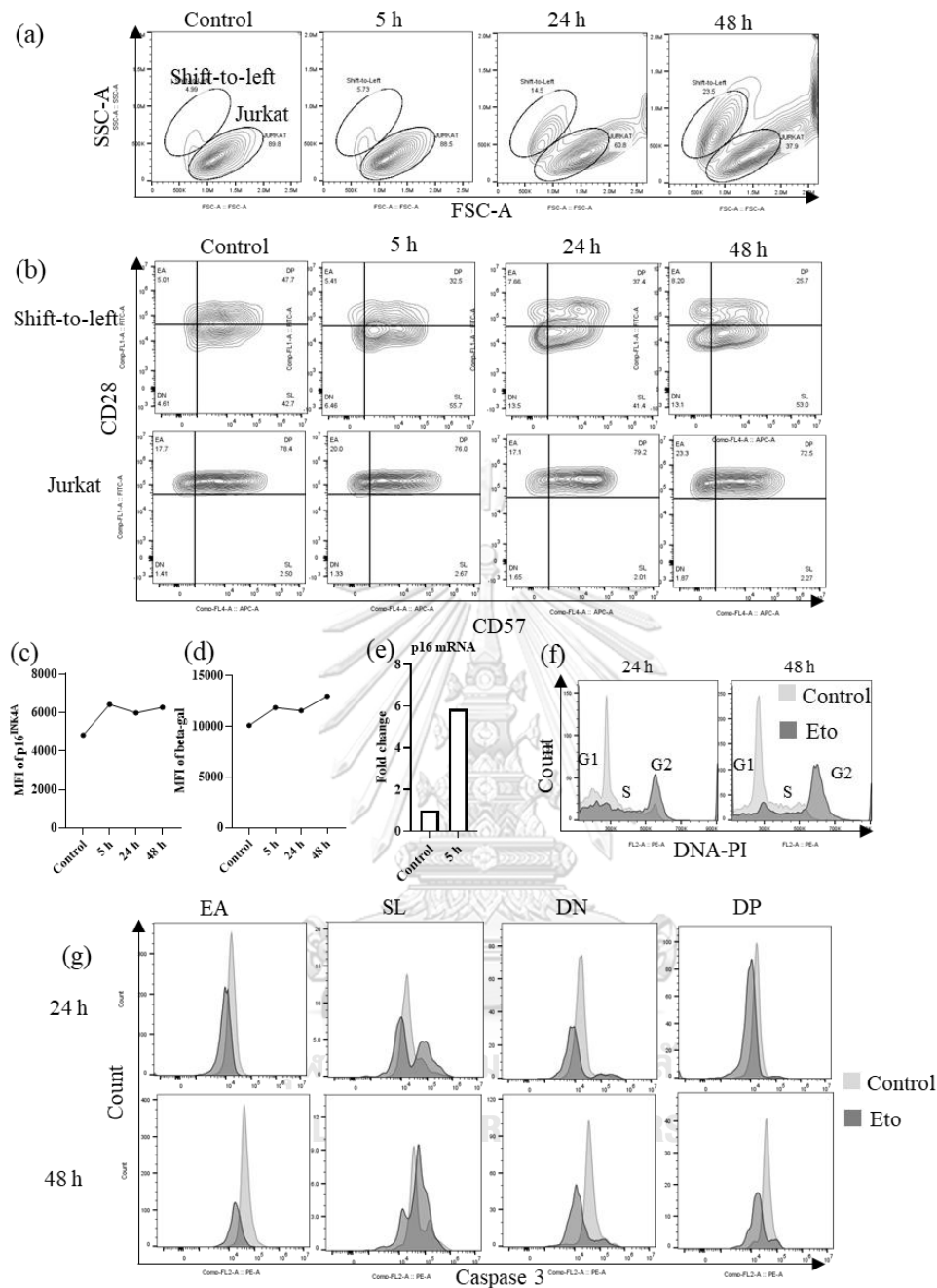
Figure 49: *Jurkat cells experiments treated with etoposide (0.5 µM/ 0.5 million cells/ ml for 24 h and 48 h).*
(a) Contour plot of control cells and etoposide-treated cells with SSC-A and FSC-A, (b) Contour plot of control cells and etoposide-treated cells with CD28 and CD57, (c) Intensity of p16^{INK4A} of control cells and etoposide-treated cells, (d) Intensity of beta-gal of control cells and etoposide-treated cells, (e) mRNA level of control cells and 5h-etoposide-treated cells, (f) histograms of DNA-PI stain of etoposide-treated cells together with controls cells, (g) histograms of MFI of Caspase-3 in EA cells, SL cells, DN cells and DP cells of etoposide-treated cells together with controls cells.

Appendix I: Changes of senescent markers expressions

T lymphocytes and monocytes from participants were examined for senescent markers, p16^{INK4A} and beta-gal. Mean fluorescent intensities were calculated from the single cell population and gating with lymphocytes region and CD3 for lymphocytes (**Fig 50a, 50b**).

Beta-gal intensity increased in CRCs: significant increase in T lymphocytes and increased IQR in monocytes (**Fig 50c**). There were no significant differences of p16^{INK4A} expressions between age-matched HCs and CRCs (**Fig 50d**). However, mRNA of p16^{INK4A} significantly increased in CRCs (**Fig 50e**).

The levels of p16^{INK4A} were observed in EA, SL, DN and DP T lymphocytes with CD28 and CD57 markers. The IQR of p16^{INK4A} increased in CRC, showing significant increase in DP cells (**Fig 50f**).
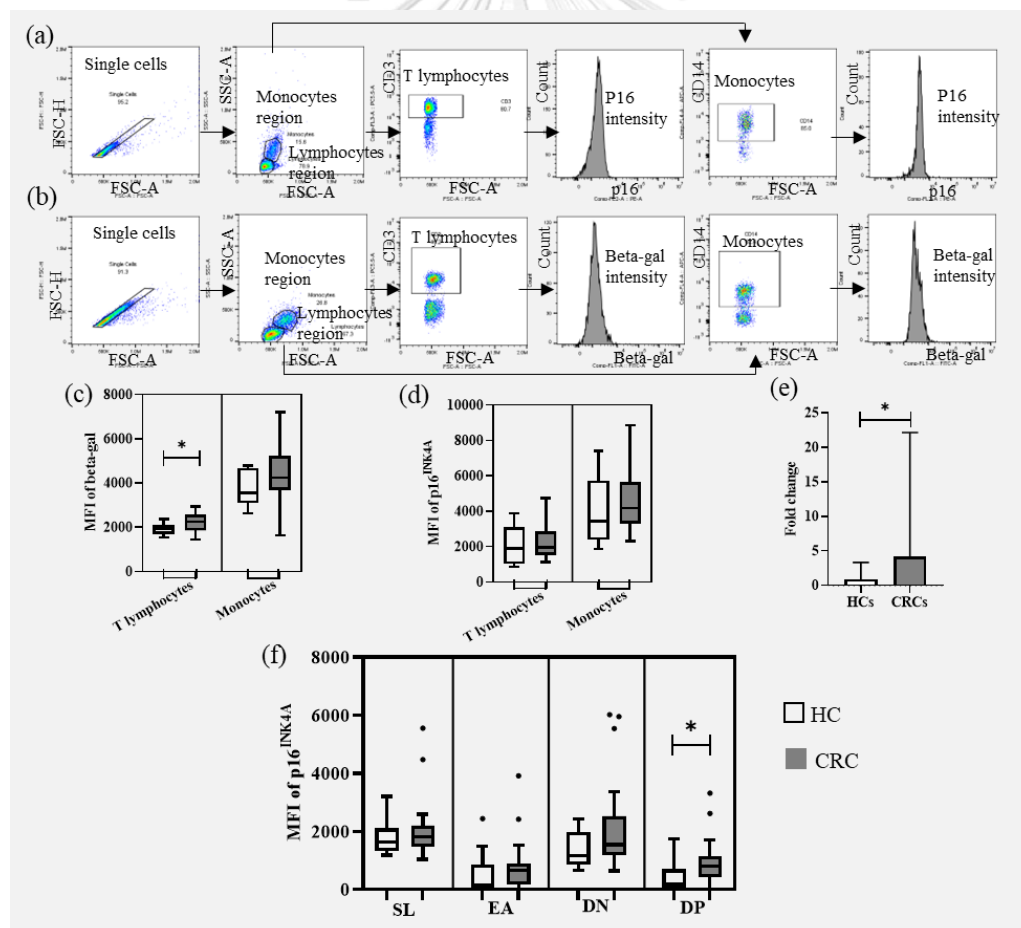
Figure 50: *p16^{INK4A} and beta-gal expression of PBMCs in age-matched HCs and CRCs. (a) gating strategy of p16^{INK4A} in PBMCs, (b) gating strategy of beta-gal in PBMCs, (c) comparison of beta-gal expression between age-matched HCs and CRC, (d) comparison of p16^{INK4A} expression between age-matched HCs and CRC, boxes*

*represent 25% to 75% of samples, lines in box represent median, whiskers represent 2/3 of IQR, dots represent outlier, * is p<0.05, (e) Fold change difference of p16^{INK4A} mRNA level between age-matched HCs and CRC, box represents median, whiskers represent 95% CI, * is p<0.05, (f) comparison of p16^{INK4A} expression in SL, EA, DN and DP T lymphocytes between age-matched HCs and CRCs, boxes represent 25% to 75% of samples, lines in box represent median, whiskers represent 3/2 of IQR, dots represent outlier, * is p<0.05.*

Appendix J: Data of ROC curve for p16^{INK4A}

Table 13: Data of ROC curve for p16^{INK4A}

|	Sensitivity%	95% CI	Specificity%	95% CI	Likelihood ratio
> 71.74	100	94.93% to 100.0%	1.266	0.06493% to 6.828%	1.013
> 72.14	100	94.93% to 100.0%	2.532	0.4498% to 8.769%	1.026
> 72.76	100	94.93% to 100.0%	3.797	1.035% to 10.58%	1.039
> 73.50	100	94.93% to 100.0%	5.063	1.986% to 12.31%	1.053
> 74.09	100	94.93% to 100.0%	6.329	2.733% to 13.97%	1.068
> 74.40	100	94.93% to 100.0%	7.595	3.527% to 15.60%	1.082
> 74.58	100	94.93% to 100.0%	8.861	4.359% to 17.18%	1.097
> 74.96	100	94.93% to 100.0%	10.13	5.221% to 18.73%	1.113
> 75.29	100	94.93% to 100.0%	11.39	6.111% to 20.25%	1.129
> 75.37	100	94.93% to 100.0%	12.66	7.023% to 21.76%	1.145
> 75.73	100	94.93% to 100.0%	13.92	7.957% to 23.24%	1.162
> 76.09	98.61	92.54% to 99.93%	13.92	7.957% to 23.24%	1.146
> 76.13	97.22	90.43% to 99.51%	15.19	8.908% to 24.70%	1.146
> 76.35	95.83	88.45% to 98.86%	15.19	8.908% to 24.70%	1.13
> 76.63	95.83	88.45% to 98.86%	17.72	10.86% to 27.58%	1.165
> 76.92	95.83	88.45% to 98.86%	18.99	11.86% to 28.99%	1.183
> 77.13	95.83	88.45% to 98.86%	20.25	12.87% to 30.40%	1.202
> 77.20	94.44	86.57% to 97.82%	20.25	12.87% to 30.40%	1.184
> 77.27	94.44	86.57% to 97.82%	21.52	13.89% to 31.79%	1.203
> 77.36	93.06	84.75% to 97.00%	21.52	13.89% to 31.79%	1.186
> 77.53	93.06	84.75% to 97.00%	22.78	14.93% to 33.17%	1.205
> 77.66	93.06	84.75% to 97.00%	24.05	15.97% to 34.54%	1.225
> 77.72	91.67	82.99% to 96.12%	24.05	15.97% to 34.54%	1.207
> 77.79	91.67	82.99% to 96.12%	26.58	18.09% to 37.24%	1.249
> 77.83	90.28	81.26% to 95.21%	26.58	18.09% to 37.24%	1.23
> 77.86	90.28	81.26% to 95.21%	27.85	19.17% to 38.58%	1.251
> 78.09	90.28	81.26% to 95.21%	29.11	20.25% to 39.91%	1.274
> 78.30	90.28	81.26% to 95.21%	30.38	21.34% to 41.23%	1.297
> 78.40	90.28	81.26% to 95.21%	31.65	22.45% to 42.55%	1.321

> 78.57	88.89	79.58% to 94.26%	31.65	22.45% to 42.55%	1.3
> 78.72	88.89	79.58% to 94.26%	32.91	23.55% to 43.85%	1.325
> 78.80	88.89	79.58% to 94.26%	34.18	24.67% to 45.15%	1.35
> 78.85	88.89	79.58% to 94.26%	35.44	25.80% to 46.44%	1.377
> 78.91	88.89	79.58% to 94.26%	36.71	26.93% to 47.72%	1.404
> 79.09	87.5	77.92% to 93.28%	36.71	26.93% to 47.72%	1.383
> 79.28	87.5	77.92% to 93.28%	37.97	28.07% to 49.00%	1.411
> 79.39	87.5	77.92% to 93.28%	39.24	29.21% to 50.27%	1.44
> 79.47	87.5	77.92% to 93.28%	40.51	30.37% to 51.53%	1.471
> 79.56	87.5	77.92% to 93.28%	41.77	31.53% to 52.78%	1.503
> 79.75	87.5	77.92% to 93.28%	43.04	32.69% to 54.03%	1.536
> 79.99	86.11	76.29% to 92.28%	43.04	32.69% to 54.03%	1.512
> 80.39	86.11	76.29% to 92.28%	45.57	35.05% to 56.50%	1.582
> 80.76	86.11	76.29% to 92.28%	46.84	36.24% to 57.73%	1.62
> 80.85	86.11	76.29% to 92.28%	48.1	37.43% to 58.95%	1.659
> 81.02	86.11	76.29% to 92.28%	49.37	38.63% to 60.16%	1.701
> 81.15	84.72	74.68% to 91.25%	49.37	38.63% to 60.16%	1.673
> 81.17	83.33	73.09% to 90.20%	49.37	38.63% to 60.16%	1.646
> 81.20	81.94	71.52% to 89.13%	49.37	38.63% to 60.16%	1.618
> 81.29	81.94	71.52% to 89.13%	50.63	39.84% to 61.37%	1.66
> 81.37	81.94	71.52% to 89.13%	51.9	41.05% to 62.57%	1.704
> 81.37	81.94	71.52% to 89.13%	53.16	42.27% to 63.76%	1.75
> 81.41	81.94	71.52% to 89.13%	54.43	43.50% to 64.95%	1.798
> 81.45	81.94	71.52% to 89.13%	55.7	44.73% to 66.13%	1.85
> 81.49	81.94	71.52% to 89.13%	56.96	45.97% to 67.31%	1.904
> 81.63	80.56	69.97% to 88.05%	56.96	45.97% to 67.31%	1.872
> 81.86	80.56	69.97% to 88.05%	58.23	47.22% to 68.47%	1.928
> 82.09	80.56	69.97% to 88.05%	59.49	48.47% to 69.63%	1.989
> 82.34	80.56	69.97% to 88.05%	60.76	49.73% to 70.79%	2.053
> 82.48	80.56	69.97% to 88.05%	63.29	52.28% to 73.07%	2.194
> 82.57	80.56	69.97% to 88.05%	64.56	53.56% to 74.20%	2.273
> 82.69	80.56	69.97% to 88.05%	65.82	54.85% to 75.33%	2.357
> 82.84	79.17	68.43% to 86.95%	65.82	54.85% to 75.33%	2.316
> 82.95	79.17	68.43% to 86.95%	67.09	56.15% to 76.45%	2.405
> 83.08	77.78	66.91% to 85.83%	67.09	56.15% to 76.45%	2.363
> 83.22	77.78	66.91% to 85.83%	69.62	58.77% to 78.66%	2.56
> 83.26	77.78	66.91% to 85.83%	70.89	60.09% to 79.75%	2.671
> 83.28	76.39	65.40% to 84.70%	70.89	60.09% to 79.75%	2.624
> 83.30	75	63.91% to 83.56%	70.89	60.09% to 79.75%	2.576
> 83.34	73.61	62.42% to 82.41%	70.89	60.09% to 79.75%	2.528
> 83.45	73.61	62.42% to 82.41%	72.15	61.42% to 80.83%	2.643

> 83.58	72.22	60.95% to 81.24%	72.15	61.42% to 80.83%	2.593
> 83.73	70.83	59.49% to 80.06%	72.15	61.42% to 80.83%	2.544
> 84.19	69.44	58.05% to 78.87%	72.15	61.42% to 80.83%	2.494
> 84.61	68.06	56.61% to 77.67%	72.15	61.42% to 80.83%	2.444
> 84.67	68.06	56.61% to 77.67%	73.42	62.76% to 81.91%	2.56
> 84.84	68.06	56.61% to 77.67%	74.68	64.11% to 82.97%	2.688
> 85.03	68.06	56.61% to 77.67%	75.95	65.46% to 84.03%	2.83
> 85.17	66.67	55.18% to 76.47%	75.95	65.46% to 84.03%	2.772
> 85.39	66.67	55.18% to 76.47%	77.22	66.83% to 85.07%	2.926
> 85.62	65.28	53.76% to 75.25%	77.22	66.83% to 85.07%	2.865
> 85.81	65.28	53.76% to 75.25%	78.48	68.21% to 86.11%	3.033
> 85.95	63.89	52.35% to 74.02%	78.48	68.21% to 86.11%	2.969
> 86.05	63.89	52.35% to 74.02%	79.75	69.60% to 87.13%	3.155
> 86.09	62.5	50.95% to 72.78%	79.75	69.60% to 87.13%	3.086
> 86.18	62.5	50.95% to 72.78%	81.01	71.01% to 88.14%	3.292
> 86.27	62.5	50.95% to 72.78%	82.28	72.42% to 89.14%	3.527
> 86.35	62.5	50.95% to 72.78%	83.54	73.85% to 90.12%	3.798
> 86.44	62.5	50.95% to 72.78%	84.81	75.30% to 91.09%	4.115
> 86.49	62.5	50.95% to 72.78%	86.08	76.76% to 92.04%	4.489
> 86.54	61.11	49.56% to 71.53%	86.08	76.76% to 92.04%	4.389
> 86.63	59.72	48.18% to 70.28%	86.08	76.76% to 92.04%	4.289
> 86.90	58.33	46.81% to 69.01%	86.08	76.76% to 92.04%	4.189
> 87.30	56.94	45.44% to 67.74%	86.08	76.76% to 92.04%	4.09
> 87.54	55.56	44.09% to 66.46%	86.08	76.76% to 92.04%	3.99
> 87.63	54.17	42.74% to 65.17%	86.08	76.76% to 92.04%	3.89
> 87.71	52.78	41.40% to 63.87%	86.08	76.76% to 92.04%	3.79
> 87.84	52.78	41.40% to 63.87%	87.34	78.24% to 92.98%	4.169
> 87.96	51.39	40.07% to 62.57%	87.34	78.24% to 92.98%	4.06
> 87.99	50	38.75% to 61.25%	87.34	78.24% to 92.98%	3.95
> 88.20	48.61	37.43% to 59.93%	87.34	78.24% to 92.98%	3.84
> 88.41	47.22	36.13% to 58.60%	87.34	78.24% to 92.98%	3.731
> 88.52	45.83	34.83% to 57.26%	87.34	78.24% to 92.98%	3.621
> 88.64	45.83	34.83% to 57.26%	88.61	79.75% to 93.89%	4.023
> 88.68	44.44	33.54% to 55.91%	88.61	79.75% to 93.89%	3.901
> 88.73	44.44	33.54% to 55.91%	89.87	81.27% to 94.78%	4.389
> 88.89	43.06	32.26% to 54.56%	89.87	81.27% to 94.78%	4.252
> 89.05	41.67	30.99% to 53.19%	89.87	81.27% to 94.78%	4.115
> 89.08	41.67	30.99% to 53.19%	91.14	82.82% to 95.64%	4.702
> 89.10	41.67	30.99% to 53.19%	92.41	84.40% to 96.47%	5.486
> 89.22	40.28	29.72% to 51.82%	92.41	84.40% to 96.47%	5.303
> 89.37	38.89	28.47% to 50.44%	92.41	84.40% to 96.47%	5.12

> 89.46	37.5	27.22% to 49.05%	92.41	84.40% to 96.47%	4.938
> 89.53	36.11	25.98% to 47.65%	92.41	84.40% to 96.47%	4.755
> 89.66	34.72	24.75% to 46.24%	92.41	84.40% to 96.47%	4.572
> 89.77	34.72	24.75% to 46.24%	93.67	86.03% to 97.27%	5.486
> 89.82	34.72	24.75% to 46.24%	94.94	87.69% to 98.01%	6.858
> 89.91	33.33	23.53% to 44.82%	94.94	87.69% to 98.01%	6.583
> 90.08	31.94	22.33% to 43.39%	94.94	87.69% to 98.01%	6.309
> 90.31	30.56	21.13% to 41.95%	94.94	87.69% to 98.01%	6.035
> 90.57	29.17	19.94% to 40.51%	94.94	87.69% to 98.01%	5.76
> 90.71	29.17	19.94% to 40.51%	96.2	89.42% to 98.96%	7.681
> 90.92	27.78	18.76% to 39.05%	96.2	89.42% to 98.96%	7.315
> 91.18	27.78	18.76% to 39.05%	97.47	91.23% to 99.55%	10.97
> 91.31	26.39	17.59% to 37.58%	97.47	91.23% to 99.55%	10.42
> 91.68	25	16.44% to 36.09%	97.47	91.23% to 99.55%	9.875
> 92.13	23.61	15.30% to 34.60%	97.47	91.23% to 99.55%	9.326
> 92.43	22.22	14.17% to 33.09%	97.47	91.23% to 99.55%	8.778
> 92.84	20.83	13.05% to 31.57%	97.47	91.23% to 99.55%	8.229
> 93.26	19.44	11.95% to 30.03%	97.47	91.23% to 99.55%	7.681
> 93.66	19.44	11.95% to 30.03%	98.73	93.17% to 99.94%	15.36
> 94.10	18.06	10.87% to 28.48%	98.73	93.17% to 99.94%	14.26
> 94.45	16.67	9.799% to 26.91%	98.73	93.17% to 99.94%	13.17
> 95.01	15.28	8.751% to 25.32%	98.73	93.17% to 99.94%	12.07
> 95.46	13.89	7.723% to 23.71%	98.73	93.17% to 99.94%	10.97
> 95.57	13.89	7.723% to 23.71%	100	95.36% to 100.0%	
> 95.72	12.5	6.718% to 22.08%	100	95.36% to 100.0%	
> 95.89	11.11	5.739% to 20.42%	100	95.36% to 100.0%	
> 96.07	9.722	4.790% to 18.74%	100	95.36% to 100.0%	
> 96.25	8.333	3.875% to 17.01%	100	95.36% to 100.0%	
> 96.37	6.944	3.003% to 15.25%	100	95.36% to 100.0%	
> 97.18	5.556	2.181% to 13.43%	100	95.36% to 100.0%	
> 98.06	4.167	1.136% to 11.55%	100	95.36% to 100.0%	
> 98.46	2.778	0.4936% to 9.574%	100	95.36% to 100.0%	
> 103.0	1.389	0.07124% to 7.457%	100	95.36% to 100.0%	

Appendix K: Data of ROC curve for CD4+ monocytes

Table 14: Data of ROC curve for CD4+ monocytes

	Sensitivity%	95% CI	Specificity%	95% CI	Likelihood ratio
> 0.5650	100	91.62% to 100.0%	6.25	0.3206% to 28.33%	1.067
> 0.7900	97.62	87.68% to 99.88%	6.25	0.3206% to 28.33%	1.041

> 1.025	97.62	87.68% to 99.88%	12.5	2.221% to 36.02%	1.116
> 1.270	95.24	84.21% to 99.15%	12.5	2.221% to 36.02%	1.088
> 1.645	95.24	84.21% to 99.15%	18.75	6.592% to 43.01%	1.172
> 1.985	95.24	84.21% to 99.15%	25	10.18% to 49.50%	1.27
> 2.725	95.24	84.21% to 99.15%	31.25	14.16% to 55.60%	1.385
> 3.735	95.24	84.21% to 99.15%	37.5	18.48% to 61.36%	1.524
> 4.400	92.86	80.99% to 97.54%	37.5	18.48% to 61.36%	1.486
> 4.830	92.86	80.99% to 97.54%	43.75	23.10% to 66.82%	1.651
> 5.305	90.48	77.93% to 96.23%	43.75	23.10% to 66.82%	1.608
> 5.755	90.48	77.93% to 96.23%	50	28.00% to 72.00%	1.81
> 6.110	88.1	75.00% to 94.81%	50	28.00% to 72.00%	1.762
> 6.620	85.71	72.16% to 93.28%	50	28.00% to 72.00%	1.714
> 6.995	83.33	69.40% to 91.68%	50	28.00% to 72.00%	1.667
> 7.215	83.33	69.40% to 91.68%	56.25	33.18% to 76.90%	1.905
> 7.445	80.95	66.70% to 90.02%	56.25	33.18% to 76.90%	1.85
> 7.830	80.95	66.70% to 90.02%	62.5	38.64% to 81.52%	2.159
> 8.025	78.57	64.06% to 88.29%	62.5	38.64% to 81.52%	2.095
> 8.180	76.19	61.47% to 86.52%	62.5	38.64% to 81.52%	2.032
> 8.395	73.81	58.93% to 84.70%	62.5	38.64% to 81.52%	1.968
> 8.515	73.81	58.93% to 84.70%	68.75	44.40% to 85.84%	2.362
> 8.655	71.43	56.43% to 82.83%	68.75	44.40% to 85.84%	2.286
> 8.785	69.05	53.97% to 80.93%	68.75	44.40% to 85.84%	2.21
> 8.935	66.67	51.55% to 78.99%	68.75	44.40% to 85.84%	2.133
> 9.055	64.29	49.17% to 77.01%	68.75	44.40% to 85.84%	2.057
> 9.275	61.9	46.81% to 75.00%	68.75	44.40% to 85.84%	1.981
> 9.485	59.52	44.49% to 72.96%	68.75	44.40% to 85.84%	1.905
> 9.745	59.52	44.49% to 72.96%	75	50.50% to 89.82%	2.381
> 10.20	59.52	44.49% to 72.96%	81.25	56.99% to 93.41%	3.175
> 11.60	59.52	44.49% to 72.96%	87.5	63.98% to 97.78%	4.762
> 13.25	54.76	39.95% to 68.78%	87.5	63.98% to 97.78%	4.381
> 14.10	52.38	37.72% to 66.64%	87.5	63.98% to 97.78%	4.19
> 15.20	50	35.53% to 64.47%	87.5	63.98% to 97.78%	4
> 17.30	47.62	33.36% to 62.28%	87.5	63.98% to 97.78%	3.81
> 18.95	45.24	31.22% to 60.05%	87.5	63.98% to 97.78%	3.619
> 19.65	42.86	29.12% to 57.79%	87.5	63.98% to 97.78%	3.429
> 20.15	40.48	27.04% to 55.51%	87.5	63.98% to 97.78%	3.238
> 21.65	38.1	25.00% to 53.19%	87.5	63.98% to 97.78%	3.048
> 24.35	35.71	22.99% to 50.83%	87.5	63.98% to 97.78%	2.857
> 26.50	33.33	21.01% to 48.45%	87.5	63.98% to 97.78%	2.667
> 27.55	30.95	19.07% to 46.03%	87.5	63.98% to 97.78%	2.476
> 28.65	28.57	17.17% to 43.57%	87.5	63.98% to 97.78%	2.286
> 31.25	26.19	15.30% to 41.07%	87.5	63.98% to 97.78%	2.095
> 34.30	23.81	13.48% to 38.53%	87.5	63.98% to 97.78%	1.905
> 35.95	23.81	13.48% to 38.53%	93.75	71.67% to 99.68%	3.81

> 37.20	21.43	11.71% to 35.94%	93.75	71.67% to 99.68%	3.429
> 39.15	19.05	9.982% to 33.30%	93.75	71.67% to 99.68%	3.048
> 40.95	16.67	8.316% to 30.60%	93.75	71.67% to 99.68%	2.667
> 47.15	16.67	8.316% to 30.60%	100	80.64% to 100.0%	
> 56.10	14.29	6.716% to 27.84%	100	80.64% to 100.0%	
> 61.15	11.9	5.194% to 25.00%	100	80.64% to 100.0%	
> 67.55	9.524	3.766% to 22.07%	100	80.64% to 100.0%	
> 73.35	7.143	2.459% to 19.01%	100	80.64% to 100.0%	
> 77.10	4.762	0.8461% to 15.79%	100	80.64% to 100.0%	
> 87.35	2.381	0.1221% to 12.32%	100	80.64% to 100.0%	

จุฬาลงกรณ์มหาวิทยาลัย

CHULALONGKORN UNIVERSITY

REFERENCES

The T Cell Marker , CD 3 Antigen and Antibodies Mini Review. 2016.

Abbas A, Lichtman A, Pillai S 2022. *Cellular and Molecular Immunology,* Philadelphia, Jeremy Bowes.

Abdalla I. Characterisation of CD8neg and CD8+ human natural killer cell subsets. 2012.

Addison EG, North J, Bakhsh I, et al (2005). Ligation of CD8alpha on human natural killer cells prevents activation-induced apoptosis and enhances cytolytic activity. *Immunology,* **116,** 354-61.

Agrawal A, Agrawal S, Gupta S (2017). Role of Dendritic Cells in Inflammation and Loss of Tolerance in the Elderly. *Frontiers in Immunology,* **8**.

Ahrends T, Spanjaard A, Pilzecker B, et al (2017). CD4(+) T Cell Help Confers a Cytotoxic T Cell Effector Program Including Coinhibitory Receptor Downregulation and Increased Tissue Invasiveness. *Immunity,* **47,** 848-61.e5.

Aiello A, Farzaneh F, Candore G, et al (2019). Immunosenescence and Its Hallmarks: How to Oppose Aging Strategically? A Review of Potential Options for Therapeutic Intervention. *Frontiers in Immunology,* **10**.

Algra AM, Rothwell PM (2012). Effects of regular aspirin on long-term cancer incidence and metastasis: a systematic comparison of evidence from observational studies versus randomised trials. *Lancet Oncol,* **13,** 518-27.

Ali A, Wang Z, Fu J, et al (2013). Differential regulation of the REGγ-proteasome pathway by p53/TGF-β signalling and mutant p53 in cancer cells. *Nat Commun,* **4,** 2667.

Alonso-Arias R, Moro-García MA, López-Vázquez A, et al (2011). NKG2D expression in CD4+ T lymphocytes as a marker of senescence in the aged immune system. *Age (Dordr),* **33,** 591-605.

Arosa FA, Porto G, Cabeda JM, et al (2000). Expansions of CD8+CD28- and CD8+TcRVbeta5.2+ T cells in peripheral blood of heavy alcohol drinkers. *Alcohol Clin Exp Res,* **24,** 519-27.

Aw D, Silva AB, Palmer DB (2009). Is thymocyte development functional in the aged? *Aging (Albany NY),* **1,** 146-53.

Baker DJ, Wijshake T, Tchkonia T, et al (2011). Clearance of p16Ink4a-positive senescent cells delays ageing-associated disorders. *Nature,* **479,** 232-6.

Bernstein HB, Plasterer MC, Schiff SE, et al (2006). CD4 expression on activated NK cells: ligation of CD4 induces cytokine expression and cell migration. *J Immunol,* **177,** 3669-76.

Bisio A, Nasti S, Jordan JJ, et al (2010). Functional analysis of CDKN2A/p16INK4a 5′-UTR variants predisposing to melanoma. *Human Molecular Genetics,* **19,** 1479-91.

Blomberg OS, Spagnuolo L, de Visser KE (2018). Immune regulation of metastasis: mechanistic insights and therapeutic opportunities. *Dis Model Mech,* **11**.

Boćko D, Frydecka I (2003). [Structure and function of lymphocyte TCR/CD3 complex]. *Postepy Hig Med Dosw,* **57,** 519-29.

Boice JA, Fairman R (1996). Structural characterization of the tumor suppressor p16, an ankyrin-like repeat protein. *Protein Sci,* **5,** 1776-84.

Boonsongserm P, Angsuwatcharakon P, Puttipanyalears C, et al (2019). Tumor-induced DNA methylation in the white blood cells of patients with colorectal cancer. *Oncol Lett,* **18,** 3039-48.

Bourlon MT, Velazquez HE, Hinojosa J, et al (2020). Immunosenescence profile and expression of the aging biomarker (p16INK4a) in testicular cancer survivors treated with chemotherapy. *BMC Cancer,* **20,** 882.

Brenner E, Schörg BF, Ahmetlić F, et al (2020). Cancer immune control needs senescence induction by interferon-dependent cell cycle regulator pathways in tumours. *Nature Communications,* **11,** 1335.

Broadley I, Pera A, Morrow G, et al (2017). Expansions of Cytotoxic CD4(+)CD28(-) T Cells Drive Excess Cardiovascular Mortality in Rheumatoid Arthritis and Other Chronic Inflammatory Conditions and Are Triggered by CMV Infection. *Front Immunol,* **8,** 195.

Bruni E, Cazzetta V, Donadon M, et al (2019). Chemotherapy accelerates immune-senescence and functional impairments of Vδ2(pos) T cells in elderly patients affected by liver metastatic colorectal cancer. *J Immunother Cancer,* **7,** 347.

Buffa S, Bulati M, Pellicanò M, et al (2011). B cell immunosenescence: different features of naive and memory B cells in elderly. *Biogerontology,* **12,** 473-83.

Buj R, Aird K (2019). p16: cycling off the beaten path. *Molecular & Cellular Oncology,* **6,** 1677140.

Burd CE, Peng J, Laskowski BF, et al (2020). Association of Epigenetic Age and p16INK4a With Markers of T-Cell Composition in a Healthy Cohort. *J Gerontol A Biol Sci Med Sci,* **75,** 2299-303.

Butcher S, Chahel H, Lord JM (2000). Review article: ageing and the neutrophil: no appetite for killing? *Immunology,* **100,** 411-6.

Byeon IJ, Li J, Ericson K, et al (1998). Tumor suppressor p16INK4A: determination of solution structure and analyses of its interaction with cyclin-dependent kinase 4. *Mol Cell,* **1,** 421-31.

Cakala-Jakimowicz M, Kolodziej-Wojnar P, Puzianowska-Kuznicka M (2021). Aging-Related Cellular, Structural and Functional Changes in the Lymph Nodes: A Significant Component of Immunosenescence? An Overview. *Cells,* **10**.

Cao Y, Fan Y, Li F, et al (2022). Phenotypic and functional alterations of monocyte subsets with aging. *Immunity & Ageing,* **19,** 63.

Casado JG, Soto R, DelaRosa O, et al (2005). CD8 T cells expressing NK associated receptors are increased in melanoma patients and display an effector phenotype. *Cancer Immunol Immunother,* **54,** 1162-71.

Cenerenti M, Saillard M, Romero P, et al (2022). The Era of Cytotoxic CD4 T Cells. *Front Immunol,* **13,** 867189.

Chatzinikolaou G, Karakasilioti I, Garinis GA (2014). DNA damage and innate immunity: links and trade-offs. *Trends Immunol,* **35,** 429-35.

Chebel A, Chien WW, Gerland LM, et al (2007). Does p16ink4a expression increase with the number of cell doublings in normal and malignant lymphocytes? *Leuk Res,* **31,** 1649-58.

Chen PY, Wu CY, Fang JH, et al (2019). Functional Change of Effector Tumor-Infiltrating CCR5(+)CD38(+)HLA-DR(+)CD8(+) T Cells in Glioma Microenvironment. *Front Immunol,* **10,** 2395.

Cheng Y, Ling Z, Li L (2020). The Intestinal Microbiota and Colorectal Cancer. *Frontiers in Immunology,* **11**.

Chidrawar SM, Khan N, Chan YL, et al (2006). Ageing is associated with a decline in peripheral blood CD56bright NK cells. *Immun Ageing,* **3,** 10.

Clinton SK, Giovannucci EL, Hursting SD (2020). The World Cancer Research Fund/American Institute for Cancer Research Third Expert Report on Diet, Nutrition, Physical Activity, and Cancer: Impact and Future Directions. *J Nutr,* **150,** 663-71.

Coillard A, Segura E (2019). In vivo Differentiation of Human Monocytes. *Frontiers in Immunology,* **10**.

Coomes SM, Kannan Y, Pelly VS, et al (2017). CD4(+) Th2 cells are directly regulated by IL-10 during allergic airway inflammation. *Mucosal Immunol,* **10,** 150-61.

Coryell PR, Goraya SK, Griffin KA, et al (2020). Autophagy regulates the localization and degradation of p16(INK4a). *Aging Cell,* **19,** e13171.

Covre LP, De Maeyer RPH, Gomes DCO, et al (2020). The role of senescent T cells in immunopathology. *Aging Cell,* **19,** e13272.

D'Arcangelo D, Tinaburri L, Dellambra E (2017). The Role of p16INK4a Pathway in Human Epidermal Stem Cell Self-Renewal, Aging and Cancer. *International Journal of Molecular Sciences,* **18,** 1591.

de Mol J, Kuiper J, Tsiantoulas D, et al (2021). The Dynamics of B Cell Aging in Health and Disease. *Front Immunol,* **12,** 733566.

De Padova S, Urbini M, Schepisi G, et al (2021). Immunosenescence in Testicular Cancer Survivors: Potential Implications of Cancer Therapies and Psychological Distress. *Frontiers in oncology,* **10,** 564346-.

Deakin AM, Singh K, Crowe JS, et al (1999). A lack of evidence for down-modulation of CD3 zeta expression in colorectal carcinoma and pregnancy using multiple detection methods. *Clin Exp Immunol,* **118,** 197-204.

den Besten G, van Eunen K, Groen AK, et al (2013). The role of short-chain fatty acids in the interplay between diet, gut microbiota, and host energy metabolism. *J Lipid Res,* **54,** 2325-40.

Deng X, Terunuma H, Nieda M (2022). Exploring the Utility of NK Cells in COVID-19. *Biomedicines,* **10**.

Dolina JS, Van Braeckel-Budimir N, Thomas GD, et al (2021). CD8(+) T Cell Exhaustion in Cancer. *Front Immunol,* **12,** 715234.

Dronca RS, Markovic S, Kottschade LA, et al (2015). Bim as a predictive T-cell biomarker for response to anti-PD-1 therapy in metastatic melanoma (MM). *Journal of Clinical Oncology,* **33,** 9013-.

Du W, Hu S, Cai S, et al (2018). Dynamic testing of stimulative and suppressive biomarkers on peripheral blood cells at early stages of immunotherapy predicts response in advanced cancer patients. *Discov Med,* **25,** 277-90.

Eagar TN, Miller SD (2023). 11 - Helper T-Cell Subsets and Control of the Inflammatory Response. In 'Clinical Immunology (Sixth Edition)', Eds Content Repository Only!, New Delhi, 151-61

Eaton SM, Burns EM, Kusser K, et al (2004). Age-related defects in CD4 T cell cognate helper function lead to reductions in humoral responses. *J Exp Med,* **200,** 1613-22.

El Hentati FZ, Gruy F, Iobagiu C, et al (2010). Variability of CD3 membrane expression and T cell activation capacity. *Cytometry B Clin Cytom,* **78,** 105-14.

Faust HJ, Zhang H, Han J, et al (2020). IL-17 and immunologically induced senescence regulate response to injury in osteoarthritis. *The Journal of Clinical Investigation,* **130,** 5493-507.

Formica V, Cereda V, Nardecchia A, et al (2014). Immune reaction and colorectal cancer: friends or foes? *World journal of gastroenterology,* **20,** 12407-19.

Franceschi C, Bonafè M, Valensin S, et al (2000). Inflamm-aging. An evolutionary perspective on immunosenescence. *Ann N Y Acad Sci,* **908,** 244-54.

Franceschi C, Garagnani P, Parini P, et al (2018). Inflammaging: a new immune–metabolic viewpoint for age-related diseases. *Nature Reviews Endocrinology,* **14,** 576-90.

Frasca D (2018). Senescent B cells in aging and age-related diseases: Their role in the regulation of antibody responses. *Exp Gerontol,* **107,** 55-8.

Fu B, Tian Z, Wei H (2014). Subsets of human natural killer cells and their regulatory effects. *Immunology,* **141,** 483-9.

Fulop T, Larbi A, Dupuis G, et al (2017). Immunosenescence and Inflamm-Aging As Two Sides of the Same Coin: Friends or Foes? *Front Immunol,* **8,** 1960.

Ganji A, Farahani I, Khansarinejad B, et al (2020). Increased expression of CD8 marker on T-cells in COVID-19 patients. *Blood Cells Mol Dis,* **83,** 102437.

George AJT, Ritter MA (1996). Thymic involution with ageing: obsolescence or good housekeeping? *Immunology Today,* **17,** 267-72.

Ghia P, Prato G, Stella S, et al (2007). Age-dependent accumulation of monoclonal CD4+CD8+ double positive T lymphocytes in the peripheral blood of the elderly. *Br J Haematol,* **139,** 780-90.

Ghiorzo P, Mantelli M, Gargiulo S, et al (2004). Inverse correlation between p16INK4A expression and NF-kappaB activation in melanoma progression. *Hum Pathol,* **35,** 1029-37.

Gill SR, Pop M, Deboy RT, et al (2006). Metagenomic analysis of the human distal gut microbiome. *Science (New York, N.Y.),* **312,** 1355-9.

Giunco S, Petrara MR, Bergamo F, et al (2019). Immune senescence and immune activation in elderly colorectal cancer patients. *Aging,* **11,** 3864-75.

Glatzová D, Cebecauer M (2019). Dual Role of CD4 in Peripheral T Lymphocytes. *Front Immunol,* **10,** 618.

Gombart AF, Yang R, Campbell MJ, et al (1997). Inhibition of growth of human leukemia cell lines by retrovirally expressed wild-type p16INK4A. *Leukemia,* **11,** 1673-80.

González-Osuna L, Sierra-Cristancho A, Cafferata EA, et al (2022). Senescent CD4+CD28− T Lymphocytes as a Potential Driver of Th17/Treg Imbalance and Alveolar Bone Resorption during Periodontitis. *International Journal of Molecular Sciences,* **23,** 2543.

Gounder SS, Abdullah BJJ, Radzuanb N, et al (2018a). Effect of Aging on NK Cell Population and Their Proliferation at Ex Vivo Culture Condition. *Anal Cell Pathol (Amst),* **2018,** 7871814.

Gounder SS, Abdullah BJJ, Radzuanb NEIBM, et al (2018b). Effect of Aging on NK Cell Population and Their Proliferation at Ex Vivo Culture Condition. *Analytical cellular pathology (Amsterdam),* **2018,** 7871814-.

Grizzi F, Bianchi P, Malesci A, et al (2013). Prognostic value of innate and adaptive immunity in colorectal cancer. *World journal of gastroenterology,* **19,** 174-84.

Gump J, Stokoe D, McCormick F (2003). Phosphorylation of p16INK4A correlates with Cdk4 association. *J Biol Chem,* **278,** 6619-22.

Guo Y, Ayers JL, Carter KT, et al (2019). Senescence-associated tissue microenvironment promotes colon cancer formation through the secretory factor GDF15. *Aging Cell,* **18,** e13013.

Gupta S, Pungsrinont T, Ženata O, et al (2020). Interleukin-23 Represses the Level of Cell Senescence Induced by the Androgen Receptor Antagonists Enzalutamide and Darolutamide in Castration-Resistant Prostate Cancer Cells. *Horm Cancer,* **11,** 182-90.

Gyurova IE, Schlums H, Sucharew H, et al (2019). Dynamic Changes in Natural Killer Cell Subset Frequencies in the Absence of Cytomegalovirus Infection. *Front Immunol,* **10,** 2728.

Hall BM, Balan V, Gleiberman AS, et al (2017). p16(Ink4a) and senescence-associated β-galactosidase can be induced in macrophages as part of a reversible response to physiological stimuli. *Aging (Albany NY),* **9,** 1867-84.

Hamm A, Prenen H, Van Delm W, et al (2016). Tumour-educated circulating monocytes are powerful candidate biomarkers for diagnosis and disease follow-up of colorectal cancer. *Gut,* **65,** 990-1000.

Hammad R, Kotb HG, Eldesoky GA, et al (2022). Utility of Monocyte Expression of HLA-DR versus T Lymphocyte Frequency in the Assessment of COVID-19 Outcome. *Int J Gen Med,* **15,** 5073-87.

Hanahan D, Weinberg RA (2011). Hallmarks of cancer: the next generation. *Cell,* **144,** 646-74.

Hara E, Smith R, Parry D, et al (1996). Regulation of p16CDKN2 expression and its implications for cell immortalization and senescence. *Mol Cell Biol,* **16,** 859-67.

Hasan MR, Ho SH, Owen DA, et al (2011). Inhibition of VEGF induces cellular senescence in colorectal cancer cells. *Int J Cancer,* **129,** 2115-23.

Hauptman N, Glavač D (2017). Colorectal Cancer Blood-Based Biomarkers. *Gastroenterology research and practice,* **2017,** 2195361-.

Hazewinkel Y, Dekker E (2011). Colonoscopy: basic principles and novel techniques. *Nat Rev Gastroenterol Hepatol,* **8,** 554-64.

Henry NL, Hayes DF (2012). Cancer biomarkers. *Molecular Oncology,* **6,** 140-6.

Hiam-Galvez KJ, Allen BM, Spitzer MH (2021). Systemic immunity in cancer. *Nature Reviews Cancer,* **21,** 345-59.

Hodge G, Mukaro V, Reynolds PN, et al (2011). Role of increased CD8/CD28(null) T cells and alternative co-stimulatory molecules in chronic obstructive pulmonary disease. *Clin Exp Immunol,* **166,** 94-102.

Holling TM, Schooten E, van Den Elsen PJ (2004). Function and regulation of MHC class II molecules in T-lymphocytes: of mice and men. *Hum Immunol,* **65,** 282-90.

Holt PR, Kozuch P, Mewar S (2009). Colon cancer and the elderly: from screening to treatment in management of GI disease in the elderly. *Best practice & research. Clinical gastroenterology,* **23,** 889-907.

Hu B, Jadhav RR, Gustafson CE, et al (2020). Distinct Age-Related Epigenetic Signatures in CD4 and CD8 T Cells. *Front Immunol,* **11,** 585168.

Hu Y, Chen D, Hong M, et al (2022). Apoptosis, Pyroptosis, and Ferroptosis Conspiringly Induce Immunosuppressive Hepatocellular Carcinoma Microenvironment and γδ T-Cell Imbalance. *Front Immunol,* **13,** 845974.

Hu Z, Gu W, Wei Y, et al (2019). NKT Cells in Mice Originate from Cytoplasmic CD3-Positive, CD4−CD8− Double-Negative Thymocytes that Express CD44 and IL-7Rα. *Scientific Reports,* **9,** 1874.

Huang Y-H, Chen M-H, Guo Q-L, et al (2020). Interleukin-10 induces senescence of activated hepatic stellate cells via STAT3-p53 pathway to attenuate liver fibrosis. *Cellular Signalling,* **66,** 109445.

Imamichi H, Lempicki R, Adelsberger J, et al (2012). The CD8 + HLA-DR + T cells expanded in HIV-1 infection are qualitatively identical to those from healthy controls. *European journal of immunology,* **42,** 2608-20.

Inadomi J, Jung B (2020). Colorectal Cancer—Recent Advances and Future Challenges. *Gastroenterology,* **158,** 289-90.

Ishigami S, Natsugoe S, Miyazono F, et al (2004). CD3 zeta expression of regional lymph node and peripheral blood lymphocytes in gastric cancer. *Anticancer Res,* **24,** 2123-6.

Jasiulionis MG (2018). Abnormal Epigenetic Regulation of Immune System during Aging. *Front Immunol,* **9,** 197.

Joseph M, Wu Y, Dannebaum R, et al (2022). Global patterns of antigen receptor repertoire disruption across adaptive immune compartments in COVID-19. *Proceedings of the National Academy of Sciences,* **119,** e2201541119.

Jumper J, Evans R, Pritzel A, et al (2021). Highly accurate protein structure prediction with AlphaFold. *Nature,* **596,** 583-9.

Kapellos TS, Bonaguro L, Gemünd I, et al (2019a). Human Monocyte Subsets and Phenotypes in Major Chronic Inflammatory Diseases. *Front Immunol,* **10,** 2035.

Kapellos TS, Bonaguro L, Gemünd I, et al (2019b). Human Monocyte Subsets and Phenotypes in Major Chronic Inflammatory Diseases. *Frontiers in Immunology,* **10**.

Kasprzak A (2021). The Role of Tumor Microenvironment Cells in Colorectal Cancer (CRC) Cachexia. *International journal of molecular sciences,* **22,** 1565.

Kim HD, Yu SJ, Kim HS, et al (2013). Interleukin-4 induces senescence in human renal carcinoma cell lines through STAT6 and p38 MAPK. *J Biol Chem,* **288,** 28743-54.

Kiss M, Caro AA, Raes G, et al (2020). Systemic Reprogramming of Monocytes in Cancer. *Frontiers in Oncology,* **10**.

Kitchen SG, LaForge S, Patel VP, et al (2002). Activation of CD8 T cells induces expression of CD4, which functions as a chemotactic receptor. *Blood,* **99,** 207-12.

Klein SL (2012). Immune cells have sex and so should journal articles. *Endocrinology,* **153,** 2544-50.

Kojima H, Inoue T, Kunimoto H, et al (2013). IL-6-STAT3 signaling and premature senescence. *JAK-STAT,* **2,** e25763-e.

Kong X, Feng D, Wang H, et al (2012). Interleukin-22 induces hepatic stellate cell senescence and restricts liver fibrosis in mice. *Hepatology (Baltimore, Md.),* **56,** 1150-9.

Krijgsman D, Hokland M, Kuppen PJK (2018). The Role of Natural Killer T Cells in Cancer-A Phenotypical and Functional Approach. *Front Immunol,* **9,** 367.

Kuipers EJ, Grady WM, Lieberman D, et al (2015). Colorectal cancer. *Nature Reviews Disease Primers,* **1,** 15065.

Lages CS, Suffia I, Velilla PA, et al (2008). Functional regulatory T cells accumulate in aged hosts and promote chronic infectious disease reactivation. *J Immunol,* **181,** 1835-48.

LaPak KM, Burd CE (2014). The molecular balancing act of p16(INK4a) in cancer and aging. *Mol Cancer Res,* **12,** 167-83.

Laphanuwat P, Jirawatnotai S (2019). Immunomodulatory Roles of Cell Cycle Regulators. *Frontiers in Cell and Developmental Biology,* **7**.

Lee MS, Menter DG, Kopetz S (2017). Right Versus Left Colon Cancer Biology: Integrating the Consensus Molecular Subtypes. *Journal of the National Comprehensive Cancer Network J Natl Compr Canc Netw,* **15,** 411-9.

Lefebvre JS, Haynes L (2012). Aging of the CD4 T Cell Compartment. *Open Longev Sci,* **6,** 83-91.

Leon KE, Tangudu NK, Aird KM, et al (2021). Loss of p16: A Bouncer of the Immunological Surveillance? *Life (Basel),* **11**.

Li J, Joo SH, Tsai MD (2003). An NF-kappaB-specific inhibitor, IkappaBalpha, binds to and inhibits cyclin-dependent kinase 4. *Biochemistry,* **42,** 13476-83.

Li J, Melvin WS, Tsai MD, et al (2004). The nuclear protein p34SEI-1 regulates the kinase activity of cyclin-dependent kinase 4 in a concentration-dependent manner. *Biochemistry,* **43,** 4394-9.

Li J, Poi MJ, Tsai M-D (2011). Regulatory mechanisms of tumor suppressor P16(INK4A) and their relevance to cancer. *Biochemistry,* **50,** 5566-82.

Li J, Tsai MD (2002). Novel insights into the INK4-CDK4/6-Rb pathway: counter action of gankyrin against INK4 proteins regulates the CDK4-mediated phosphorylation of Rb. *Biochemistry,* **41,** 3977-83.

Li M, Yao D, Zeng X, et al (2019). Age related human T cell subset evolution and senescence. *Immunity & Ageing,* **16,** 24.

Li X, Yao W, Yuan Y, et al (2017). Targeting of tumour-infiltrating macrophages via CCL2/CCR2 signalling as a therapeutic strategy against hepatocellular carcinoma. *Gut,* **66,** 157-67.

Lian J, Yue Y, Yu W, et al (2020). Immunosenescence: a key player in cancer development. *Journal of Hematology & Oncology,* **13,** 151.

Lin C-C, Liao T-T, Yang M-H (2020). Immune Adaptation of Colorectal Cancer Stem Cells and Their Interaction With the Tumor Microenvironment. *Frontiers in Oncology,* **10**.

Liu C, Wang Y, Li S, et al (2021). Early change in peripheral CD4+ T cells associated with clinical outcomes of immunotherapy in gastrointestinal cancer. *Immunotherapy,* **13,** 55-66.

Liu Y, Sanoff HK, Cho H, et al (2009). Expression of p16(INK4a) in peripheral blood T-cells is a biomarker of human aging. *Aging cell,* **8,** 439-48.

Loktionov A (2020). Biomarkers for detecting colorectal cancer non-invasively: DNA, RNA or proteins? *World journal of gastrointestinal oncology,* **12,** 124-48.

Ma S, Wang C, Mao X, et al (2019). B Cell Dysfunction Associated With Aging and Autoimmune Diseases. *Front Immunol,* **10,** 318.

MacFarlane AWt, Jillab M, Plimack ER, et al (2014). PD-1 expression on peripheral blood cells increases with stage in renal cell carcinoma patients and is rapidly reduced after surgical tumor resection. *Cancer Immunol Res,* **2,** 320-31.

MacGregor RR, Shalit M (1990). Neutrophil Function in Healthy Elderly Subjects. *Journal of Gerontology,* **45,** M55-M60.

Madu A, Ocheni S, Ibegbulam O, et al (2013). Pattern of CD4 T-lymphocyte Values in Cancer Patients on Cytotoxic Therapy. *Ann Med Health Sci Res,* **3,** 498-503.

Mager LF, Wasmer M-H, Rau TT, et al (2016). Cytokine-Induced Modulation of Colorectal Cancer. *Frontiers in oncology,* **6,** 96-.

Maijó M, Clements SJ, Ivory K, et al (2014). Nutrition, diet and immunosenescence. *Mech Ageing Dev,* **136-137,** 116-28.

Malumbres M (2014). Cyclin-dependent kinases. *Genome Biology,* **15,** 122.

Mamatha P, Ershler WB, Longo DL (2009). BONE MARROW, THYMUS AND BLOOD: CHANGES ACROSS THE LIFESPAN. *Aging health,* **5,** 385-93.

Mansfield AS, Nevala WK, Dronca RS, et al (2012). Normal ageing is associated with an increase in Th2 cells, MCP-1 (CCL1) and RANTES (CCL5), with differences in sCD40L and PDGF-AA between sexes. *Clin Exp Immunol,* **170,** 186-93.

Marrero YT, Suárez VM, Abraham CMM, et al (2023). Peripheral double negative T: A look at senescent Cubans. *Exp Gerontol,* **171,** 112006.

Mathur SK, Schwantes EA, Jarjour NN, et al (2008). Age-related changes in eosinophil function in human subjects. *Chest,* **133,** 412-9.

Matsuoka M, Jeang KT (2011). Human T-cell leukemia virus type 1 (HTLV-1) and leukemic transformation: viral infectivity, Tax, HBZ and therapy. *Oncogene,* **30,** 1379-89.

McLaughlin B, O'Malley K, Cotter TG (1986). Age-related differences in granulocyte Chemotaxis and degranulation. *Clinical Science,* **70,** 59-62.

Meirson T, Gil-Henn H, Samson AO (2019). Invasion and metastasis: the elusive hallmark of cancer. *Oncogene*.

Mengos AE, Gastineau DA, Gustafson MP (2019). The CD14(+)HLA-DR(lo/neg) Monocyte: An Immunosuppressive Phenotype That Restrains Responses to Cancer Immunotherapy. *Front Immunol,* **10,** 1147.

Milde-Langosch K, Bamberger AM, Rieck G, et al (2001). Overexpression of the p16 cell cycle inhibitor in breast cancer is associated with a more malignant phenotype. *Breast Cancer Res Treat,* **67,** 61-70.

Mishra S, Srinivasan S, Ma C, et al (2021). CD8(+) Regulatory T Cell - A Mystery to Be Revealed. *Front Immunol,* **12,** 708874.

Mørch AM, Bálint Š, Santos AM, et al (2020). Coreceptors and TCR Signaling - the Strong and the Weak of It. *Front Cell Dev Biol,* **8,** 597627.

Moretta L (2010). Dissecting CD56dim human NK cells. *Blood,* **116,** 3689-91.

Moretto R, Cremolini C, Rossini D, et al (2016). Location of Primary Tumor and Benefit From Anti-Epidermal Growth Factor Receptor Monoclonal Antibodies in Patients With RAS and BRAF Wild-Type Metastatic Colorectal Cancer. *Oncologist,* **21,** 988-94.

Moro-García MA, Alonso-Arias R, López-Larrea C (2013). When Aging Reaches CD4+ T-Cells: Phenotypic and Functional Changes. *Front Immunol,* **4,** 107.

Mosavi LK, Cammett TJ, Desrosiers DC, et al (2004). The ankyrin repeat as molecular architecture for protein recognition. *Protein Sci,* **13,** 1435-48.

Mucida D, Husain MM, Muroi S, et al (2013). Transcriptional reprogramming of mature CD4+ helper T cells generates distinct MHC class II-restricted cytotoxic T lymphocytes. *Nat Immunol,* **14,** 281-9.

Müller-Durovic B, Grählert J, Devine OP, et al (2019). CD56-negative NK cells with impaired effector function expand in CMV and EBV co-infected healthy donors with age. *Aging (Albany NY),* **11,** 724-40.

Muss H, Krishnamurthy J, Alston S, et al (2011). P16 INK4a expression after chemotherapy in older women with early-stage breast cancer. *Journal of Clinical Oncology,* **29,** 9002-.

Mutirangura A (2019). A Hypothesis to Explain How the DNA of Elderly People Is Prone to Damage: Genome-Wide Hypomethylation Drives Genomic Instability in the Elderly by Reducing Youth-Associated Gnome-Stabilizing DNA Gaps. In 'Epigenetics', Eds IntecOpen, 65-75

Myöhänen SK, Baylin SB, Herman JG (1998). Hypermethylation can selectively silence individual p16ink4A alleles in neoplasia. *Cancer Res,* **58,** 591-3.

Nakamura T, Sonoda KH, Faunce DE, et al (2003). CD4+ NKT cells, but not conventional CD4+ T cells, are required to generate efferent CD8+ T regulatory cells following antigen inoculation in an immune-privileged site. *J Immunol,* **171,** 1266-71.

Natividad JM, Verdu EF (2013). Modulation of intestinal barrier by intestinal microbiota: pathological and therapeutic implications. *Pharmacol Res,* **69,** 42-51.

Nelson A, Lukacs JD, Johnston B (2021). The Current Landscape of NKT Cell Immunotherapy and the Hills Ahead. *Cancers (Basel),* **13**.

Ng L, Wan TM-H, Man JH-W, et al (2017). Identification of serum miR-139-3p as a non-invasive biomarker for colorectal cancer. *Oncotarget,* **8,** 27393-400.

Nguyen LH, Goel A, Chung DC (2019). Pathways of Colorectal Carcinogenesis. *Gastroenterology*.

Nicita-Mauro V, Basile G, Maltese G, et al (2008). Smoking, health and ageing. *Immunity & ageing : I & A,* **5,** 10-.

Nixon AB, Schalper KA, Jacobs I, et al (2019). Peripheral immune-based biomarkers in cancer immunotherapy: can we realize their predictive potential? *Journal for ImmunoTherapy of Cancer,* **7,** 325.

Oh DY, Kwek SS, Raju SS, et al (2020). Intratumoral CD4(+) T Cells Mediate Anti-tumor Cytotoxicity in Human Bladder Cancer. *Cell,* **181,** 1612-25.e13.

Oh SA, Li MO (2013). TGF-β: guardian of T cell function. *J Immunol,* **191,** 3973-9.

Ohkusa T, Yoshida T, Sato N, et al (2009). Commensal bacteria can enter colonic epithelial cells and induce proinflammatory cytokine secretion: a possible pathogenic mechanism of ulcerative colitis. *J Med Microbiol,* **58,** 535-45.

Okamura T, Taniguchi S, Ohkura T, et al (2003). Abnormally high expression of proteasome activator-gamma in thyroid neoplasm. *J Clin Endocrinol Metab,* **88,** 1374-83.

Olingy CE, Dinh HQ, Hedrick CC (2019). Monocyte heterogeneity and functions in cancer. *Journal of Leukocyte Biology,* **106,** 309-22.

Ong BA, Vega KJ, Houchen CW (2014). Intestinal stem cells and the colorectal cancer microenvironment. *World journal of gastroenterology,* **20,** 1898-909.

Ong S-M, Hadadi E, Dang T-M, et al (2018). The pro-inflammatory phenotype of the human non-classical monocyte subset is attributed to senescence. *Cell Death & Disease,* **9,** 266.

Ostan R, Bucci L, Capri M, et al (2008). Immunosenescence and Immunogenetics of Human Longevity. *Neuroimmunomodulation,* **15,** 224-40.

Ostan R, Monti D, Gueresi P, et al (2016). Gender, aging and longevity in humans: an update of an intriguing/neglected scenario paving the way to a gender-specific medicine. *Clinical science (London, England : 1979),* **130,** 1711-25.

Overgaard NH, Jung JW, Steptoe RJ, et al (2015). CD4+/CD8+ double-positive T cells: more than just a developmental stage? *J Leukoc Biol,* **97,** 31-8.

Pancione M, Giordano G, Remo A, et al (2014). Immune Escape Mechanisms in Colorectal Cancer Pathogenesis and Liver Metastasis. *Journal of Immunology Research,* **2014,** 686879.

Pangrazzi L, Reidla J, Carmona Arana JA, et al (2020). CD28 and CD57 define four populations with distinct phenotypic properties within human CD8(+) T cells. *Eur J Immunol,* **50,** 363-79.

Papadogianni G, Ravens I, Dittrich-Breiholz O, et al (2020). Impact of Aging on the Phenotype of Invariant Natural Killer T Cells in Mouse Thymus. *Front Immunol,* **11,** 575764.

Pawelec G (2017). Immunosenescence and cancer. *Biogerontology,* **18,** 717-21.

Pawelec G (2018). Age and immunity: What is "immunosenescence"? *Experimental Gerontology,* **105,** 4-9.

Petersone L, Edner NM, Ovcinnikovs V, et al (2018). T Cell/B Cell Collaboration and Autoimmunity: An Intimate Relationship. *Front Immunol,* **9,** 1941.

Phetsouphanh C, Aldridge D, Marchi E, et al (2019). Maintenance of Functional CD57+ Cytolytic CD4+ T Cells in HIV+ Elite Controllers. *Front Immunol,* **10,** 1844.

Pilger D, Seymour LW, Jackson SP (2021). Interfaces between cellular responses to DNA damage and cancer immunotherapy. *Genes Dev,* **35,** 602-18.

Poli A, Michel T, Thérésine M, et al (2009). CD56bright natural killer (NK) cells: an important NK cell subset. *Immunology,* **126,** 458-65.

Popov N, Gil J (2010). Epigenetic regulation of the INK4b-ARF-INK4a locus: in sickness and in health. *Epigenetics,* **5,** 685-90.

Prall F, Dührkop T, Weirich V, et al (2004). Prognostic role of CD8+ tumor-infiltrating lymphocytes in stage III colorectal cancer with and without microsatellite instability. *Human Pathology,* **35,** 808-16.

Prattichizzo F, Bonafè M, Olivieri F, et al (2016). Senescence associated macrophages and "macroph-aging": are they pieces of the same puzzle? *Aging,* **8,** 3159-60.

Puttipanyalears C, Denariyakoon S, Angsuwatcharakon P, et al (2021). Quantitative STAU2 measurement in lymphocytes for breast cancer risk assessment. *Scientific Reports,* **11,** 915.

Quezada SA, Simpson TR, Peggs KS, et al (2010). Tumor-reactive CD4(+) T cells develop cytotoxic activity and eradicate large established melanoma after transfer into lymphopenic hosts. *J Exp Med,* **207,** 637-50.

Qv L, Mao S, Li Y, et al (2021). Roles of Gut Bacteriophages in the Pathogenesis and Treatment of Inflammatory Bowel Disease. *Front Cell Infect Microbiol,* **11,** 755650.

Raskov H, Orhan A, Christensen JP, et al (2021). Cytotoxic CD8+ T cells in cancer and cancer immunotherapy. *British Journal of Cancer,* **124,** 359-67.

Rawla P, Sunkara T, Barsouk A (2019). Epidemiology of colorectal cancer: incidence, mortality, survival, and risk factors. *Przeglad gastroenterologiczny,* **14,** 89-103.

Rayess H, Wang MB, Srivatsan ES (2012). Cellular senescence and tumor suppressor gene p16. *Int J Cancer,* **130,** 1715-25.

Rea IM, McNerlan SE, Alexander HD (1999). CD69, CD25, and HLA-DR activation antigen expression on CD3+ lymphocytes and relationship to serum TNF-alpha, IFN-gamma, and sIL-2R levels in aging. *Exp Gerontol,* **34,** 79-93.

Reif de Paula T, Simon HL, Profeta da Luz MM, et al (2021). Right sided colorectal cancer increases with age and screening should be tailored to reflect this: a national cancer database study. *Techniques in Coloproctology,* **25,** 81-9.

Ricci C, Cova M, Kang YS, et al (1990). Normal age-related patterns of cellular and fatty bone marrow distribution in the axial skeleton: MR imaging study. *Radiology,* **177,** 83-8.

Romagosa C, Simonetti S, López-Vicente L, et al (2011). p16Ink4a overexpression in cancer: a tumor suppressor gene associated with senescence and high-grade tumors. *Oncogene,* **30,** 2087-97.

Roncucci L, Ponz de Leon M, Scalmati A, et al (1988). The influence of age on colonic epithelial cell proliferation. *Cancer, 62,* 2373-7.

Roy S, Bagchi B (2020). Fluctuation theory of immune response: A statistical mechanical approach to understand pathogen induced T-cell population dynamics. *The Journal of Chemical Physics,* **153,** 045107.

Russo AA, Tong L, Lee J-O, et al (1998). Structural basis for inhibition of the cyclin-dependent kinase Cdk6 by the tumour suppressor p16INK4a. *Nature,* **395,** 237-43.

Ryan G (2010). CD3 conformation is crucial for signalling. *Nature Reviews Immunology,* **10,** 7-.

Salam N, Rane S, Das R, et al (2013a). T cell ageing: effects of age on development, survival & function. *Indian J Med Res,* **138,** 595-608.

Salam N, Rane S, Das R, et al (2013b). T cell ageing: effects of age on development, survival & function. *The Indian journal of medical research,* **138,** 595-608.

Salminen A, Kaarniranta K, Kauppinen A (2020). ER stress activates immunosuppressive network: implications for aging and Alzheimer's disease. *Journal of Molecular Medicine,* **98,** 633-50.

Sambandam A, Maillard I, Zediak VP, et al (2005). Notch signaling controls the generation and differentiation of early T lineage progenitors. *Nat Immunol,* **6,** 663-70.

Sandhu C, Peehl DM, Slingerland J (2000). p16INK4A mediates cyclin dependent kinase 4 and 6 inhibition in senescent prostatic epithelial cells. *Cancer Res,* **60,** 2616-22.

Sanoff HK, Deal AM, Krishnamurthy J, et al (2014). Effect of cytotoxic chemotherapy on markers of molecular age in patients with breast cancer. *J Natl Cancer Inst,* **106,** dju057.

Saraiva D, Jacinto A, Braga S, et al 2018. *120PA new biomarker of breast cancer stage and patient response to neoadjuvant chemotherapy: HLA-DR expression in cytotoxic and regulatory T cells*.

Sawicka M, Pawlikowski J, Wilson S, et al (2013). The Specificity and Patterns of Staining in Human Cells and Tissues of p16INK4a Antibodies Demonstrate Variant Antigen Binding. *PLOS ONE,* **8,** e53313.

Schauer D, Starlinger P, Reiter C, et al (2012). Intermediate Monocytes but Not TIE2-Expressing Monocytes Are a Sensitive Diagnostic Indicator for Colorectal Cancer. *PLOS ONE,* **7,** e44450.

Schuster IS, Coudert JD, Andoniou CE, et al (2016). "Natural Regulators": NK Cells as Modulators of T Cell Immunity. *Front Immunol,* **7,** 235.

Sconocchia G, Keyvanfar K, El Ouriaghli F, et al (2005). Phenotype and function of a CD56+ peripheral blood monocyte. *Leukemia,* **19,** 69-76.

Seidelin JB (2004). Colonic epithelial cell turnover: possible implications for ulcerative colitis and cancer initiation. *Scandinavian Journal of Gastroenterology,* **39,** 201-11.

Serra S, Chetty R (2018a). p16. *Journal of Clinical Pathology,* **71,** 853-8.

Serra S, Chetty R (2018b). Structure_p16. *Journal of Clinical Pathology,* **71,** 853-8.

Serrano M (1997). The tumor suppressor protein p16INK4a. *Exp Cell Res,* **237,** 7-13.

Serrano M, Hannon GJ, Beach D (1993). A new regulatory motif in cell-cycle control causing specific inhibition of cyclin D/CDK4. *Nature,* **366,** 704-7.

Shain AF, Wilbur DC, Stoler MH, et al (2018). Test Characteristics of Specific p16 Clones in the Detection of High-grade Squamous Intraepithelial Lesions (HSIL). *International Journal of Gynecological Pathology,* **37**.

Shanker A, Buferne M, Schmitt-Verhulst AM (2010). Cooperative action of CD8 T lymphocytes and natural killer cells controls tumour growth under conditions of restricted T-cell receptor diversity. *Immunology,* **129,** 41-54.

Shin SA, Moon SY, Park D, et al (2019). Apoptotic cell clearance in the tumor microenvironment: a potential cancer therapeutic target. *Arch Pharm Res,* **42,** 658-71.

Silva-Filho JL, Caruso-Neves C, Pinheiro AAS (2014). IL-4: an important cytokine in determining the fate of T cells. *Biophys Rev,* **6,** 111-8.

Sipos F, Műzes G, Galamb O, et al (2010). The Possible Role of Isolated Lymphoid Follicles in Colonic Mucosal Repair. *Pathology & Oncology Research,* **16,** 11-8.

Sorrentino C, D'Antonio L, Fieni C, et al (2021). Colorectal Cancer-Associated Immune Exhaustion Involves T and B Lymphocytes and Conventional NK Cells and Correlates With a Shorter Overall Survival. *Front Immunol,* **12,** 778329.

Soysal P, Stubbs B, Lucato P, et al (2016). Inflammation and frailty in the elderly: A systematic review and meta-analysis. *Ageing Research Reviews,* **31,** 1-8.

Stahl EC, Brown BN (2015). Cell Therapy Strategies to Combat Immunosenescence. *Organogenesis,* **11,** 159-72.

Strioga M, Pasukoniene V, Characiejus D (2011). CD8+ CD28- and CD8+ CD57+ T cells and their role in health and disease. *Immunology,* **134,** 17-32.

Sun JC, Beilke JN, Bezman NA, et al (2011). Homeostatic proliferation generates long-lived natural killer cells that respond against viral infection. *J Exp Med,* **208,** 357-68.

Sun L, Brown R, Chen S, et al (2012). Aging induced decline in T-lymphopoiesis is primarily dependent on status of progenitor niches in the bone marrow and thymus. *Aging (Albany NY),* **4,** 606-19.

Sun P, Nallar SC, Raha A, et al (2010). GRIM-19 and p16(INK4a) synergistically regulate cell cycle progression and E2F1-responsive gene expression. *J Biol Chem,* **285,** 27545-52.

Sunthamala N, Sankla N, Chuerduangphui J, et al (2020). Enhancement of specific T-lymphocyte responses by monocyte-derived dendritic cells pulsed with E2 protein of human papillomavirus 16 and human p16INK4A. *PeerJ,* **8,** e9213.

Surh CD, Sprent J (2008). Homeostasis of Naive and Memory T Cells. *Immunity,* **29,** 848-62.

Sznurkowski JJ, Żawrocki A, Biernat W (2017). Local immune response depends on p16 INK4a status of primary tumor in vulvar squamous cell carcinoma. *Oncotarget,* **8**.

Tang Y-p, Xie M-z, Li K-z, et al (2020). Prognostic value of peripheral blood natural killer cells in colorectal cancer. *BMC Gastroenterology,* **20,** 31.

Teissier T, Boulanger E, Cox LS (2022). Interconnections between Inflammageing and Immunosenescence during Ageing. *Cells,* **11,** 359.

Tillinger W, Jilch R, Waldhoer T, et al (2013). Monocyte human leukocyte antigen-DR expression-a tool to distinguish intestinal bacterial infections from inflammatory bowel disease? *Shock,* **40,** 89-94.

Tippalagama R, Singhania A, Dubelko P, et al (2021). HLA-DR Marks Recently Divided Antigen-Specific Effector CD4 T Cells in Active Tuberculosis Patients. *J Immunol,* **207,** 523-33.

Tominaga K, Suzuki HI (2019). TGF-β Signaling in Cellular Senescence and Aging-Related Pathology. *International journal of molecular sciences,* **20,** 5002.

Trautmann A, Rückert B, Schmid-Grendelmeier P, et al (2003). Human CD8 T cells of the peripheral blood contain a low CD8 expressing cytotoxic/effector subpopulation. *Immunology,* **108,** 305-12.

Tsygankov D, Liu Y, Sanoff HK, et al (2009). A quantitative model for age-dependent expression of the p16INK4a tumor suppressor. *Proceedings of the National Academy of Sciences of the United States of America,* **106,** 16562-7.

Tu J, Zhang H, Yang T, et al (2022). Aging-associated REGγ proteasome decline predisposes to tauopathy. *J Biol Chem,* **298,** 102571.

Unsinger J, Kazama H, McDonough JS, et al (2009). Differential lymphopenia-induced homeostatic proliferation for CD4+ and CD8+ T cells following septic injury. *J Leukoc Biol,* **85,** 382-90.

Valle A, Barbagiovanni G, Jofra T, et al (2015). Heterogeneous CD3 expression levels in differing T cell subsets correlate with the in vivo anti-CD3-mediated T cell modulation. *J Immunol,* **194,** 2117-27.

Vallejo AN (2005). CD28 extinction in human T cells: altered functions and the program of T-cell senescence. *Immunol Rev,* **205,** 158-69.

van Leeuwen EM, Remmerswaal EB, Vossen MT, et al (2004). Emergence of a CD4+CD28- granzyme B+, cytomegalovirus-specific T cell subset after recovery of primary cytomegalovirus infection. *J Immunol,* **173,** 1834-41.

van Panhuys N (2016). TCR Signal Strength Alters T-DC Activation and Interaction Times and Directs the Outcome of Differentiation. *Front Immunol,* **7,** 6.

Varchetta S, Mele D, Oliviero B, et al (2021). Unique immunological profile in patients with COVID-19. *Cellular & Molecular Immunology,* **18,** 604-12.

Vasen HF, Tomlinson I, Castells A (2015). Clinical management of hereditary colorectal cancer syndromes. *Nat Rev Gastroenterol Hepatol,* **12,** 88-97.

Vicente R, Mausset-Bonnefont AL, Jorgensen C, et al (2016). Cellular senescence impact on immune cell fate and function. *Aging Cell,* **15,** 400-6.

von Boehmer H, Fehling HJ (1997). STRUCTURE AND FUNCTION OF THE PRE-T CELL RECEPTOR. *Annual Review of Immunology,* **15,** 433-52.

Waidhauser J, Schuh A, Trepel M, et al (2020). Chemotherapy markedly reduces B cells but not T cells and NK cells in patients with cancer. *Cancer Immunol Immunother,* **69,** 147-57.

Wang C, Liu X, Li Z, et al (2015). CD8+NKT-like cells regulate the immune response by killing antigen-bearing DCs. *Scientific Reports,* **5,** 14124.

Wang X, Zhang S, Dong M, et al (2020). The proinflammatory cytokines IL-1β and TNF-α modulate corneal epithelial wound healing through p16Ink4a suppressing STAT3 activity. *Journal of Cellular Physiology,* **235,** 10081-93.

Watchmaker PB, Lahl K, Lee M, et al (2014). Comparative transcriptional and functional profiling defines conserved programs of intestinal DC differentiation in humans and mice. *Nat Immunol,* **15,** 98-108.

Weiskopf D, Weinberger B, Grubeck-Loebenstein B (2009). The aging of the immune system. *Transpl Int,* **22,** 1041-50.

Weng NP (2006). Aging of the immune system: how much can the adaptive immune system adapt? *Immunity,* **24,** 495-9.

Wilkinson AN, Lieberman D, Leontiadis GI, et al (2019). Colorectal cancer screening for patients with a family history of colorectal cancer or adenomas. *Can Fam Physician,* **65,** 784-9.

Wong KL, Yeap WH, Tai JJ, et al (2012). The three human monocyte subsets: implications for health and disease. *Immunol Res,* **53,** 41-57.

Woolaver RA, Wang X, Krinsky AL, et al (2021). Differences in TCR repertoire and T cell activation underlie the divergent outcomes of antitumor immune responses in tumor-eradicating versus tumor-progressing hosts. *Journal for ImmunoTherapy of Cancer,* **9,** e001615.

Wu L, Van Kaer L (2011). Natural killer T cells in health and disease. *Front Biosci (Schol Ed),* **3,** 236-51.

Wu TD, Madireddi S, de Almeida PE, et al (2020). Peripheral T cell expansion predicts tumour infiltration and clinical response. *Nature,* **579,** 274-8.

Wu Z, Zheng Y, Sheng J, et al (2022). CD3(+)CD4(-)CD8(-) (Double-Negative) T Cells in Inflammation, Immune Disorders and Cancer. *Front Immunol,* **13,** 816005.

Xia S, Zhang X, Zheng S, et al (2016). An Update on Inflamm-Aging: Mechanisms, Prevention, and Treatment. *Journal of Immunology Research,* **2016,** 8426874.

Xiong Y, Wang Y, Tiruthani K (2019). Tumor immune microenvironment and nano-immunotherapeutics in colorectal cancer. *Nanomedicine: Nanotechnology, Biology and Medicine,* **21,** 102034.

Xu W, Wong G, Hwang YY, et al (2020). The untwining of immunosenescence and aging. *Semin Immunopathol,* **42,** 559-72.

Yang J, Zhang L, Yu C, et al (2014). Monocyte and macrophage differentiation: circulation inflammatory monocyte as biomarker for inflammatory diseases. *Biomarker research,* **2,** 1-.

Yang L, Zhu Y, Tian D, et al (2021). Transcriptome landscape of double negative T cells by single-cell RNA sequencing. *Journal of Autoimmunity,* **121,** 102653.

Yap NY, Ong TA, Pailoor J, et al (2023). The significance of CD14 in clear cell renal cell carcinoma progression and survival prognosis. *Biomarkers,* **28,** 24-31.

Zaidi S, Motabi I, Al-Shanqeeti A (2015). Neural cell adhesion molecule (cluster of differentiation 56) in health and disease. *Journal of Applied Hematology,* **6,** 93-105.

Zanoni I, Granucci F (2013). Role of CD14 in host protection against infections and in metabolism regulation. *Front Cell Infect Microbiol,* **3,** 32.

Zhang D, Chen G, Manwani D, et al (2015). Neutrophil ageing is regulated by the microbiome. *Nature,* **525,** 528-32.

Zhang FF, Cudhea F, Shan Z, et al (2019). Preventable Cancer Burden Associated With Poor Diet in the United States. *JNCI cancer spectrum,* **3,** pkz034-pkz.

Zhang H, Weyand CM, Goronzy JJ (2021a). Hallmarks of the aging T-cell system. *The FEBS Journal,* **288,** 7123-42.

Zhang J, He T, Xue L, et al (2021b). Senescent T cells: a potential biomarker and target for cancer therapy. *EBioMedicine,* **68,** 103409.

Zhang L, Chen X, Zu S, et al (2022). Characteristics of circulating adaptive immune cells in patients with colorectal cancer. *Scientific Reports,* **12,** 18166.

Zhang L, Pan J, Chen W, et al (2020a). Chronic stress-induced immune dysregulation in cancer: implications for initiation, progression, metastasis, and treatment. *Am J Cancer Res,* **10,** 1294-307.

Zhang L, Yu X, Zheng L, et al (2018). Lineage tracking reveals dynamic relationships of T cells in colorectal cancer. *Nature,* **564,** 268-72.

Zhang W, Ren J, Lu J, et al (2021c). Elucidating the Relationship between ROS and Protein Phosphorylation through In Situ Fluorescence Imaging in the Pneumonia Mice. *Analytical Chemistry,* **93,** 10907-15.

Zhang WJ, Zheng SS (2005). In vitro study of immunosuppressive effect of apoptotic cells. *J Zhejiang Univ Sci B,* **6,** 919-25.

Zhang Y, Rajput A, Jin N, et al (2020b). Mechanisms of Immunosuppression in Colorectal Cancer. *Cancers,* **12,** 3850.

Zhao Y, Shao Q, Peng G (2020). Exhaustion and senescence: two crucial dysfunctional states of T cells in the tumor microenvironment. *Cellular & Molecular Immunology,* **17,** 27-35.

Zhen A, Krutzik SR, Levin BR, et al (2014). CD4 ligation on human blood monocytes triggers macrophage differentiation and enhances HIV infection. *Journal of virology,* **88,** 9934-46.

Zheng R, Zhang Y, Zhang K, et al (2022). The Complement System, Aging, and Aging-Related Diseases. *Int J Mol Sci,* **23**.

Zheng Y, Liu X, Le W, et al (2020). A human circulating immune cell landscape in aging and COVID-19. *Protein Cell,* **11,** 740-70.

Zhu J (2018). T Helper Cell Differentiation, Heterogeneity, and Plasticity. *Cold Spring Harb Perspect Biol,* **10**.

Ziegler-Heitbrock L, Ancuta P, Crowe S, et al (2010). Nomenclature of monocytes and dendritic cells in blood. *Blood,* **116,** e74-e80.
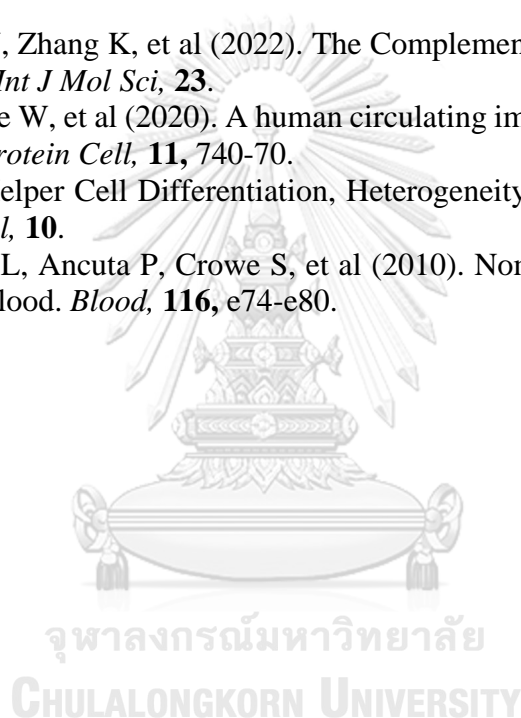
VITA

NAME	Ms. Khin Aye Thin
DATE OF BIRTH	19 February 1984
PLACE OF BIRTH	Taunggyi
INSTITUTIONS ATTENDED	University of Medical Technology, Yangon, Myanmar.
HOME ADDRESS	B14, Chanthar Shwe Pyi Housing, 10 Wards, Dagon East Township, Yangon, 11451, Myanmar.

PUBLICATION

Thin KA, Angsuwatcharakon P, Edwards SW, Mutirangura A & Puttipanyalears C. (2022). Upregulation of p16INK4A in Peripheral White Blood Cells as a Novel Screening Marker for Colorectal Carcinoma. Asian Pac J Cancer Prev, 23, 3753-61. doi: 10.31557/APJCP.2022.23.11.3753. PMID: 36444588; PMCID: PMC9930939.

Thin KA, Khin AA, Wah ST, Lwin CM & Soe MK. (2020). ABO blood group secretor status correlates with autoimmune diseases in Myanmar patients. Australian Journal of Medical Science, 41(2), 50-4.

Thin KA, Khin AA, Soe WPP & Oo MHHH. (2019) Detection of Aflatoxin M1 from Milk by ELISA Method. Conference Proceeding, Myanmar Universities' Research Conference. 1, 81-6.

Thin KA, Kyaw WK, Khin AA, Zaw MSM & Aung EEM. (2018). Screening of Microalbuminuria and Estimated Glomerular Filtration Rate in Type 2 Diabetes Mellitus for Early Detection of Renal Dysfunction. Myanmar Health Sciences Research. 30(2), 107-10.

Khin AA, Kyaw WK & Thin KA. (2018). Detection of Antinuclear Antibodies in Systemic Lupus Erythematosus Patients using Indirect Immunofluorescence and line Immunoassay Methods. Myanmar Health Sciences Research. 30(3), 236-41.

Thin KA, Oo KY & Khin AA. (2013). Comparative study of HIV DNA detection from whole blood and dried blood spot for early infant diagnosis, Conference of Scientific Research on HIV/AIDS between 2011-2013, Vietnam. 1, 104-6.